Advances in Mechanical Engineering

Advances in Conceptual Design Theories, Methodologies, and Applications

Guest Editors: Dongxing Cao, Shengfeng Qin, and Yu-Shen Liu

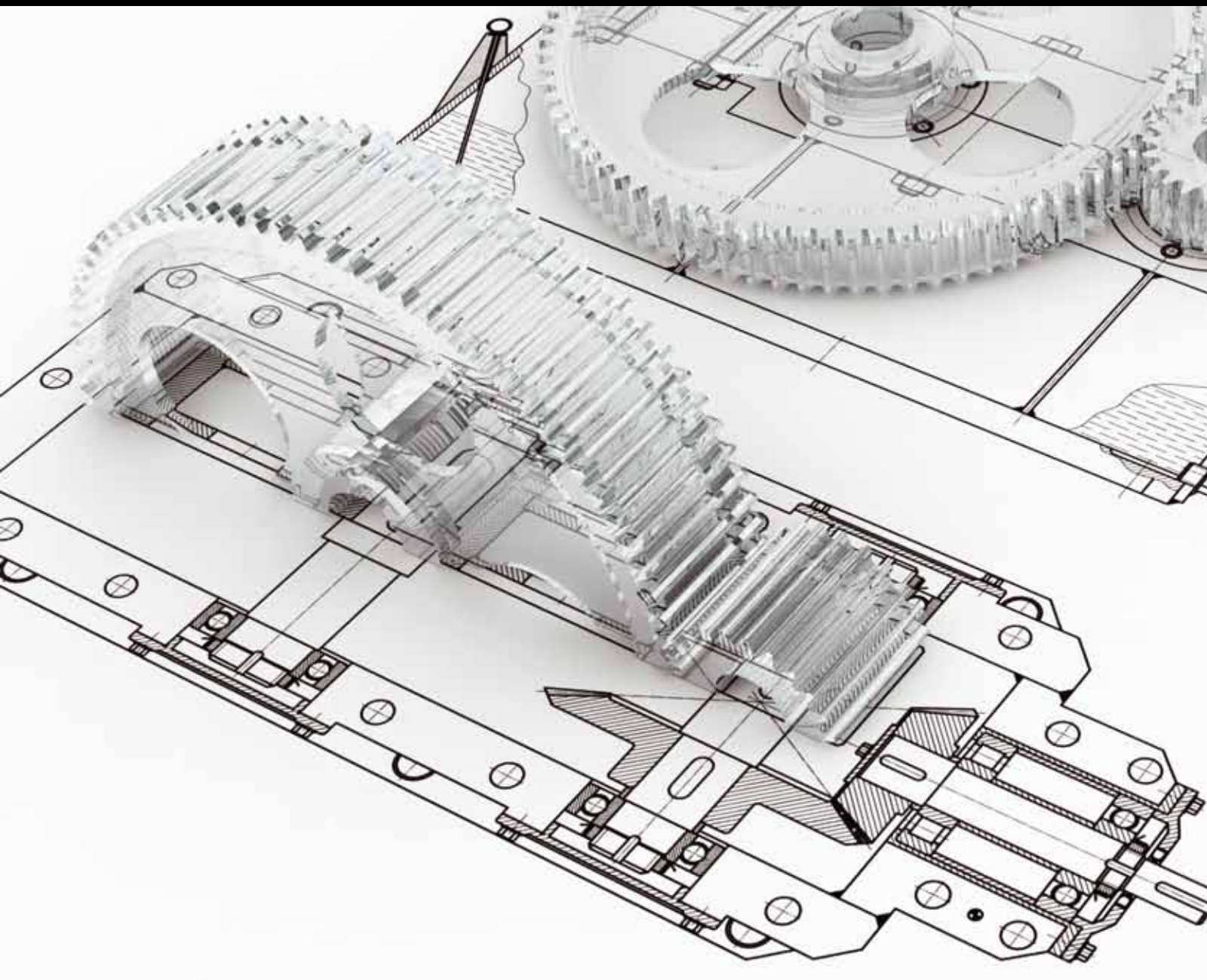

Advances in Conceptual Design Theories, Methodologies, and Applications

Advances in Mechanical Engineering

Advances in Conceptual Design Theories, Methodologies, and Applications

Guest Editors: Dongxing Cao, Shengfeng Qin, and Yu-Shen Liu

Editorial Board

Contents

Hindawi Publishing Corporation
Advances in Mechanical Engineering
Volume 2013, Article ID 207492, 3 pages
http://dx.doi.org/10.1155/2013/207492

Editorial

Advances in Conceptual Design Theories, Methodologies, and Applications

Dongxing Cao,[1] Shengfeng Qin,[2] and Yu-Shen Liu[3]

[1] *School of Mechanical Engineering, Hebei University of Technology, Tianjin 300130, China*
[2] *Department of Design, Northumbria University, Newcastle upon Tyne NE1 8ST, UK*
[3] *School of Software, Tsinghua University, Beijing 100084, China*

Correspondence should be addressed to Dongxing Cao; dongxingcao@gmail.com

Received 25 November 2013; Accepted 25 November 2013

Conceptual design lies in the early stage of a complex product development process, requiring not only considering the product's function and structure but also its social and environmental impacts. The design and decision made at the conceptual design stage have a significant influence on the success of the product development. Thus, exploring advanced conceptual design theories and methodologies and their applications has been considered as an important stage of a new product development, and it is currently a hot research topic in the engineering design field. The existing design methodologies have achieved extensive applications in engineering design, such as axiomatic design, collaborative design, agent-based design, and nfused design. Computer-aided design is widely seen as an enabling technology for supporting the scheme evaluation, geometric modeling, and structural feature design of new product development. Furthermore, within the industry engineering areas, there are strong commercial drivers to reuse and extend existing methodologies. Sometimes they are often undertaken in a highly coupled manner for a specific product design. However, as the complexity of product system and the diversity of product functions increase, the need for advanced design methods and tools becomes stronger. Therefore, conceptual design, as a rapidly changing field, developing new and advanced theories and methodologies dedicated to product innovation is required.

This special issue of Advances in Mechanical Engineering is dedicated to exploring the conceptual design theories, methodologies, and applications. We invite investigators from different countries and regions to contribute to this special issue with the original research articles as well as the review articles on engineering design.

This issue aims to stress the importance of using conceptual design and advances in the conceptual design theories. This special issue contains thirteen papers dealing with theories, methodologies, and applications of conceptual design in mechanical engineering. We hope that it is valuable to readers for their own research work.

The papers in this issue represent multifaceted contributions as well as the availability and usability of conceptual design in new product development. Three taxonomies, including theories, methodologies, and their applications, are differentiated. A brief overview of each paper as follows.

Firstly, R. Gaha et al. presented a literature review of different works based on feature technology to ecodesign products in their paper "Ecodesigning with CAD Features: analysis and proposals". Environment has become an important factor for product design, especially for a kind of devices of producing gas against environment. They divide ecodesign into two parts. The first one concerns CAD-Life Cycle Assessment, such as methodologies, prototype tools, and the second one implements feature technology to reduce the environmental impact of one life cycle stage, such as material selection and manufacturing.

Secondly, advanced conceptual design theories are proposed by five research papers. The first paper by Y. and Chakrabarti "Physical realizations: transforming into physical embodiments of concepts in the design of mechanical

movements" represented a kind of the method of concept generation, which could be used to support designers to systematically search for physical objects from a given input in terms of simplified functional, spatial, and mechanical movement requirements. Although it is similar to traditional method proposed 20 years ago, it is an effective means for resolving simple input/output and multi-input/output. Ying-Chieh Liu and Amaresh Chakrabarti proposed a method of conceptual generation to come up with possible physical embodiments to offer to designers for exploration and evaluation. They investigated the issue of how to transform a variety of possible initial solutions to the specified problems in terms of abstraction of mechanical movements and the synthesis of possible generic physical embodiments and report an implemented method that could automatically generate these embodiments. The underlying principle of this method is to make it possible to link common attributes between a specific abstract representation and its possible physical objects. The second paper by D. Cao et al. "Port-based ontology modeling for robot leg conceptual design" proposed a method of port-based ontology modeling for product conceptual design. It is an advanced design method, different from the existing design theories, such as axiomatic design QFD, to be conducted to model the process of product conceptual design. It can not only be used to model the early stage of product design, but also to implement embodiment design. D. Cao et al. considered that a port can be assumed as a real or virtual interface of the component which can exchange information with its outer environment, and it is the basis of the component concept and configuration generation. In this paper, they give a port-based ontology representation for robot conceptual design. Component knowledge and the primitive concepts are presented on the basis of port ontology. The taxonomy of port-based ontology is built to map the component connections and interactions to cluster functional blocks, and the semantic synthesis is employed to describe component ontology. At the same time, an approach is proposed for computing semantic similarity by mapping terms to function ontology and by examining their relationships based on port ontology language. Furthermore, the construction process of port-based ontology concepts is described, and its elements are related to the similarity values between concepts. The third paper by K. Li et al. "Research on SDG-based qualitative reasoning in conceptual design" reported a SDG-based qualitative reasoning for concept generation. The main task of conceptual design involves the generation of concepts to fulfill required functions and the evaluation of these concepts to select the most promising ones for further development. K. Li et al. adopted the signed directed graph (DSG) to reveal the inherent causal relationship and interactions among the variables, and find qualitative interactions between design variables and design purposes with the help of causal sequence analysis and constraint propagation. In the case of incomplete information, qualitative reasoning, which has the function of qualitative behavior prediction, can improve conceptual design level aided by the computer. To some extent, qualitative reasoning plays a supplementary role in evaluating scheme and predicting function. Next paper by Y. Kang and D. Tang "Matrix-based conceptual solution generation approach of multifunction product" puts up with a matrix-based conceptual generation method. It is an effective approach for matrix modeling design concept, such as axiomatic design, incidence matrix, and QFD. Y. Kang and D. Tang proposed a matrix-based conceptual solution generation approach to integrate two single-function products to a multifunction product. In the approach, the functions are represented by the functional basis and are used to construct the function model of the single-function product. The function similarity matrix of two single-function products is constructed based on the quantified similarity index of two subfunctions. Also the function-component matrix of each single-function product is constructed. The component-component matrix of two single-function products can be acquired by the function-component matrix multiplied by the function similarity matrix. There are three kinds of the component relationships in the component-component matrix: no-correlation, simple-correlation, and complex-correlation. The components of two single-function products are, respectively, removed, modified, and reserved according to the different correlation relationships. The design solution of a new multifunction product can be obtained by combining the reserved and modified components. The final paper by Y. Feng et al. "Equilibrium design based on design thinking solving: an integrated multicriteria decision-making methodology" used an integrated multicriteria decision-making methodology for concept evaluation. Y. Feng et al. proposed a multi-criteria decision making model to acquire the optimum one among different product design schemes. VIKOR method was introduced to compute the ranking value of each scheme. A multiobjective optimization model for criteria weight was established. In this paper, projection pursuit method was employed to identify the criteria weight set which could keep classification information of original schemes to the greatest extent, while PROMETHEEII was adopted to keep sorting information. Dominance-based multiobjective simulated annealing algorithm (D-MOSA) was introduced to solve the optimization model.

Thirdly, different methodologies have been used to improve the process of conceptual design, such as customer preference modeling, knowledge-based reasoning, and generic algorithm. They have different features and have achieved the expected results. We collected four papers to be used to represent conceptual design. The first paper by D. Cao et al. "Customer preference-based information retrieval to build module concepts" proposed customer preference information retrieval method to model concepts. How to obtain the new concepts from users' requirements and design information? How to deal with these documents? They are the fundamental work for generating alternative design concepts. D. Cao et al. viewed preference as an outer feeling of a product and also as a reflection of human's inner thought. It dominates the designers' decisions and affects people's purchase intention. In the paper, a model of preference elicitation from customers is proposed to build module concepts. The attributes of customer preference are classified in a hierarchy and make the surveys to build customer preference concepts. The documents or catalogs of design requirements, perhaps containing some textual description and geometric

data, are normalized by using semantic expressions. Some semantic rules are developed to describe low-level features of customer preference to construct a knowledge base of customer preference. Designers' needs are used to map customer preference for generating module concepts. The second paper by D. Karayel et al. "Integrated knowledge-based system for machine design" integrated knowledge for mechanical product design. When a method is used to a general product design, it is certain to be of the merits and demerits. An effective measure is to develop the merits and avoid the defect by integrating and combining them together. D. Karayel et al. developed an integrated design system (IDS) approach to various stages of the mechanical design process including rapid prototyping. The system consists of design, analysis, calculation, rapid prototyping, and library modules, and it blends artificial intelligence methods, CAD-CAM, and technical computing packages into a single environment. The third paper by C. Hu et al. "A simulation model design method for distributed/cloud-based simulation environment" sets up simulation environment to model design process. A variety of simulation models have been developed in specific organizations or enterprises to conduct the design process. However, they are difficult for reuse in the process of design. C. Hu et al. proposed computer simulation as a valid tool for the conceptual design of complex products involving multiple disciplines. The paper provides a simple implementation of simulation model reuse for distributed/cloud-based simulation environment and creates the simulation models' meta-model and ontology for the universal description. They proposed four rules to design/reprogram a simulation model into service-oriented form for its interoperability and established the ontology of service-oriented simulation model. The fourth paper by P. Gao and S. Yan "Fuzzy dynamic reliability model of dependent series mechanical systems" developed a reliability model for mechanical system. As the difficulties in describing the strength degradation process of components under fuzzy load and considering the failure dependence between different components in a system, conventional static fuzzy reliability models cannot be directly extended for dynamic reliability analysis of mechanical systems. To deal with these problems, P. Gao and S. Yan proposed fuzzy dynamic reliability models of mechanical systems in terms of stress and strength. The proposed models can be used to represent the dynamic characteristics of fuzzy reliability and analyze the influences of the variation in the parameters of fuzzy stress and strength on the failure dependence of components in a system and the dynamic behavior of fuzzy system reliability.

At last, the application of conceptual design theories has achieved a great success in industry engineering areas. We collected three papers to represent the applied results. The first paper by J. Li et al. "Conceptual design of deployment structure of morphing nose cone" adopted genetic algorithm to obtain the deployment structure of morphing nose cone. For a reusable space vehicle or a missile, the shape of the nose cone has a significant impact on the drag of the vehicle. J. Li et al. proposed the concept of morphing nose cone to reduce the drag when the reentry vehicle flies back into the atmosphere. The conceptual design of the structure of morphing nose cone is conducted. Mechanical design and optimization approach are developed by employing genetic algorithm to find the optimal geometric parameters of the morphing structure. The second paper by Z. Li and D. Cao, "Conceptual design of compliant mechanism based on port ontology" applied port ontology to conceptual design of compliant mechanism. Port-based ontology (PBO) is used to represent and organize product design information and support product conceptualization. Port is used to map and link components together. It plays an important role in capturing component information. Z. Li and D. Cao established a design method of compliant mechanism based on port ontology. The paper constitutes coding rules and constructs PBO knowledge base of compliant mechanism, which includes stiffness-base and inherent frequency-base of flexible cells. The incidence matrix is built to denote the relationship of components, and the schemes are generated by adopting the genetic algorithm based on incidence matrix. The scheme populations for training neural network (NN) are generated by parameters distributing, and the preferential scheme is to be selected via the trained NN. The third paper by M. H. Shojaeefard et al. "Optimum design of 1st gear ratio for 4WD vehicles based on vehicle dynamic behaviour" adopted optimum approach to obtain the gear ratio for 4WD vehicles. M. H. Shojaeefard et al. presented an approach that allows optimizing gear ratio and vehicle dimension to achieve optimum gear transmission. Augmented Lagrangian multiplier method, defined as classical method, is utilized to find the optimum gear ratios and the corresponding number of gear teeth applied to all epicyclical gears. This method is able to calculate and also to optimize the gear ratio based on dynamic of 4WD vehicles.

The emergence of increasingly newer theories and methodologies of conceptual design will constantly be proposed with the development of sciences and technologies. The more mathematic tools and algorithms will be applied to the stage of conceptual design, even to some specific case studies. We believe that this special issue is valuable to readers from engineering design field. We would like to acknowledge all authors and all reviewers anonymously contributed to this special issue. It is that your efforts make this special issue possible. We would be interested to receive any comments either to the members of Editorial Board or to any readers.

Dongxing Cao
Shengfeng Qin
Yu-Shen Liu

Hindawi Publishing Corporation
Advances in Mechanical Engineering
Volume 2013, Article ID 657960, 10 pages
http://dx.doi.org/10.1155/2013/657960

Research Article

Port-Based Ontology Modeling for Robot Leg Conceptual Design

Dongxing Cao,[1] Ming Wang Fu,[2] Jiajia Mi,[1] and Zhanwei Li[1]

[1] *School of Mechanical Engineering, Hebei University of Technology, Tianjin 300130, China*
[2] *School of Mechanical Engineering, The Hong Kong Polytechnic University, Hung Hom, Hong Kong*

Correspondence should be addressed to Dongxing Cao; dongxingcao@gmail.com

Received 12 April 2013; Accepted 12 September 2013

Academic Editor: Shengfeng Qin

Port, as an interface of the component, can be used to exchange information with its outer environment. It is the basis of the component concept and configuration generation. In this paper, port-based ontology representation is first given, and component knowledge and the primitive concepts are presented to describe robot leg ontological concepts. Secondly, the taxonomy of port-based ontology is built to map the component connections and interactions to cluster functional blocks, and their semantic synthesis is employed to describe component ontology. Next, an approach is proposed for computing semantic similarity by mapping terms to function ontology and by examining their relationships based on port ontology language. Furthermore, the construction process of port-based ontology concepts is described and its elements are related to the similarity between two concepts. Finally, a robot leg example is shown to illustrate the proposed approach.

1. Introduction

A port is viewed as the location of intended interaction of two components or a component and its environment [1]. It plays an important role in the component concept generation. It constitutes the interface of a component and defines its boundary. Singh and Bettig [2] defined assembly ports as one or more low-level geometric entities that undergo mating constraints to join parts. They adopted the port-based composition to describe the hierarchical configurations of complex engineering design and realized assembly design through determining port compatibility and connectability. Breedveld [3] described a port as the "point" of interaction of a system, subsystem, or element with its environment in order to realize the port-based modeling of dynamic systems on the basis of bond graphs. Campbell et al. [4] developed a functional representation based on the ports of connectivity with other components to describe how energy and signals are transformed between ports. Horváth et al. [5] defined a port as the place of action for a physical effect. Based on energy flow, they classified contact ports into inports and out-ports and considered certain physical effects as occurring inside the objects and others as occurring between the objects. To formalize port descriptions, ontologies are introduced to be used for port representation, in which the classes include the ports themselves along with the attributes that allow designers to define the ports. These classes are a subset of artifact ontology, which can describe not only the interface, but also the internal characteristics of components and subsystems. Also, they adopted design concept ontology as a comprehensive methodology for managing conceptual design, including structure, shape, and functionality. Ozawa et al. [6] proposed a common ontology to support different information-level sharing between humans and multiple modeling and simulation software agents. Unified taxonomies and keyword networks can be built to support model retrieval and repository management available to designers in these domain ontologies [7]. In addition, there has been significant research into functional representation. Stone and Wood [8] presented the concept of functional basis—a formal function representation and a standardized set of function-related terminologies to support functional modeling—which consists of function and flow sets. Any functions can be described in the form of simple function sets. Furthermore, when the functional structure of a product is built, different functional classifications can be identified based on the functions themselves. Functions may be used for conveying the designers' intent. This is illustrated

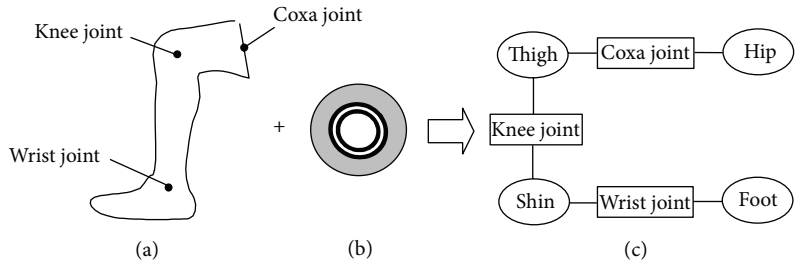

Figure 1: Leg and wheel structure corresponding graph representation.

in the design process developed by Kirschman and Fadel [9]. They presented the taxonomy of elemental mechanical functions and derived four basic types of functions, which are related to the concepts of motion, power/matter, control, and enclosure, of which each can be used with many decomposition techniques. De Kleer [10] defined function as a causal pattern between variables. The functional symbols in the natural language with the "verb + noun" style represent the designers' intention. Ontology representations not only convey and encapsulate both syntax and semantics, but also allow computer programs to share, exchange, extend, reuse, and translate information. The representations can be based on either frame-based logic or description logic.

An approach to port-based ontology that primarily focuses on performing the activity for design concept is proposed in this paper. It is difficult to build an appropriate configuration for a specific product if the developed product is not yet known. Thus, there is a tremendous need to develop an effective technology that can capture component concepts that are involved in product development. The proposed port-based ontology attempts to address this issue. The remainder of this paper is organized as follows. Section 2 gives a port-based ontology representation. Section 3 establishes component ontology knowledge base. Section 4 presents function ontology concepts, gives port attributes and taxonomies in a hierarchy, and discusses port ontology concept measures. Port-based ontology modeling process is described in Section 5. A case study and analysis of results are presented in Section 6. Finally, concluding remarks and further research are given in Section 7.

2. Port-Based Ontological Representation

A port can be viewed as the joint of human body. And it properly connects each part and makes it collaboratively work. It plays an important role in functional design of robot leg system based on port description. The total function characterizes general purpose of the designed product [11]. It may need to be decomposed into a set of subfunctions in the hierarchy. During this phase, we should carefully define component interfaces with ports and specify the associated port form.

Figure 1 gives a graph representation with leg and wheel configuration, in which Figure 1(a) presents three main joints of the leg: coxa joint, knee joint, and wrist joint. They have different functions corresponding the ports, respectively. Each port plays a different role in implementing leg's motion. Figure 1(b) indicates a wheel, and Figure 1(c) gives graph representation for robot leg system. However, it is actually difficult to go walking as human being from a technique standpoint. Thus, it is feasible to combine leg with wheels together for the robot leg. As a matter of convenience, we focus on establishing design components for implementing the specific function according to port-based ontological description.

Assume that a system (S) consists of n ports and it has m connectors (CON). Therefore, we can formally represent a product system as follows:

$$S = \sum_{k=1}^{n} \sum_{l=1}^{m} P_k \mathrm{CON}_l$$
$$\mathrm{CON}_l = \mathrm{INT}\left(\mathrm{CO}_i, \mathrm{CO}_j\right) \quad i \neq j, \tag{1}$$

where P means ports, which exist in between two components or simple component; CO indicates the components, and INT stands for the interaction between components, in which i, j, k, l, n, and m are the positive integers.

In (1), CONs represent the action between two components. They can realize some specific functions, such as "fastening parts," "transmitting torques," "bounding parts". Sometimes they constitute the prototype components.

3. Knowledge Base Establishment

3.1. Port Compatibility Rules. A component is a design object with a complete specification describing how it is connected to other components in a configuration. For example, a shaft is assembled into the wheel by an axle link or two shafts are linked by a shaft coupling. They collectively form a port or an interface with each other. Then, a configuration is generated when two or more components are connected with each other via their interface as shown in Figure 2.

Compatibility checking occurs when two component models are connected. The port-based description can be conducted by the logic representation, which verifies whether all the attributes of the two ports satisfy the compatibility requirements specified in the port ontology. In a logic description, the port definitions and compatibility rules are stored in the knowledge base which is a collection of axioms for describing the true conditions of the port connection domain. When a port is established, the system queries the

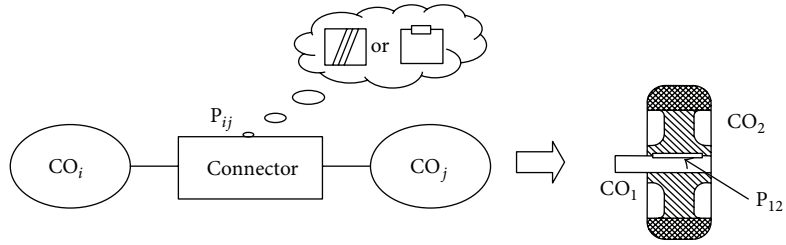

Figure 2: Port model between two components.

Table 1: The static connector types of two components.

Names	Fastener link (FK)	Weld link (WL)	Shaft coupling (SC)	Key link (KL)	Pin link (PL)
Types					

logic representation to verify if the connected port instances satisfy all the rules. For example, to connect a circular-hole port, the port must have either a pin shape or an axle shape form attribute. A system can be established as a configuration of components by connecting the components at their ports. At the same time, the connected two ports need to be compatible, or else they do not connect together; for example, a square plug does not fit a round hole. In this paper, we illustrate how the port ontology can be used to define general rules for port compatibility. The port ontology, has been defined, but it does not include the concept of compatibility yet. We can use the phrase named "is-compatible-with" to identify the port types that are compatible with each other [12]. For example, we can define the compatibility of a circular-hole port whose rule explicitly specifies that only the axle port and pin port can be connected to a circular-hole-port. This research defines the port topological properties (PTP) as a flexible mechanism to link and configure different ontologies into larger ones.

Assume that X represents the set of components in a product and a relation R_{port} can be defined in such way that it denotes port compatibility below

$$P = xR_{\text{port}}y \quad \left(x, y \in X;\ R_{\text{port}} \in \text{rules}\right), \tag{2}$$

where x and y are components in X. R_{port} stands for a compatibility; that is, they exist in relativity, which contains an equivalent relation, a public relation, an inclusion relation, and a transfer relation. These relations are defined as follows.

3.1.1. Equivalent Relation. If x and y have the same port type and port attribute, namely, $x \equiv y$ in mathematics, they are of compatibility and can form a mutual port, that is, $xR_{\text{port}}y$. For instance, key link, pin link, shaft coupling, and so forth are often viewed as a kind of typtical equivalent relations shown in Table 1.

3.1.2. Public Relation. If x and y have the public port type and port attribute, then $x \cap y \neq \emptyset$ can be defined from a mathematical perspective. They are also compatible and can form a shared port, that is, $xR_{\text{port}}y$. For instance, common components or parts in a product system are generally viewed as public relation.

3.1.3. Inclusion Relation. If the port types and port attributes of x completely belong to y and are unreversed, then it can be represented as $x \subset y$ and $y \not\subset x$. They are also compatible and form an oriented port, that is, $xR_{\text{port}}y$. For instance, some components with support functions or packing functions can be considered as inclusion relation.

3.1.4. Transfer Relation. If x, y, and z satisfy $x \subset y$ and $y \subset z$, then $x \subset z$; the ports x, y, and z will be of conduction attribute, namely, $xR_{\text{port}}yR_{\text{Port}}z$. For instance, worm gear, cone gear, rack pinion, and so forth are often viewed as transfer relation shown in Table 2.

The connectors are the basis of connecting two components to implement the specific relations. There are number of connectors which have different functions, such as motion, orientation, and dynamic requirements. There are two kinds of connectors, that is, static connectors and kinetic connectors. Table 1 presents the static connectors, such as fastener link, weld, shaft coupling, key link, and pin link. Meanwhile, Table 3 gives the kinetic connectors, such as worm gear, cone gear, gear mechanism, belt gear, and rack pinion. They constitute a set of connectors for the knowledge base of alternative design.

The above-mentioned relational rules are solely based on port names and their attributes. However, if a new port class is added to the port ontology, it is not suitable for only using port names. This needs to update compatibility rules. An effective measure is to use attributes to present the compatibility constraints. A circular port can be connected between shaft and gear with similar geometric features as shown in Figure 2. When foot wheel contacts the earth surface, a port is formed. If robot leg walks along on the ground, then a drive is forced on a shaft which generates a port between shaft and

Table 2: The kinetic connector types of two components.

Names	Worm gear (WG)	Cone gear (CG)	Gear mechanism (GM)	Belt gear (BG)	Rack pinion (RP)
Types	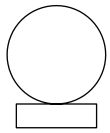	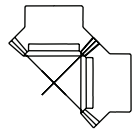	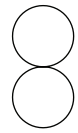	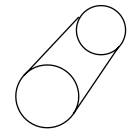	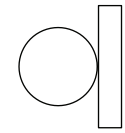

Table 3: The prototype components of constraint joints.

Names	Spherical joint (SJ)	Revolute joint (RJ)	Cylindrical joint (CJ)	Prismatic joint (PJ)	Cross-pin joint (CP)
Types	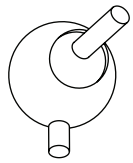	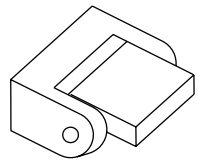	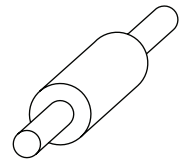	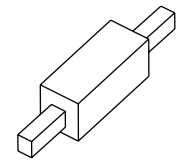	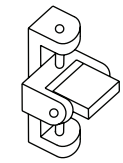
Dofs	3	1	2	1	2

wheel. We could express this rule using low-level geometric constraints on the type and dimensions of port features. If two components are compatible, they certainly possess relativity. We can also evaluate the compatibility of both components by evaluating the semantic relativity [13].

3.2. Prototype Component Base. The prototype component corresponds to the basic function unit, and it cannot be separated further. Port is used to configure a particular component and is restricted within the configuration interface for the component. Multijoints are the basis unit for constructing robot leg system. General joints are described as follows [14].

A spherical joint, shown in column one in Table 3, is satisfied with the condition that the center of the ball coincides with the center of the socket. Then, terminal equations are three scalar constraint relationships that restrict the relative positions between the components in the following:

$$\left[e^x \;\; e^y \;\; e^z\right]^T \delta_{r3} = \left[0 \;\; 0 \;\; 0\right]^T, \tag{3}$$

where e^x, e^y, and e^z are unit vectors and δ_{r3} represents the relative virtual displacement between the components. Essentially, three constraint relationships are imposed, and there is no relative displacement at the joint in the x-y-z directions, but three virtual angular rotations are free. Therefore, the dof equates to three.

A revolute joint, shown in column two in Table 3, is constructed with bearings which only allows relative rotation about a common axis in a pair of components but precludes relative translation along the axis. The five terminal constraint equations are

$$\left[e^x \;\; e^y \;\; e^z\right]^T \delta_{r3} = \left[0 \;\; 0 \;\; 0\right]^T \qquad \left[e^x \;\; e^y\right]^T \delta_{\theta 2} = \left[0 \;\; 0\right]^T, \tag{4}$$

where $\delta_{\theta 2}$ represents the relative virtual angular rotation between the components and dof equates to one.

A cylindrical joint between components is shown in column three in Table 3. It permits relative translation and relative rotation between two components along a common axis. The four terminal constraint equations are

$$\left[e^x \;\; e^y\right]^T \delta_{r2} = \left[0 \;\; 0\right]^T \qquad \left[e^x \;\; e^y\right]^T \delta_{\theta 2} = \left[0 \;\; 0\right]^T. \tag{5}$$

A prismatic joint, shown in column four in Table 3, allows relative translation along a common axis between two components but precludes relative rotation about the axis. The five terminal constrained equations are

$$\left[e^x \;\; e^y\right]^T \delta_{r2} = \left[0 \;\; 0\right]^T \qquad \left[e^x \;\; e^y \;\; e^z\right]^T \delta_{\theta 3} = \left[0 \;\; 0 \;\; 0\right]^T. \tag{6}$$

Above-mentioned constraint joints are shown in Table 3. Also, the other connectors can be obtained, and they are the common connecting mechanisms shown in Table 3. These components can be put into knowledge base for indexing and reusing.

4. Functional Ontology Concepts

4.1. Port Attributes and Port Taxonomy. In mechanical system, common components, such as gear, bearing, fastener, gimbal, shaft coupling, and spring, are named the prototype components. They are the basis of prototype concept generation. And they can be well defined by a set of structural attributes. The connector is defined by an action of two basic mechanisms with physical law or geometric axiom, and it provides constraint on them to implement the specific functions. On the basis of constraint characteristic, mechanical products can be classified into three kinds of form, that is, static constraint, kinetic constraint, and motional force transfer as shown in Table 4. The physical effect of the connectors has Hooke's law, Newton's law, friction principle, and so on. Their representation includes geometric constraint or primitive components, named mechanical standard parts, such as fastener, spring, and bearing. They are referred to as the standard connectors in mechanical engineering field.

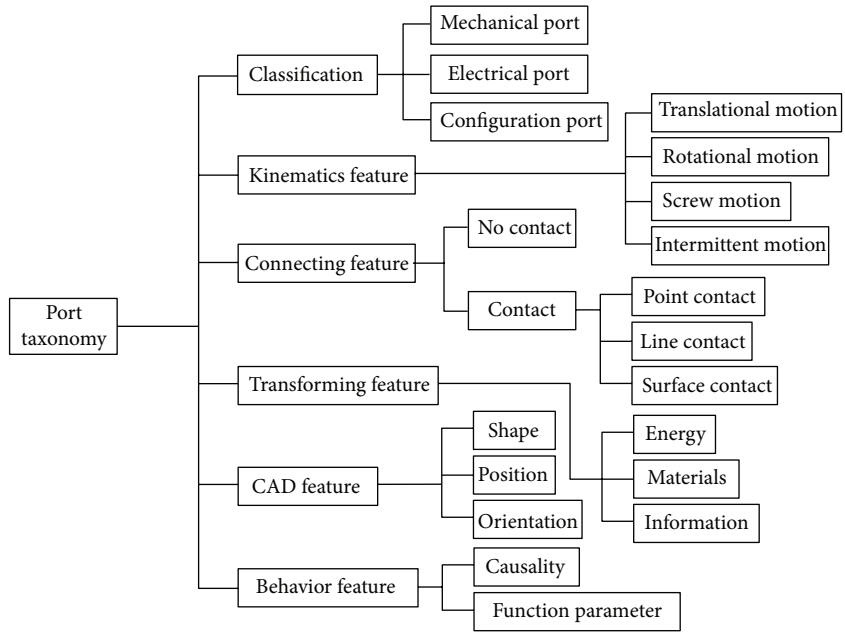

Figure 3: Port taxonomy.

Table 4: Connectors of mechanical components.

Functions	Behaviors	Types of connectors
Fastener connectors	Fastening	Fasteners
	Jointing	Binder
Kinematic constraint connectors	Rolling	Bearing
	Sliding	Slide rail
Force transfer connectors	Airproof	Sealing ring
	Speed change	Gear drive

In general, port attributes include function, behavior, and structure, in which function attribute contains port classification, connecting form, and kinetic and transforming way. Behavioral attribute indicates causality and physical parameters. And structural attribute means shape, position, and orientation. They are the basis of port ontology modeling, and their taxonomies are shown in Figure 3.

4.2. Port Ontology Concept Measures. It is easy to obtain an ontology concept by using attribute representation of port ontology. Therefore, it is very important to distinctly analyze port attributes before naming concept ontology. Attribute representation of a port is shown in Figure 3. This taxonomy allows the users to quickly find components in an ontology library by mapping operation, which contains component models and an alternative way to access components in the library. For example, two mechanical contacted parts have the same attribute of transferring mechanical energy, and they easily form a mechanical port.

Prototype concepts are the basic unit of function concepts and are interdependently defined with each other. They are defined by using a set of prototype terms and viewed as a semantic description of functional elements. A connector is defined as the interaction between two components and it is the location of generating physical effect [1, 15].

As the phrase of "verb + noun" is used to represent the function, the semantic description of functional elements can be quantitatively obtained by indexing its verb and noun terms. Therefore, functional concept (δ_i) is related to verb (V_i) and noun (N_i) and represented as follows:

$$\delta_i = \{V_i, N_i \mid V_i \subset \text{Verbs}, N_i \subset \text{Nouns}\}. \quad (7)$$

Specifically, the similarity (SIM) between two prototype concepts can be represented as follows:

$$\text{SIM}(\delta_i, \delta_j) = \frac{\text{The number of matching terms with each}}{\text{The total number of terms}}, \quad (8)$$

where δ stands for the prototype concept; that is, (δ_i, δ_j) refers to two different prototype concepts.

The connectivity of different prototype concepts can be quantitatively measured on the basis of the similarity calculation [13]. Based on the function, four typical connections are identified among primitive design concepts in the following [5].

(i) *Cause Connection* (CC). A design concept necessitates the function delivered by another design concept to achieve a needed function. It has a feature with transfer relation. For example, a gear can realize rotation from the other gear drive.

(ii) *Equal Connection* (EC). If two design concepts present the same function based on similar or dissimilar constituents, such as entities, situations, and phenomena, then they form equal connectors. It has

a feature with equal relation. For example, fastener link and weld are two kinds of equal connectors.

(iii) *Share Connection* (SC). Simultaneously possesses one ontology concept when SC distributes in different locations and spaces with several functions. It has a feature with public relation. For example, a concept of fastener ontology is used to share static connector for different components.

(iv) *Bind Connection* (BC). BC expresses the assertion that there is no interdependence between two or more design concepts. It has a feature with inclusion relation. And the bind connection of the design concepts will depend on the constraints' relationships.

Four form connections are the foundation of generating module concepts. A module can be formed by combining different connections with more components. In the process of primitive concept acquisition, it is possible to distinguish properties from the specific domain. These properties can be explored by describing port ontology. In the practical application, these distinctions refer to groups of properties that are known as port concept. For example, a robot leg system can be viewed as several functional modules, and each module exists in many components and connectors. Identifying and separating these basic connections will be important for structuring a new prototype concept in port-based ontology. It can give rise to a strong internal connection or a weak coupling connection. According to the above analysis, four kinds of connection relations can be uniformly represented as follows:

$$\mathrm{CON} = \left\{\mathrm{INT}\left(\mathrm{CO}_i, \mathrm{CO}_j\right) \mid i \neq j; \mathrm{INT} \subset \mathrm{CC}, \mathrm{EC}, \mathrm{SC}, \mathrm{BC}\right\}. \tag{9}$$

To determine the connection degree between primitive concepts, the similarity degree (SIM) is defined as the similarity evaluation of two primitive concepts given in (8). In the practical application, the ontological relation between concepts can be determined by using the primitive concept classification and a set of familiar attributes. For example, the robot leg is the basic mechanism to implement robot walk, and it can go ahead, back, and get across the obstacles. It plays an important role in determining robot joints and components to construct port-based ontology, that is, to obtain a stronger inner connecting or a weak coupling relation.

5. Port-Based Ontology Modeling

The functions are decomposed by matching the primitive function concepts of knowledge base. They describe the physical effects corresponding the port connectors. Port-based ontological semantics also describe connection information and structure information between primitive components. Primitive functions or subfunctions are aggregated into the total function in a bottom-up manner. Behavioral description specifies the connectivity and causality which constitutes a hierarchical semantic net by behavioral semantic mapping and it makes efforts to bridge the gap between port function and port structure [16]. Configuration describes which components are involved and whether they are mapped or interact with each other. They specify the relations of component position, topology, and kinematics. The positional relation quantitatively describes how the artifact is positioned and oriented in a three-dimensional space presented in (3), (4), (5), and (6). The topological relation interprets the condition of their physical connections. Contacts can be direct or indirect. Contacts can also be further specified among the individual points on the surface, domains on the surface, and complete the surface [5]. Configuration is identified by primitive form mapping in a hierarchy.

The attributes are lower-level concepts for defining ports. The attributes are divided into three main categories: function, behavior, and structure [17]. When a port is defined by function attributes, its attributes describe the intended use of the port. Port attributes are crucial to constructing the concept ontology process. Therefore, it is very important to distinctly analyze port attributes before defining concept ontology.

As the language is governed by grammar or a set of rules, it is possible to algorithmically process language to identify patterns and extract information [18]. In English language, verbs and nouns or more generally noun phrases are used. Their grammar functions can be either the subject or the object of the verb, and the typical construction of English sentences is subject-verb-object (SVO). We use this language model to identify verbs to connect engineering lexicons.

We defined port concepts with intention-rich functional concepts. However, most of "verb + noun" phrases often slack such intention of functional representation. They have no machine understandable definition of concepts. In the function behavioral structure (FBS) model, the function symbol in natural language in the verb + noun style represents the intention of designers. We tried to identify this kind of function concepts as hiding in function semantic structure. A function of a component cannot be determined until the component is installed in a specific system with a specific configuration [2]. Although a function of a component depends on other components, the description itself should be local. In such cases, a group of functions is sometimes formed by a set of components across the intersubsystem boundary.

Function semantic expression from users' requirements describes the process of port ontology generation. In the following illustration, the semantic expressions of a robot leg system are extracted from the users' design description and are given as follows.

> Run up thigh to add the height of body, while putting down thigh to reduce the height of body.
>
> Leg is a part of robot body, and also thigh is a part of leg.
>
> Foot wheel is the foot of robot, and it can make the robot walk.
>
> Drive KJ-motor to reduce the span in a clockwise direction.

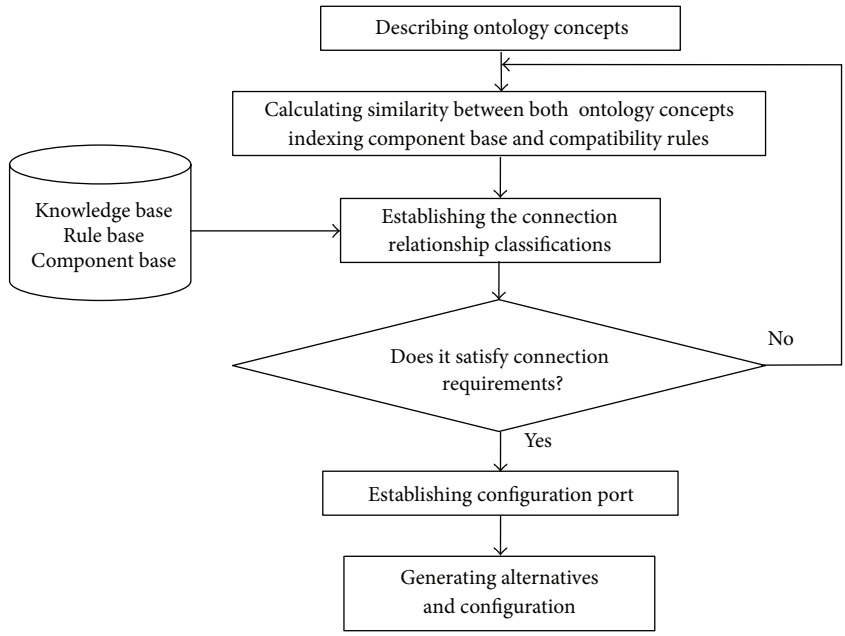

Figure 4: Port-based ontology modeling process.

Drive WJ-motor to make foot wheel rotation.

Knee joint has the function of driving shin rotation.

Connect WG1 with hip together.

Assemble key link to shaft and foot wheel.

Fix WJ-motor to the end of shin.

Assemble shaft into bevel gear.

...

Return.

These semantic expressions include a phrase of "verb + noun", that is, "is_a" link, "part_whole" relation, "has_function" relation, and so on. "Noun" and "noun phrase" are composed of the keywords of function concepts [19]. Actually, there are different types of artifact ontologies. They are firstly filtrated by several rules. Secondly, the selected artifacts are included and subsequently are specialized to an engineering domain by instantiation, term, and concept mappings and additional specific axioms. Finally, a larger ontology is synthesized by the compatibility to connect corresponding artifact ontologies. We developed formal steps to implement port-based ontology modeling shown in Figure 4 as follows:

(i) describe the component functions to build port ontology and lexicon;

(ii) pick up the various semantic relations to formalize users' requirements for regular term arrangement;

(iii) establish a hierarchical functional concept to conveniently obtain primitive concepts;

(iv) measure the shortest path between two functional concepts by using the semantic similarity;

(v) distinguish compatibility port ontology to cluster into a fit component configuration.

6. Case Study and Result Analysis

The leg is a part of robot body and it is the main component to realize robot motion. The dofs determine the complexity of robot motion and routing problem. It is a much familiar and simple robot leg for two dofs and foot bottom truckle. It is easy to realize for simplifying leg motion paths. According to users' requirements and human being's leg structure, three joints, called ports, are needed to realize leg's functions as shown in Figure 1. Thigh and hip are linked by coax joint, and thigh and shin are linked by knee joint. Five basic components $P_1 \sim P_5$ are easily established to configure robot leg. Figure 3 presents the connector model of two components for robot leg. The connector C_{12}, that is, key link, connects between P_1 and P_2, since P_1 and P_2 are common linearity with each other. We select one of the static connectors, such as SC, KL, and PK, as shown in Table 1. In addition, as P_1 and P_2 locate on different surfaces, it is a fit choice for KL. It can be obtained from knowledge reasoning through indexing component base. So, a key link will be selected to satisfy the robot leg requirements. Also, port P_{23} will be generated between shin and shaft. As P_2 and P_3 consist in the relationship of plane motion, we select kinetic and static connectors, that is, CG and KL, as shown in Tables 1 and 2. All ports will be obtained by semantic description and knowledge reasoning on account of port-based ontology as shown in Table 5. The configuration relationships of ports and connectors are shown in Figure 5(a).

The rotation is the main function that joint legs realize. It is also a main way for implementing the robot leg functions. An additional function is needed to realize the robot leg

Table 5: The verbs and nouns of describing robot leg port concepts.

Ports	Port generations	Verbs	Nouns	Examples
P_{12}	(shaft, foot wheel)	Assemble, rotate, connect, transform	Shaft, foot wheel, key link	Assemble shaft to foot wheel
P_{23}	(Shin, shaft)	Transform, connect, fasten	Shin, shaft, WJ-motor, CG, key link	Transform torque from WJ-motor to shaft
P_{34}	(thigh, shin)	Connect, rotate, assemble	Thigh, shin, WG2, shaft coupling, key link, KJ-motor	Fasten KJ-motor to worm through key link
P_{45}	(hip, thigh)	Fasten, assemble, has, is_a	Hip, thigh, WG1, shaft coupling, key link, CJ-motor	Fasten WG1 to hip through bolted connection

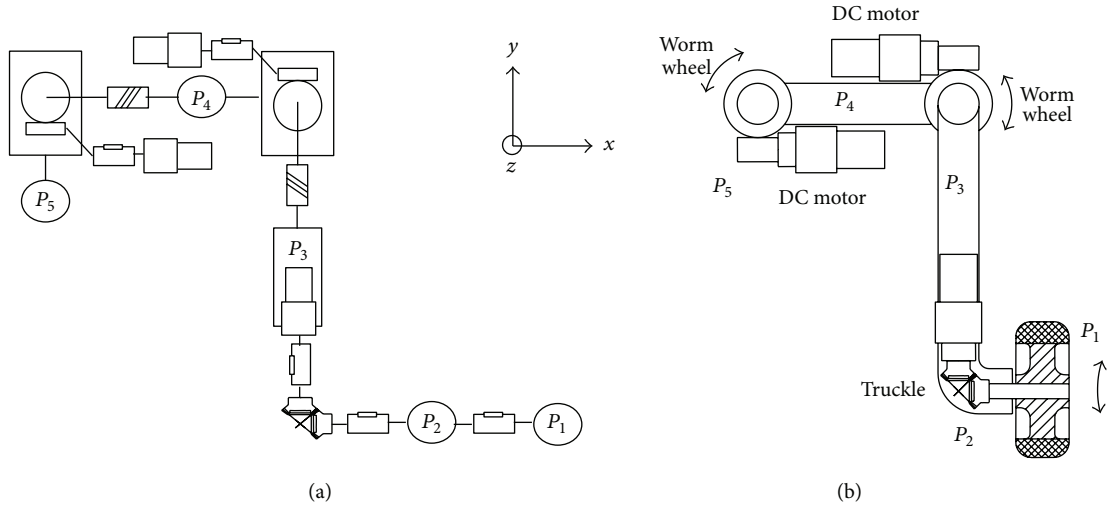

Figure 5: A robot leg configuration.

functions, such as the motion state of the thigh, the motion state of the shin, or the additional mechanism to realize the robot motion. In doing so, a set of phrases and relations are established to describe additional functions. For example, rotate thigh, move hip, rotate foot wheel, drive CJ-motor, and so forth. These phrases can describe the function of a robot and realize the requirements of robot motion. Thus, the function concepts of robot are obtained. And they have the corresponding port functional semantic attributes, as shown in Table 5.

To effectively realize the function of the robot leg, according to design requirements, we will transversally extend total function of the robot leg into several function modules. They form a port-based ontology structure in which each function is described by using different ontology concepts, such as "verb +noun" drawn from design requirements [20].

Different function concepts are represented on the basis of "verb + noun" phrases. Some relationships should be extracted, such as is_a, part_whole, has_function, and has_feature [13]. At present, we have only collected the function taxonomy of robot leg. Four types of relationships are described in Table 6. The number of concepts depends on the users' requirements and the definition of concepts. The standard worksheets have been developed to easily acquire port ontology and lexicon. At the same time, they can automatically upload the required data into the Protégé editor [18], which is one of the most widely used ontology editors. Protégé provides a visual tool for port ontology editing, including concept, taxonomy, and relationship building along with ontology visualization.

Figure 5 presents the process of clustering concepts into a configuration of the robot leg. It calculates the correlations between the matched concepts of terms to determine the connection of two concepts. For a set of concepts, a concept is highly correlated with others if it is less distant from them, that is, semantically closer, or contains more words that match the specific terms, that is, are lexically closer [7]. At the same time, component generation depends on the function taxonomy. Figure 5(a) gives different weight scores and their concept similarity measures results corresponding to robot leg configuration which contains 6 function concepts, 18 function terms, and 9 components for clustering robot leg. Figure 5(b) presents the structure of robot assembly. Table 7 gives different function concepts corresponding to the primitive connectors, attributes, and port types as part of the functional semantic description after the designers

Table 6: Classification of the relationships.

Relationships	Concepts	Definitions	Examples
Is_a	Key link, connector	Relationships between parent and son or special and general	Is_a (key link, connector)
Part_whole	Thigh, robot leg	Relationships between part and whole	Part_whole (thigh, robot leg)
Has_function	CG, foot wheel	Refer to the connection between two ontology concepts	Has_function (CG, foot wheel)
Has_feature	Worm wheel, worm	Physical attributes or geometric attributes	Has_feature (worm, worm wheel)

Table 7: Measure between two function concepts.

Function concepts	Primitive connectors	Causality	Attributes	Port types
Transform motion/realize rotation	Key link	EC, SC	Surface contact	Mechanical port
Drive wrist joint motion/realize rotation	WJ-motor, CG, key link	CC, EC	Line contact, surface contact	Mechanical port
Drive knee joint motion/move shin	WG2, shaft coupling, key link, KJ-motor	CC, BC, EC	Line contact, surface contact	Mechanical port
Move thigh/drive coxa joint motion	WG1, shaft coupling, key link, CJ-motor	CC, BC, EC	Line contact, surface contact	Mechanical port

have made use of effective semantic inference. The causality indicates that they include cause connection, equal connection, share connection, and bind connection for two function concepts.

7. Concluding Remarks

This paper describes port-based ontology modeling for robot leg concepts, determines port types, and extends port attributes in a hierarchy. One of the main goals of the research was to clarify the relationship of component ontology concepts associated with functionality, that is, is_a relation, part_whole relation, and has_function relation. Although the functional decomposition trees can be used to represent the scheme design, the approach often leads to combinational explosion. In this paper, the semantic similarity approach is applied to port-based ontology and specified by users to enable the system to generate various function modules. Port-based ontology may be used in the conceptual design of the electromechanical system by providing the function module; that is, it can quantitatively realize semantic measures and effectively build function modules. Function concepts and corresponding terms are related to design requirement descriptions. However, further research needs to consider the following.

(i) To get the correct results of semantic measures, the accuracy of function concept description and port-based ontology information retrieval are very important. In most cases, the number of components, function concepts, and terms is not completely corresponding to each other, and they exist in one-to-many or many-to-one relationships. Axiomatic design should be adopted to clarify these relationships.

(ii) The paper only focuses on a simple robot leg conceptual design; however, actually it is more complicated about conceptual design of a complex product, and it needs to build some fit modules through using effective clustering algorithm. It is worth further investigating in the future.

(iii) Each designer has different functional semantic description for the same product; perhaps they obtain a different function ontology concept and further generate the other alternatives. This depends on designers' backgrounds, educations, and preferences. Therefore, we will focus on them in the future.

Acknowledgments

This research is sponsored by the National Nature Science Foundation of China (NSFC) under Grant no. 50775065 and no. 51275152 and Nature Science Foundation of Hebei Province under Grants E2008000102 and E2013202123.

References

[1] V. Liang and C. J. J. Paredis, "A port ontology for conceptual design of systems," *Journal of Computing and Information Science in Engineering*, vol. 4, no. 3, pp. 206–217, 2004.

[2] P. Singh and B. Bettig, "Port-compatibility and connectability based assembly design," *Journal of Computing and Information Science in Engineering*, vol. 4, no. 3, pp. 197–205, 2004.

[3] P. C. Breedveld, "Port-based modeling of dynamic systems in terms of bond graphs," in *Proceeding of the 5th Vienna on Mathematical Modeling*, Vienna, Austria, February 2006.

[4] M. I. Campbell, J. Cagan, and K. Kotovsky, "Agent-based synthesis of electromechanical design configurations," *Journal of Mechanical Design*, vol. 122, no. 1, pp. 61–69, 2000.

[5] I. Horváth, K. Dorozsmai, and V. Thernesz, "A feature-object-based practical methodology for integration of conceptual and morphological design," in *Proceedings of the Lancaster International Workshop on Engineering Design (CACD '94)*, pp. 131–149, Lancaster University EDC, Lancaster University, 1994.

[6] M. Ozawa, M. R. Cutkosky, and B. J. Howley, "Model sharing among agents in a concurrent product development team," in *Proceedings of the Workshop on Knowledge Intensive CAD, KIC-3, IFIP5. 2 Working Group*, Tokyo, Japan, 1998.

[7] Z. Li, V. Raskin, and K. Ramani, "Developing engineering ontology for information retrieval," *Journal of Computing and Information Science in Engineering*, vol. 8, no. 1, pp. 1–13, 2008.

[8] R. B. Stone and K. L. Wood, "Development of a functional basis for design," *Journal of Mechanical Design*, vol. 122, no. 4, pp. 359–370, 2000.

[9] C. F. Kirschman and G. M. Fadel, "Classifying functions for mechanical design," *Journal of Mechanical Design*, vol. 120, no. 3, pp. 475–490, 1998.

[10] J. De Kleer, "How circuits work," *Artificial Intelligence*, vol. 24, no. 1–3, pp. 205–280, 1984.

[11] Y. Kitamura, T. Sano, K. Namba, and R. Mizoguchi, "A functional concept ontology and its application to automatic identification of functional structures," *Advanced Engineering Informatics*, vol. 16, no. 2, pp. 145–163, 2002.

[12] C. J. J. Paredis, A. Diaz-Calderon, R. Sinha, and P. K. Khosla, "Composable models for simulation-based design," *Engineering with Computers*, vol. 17, no. 2, pp. 112–128, 2001.

[13] D. Cao, K. Ramani, M. Wang Fu, and R. Zhang, "Port-based ontology semantic similarities for module concept creation," in *Proceedings of the ASME International Design Engineering Technical Conferences and Computers and Information in Engineering Conference (IDETC/CIE '09)*, pp. 141–150, San Diego, Calif, USA, September 2009.

[14] D. Cao, W. Feng, P. Qu, and C. Yu, "Port-based ontology modeling for robot leg configuration design," in *Proceedings of the 10th International Conference on Frontiers of Design and Manufacturing*, Chongqing, China, June 2012.

[15] D. Cao, Y. Gu, M. W. Fu, and H. Jia, "Port-based ontology modeling for product conceptual design," in *Proceedings of the ASME International Design Engineering Technical Conferences and Computers and Information in Engineering Conference (IDETC/CIE '08)*, pp. 163–172, New York, NY, USA, August 2008.

[16] J. B. Dahmus, J. P. Gonzalez-Zugasti, and K. N. Otto, "Modular product architecture," *Design Studies*, vol. 22, no. 5, pp. 409–424, 2001.

[17] U. Roy, N. Pramanik, R. Sudarsan, R. D. Sriram, and K. W. Lyons, "Function-to-form mapping: model, representation and applications in design synthesis," *CAD Computer Aided Design*, vol. 33, no. 10, pp. 699–719, 2001.

[18] S. C. J. Lim, Y. Liu, and W. B. Lee, "Product analysis and variants derivation based on a semantically annotated product family ontology," in *Proceedings of the ASME International Design Engineering Technical Conferences and Computers and Information in Engineering Conference (DETC '09)*, pp. 817–826, San Diego, Calif, USA, September 2009.

[19] E. Bozsak, M. Ehrig, S. Handschuh et al., "KAON-Towards a large scale semantic web," in *Proceedings of the 3rd International Conference on E-Commerce and Web Technologies*, K. Bauknecht, A. Mintjoa, and G. Quirchmayr, Eds., pp. 304–313, Springer, Heidelberg, Germany, 2002.

[20] Z. Wu and M. Palmer, "Verb semantics and lexical selection," in *Proceedings of the 32nd Annual Meeting of the Associations for Computational Linguistics (ACL '94)*, pp. 133–138, Las Cruces, New Mexico, 1994.

Hindawi Publishing Corporation
Advances in Mechanical Engineering
Volume 2013, Article ID 531714, 11 pages
http://dx.doi.org/10.1155/2013/531714

Review Article

Ecodesigning with CAD Features: Analysis and Proposals

Raoudha Gaha,[1] Abdelmajid Benamara,[1] and Bernard Yannou[2]

[1] *Laboratoire Genie Mecanique, Ecole Nationale Ingenieurs Monastir, Universite Monastir, rue Ibn Aljazzar, 5019 Monastir, Tunisia*
[2] *Laboratoire Genie Industriel, Ecole Centrale Paris, Grande Voie des Vignes, 92290 Chatenay-Malabry, France*

Correspondence should be addressed to Raoudha Gaha; raoudha.gaha@gmail.com

Received 17 March 2013; Revised 17 September 2013; Accepted 25 October 2013

Academic Editor: Dongxing Cao

The integration of environmental aspects in design frameworks has become a necessity for manufacturers to maintain their market position. This is especially true in the Computer Aided Design (CAD) phase, which is the last phase in the design process. At this stage, more than 80% of choices have been made. However, the environmental impacts generated by the remaining choices are significant. Features Technology (FT), the core of the CAD phase, is used to integrate environmental aspects. This paper presents a literature review of different works based on FT to ecodesign products. First, we present an overview of features in CAD systems. Second, we present a critical review of works done on ecodesigning with features that we divide into two subsections: the first one concerns CAD-Life Cycle Assessment (LCA) integration (methodologies, prototype tools, and commercial tools), and the second one, works using FT in CAD phase to reduce the environmental impact of one life cycle stage such as material selection or manufacturing. Finally, we propose an approach based on FT for ecodesigning products to promote simple new ecodesign tools which will help the inexperienced designer.

1. Introduction

In the earlier stages of design process, the reduction of Environmental Impacts (EIs) was the purpose of much research. This was due to the increasing demand for eco-friendly products. The amount of data provided by Computer Aided Design (CAD) systems enables a complete Life Cycle Assessment (LCA). Features technology (FT) provides the necessary data to realize a life cycle inventory (LCI), which is the second stage of an LCA according to ISO 14040. We propose a model to integrate CAD and LCA systems based on features. The objective is to extract data and provide an environmental evaluation which would be comprehensible to a designer; the model should deal with different possible scenarios and show the optimal solution. A number of steps are necessary to attempt this: necessary data for LCI must be extracted (raw material, manufacturing process possible, transportation, use, and end-of-life scenarios); possible scenarios need to be evaluated; the designer must be shown the influence of his/her choices in real time; the optimal scenario must be selected. That is why the integration between CAD/LCA tools has greatly evolved. There are tools for real-time evaluation such as solidworks sustainability [1], in which the designer can visualize the impact of his/her choices till features attribution. But several gaps and problems persist. In this research, firstly, we present an overview of features in CAD systems. Secondly, we review related studies done on ecodesigning with features in CAD phase. Finally, we propose an approach based on FT in order to present an environmental assistance to the CAD designer.

2. Overview of Features

The evolution of CAD systems has allowed nongeometric information to be integrated in a purely geometrical model (e.g., engineering constraints, tolerances, or material) through high technological entities (features) that have been introduced in most current CAD systems. Shah and Mantyla [2] present needs and advantages of features over geometric models. They configure features as objects that represent the designer's intent; this intention is maintained during the different phases of product development. According to Bidarra and Bronsvoort, modeling features compared to conventional geometric modeling enables the combination of functional and engineering information on the form in a product model [3]. For Ghodous, this FT facilitates the integration between

different phases of product development such as design and manufacturing [4]. With the features approach, the geometrical objects are formed by an assembly of simple elements, such as a chamfer in a mechanical part. The final geometric form of the part results from the application of a sequence of features configured and integrated into the 3D model.

2.1. Features Definitions. Different definitions have been proposed for features. For Wilson and Pratt, features present a field of interest in a product model [5]. In Smith and Dagli's work, features are defined as high-level design primitives with their attributes, their qualifiers, and restrictions which affect the functionality and/or the ability for the product to be manufactured; that is, they can describe the shape (size and dimensions), precision (tolerances and finish), or material (type, properties, and processing) and vary with the product and the manufacturing process [6]. In the design field, according to Shah and Mathew, features are the elements used in generation, analysis, and evaluation of a product model [7]. In manufacturing, Salomons defines a feature as product data, related to functional specifications, manufacturing processes, or physical design properties [8]. In design and manufacturing, Pratt and Bedford consider shape features as elements conforming to rules that enable their recognition and classification [9].

2.2. Types of Features. Different types of features have been elaborated: Shape Features Constraint Features, Precision Features (or tolerance), Assembly Features, Functional Features (sets of features related to specific functions which may include information on design intent, nongeometric parameters related to function or performance, etc.), Material Features, and Primitive Features.

2.3. Features Representation. Most research on the geometric representation of features shape is oriented to volume representation (3D), in combination with surface representation. For example, we can cite the representation based on Boundary Representation (B-REP), and on Constructive Solid Geometry (CSG), as well as hybrid representation as shown in Wang and Ozsoy [10].

2.4. Techniques of Features Creation. Several techniques have been developed for the creation of models based on features. These techniques are divided into two main approaches according to Allada and Anand [11] and Shah and Mantyla [2].

(i) Features recognition: features are recognized from a geometric model applying rules of recognition. More features models, describing the same product, can therefore be derived.

(ii) Design features: a product model is developed based on predefined features. In this case, a product's explicit geometry is created from the features model.

In order to obtain a feature-based model, feature recognition and feature-based design are the two main approaches used. To evaluate a part environmentally, nongeometric data has to be attached to the designed object. However, the recognition approach causes the loss of all nongeometric data, which can be provided with feature-based design approach. Hence, the interest is oriented to the latter approach for ecodesigning products in the detail design phase.

3. Ecodesigning with CAD Features: State of the Art

In order to help companies design "green" and sustainable products, it is necessary to implement integration between CAD tools and sustainable methods, both of which are related to the product Life Cycle. Such digital integration allows the Ecodesign process to be supported in the early stages of product development. Retrieving part of the information available from the CAD system (e.g., volume, geometry, material, and the energy needed to form the part) is necessary to realize an environmental evaluation. FT—also called "green feature" by Xin et al. [12], has been successful due to its high level of representation and modeling capabilities. In this section, we present how FT can be used to develop new Ecodesign tools (CAD/LCA integrated tools) covering the Environmental Evaluation (EE) of all life cycle stages. We then show how it can be used on CAD phase to reduce EIs of a stage such as material selection or a green manufacturing process. Figure 1 presents the two essential categories of research on the topic "Ecodesign with CAD features": CAD-LCA integration and Ecodesigning one life cycle stage. Each category is divided into three subcategories.

3.1. CAD/LCA Integrated Tools and Methodologies Based on Feature Technology. Bonvoisin and Thiede describe a part, in CAD systems, as a 3D model, composed of a set of features which describe the part's geometry. It is used for the realization of a process plan which is defined by a set of operations. An operation is a treatment unit of one or many features by a machine. A feature can be realized by one or many operations [13]. Mäntylä et al. show that features are generally expected to form a basis for linking CAD with downstream manufacturing applications and for organizing databases for design data [14]. As described in ISO 14040, an LCA requires several iterations between goal scope definitions, inventoryanalysis, and impact analysis [15]. Hence, Life Cycle Inventory (LCI) is strongly linked to CAD features, essentially in retrieving necessary data. Figure 2 presents a simplified model for the Life Cycle Inventory Analysis (LCIA) phase. FT, then, is the core of most CAD/LCA integrations whether methodologies, tool prototypes, or realized tools. We have chosen to focus primarily on studies that help us establish our approach.

3.1.1. Methodologies Based on Features for CAD/LCA Integration. Data exchange is an important step in the integration. For this reason, data extraction, data transfer, and data exchange are initially the most important tasks resolved by research such as Otto et al. [16, 17]. Otto presents a framework, where a data transfer between the two systems is

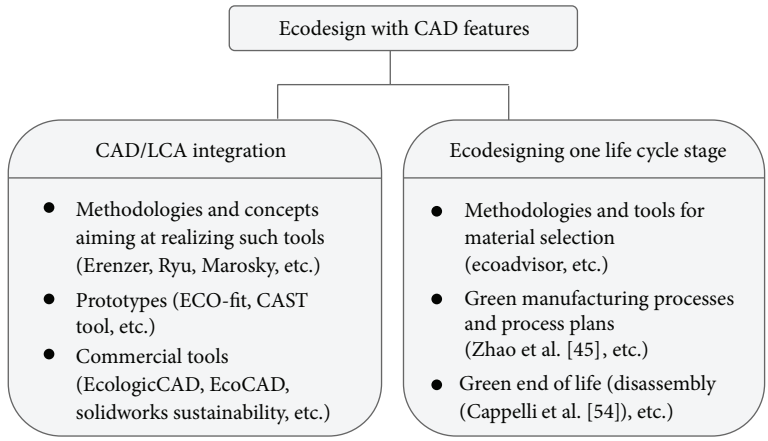

Figure 1: Essential axis in the topic "Ecodesign with CAD features".

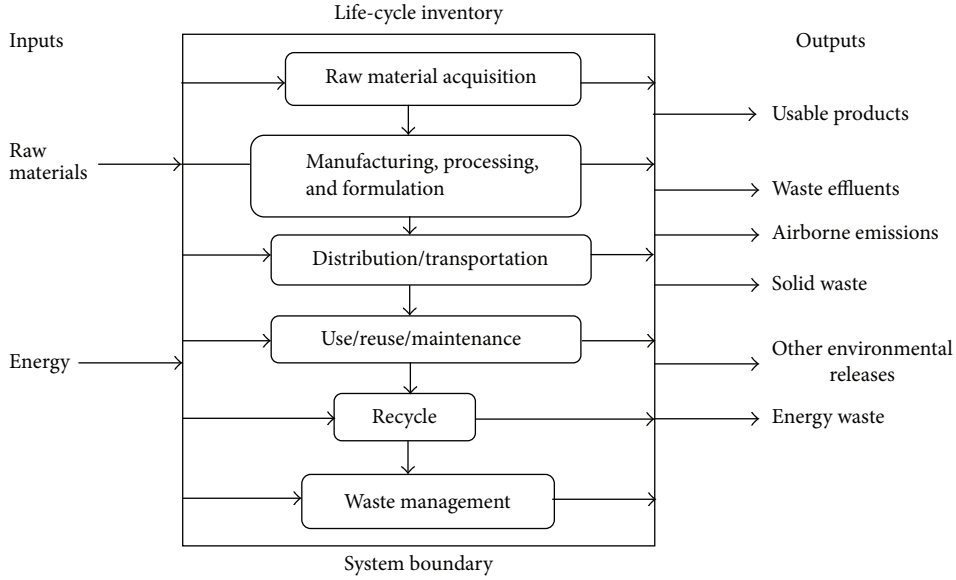

Figure 2: LCIA proposed framework by SETAC [18].

performed. The LCA required data is extracted from a geometric model based on features.

Within the approach taken, efficient access to the LCI-relevant data is realized by using a search index in order to extract the necessary features for practicing an LCA. FT supports data migration in order to identify input-output entities in the conceptual design phase [19] and in the detailed design phase [20].

The data provided by features can be divided into explicit information, which is related to part geometry, and implicit information, which is related to part process [16, 21, 22]. Success is obtained when data extraction and migration between two different types of software are carried out; thus for a digital tool, data exchange is necessary. Marosky [22] explores these works and presents a structure of an algorithm that allows mutual data transfer between CAD (SolidEdge) and LCA tool (SimaPro). This transfer is based on extracting data from a product CAD model which consists of assemblies, subassemblies, parts, and features. The objective is to evaluate the environmental impact of a component as well as the whole product. In a previous paper [23], we proposed a simple ecodesign tool by integrating CAD and LCA. Geometric characteristics of a CAD model were analyzed to estimate their environmental influences during all the phases of a product life cycle. The tool consists of a special geometric data base containing the impacts of all existing design technical solutions of a product; critical geometric features and forms concerning environmental impact are identified, after which designers can select the optimal solution in terms of feasibility and ecology. However, when it is a case of a new product, the designer may encounter problems using this tool (Chui and Chu [24]). The data extracted from CAD systems represents an LCA model; this model helps us to approximate the environmental impact of a virtual product. Although a model for a complete LCA has yet to be developed, we can cite Yangl who presents a new Rapid Life Cycle Assessment (RLCA) model based on features [25], in which corresponding design parameters of a product concept are indentified based on

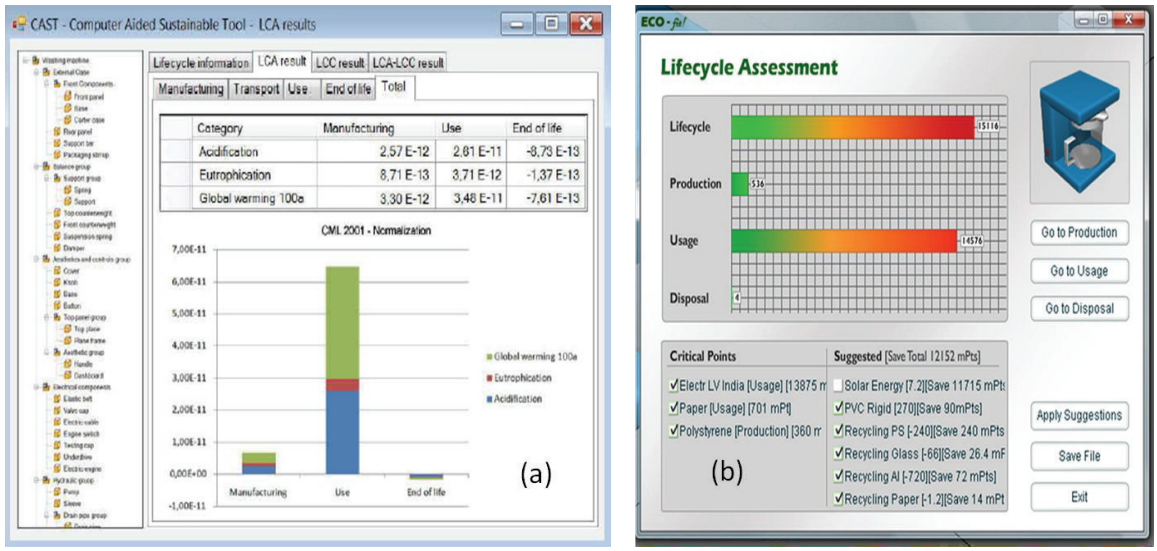

(a) (b)

Figure 3: Screenshots of "CAST Tool" (a) and "ecofit" (b) the proposed CAD-LCA software prototypes [26, 27].

the mapping relationship between "green features" and conceptual design information. "Green features" is a group of green design information covering the entire lifecycle of products [12]. Green features are characterized by green attributes, and different green features have different attributes. For example, a material feature has such attributes as material type and material quantity; a manufacturing feature has such attributes as manufacturing energy consumption and manufacturing emissions.

The lack of common format between CAD and LCA systems has been resolved thanks to FT. However, all methods consider a CAD geometric representation as a collection of data to assess the environmental impact of one life cycle scenario. We note that presenting alternative scenarios and their impacts is still to be developed. However in reality, a part can be realized in different ways. Also, it is necessary to provide a digital real tool to be used in industries. For example, we found prototype tools for CAD-LCA integration where features, extracted from CAD systems, are the core of an LCA model. In the following section we present these prototypes.

3.1.2. Prototype Tools Based on Features for CAD/LCA Integration. Realizing a CAD/LCA integrated tool is an aim of researchers to help nonexpert designers to ecodesign products in terms of the environment. In the literature, we have identified prototypes of tools based on the extraction of CAD data from features in order to evaluate environmental impacts of products, such as the "DEMONSTRATOR" developed by Mathieux et al. [28]. This prototype tool binds CATIA (a CAD software) and EIME (an LCA software). CATIA is connected to a Product Life Management (PLM) system that extracts all data provided by different used features. The established system then selects necessary LCA data and transfers them to EIME to calculate and show the environmental impact. Following Jain [27], we deduce that the use of the integration between PLM and CAD systems is useful to develop our approach. Jain presents a plugin (Eco-fit) designed for 3DS-max using the Eco-indicator99 (EI99), an ecoassessment methodology and database designed to evaluate CAD-based products. A screenshot of this tool appears in Figure 3. There is also "EcoCAD" presented by Cappelli et al. [29], which is based on the analysis of the tree structure of a CAD project composed of assemblies, subassemblies, parts, and features. The lack of these prototypes is their dependence on tools used in the authentication of their proposed methodologies. Like the module implemented in SolidEge, Abad-Kelly et al. [30] also connected Solidworks (CAD) and SimaPro (LCA) using macros. Computer aided sustainable tool "CAST Tool" presented by Morbidoni et al. [26] tried to overcome this gap by providing a prototype with an open access database, allowing products to be evaluated regardless of the CAD or LCA systems used (cf. screenshot Figure 3). This work is compared essentially to the sustainability module of the commercial tool "Solidworks Sustainability" [1]. Benefits are essentially due to selecting more than one production process, introducing lifecycle scenarios and extracting the right amount of geometrical and nongeometrical data from the CAD data structure and PLM databases. "CAST Tool" overcomes many weaknesses such as the single scenario introduced where the evaluation of different possible scenarios is available. However, the evaluation is postmodeling that is realized on a final part where modifications are difficult to implement, especially when it is a complex part. This explains the need for a real-time evaluation tool. A real CAD-LCA integrated tool is also needed. In the following section, some of the existing commercial tools are presented.

3.1.3. Tools Based on Features for CAD/LCA Integration. Commercial CAD-LCA integrated tools are essentially based on data exchange between the two different systems

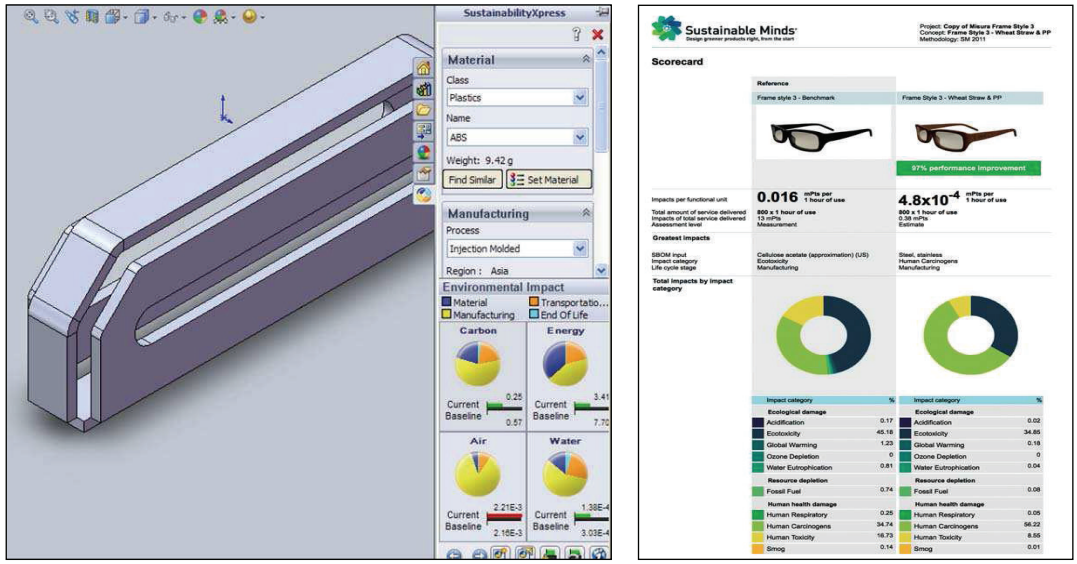

(a) (b)

Figure 4: Screenshots of "solidworks sustainability" (a) [1] and "sustainable minds" (b) [31]: the CAD-LCA commercial software tools.

(CAD and LCA). Output data from the CAD system represents the input data for the LCA system. This data is essentially information provided from different types of features attributed by the designer. "EcologiCAD" is one CAD-LCA integrated tool which aims at the environmental evaluation of virtual product prototypes. It is developed by Leibrecht [32]. It is based on a client-server concept, where the information model represents the server. The information model also provides functionality to further applications via an application programmable interface (API). "SolidWorks Sustainability 2010" [1], developed by Dassault Systems, allows environmental assessment in real time once a feature has been attributed. It evaluates the environmental impacts associated with the material and manufacturing selections chosen by the designer and is most applicable for detailed design, as complete dimensions and tolerances are required for the simulation. Hence, to estimate the potential ecological footprint for another product with the same design requirements, it is necessary to provide a new full-scale CAD model.

Sustainable minds provide a smooth Graphical User Interface (GUI). Its advantage relative to the other software is having the ability to see tradeoffs between different designs of a product. It can be used at all stages of Conceptual Design, based on the extracted information from attributed features. The outputs are in equivalent CO_2 emission or the commonly used North American single-figure process values for impact assessment [31]. This may be incomprehensible for nonenvironmental expert designers. It is thus necessary to provide a translation of such outputs into the designer field knowledge. In Figure 4, we present screenshots of "Solidworks Sustainability" and "Sustainable Minds."

3.2. Feature Technology for a Single Green Life Cycle Stage. Several studies have been undertaken to assist the designer in the CAD stage in predicting and reducing the environmental impact of a product life cycle stage (material or machining process selection; adopting an environmentally conscious process plan; or promoting disassembly to facilitate recycling or reuse).

3.2.1. Material Selection. The first stage of a product life cycle is material selection. Attention focuses on reducing extracted resources; using recyclable materials and many other precautions can be taken in this step. Abdalla and Ebeid divide material selection into two phases, material quantity and material type. Material quantity is dedicated to conserving environmental resources where designers try to minimize the amount of materials used in manufacturing the product [33]. The amount of material of a part is determined by summing different attributed geometric features. Taking into account environmental aspects till the design phase implies optimizing the volume of the designed shape, as well as selecting the most ecological and adequate material. Hence, the objects of this design phase are resources use reduction, for example, by choosing recyclable materials. For this, software tools such as "Eco-Audit" have been developed. This tool is mostly relevant for detailed design. The advantages of this software are that it is possible to explore alternative options relatively easily in the design stages, and it can apply to 19 material processes. Granta Design [34] and Autodesk Inventor CAD software are integrated. In the same way, Granta Design developed "Eco Materials Advisor" where it is possible to propose similar alternative materials. CES selector is also a software package developed by Granta Design and Cambridge University [35]. It is a material and process selection software using a systemic procedure based on design constrains (constraint features). A screenshot of this tool is presented in Figure 5.

3.2.2. Environmentally Conscious Transport. The geometry of a product has an influence on its transport phase [36], because

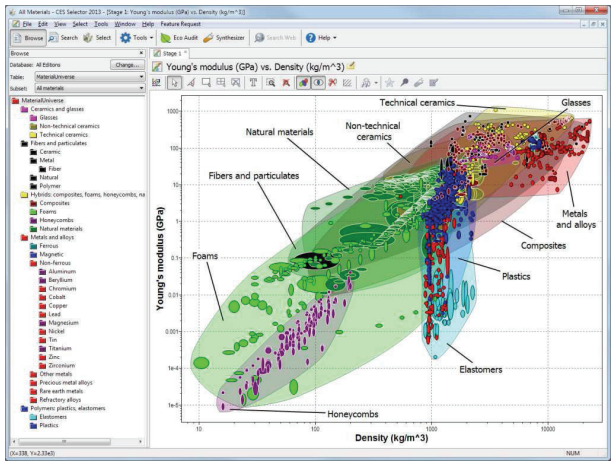

Figure 5: Screenshot of granta design tool "CES selector."

to calculate transport impacts it is necessary to introduce two essential parameters: a product weight and volume box. Weight and volume boxes are being reduced, especially when many products are being transported. For example, for an old geometric model a transported quantity is "X" and for an ecodesigned geometric model (box volume and weight reduced) the product quantity transported is "$a * X$" where ($a > 1$). Relating the environmental impact of this phase to part geometry is clearly an area for future research.

3.2.3. Environmentally Conscious Manufacturing Process. A feature is a local shape of a product directly related to the manufacturing process. It is used to reduce the environmental impact of the different parameters in the production phase. The majority of studies found in the literature takes into account the following three axes: evaluation of process EIs; selection of green process planning from different alternatives; and selection of green process parameters such as cutting fluid or machining tool. The integration of CAD and Computer Aided Process Planning (CAPP) is successful in generating different possible process plans in real time and their EIs. Moreover, it is possible to select the most appropriate machining tool with low EIs and also the optimum scenario. These benefits are possible thanks to features models that provide the necessary data for an LCI. We present below the most important works that guided us.

(1) Evaluation of EIs of a Process Plan and Selecting the Greenest One. The evaluation of manufacturing environmental impacts is present in much research. It is oriented to reducing or avoiding processes which have an impact on ecosystems, human health, and so forth. Sheng et al. [37], Munoz and Sheng [38], and Sheng and Srinivasan [39] analyze, in their respective work, the environmental impact of dissimilar waste streams. They apply a scoring system which evaluates factors such as toxicity, carcenogenesis, irritation, flammability, and reactivity, reducing complexity of processing alternatives through a feature-based approach. A hierarchical part planning strategy for environmentally conscious machining is developed [39], and it is shown that a feature can be machined with different scenarios. The purpose is to choose the least impact set of machining sequences. Figure 6 shows the example considered by Sheng to demonstrate the influence of changing the order of machining sequences on environmental impacts of a production process. However, machining a part can be realized feature by feature or by set of features. In [37] Sheng et al. decompose the environmental impact component into "micro" analyses of individual features [40] and "macro" analyses of feature interactions [41]. To evaluate the resources and environment attributes of a/manufacturing process, Zhang et al. [42] present an Input-Process-Output (IPO) model and an evaluation index system based on a scatter degree combination evaluation method to solve the inconsistency produced by different evaluation methods in order to select the greenest process plan. This task presents the core of several works.

More than the evaluation of EIs, features are useful for selecting green process planning, such as the multiobjective optimization decision-making framework model of process planning for green manufacturing established by Cao et al. [43] to put forward a new process planning strategy for green manufacturing and to develop a process planning software tool. In 2006, Tan et al. [44] developed a new production process which determines a method focusing on sustainable manufacturing. It is based on case-based reasoning, expert systems, and FT for designing a new component's process flow. A sustainable development assessment is the basis of this process flow.

Cao and Tan methods developed for green CAPP selection have to be developed in order to be used as a numerical methods integrated in CAD systems. Zhao et al. [45] also propose a method for environmentally conscious process planning. The method begins with an existing process plan and then identifies impactful process steps and associated design features, in terms of manufacturing cost and environmental impact. Alternative processes that can achieve these features are then considered to generate alternative process plans. This might be useful to integrate into CAD-LCA integrated systems to help a designer compare different alternatives till features attribution. Nawata and Aoyama [46] propose a new life-cycle design system specifically applicable to machined parts. The system automatically generates life-cycle assessment (LCA) feedback for the design process through the effective linkage of life-cycle inventory data with computer-aided design/computer-aided manufacturing (CAD/CAM) data by feature-based modeling. Hence, the important deduction that can be retained from CAD/CAM/CAPP integration is allowing the generation of different possible alternative machining scenarios.

Each scenario has environmental impacts related to the parameters of the process plan attributed. FT, in CAD phase, can help the designer select, from possible alternatives, the greenest process.

(2) Selection of Green Process Parameters. Manufacturing process planning is based on a set of parameters such as cutting tool, cutting fluid, or machining tool. Tan et al. [47] used FT in selecting the most ecological cutting fluid and machining tool because they are important parameters in developing

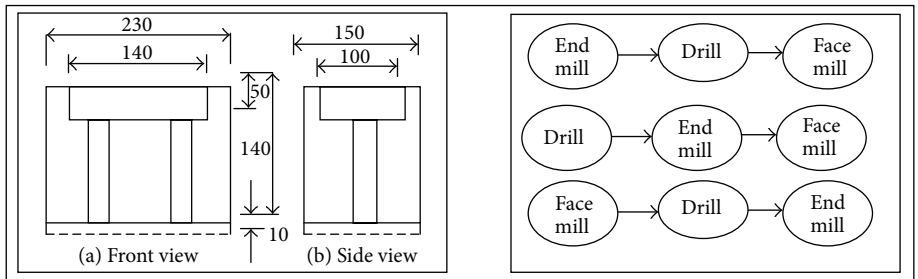

Sequence	1	2	3
Energy (MJ)	4.7	5.5	4.8
Weighted mass	15.3	16.4	14.4
Process time (min)	12.1	10.2	13

Figure 6: Influence of machining sequences order on the EIs of a part consisting of three types of features: a pocket, a hole, and a finished planar face [39].

green products. In a similar vein, the selection of an ecological machine tool is the aim of Jiang and Zhang's study [48], where they develop the model called Vector Projection Method. This method, based on FT, creates a reference index system to justify machine tool selection, by considering resource consumption and environmental impact due to part features which needs an energy input/expenditure (electric mechanic, pneumatic, etc.) to be realized. Estimating the required energy and optimizing it presents a challenge for green manufacture. Possible production energy consumption scenarios in a feature level are studied by Deshpande et al. [49] and assessed through MTConnect standard methodology. Other process parameters, such as finish cut and feed rate, generate EIs due to their relation to the part quality. Helu et al. [50], using FT, develop a methodology showing that the impact of green machining strategies such as part quality on achieved surface quality is most influenced by the finish cut(s) and feed rate. Improving part quality can also reduce life cycle EIs.

CAD and CAPP integrations are able to provide more Life Cycle scenarios for the part in a real time. It is therefore necessary to integrate these benefits into CAD-LCA integrated tools to realize environmental evaluation in real time and also choose the greenest process plan from existing possible scenarios. These contributions can be accompanied by a green end of life with promotion of design phase disassembly and recyclability.

3.2.4. Design for Green End of Life. For many products, the End of Life (EoL) phase is the worst phase in terms of sustainability. In the last decade, much research has focused on minimizing the environmental impact of this phase till the design process. FT is used in the CAD phase to select an optimal product structure from the design alternatives corresponding to lower assembly/disassembly costs, while complying with specified recycling and recovering rates. It also chooses a small set of parts to be disassembled to meet with the green directives and suggests an economical disassembly process (Chu et al. [51]). Zhang and Kuo [52] develop a graph-based heuristic approach to generate a disassembly tree in order to undertake the disassembly analysis and study the product structure and disassembly, ensuring the recording of the physical properties of components such as weight and volume. Güngör [53] proposes a method which is applicable to the detail design phase. The importance of connectors between different geometric features attributed in Design for Disassembly (DfD) is indicated. These features are evaluated with an Analytic Network Process (ANP) method.

Optimizing the disassembly sequence of mechanical systems is very useful in order to improve maintenance and recycling activities (i.e., to reduce costs, times, and number of operations). A new virtual disassembly environment, based on two different algorithms, is presented by Cappelli et al. [54] by using features such as those shown in Figure 7. Takao and Niall [55] with their support system design consider the recycling from its start point. It reduces the amount of waste at the EoL over time reduction disassembly. Abu Bakar and Rahimifard present a Computer-Aided Recycling Process Planning for EoL Electrical and Electronic Equipment [56].

4. Proposed Approach for Ecodesigning with CAD Features

Resulting from this literature review, Figure 8 shows a summary of ecodesign works on CAD phase based on FT. Ecodesign could focus on one life cycle stage or take into account all life cycle stages. A framework of the four most important benefits found in the state of the art above based on FT is shown in Figure 8. This framework has served in our previous work to develop a new methodology based on FT to integrate CAD-LCA systems [57]. This methodology considers benefits extracted above from the literature review presented. However the methodology presented requires development. Figure 9 represents a model of a new Ecodesign tool applying

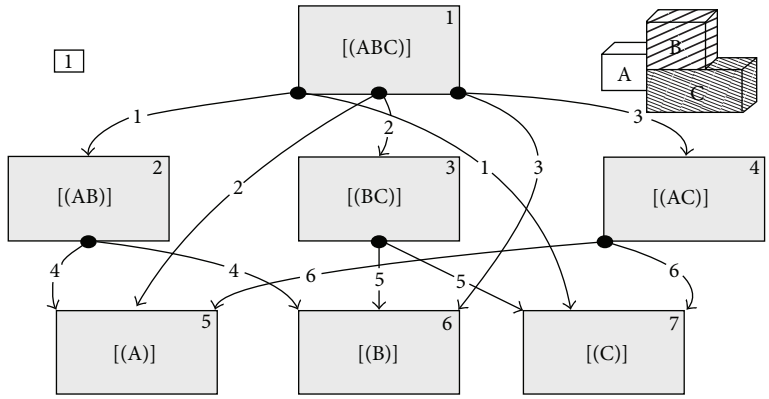

Figure 7: Possible scenarios of disassembly sequences [56].

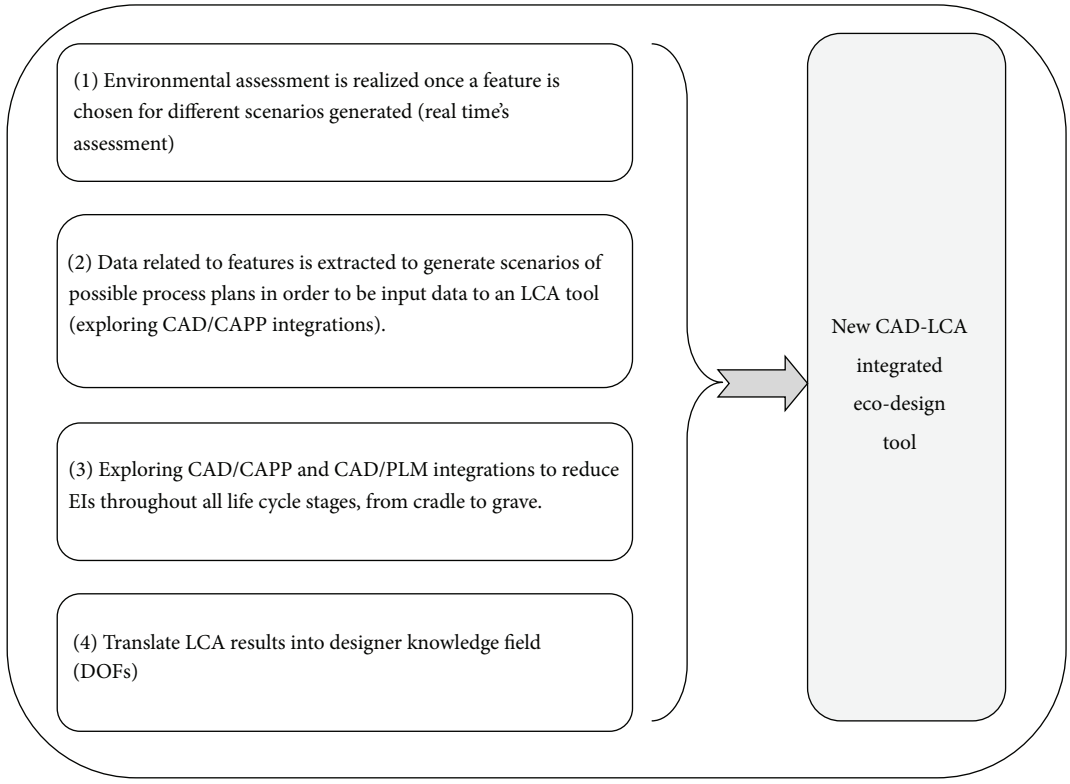

Figure 8: Benefits framework of FT in ecodesign.

the approach proposed above. It is composed of a connector which collects necessary data for an LCA tool from CAD, CAM, CAPP, and PLM systems. Once the environmental evaluation is completed, graphical representation is shown to the designer. The graphic allows, at the user interface, the optimal scenario to be selected from those proposed. The necessity of reducing products' EIs has led researchers to develop new ecodesign tools in order to help designers choose the ecological solutions in CAD phase where Degrees of Freedom (DoFs) in the acting zone are limited [58].

The data transfer of the majority of CAD-LCA integrated tools and methodologies, found in the literature, is based on FT. This technology has been used in generating scenarios in CAPP and for the choice of optimal scenarios/solutions in terms of cost. Based on functionalities offered by FT and CAD/PLM integrations, we propose a new Ecodesign framework. Exploring this approach, a new Ecodesign tool, "Green-CAD," with two interesting features will be developed. First, this tool can extract features data in order to generate scenarios of possible process plans. These scenarios represent input data to a tool (exploring CAD/CAPP integrations).

Second, an environmental assessment can be undertaken once a feature is chosen for different generated scenarios (real time EE which is based on exploring CAD/CAPP and CAD/PLM integrations to reduce EI throughout all life cycle stages from cradle to grave).

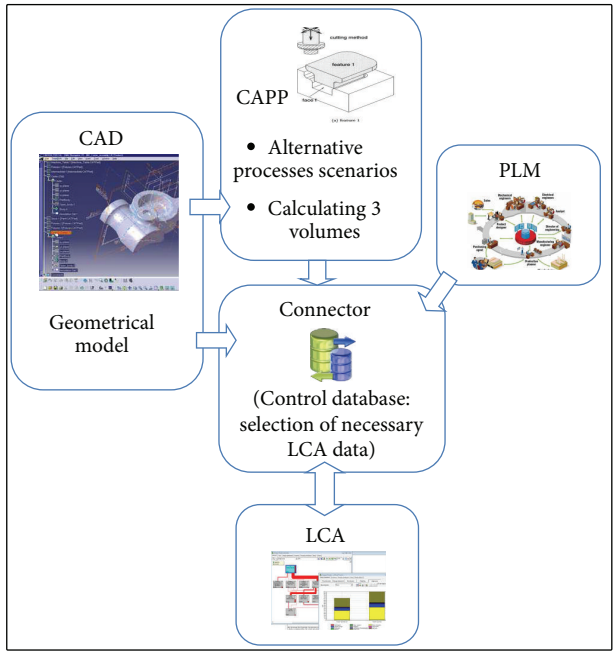

Figure 9: Framework of a new ecodesign tool with CAD/CAPP/PLM integration.

5. Conclusion

Despite the number of studies that explore CAD features for ecodesigning products at each stage of the product design process, industries do not yet efficiently integrate environmental aspects in design processes. Through our literature review and research observations, it appears that digital tools are needed to help nonexpert environmental designers. The latter needs to include environmental aspects of their virtual prototypes in the CAD phase by promoting the environmental impacts reduction in all product life cycle stages, from cradle-to-gate till the features attribution. We have presented a framework that might help resolve some difficulties that currently prevent product designers from systematically integrating environmental considerations in their activities. This framework links benefits acquired in different life cycle stages in reducing environmental impacts. It is based on FT and requires the development of more efficient CAD-LCA integrated tools (material selection, environmentally conscious process plan, energy consumption, disassembly, etc.).

In our future research work, a comprehensive model of the interactions and information flows between CAD systems and LCA software will be established, and the model will be developed into a prototype tool that will be tested through a case study.

References

[1] DS, Dassault Systems, "SolidWorks Sustainability," http://www.solidworks.com/sustainability/.

[2] J. J. Shah and M. Mantyla, *Parametric and Feature Based CAD/CAM: Concepts, Techniques, and Applications*, John Wiley & Sons, New York, NY, USA, 1995.

[3] R. Bidarra and W. F. Bronsvoort, "Semantic feature modelling," *Computer-Aided Design*, vol. 32, no. 3, pp. 201–225, 2000.

[4] P. Ghodous, "Modélisation intégrée de données de produit et de processus de conception," Tech. Rep., Université Claude Bernard, Lyon, France, 1996.

[5] P. R. Wilson and M. J. Pratt, "A taxonomy of form features for solid modeling," in *Geometric Modeling for CAD Applications*, pp. 125–135, Elsevier Science, North Holland, The Netherlands, 1988.

[6] A. E. Smith and C. H. Dagli, "Manufacturing feature identification for intelligent design," in *Intelligent Systems in Design and Manufacturing*, pp. 213–230, ASME Press, Boston, Mass, USA, 1995.

[7] J. J. Shah and A. Mathew, "Experimental investigation of the step form-feature information model," *Computer-Aided Design*, vol. 23, no. 4, pp. 282–296, 1991.

[8] O. W. Salomons, "Computer support in the design of mechanical products: constraint specification and satisfaction in feature based design for manufacturing," University of Twente: Enschede, The Netherlands, 2000.

[9] M. J. Pratt and M. K. Bedford, "Aspects of form feature modeling," in *Geometric Modeling: Methods and Applications*, Computer Graphics—Systems and Applications, pp. 227–250, Springer, Berlin, Germany, 1991.

[10] N. Wang and T. M. Ozsoy, "A scheme to represent features, dimensions, and tolerances in geometric modeling," *Journal of Manufacturing Systems*, vol. 10, no. 3, pp. 233–240, 1991.

[11] V. Allada and S. Anand, "Feature-based modelling approaches for integrated manufacturing: state-of-theart survey and future research directions," *International Journal of Computer Integrated Manufacturing*, vol. 8, no. 6, pp. 411–440, 1995.

[12] L.-l. Xin, X.-J. Jia, F.-Y. Fang, X.-W. Wang, and X.-X. Chen, "Green feature modeling for mechanical and electrical product conceptual design," *Computer Integrated Manufacturing Systems*, vol. 18, no. 4, pp. 713–718, 2012.

[13] J. Bonvoisin and S. Thiede, "Vers une estimation de l'énergie de fabrication d'un produit dès sa conception," in *13ème Colloque National AIP-PRIMECA-Démarche et Innovation dans la Conception et la Production des Systèmes Intégrés*, March 2012.

[14] M. Mäntylä, D. Nau, and J. Shah, "Challenges in feature-based manufacturing research," *Communications of the ACM*, vol. 39, no. 2, pp. 77–85, 1996.

[15] "Environmental management—life cycle assessment—principles and framework," ISO 14040:2006, 2006.

[16] H. E. Otto, K. G. Mueller, and F. Kimura, "A framework for structured data retrieval in LCA using feature technology," in *Proceedings of the 2nd International Symposium on Environmentally Conscious Design and Inverse Manufacturing (EcoDesign '01)*, pp. 250–255, Tokyo, Japan, December 2001.

[17] H. Otto, F. Mandorli, M. Germani, and F. Kimura, "Integration of solid modeling with LCA using feature technology: an application for SME," in *Proceedings of the International Symposium on Environmentally Conscious Design and Inverse Manufacturing (EcoDesign '03)*, Tokyo, Japan, December 2003.

[18] I. Sridhar, "Materials selection for green design," in *Environmentally Conscious Mechanical Design*, pp. 319–350, Wiley, Hoboken, NJ, USA, 2007.

[19] M. Ernzer and H. Birkhofer, "From product ideas to sustainable products—life cycle design suitable for product designer," in *Proceedings of the Engineering Design Conference (EDC '02)*, pp. 647–656, Kings College London, London, UK, July 2002.

[20] M. Germani, F. Mandorli, and H. E. Otto, "CAD—LCA data migration supported by feature technology and attributed structures," in *Proceedings of the Global Conference on Sustainable Product Development and Life Cycle Engineering*, pp. 379–384, 2004.

[21] J. Ryu, I. Kim, E. Kwon, and T. Hur, "Simplified life cycle assessment for eco-design," in *Proceedings of the 3rd International Symposium on Environmentally Conscious Design and Inverse Manufacturing (EcoDesign '03)*, pp. 8459–463, Tokyo, Japan, December 2003.

[22] N. Marosky, "Challenges of data transfer between CAD and LCA software tools," in *Proceedings of the 3rd International Conference on Life Cycle Management*, University of Zurich, Irchel, Switzerland, August 2007.

[23] R. Gaha, A. Benamara, and B. Yannou, "Influence of geometrical characteristics on eco-designed products," in *Proceedings of the International Conference on Innovative Methods in Product Design*, pp. 242–247, Venice, Italy, June 2011.

[24] M.-C. Chiu and C.-H. Chu, "Review of sustainable product design from life cycle perspectives," *International Journal of Precision Engineering and Manufacturing*, vol. 13, no. 7, pp. 1259–1272, 2012.

[25] X. Yang, F. Li, X. Wang, and L. Wang, "A green-feature based LCA backtracking mechanism," in *proceedings of the Electronics Goes Green (EGG '12)*, pp. 1–6, Berlin, Germany, september 2012.

[26] A. Morbidoni, C. Favi, and M. Germani, "CAD-integrated LCA tool: comparison with dedicated LCA software and guidelines for the improvement," in *Glocalized Solutions for Sustainability in Manufacturing*, pp. 569–574, Springer, Berlin, Germany, 2011.

[27] P. Jain, *Design of an interactive eco-assessment GUI tool for computer aided product design [Ph.D. thesis]*, Indian Institute of Technology, Kharagpur, India, 2009.

[28] F. Mathieux, L. Roucoules, L. Lescuyer, and Y. Bouzidi, "Opportunities and challenges for connecting environmental assessment tools and cad software," in *Proceedings of the 2nd International Conference on Life Cycle Management*, Barcelona, Spain, Septembre 2005.

[29] F. Cappelli, P. Citti, M. Delogu, and M. Pierini, "Strumento informatico integrato in ambiente cad per l'analisi preventiva degli impatti ambientali dei processi/prodotti in fase di produzione," in *36a Convegno Nazionale AIAS*, Ischia, Italy, September 2007.

[30] J. Abad-Kelly, D. Cebrián, and V. Chulvi, "An ontology-based approach to integrating life cycle analysis and computer aided design," in *Proceedings of the 12th International Congress on Project Engineering*, pp. 161–172, Zaragoza, Spain, July 2008.

[31] Sustainable Minds LLC, "Connecting ecodesign with LCA for a new generation of greener products," 2010, http://www.sustainableminds.com/ecodesign-and-lca.

[32] S. Leibrecht, "Fundamental principles for CAD-based ecological assessments," *International Journal of Life Cycle Assessment*, vol. 10, no. 6, pp. 436–444, 2005.

[33] H. S. Abdalla and M. A. Ebeid, "A holistic approach for sustainable product design," in *Global Product Development*, pp. 329–338, Springer, Berlin, Germany, 2011.

[34] http://www.grantadesign.com/education/edupack2009.htm.

[35] M. F. Ashby, *Materials Selection in Mechanical Design*, Elsevier, Amsterdam, The Netherlands, 3rd edition, 2005.

[36] R. Gaha, A. Benamara, and B. Yannou, "Eco-conception et CAO paramétrique," in *Colloque des Sciences de la Conception et de l'Innovation*, Sousse, Tunisie, Juillet 2010.

[37] P. Sheng, M. Srinivasan, and S. Kobayashi, "Multi-objective process planning in environmentally conscious manufacturing: a feature-based approach," *CIRP Annals—Manufacturing Technology*, vol. 44, no. 1, pp. 433–437, 1995.

[38] A. A. Munoz and P. Sheng, "An analytical approach for determining the environmental impact of machining processes," *Journal of Materials Processing Technology*, vol. 53, no. 3–4, pp. 736–758, 1995.

[39] P. Sheng and M. Srinivasan, "Hierarchical part planning strategy for environmentally conscious machining," *CIRP Annals—Manufacturing Technology*, vol. 45, no. 1, pp. 455–460, 1996.

[40] M. Srinivasan and P. Sheng, "Feature-based process planning for environmentally conscious machining—part 1: microplanning," *Robotics and Computer-Integrated Manufacturing*, vol. 15, no. 3, pp. 257–270, 1999.

[41] M. Srinivasan and P. Sheng, "Feature based process planning in environmentally conscious machining—part 2: macroplanning," *Robotics and Computer-Integrated Manufacturing*, vol. 15, no. 3, pp. 271–281, 1999.

[42] H. Zhang, X. Zhang, and Y. Wang, "The evaluation of resources and environment attributes of manufacturing process based on scatter degree combination evaluation method," *Applied Mechanics and Materials*, vol. 37, pp. 1466–1472, 2010.

[43] H.-J. Cao, F. Liu, Y. He, and H. Zhang, "Study on model set based process planning strategy for green manufacturing," *Computer Integrated Manufacturing Systems*, vol. 8, no. 12, pp. 978–982, 2002.

[44] X. Tan, F. Liu, D. Liu, L. Zheng, H. Wang, and Y. Zhang, "Improved methods for process routing in enterprise production processes in terms of sustainable development II," *Tsinghua Science and Technology*, vol. 11, no. 6, pp. 693–700, 2006.

[45] F. Zhao, V. R. Murray, K. Ramani, and J. W. Sutherland, "Toward the development of process plans with reduced environmental impacts," *Frontiers of Mechanical Engineering*, vol. 7, no. 3, pp. 231–246, 2012.

[46] S. Nawata and T. Aoyama, "Life-cycle design system for machined parts-linkage of LCI data to CAD/CAM data," in *Proceedings of the 2nd International Symposium on Environmentally Conscious Design and Inverse Manufacturing (EcoDesign '01)*, Tokyo, Japan, December 2001.

[47] X. C. Tan, F. Liu, H. J. Cao, and H. Zhang, "A decision-making framework model of cutting fluid selection for green manufacturing and a case study," *Journal of Materials Processing Technology*, vol. 129, no. 1–3, pp. 467–470, 2002.

[48] Z. Jiang and H. Zhang, "A vector projection method to evaluating machine tool alternatives for green manufacturing," in *Proceedings of the International Technology and Innovation Conference (ITIC '06)*, pp. 640–643, Hangzhou, China, November 2006.

[49] A. Deshpande, J. Snyder, and D. Scherrer, "Feature level energy assessments for discrete part manufacturing," in *Proceedings of the 39th Annual North American Manufacturing Research Conference (NAMRC '11)*, pp. 190–197, Corvallis, Ore, USA, June 2011.

[50] M. Helu, B. Behmann, H. Meier, D. Dornfeld, G. Lanza, and V. Schulze, "Impact of green machining strategies on achieved surface quality," *CIRP Annals—Manufacturing Technology*, vol. 61, no. 1, pp. 55–58, 2012.

[51] C.-H. Chu, Y.-P. Luh, T.-C. Li, and H. Chen, "Economical green product design based on simplified computer-aided product structure variation," *Computers in Industry*, vol. 60, no. 7, pp. 485–500, 2009.

[52] H. C. Zhang and T. C. Kuo, "Graph-based approach to disassembly model for end-of-life product recycling," in *Proceedings of the 19th (IEEE/CPMT) International Electronics Manufacturing Technology Symposium (IEMT '96)*, pp. 247–254, Austin, Tex, USA, October 1996.

[53] A. Güngör, "Evaluation of connection types in design for disassembly (DFD) using analytic network process," *Computers and Industrial Engineering*, vol. 50, no. 1–2, pp. 35–54, 2006.

[54] F. Cappelli, M. Delogu, M. Pierini, and F. Schiavone, "Design for disassembly: a methodology for identifying the optimal disassembly sequence," *Journal of Engineering Design*, vol. 18, no. 6, pp. 563–575, 2007.

[55] B. Takao and M. Niall, "An ecological design support tool for recyclability," Tech. Rep., Industrial Electronics and Systems, Mitsubishi Laboratory, 1999.

[56] M. S. Abu Bakar and S. Rahimifard, "Computer-aided recycling process planning for end-of-life electrical and electronic equipment," *Proceedings of the Institution of Mechanical Engineers, Part B*, vol. 221, no. 8, pp. 1369–1374, 2007.

[57] R. Gaha, A. Benamara, and B. Yannou, "A feature-based methodology for eco-designing parts on detail phase," in *Design and Modeling of Mechanical Systems*, pp. 645–654, Springer, Berlin, Germany, 2013.

[58] R. Gaha, A. Benamara, and B. Yannou, "Eco-design of a basin mixer in geometric modeling phase," *Key Engineering Materials*, vol. 572, pp. 7–11, 2014.

Hindawi Publishing Corporation
Advances in Mechanical Engineering
Volume 2013, Article ID 318173, 11 pages
http://dx.doi.org/10.1155/2013/318173

Research Article

Physical Realizations: Transforming into Physical Embodiments of Concepts in the Design of Mechanical Movements

Ying-Chieh Liu[1] and Amaresh Chakrabarti[2]

[1] *Department of Industrial Design, Chang Gung University, Taoyuan 333, Taiwan*
[2] *Centre for Product Design and Manufacturing, Indian Institute of Science, Bangalore 560012, India*

Correspondence should be addressed to Ying-Chieh Liu; ycl30@mail.cgu.edu.tw

Received 8 May 2013; Revised 10 October 2013; Accepted 12 October 2013

Academic Editor: Dongxing Cao

Conceptual design involves identification of required functions of the intended design, generation of concepts to fulfill these functions, and evaluation of these concepts to select the most promising ones for further development. The focus of this paper is the second phase—concept generation, in which a challenge has been to develop possible physical embodiments to offer designers for exploration and evaluation. This paper investigates the issue of how to transform and thus synthesise possible generic physical embodiments and reports an implemented method that could automatically generate these embodiments. In this paper, a method is proposed to transform a variety of possible initial solutions to a design problem into a set of physical solutions that are described in terms of abstraction of mechanical movements. The underlying principle of this method is to make it possible to link common attributes between a specific abstract representation and its possible physical objects. For a given input, this method can produce a set of concepts in terms of their generic physical embodiments. The method can be used to support designers to start with a given input-output function and systematically search for physical objects for design consideration in terms of simplified functional, spatial, and mechanical movement requirements.

1. Introduction

Conceptual design is the process of exploring promising concepts (e.g., sketches); this often starts with reasoning about design from a functional point of view and involves a series of transformations with increasing detail. In general, there are three phases in conceptual design [1], namely, (1) *function analysis*—to develop and describe the functions required, (2) *concept generation*—to generate possible physical concepts from required functions, and (3) *concept evaluation*—to evaluate these concepts so as to select the most promising ones.

In the second phase of conceptual design, generating a range of physical concepts is seen by many as a challenging task [2]. Also, developing a method that generates these concepts is widely accepted as a principal issue to be resolved for improving current engineering design synthesis [3]. From the literature, methods proposed for generation of physical concepts include the following.

(i) Morphological Charts. A morphological chart, as used in design research, is a matrix where columns present different functional requirements of a design and rows represent alternative working principles that can fulfill each function. Each combination with a working principle from each column represents a concept. After identifying the functional requirements, one or more working principles are found for every function required. These principles are then combined using a morphological chart in order to meet all the functions; principal researchers include Hundal and Langholtz [4], Roozenburg and Eekels [5], Cross [6], and Pahl et al. [7]. A limitation of this method is that there is little guidance for how to transform these working principles into physical descriptions of the device (i.e., physical concepts). Moreover,

whether working principles can be combined or not is implicitly decided by designers.

(ii) Catalogue of Elements. To solve the problem of generating physical concepts from required functions, one possible way is to develop a catalogue of building blocks (i.e., elements commonly found in designs). These elements with their function are first identified and listed for use by designers, for example, see Kota and Chiou [8] and Li et al. [9], who developed two levels of building blocks—motion and physical. Physical building blocks describe a set of physical artefacts that embody the motion building blocks. The link between requirements and their physical building blocks is explicitly described in a matrix. Roth [10, 11] developed a more elaborate, multiple-level solution representation to provide guidance from abstract function structures, through physical embodiments, to detailed designs. However, as to how these elements are combined is still dependent on designers' intuition. A similar work developed into a computational framework is reported by Han and Lee [12].

(iii) Catalogue of Solutions. This provides a list of existing solutions for a given requirement. Researchers such as Murakami and Nakajima [13] and Gu et al. [14] proposed computerized methods for retrieving mechanism concepts. Mechanism concepts and their kinematic behaviour are first analyzed and stored in a library, along with additional information such as motion type. To retrieve mechanism concepts, designers specify the required behaviour in a time history of input and output and/or motion type. However, this method is limited to retrieving complete mechanism concepts rather than generating them by combining building blocks. The usefulness of this approach heavily relies on how extensive the catalogue of mechanisms is. One problem with this approach is that the granularity of building blocks is coarse; therefore, it lacks flexibility in providing as wide a range of concepts as would be possible if the building blocks underlying the designs stored in the catalogue were considered.

This paper investigates the issue of how to transform and thus synthesise possible physical concepts and proposes an implemented method for automated physical synthesis. This research extends earlier research on a *functional synthesis* approach that produces a wide variety of abstract concepts to mechanical design problems, which involve transmission and conversion of mechanical forces and motions [15]. For a given design problem, this approach can produce an exhaustive set of concepts in terms of their spatial configurations. These are then offered to designers for exploration. This approach has been tested by means of case studies and hands-on experiments involving experienced designers [15]. It was found that the number and variety of solutions generated by using this approach were always larger than those of the designers. This demonstrated its potential for enhancing designers' chances of developing promising concepts. However, these experiments also revealed a problem with the approach: the representation of solutions was too abstract to adequately visualise their potential embodiments. To tackle this problem, this paper proposes a method of transformation—to develop generic physical embodiments for abstract functional representations of solutions.

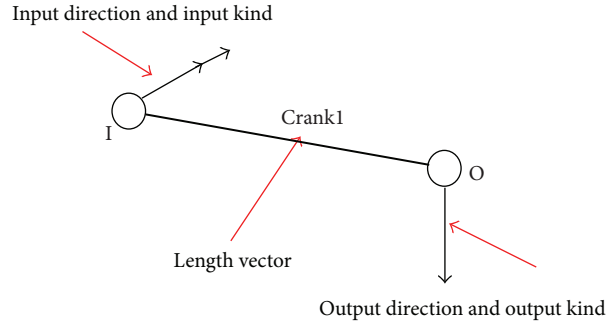

Figure 1: The definition of a spatial element.

2. Method

To start off the method, spatial elements, in this research, are taken as the input to the process; these spatial elements are expressed as the directional and spatial aspects of existing embodiments at a specific time-instant. A spatial element has five parts: input kind (force or torque), input direction (restricted to $i+$, $j+$, $k+$, $i-$, $j-$, or $k-$ directions), length vector, output kind, and output direction [16], as shown in Figure 1. The input or output direction is related to the directional aspect of existing embodiments, while the length vector is related to the spatial aspect. The length vector (called the pin part) is defined as a vector with a qualitative distance from the input point to the output point (each described as a dot part in Figure 1) and is assigned as a vector parallel to the i, j, or k orientation. However, in many cases, the real vector (from the input point to the output point) of existing embodiments is not parallel to the i, j, or k direction. The input and output points are related to the contacting areas of existing embodiments and are defined as the centre points of the areas connected to the subsequent elements, such as the centre of a circle, a square, and a line. Further details upon the definition of spatial element can be seen in previous research [16].

Before presenting the reasoning method by which a spatial element can be linked to possible physical objects that can embody it, three terms, function, behaviour, and structure, are defined.

(i) Function. It is taken here as the intended behaviour and is viewed as an intended transformation between a set of input-output characteristics. These characteristics are (1) number, (2) kind, (3) direction, (4) magnitude, (5) position, and (6) motion. Take a door latch design as an example. The handle output is a rotation (i.e., the characteristic of motion) with direction in a skew way (i.e., the characteristic of direction), and the latch output is a translation (i.e., the characteristic of motion) to enable disengagement of the latch from the doorframe with input-output relative position. It requires a generation of design solutions taking the torque (i.e., the characteristic of kind) input of the handle and producing a (i.e., the characteristic of number) force output.

(ii) Structure. It is defined as a component or an assembly of components that describes geometric aspects of an object. Component is an individual geometric entity, such as a rod, a pin, a spring, or a shaft.

(iii) Behaviour. It is defined as what a designed system or an object actually does within the motional aspects of the I-O characteristics.

A spatial element has limited information on what the structure of its physical object can be. Therefore, it is necessary to explore the link between spatial and physical descriptions of objects. One possible way is to apply various input motions to a structure, resulting in the creation of various or similar behaviours. By analysing the structure and its behaviour, the possible functions of the structure could be decided. By considering the representation of existing structures, it should be possible to abstract them into the spatial element level. Comparing these transformed objects at the spatial element level with the database of spatial elements, it would be possible to find physical objects for each database spatial element.

Note that behaviour, in the reasoning process, provides the linkage between function and its possible structures, and these structures are then abstracted to the spatial element level. A method based on these Structure-Behaviour-Function (S-B-F) links, as well as on abstracting the level of structures, is thereby built in this work.

To summarize, in order to obtain the input and output point, the contacting area of the physical object is specified, thereby defining its input and output point. To obtain the input and output kind, the physical object is analyzed by means of its S-B-F link. To obtain the length vector, the vector pointing from the input point to the output point is first identified and thus abstracted into the closest among the length vectors parallel to the i, j, or k direction. Figure 2 is a summary of the procedure by which possible physical objects to embody a spatial element can be derived by understanding the structure-behaviour-function relationships of many objects, and abstracting these objects into the spatial element level.

To elaborate the proposed method of transforming a spatial element into its physical embodiments, three steps are proposed: (1) develop the relationships between each spatial element and its possible physical objects, (2) develop rules for ensuring interface compatibility between any two connecting elements, and (3) develop reasoning procedures to replace each abstract spatial configuration with all its possible generic physical embodiments to complete the task of transforming a spatial configuration into geometric configurations (physical embodiments). Using this method, alternative generic physical embodiments for a spatial configuration can be generated.

2.1. Establishing Relationships between Each Spatial Element and Its Physical Objects

2.1.1. Generic Physical Elements and Physical Objects. For transformation of a spatial element into its physical objects, there are two questions to be answered: (1) what are the possible forms representing the pin part of the spatial element, (see Figure 3)? (2) what are the possible interfaces representing the dot parts?

To answer Question 1, two generic attributes are identified from the structural aspects of the spatial element.

(i) Form. This is the abstract geometric representation of an object and is the main attribute that transfers or transforms motions within itself. There are different geometric forms, such as plate, semi disk, block, and rod.

(ii) Support Interface. This provides support that interacts with the structure's environment and sometimes contains the geometric coordinate of the object, such as the centre of a circle. Common support interfaces are revolute pairs (turning pairs), prismatic pairs, screw pairs, cylindrical pairs, spherical pairs, and planar pairs.

To answer Question 2, one generic attribute is defined.

(iii) Motion Interface. This constitutes areas through which objects contact each other in order to transfer motion. This attribute provides interactions between two connecting objects. There are at least two areas in each object: the input and output areas. The types of the motion interface considered are *traction*, *tooth*, *groove*, *plane*, or *hinge*. (Traction is the surface made rough. Tooth is the surface made of teeth and may be straight, helical, double helical, or others. Groove is the surface composed of a negative (such as a heart-shaped groove or slot) and a positive (such as a pin-like bar) part. Plane is the surface made of a plane or a curved surface which is perpendicular, or otherwise to x, y, or z axis. Hinge is the surface made of a negative (such as a hole-shaped cylinder) and a positive (such as a pin) part.)

If we analyze the structural aspect of a spur gear, the form is *plate*, the support interface is a *revolute pair*, and the motion interface is the meshing of the gear *teeth*. The interface of any two objects is similar to what Reuleaux (1963) called a "kinematic pair." Generic physical elements representing a spatial element have a generic representation composed of form, support interface, and motion interface. Each element represents many physical (standard) objects. For example, an element composed of a plate as the generic form, tooth as the motion interface, and a revolute pair as the support interface generically represents all sorts of gears. The relationship between generic physical elements and physical objects is shown in Figure 3. In Figure 3, the first line represents a generic physical element, which is composed of a generic form, support interface, and motion interface. Each physical object consists of its generic physical element added to its specific descriptors. Take a generic physical element with a plate as the form, a tooth as the motion interface, and a revolute pair as the support interface. If its descriptors are circle, spur tooth, and bearing, respectively, the standard object is a spur gear. If we change the form descriptor to a rectangle and the remaining parts are the same, the resulting standard object is a rectangular spur gear.

After linking each spatial element to its physical objects, these physical objects can be further classified into generic physical elements. The procedure for classifying standard objects into generic physical elements is to remove form,

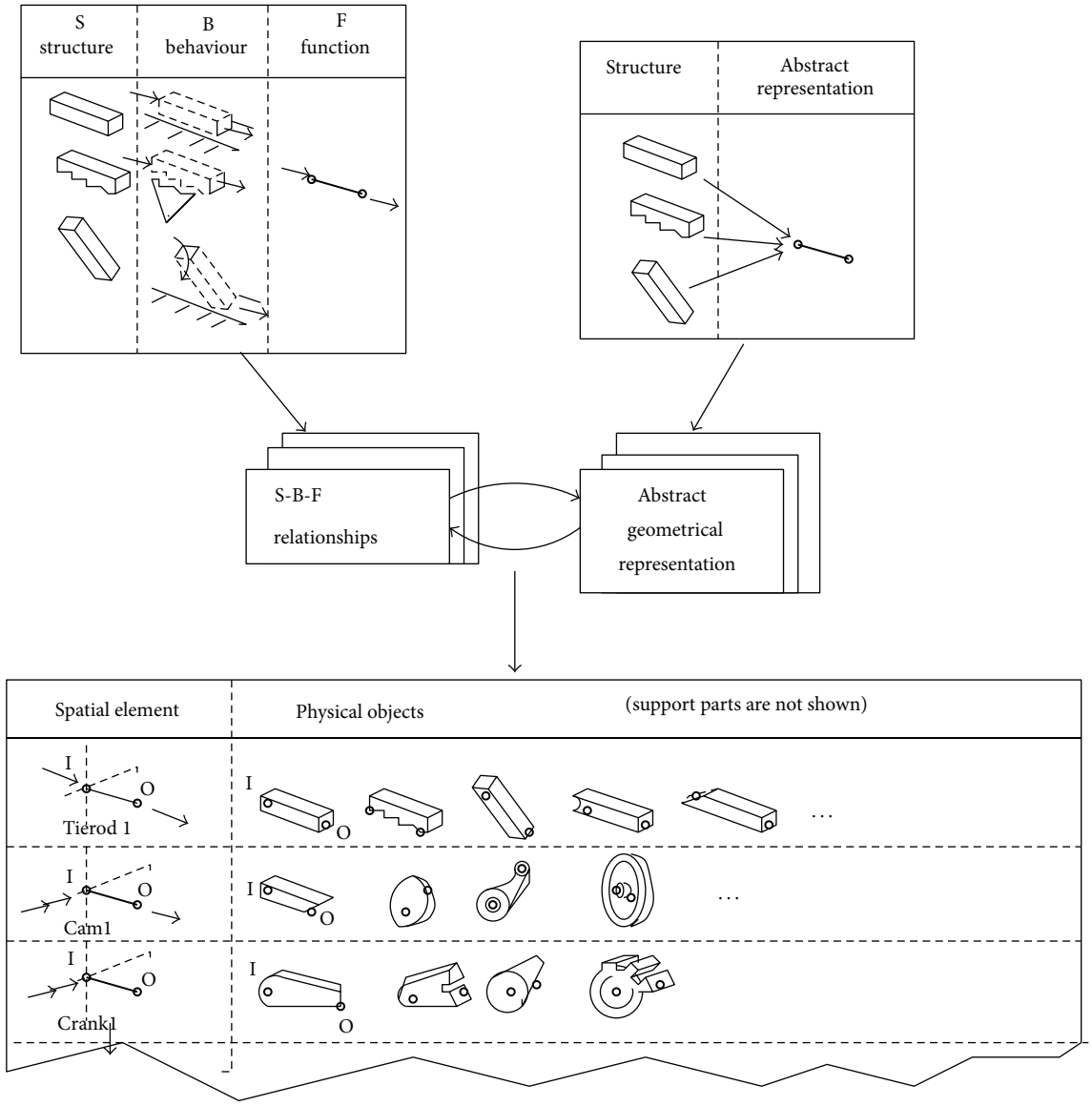

Figure 2: A method based on the Structure-Behavior-Function (S-B-F) links, between standard objects and their spatial elements.

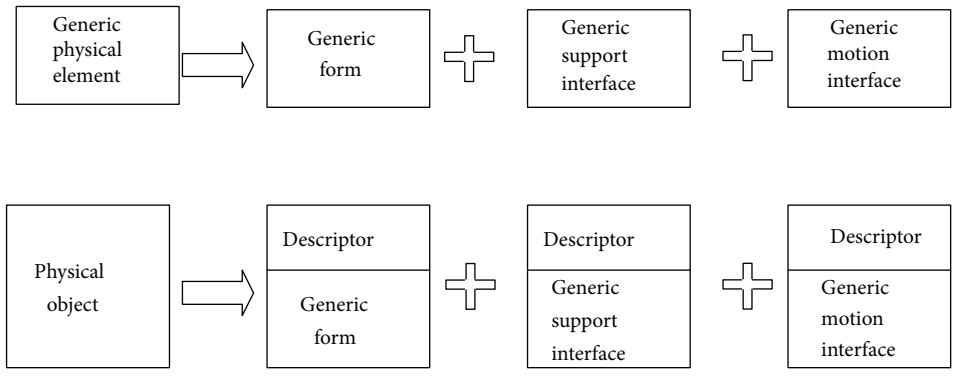

Figure 3: Representations of generic physical elements and physical objects.

support interface, and motion interface specific descriptors from each standard object.

2.2. Ensuring Interface Compatibility. When transforming into its physical embodiments, it has to be ensured that any solution composed of more than one spatial element has compatibility between its connecting elements. Both structural and behavioural aspects of generic physical elements contribute to the issue of compatibility. Analysis of these two aspects reveals that compatibility contains (1) *configuration compatibility* and (2) *motion interface compatibility*.

Configuration compatibility is that the space taken by one individual element cannot be occupied by the other. However, each element in our method is qualitatively represented, and the coordinates and dimensions of the object are not quantified. Therefore, it is supposed that any two connecting elements are located and dimensioned so as to meet configuration compatibility.

As far as the motion interface compatibility between two components is concerned, three important attributes need to be considered.

(i) Contact Normal Vector. The common denominator of the contacting situations is that the normal vectors of two contacting surfaces are coincident, with the exception of a point contact where the normal vector of the contacting point can be defined with any possible direction in space. In this research, a contacting vector is restricted to be oriented along $i+$, $j+$, $k+$, $i-$, $j-$, or $k-$ direction. However, in some realistic situations, the contacting vectors are not along one of these directions. For these situations, their normal vectors are approximated to be along $i+$, $j+$, $k+$, $i-$, $j-$, or $k-$ direction. Examples of contact normal vectors are shown later.

(ii) Contact Motion. The connection of two connecting objects permits a certain kind of motion. The motion of two connecting objects dictates the interface. For example, if the motion of the contacting surfaces of two objects is the same, their interface can be a *fixed* interface. However, if the motion of the contacting surface of one object is not always the same as that of the other, the connection must allow relative motion. The contacting area of two contacting surfaces in general is therefore defined to be either *fixed* or *changeable*.

(iii) Contact Type. The type of interface of the contacting area of two objects must match. Contact type describes the form of the contacting area of two objects, such as *plane*, *traction*, *tooth*, *hinge,* or *groove*.

To summarise, each contacting area has three attributes: contact *normal* vector, contact *motion*, and contact *type*. Examples of various interfaces are shown in Figure 4. In Figure 4(a), the contact normal vector, motion, and form of a rack are specified as $j+$ (even though the real contact normal vector is not in $j+$), changeable, and tooth. In Figure 4(b), the contact normal vector, motion, and form of the bevel gear are specified as $j+$ (again, even though the real contact normal vector is not in $j+$), changeable, and tooth. The contact normal vector, motion, and form of the brush wheel are $j+$, changeable and traction, as shown in Figure 4(c). The contact normal vector, motion, and form of the shaft are $i-$, fixed, and plane, as shown in Figure 4(d). In Figure 4(e), the contact normal vector, motion, and form of a groove cam are $k+$ (even though the real contact normal vector is not exactly in $k+$). And finally, in Figure 4(f), the contact normal vector, motion, and form of a rod are $i-$, changeable, and plane.

2.3. Developing Reasoning Procedure. The motion interface in each generic physical element has various possible input and output areas. An example of a block element derived from a spatial element is shown in Figure 5. Five input areas with their contact types, motions, and normal vectors (shown in the top chart) and five output areas (shown in the bottom chart) enable each generic physical element to connect with different elements oriented in a three-dimensional space.

The rules for ensuring motion interface compatibility (see Figure 6) are summarized as follows: two connecting objects must match in terms of their normal vector, motion, and type at their contacting surfaces.

The procedure for generating all possible physical embodiments is as follows: each spatial element in a spatial solution has various alternative generic physical elements with various forms, support interfaces, and motion interfaces. Considering all possible combinations of the elements' generic physical elements, alternative physical embodiments of the solution, which meet the rule of motion interface compatibility for all connecting elements, are generated. Connections between these elements contain kinds, directions of the kinds, positions of the elements, and the motion interface with the matching normal vector, motion, and type.

The matching process between two sets of objects (each set containing alternative physical embodiments of a spatial element) is to first select an alternative from each set, followed by deciding whether the output area of the former element or the input area of the latter element obeys the rule for motion interface compatibility. This process has to be repeated for all alternative combinations.

3. Examples

3.1. Example of Spatial Element and Its Physical Realizations. Figures 7–10 present various generic physical elements for the four spatial elements. Each generic element is as shown in the columns of the top row with its name shown in the second row. The attributes of possible input and output areas of the physical element are shown in each column of the bottom row.

The derivation of generic physical elements in the database is based on two concerns.

(i) Motion. Elements providing different kinematic motions, such as continuity or reciprocity, need to be distinguished. For instance, the generic element of a plate and a semidisk from the *torque-to-force* spatial element need to be

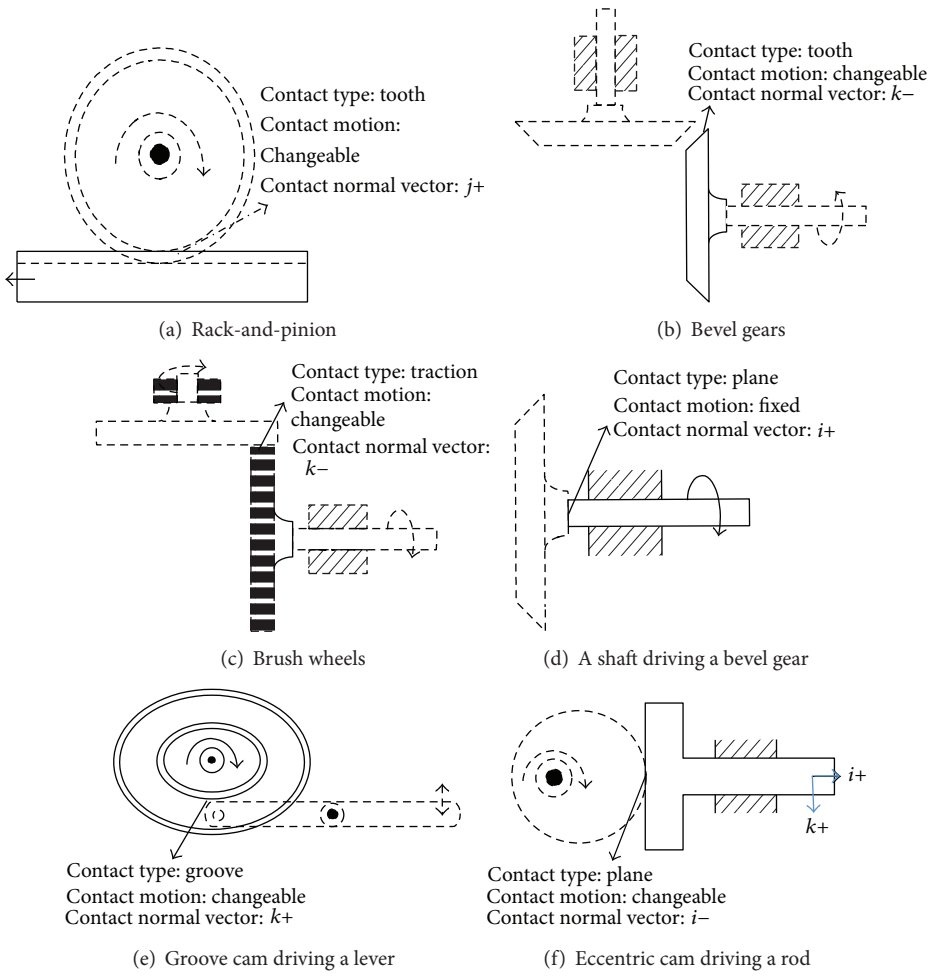

Figure 4: Examples of various motion interfaces with their contact types, motions, and normal vectors.

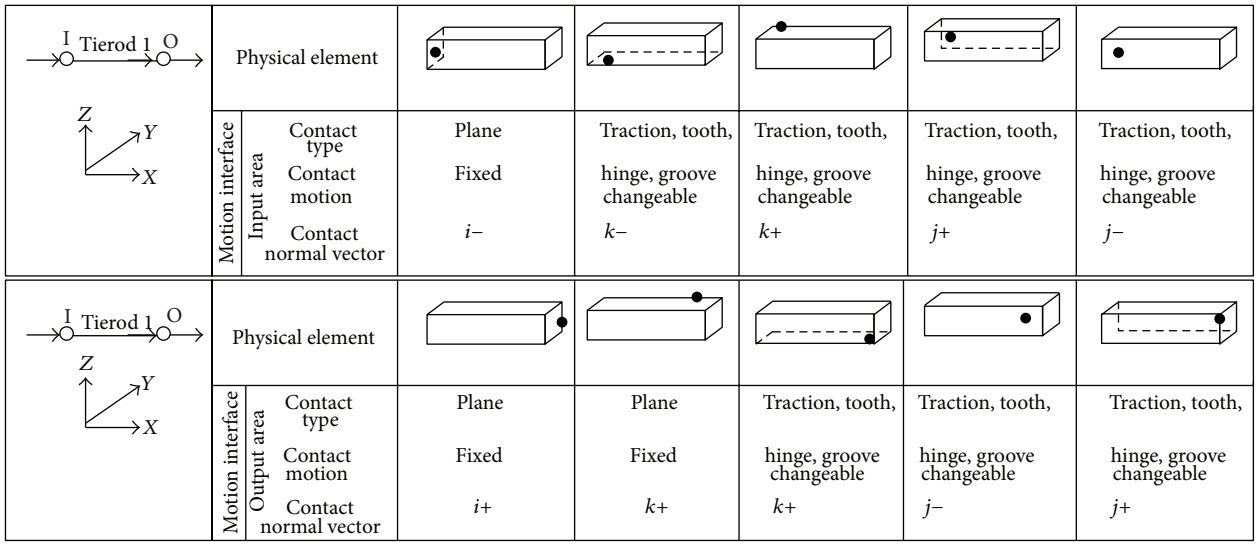

● : Input area and output area

Figure 5: Motion interface of a block element derived from a spatial element.

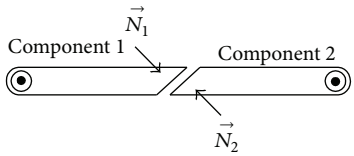

$\vec{N}_1 + \vec{N}_2 = \vec{0}$

$\vec{N}_1$: normal vector of component 1

$\vec{N}_2$: normal vector of component 2

(a) Contact normal vector matching

Changeable	⊕	Changeable	→	Changeable
Fixed	⊕	Fixed	→	Fixed
Changeable	⊕	Fixed	→	Not applicable
Fixed	⊕	Changeable	→	Not applicable

(b) Contact motion matching

Groove	⊕	Groove	→	Match
Traction	⊕	Traction	→	Match
Plane	⊕	Plane	→	Match
Hinge	⊕	Hinge	→	Match
Tooth	⊕	Tooth	→	Match

(c) Contact type matching

Figure 6: Rules for motion interface compatibility.

distinguished, because one can generate a continuous output and the other cannot.

(ii) Spatial Constraint. Elements having different types need to be distinguished. For example, the distinction between Wedge1 and Wedge3 generic element derived from the Wedge spatial element is because their spatial constraints are located in different places.

Figure 7 shows the results of transforming a *torque-to-force* spatial element into generic physical elements. Each generic physical element consists of a generic form, support interface, and motion interface. Three generic forms—plate, semidisk, and block—are shown in this figure. The generic support interface is a revolute pair which is situated at the centre of the plane generic form and is situated at the top of the semidisk and block forms. A revolute pair provides one degree of freedom (rotation) to its generic physical form. Each generic interface has an input area and output area. The input area of a plate generic form is a plane and the output area is either a tooth or a traction. Similarly, the input area of a semidisk generic form is a plane and the output area is either a tooth or traction. The input area of a block generic form has the input area as a plane and the output area as plane, hinge, or groove. The presentation of various input and output areas for a generic element is not shown in this figure.

Figure 8 shows the results of transforming a *force-to-torque* spatial element to generic physical elements. Three generic forms—plate, semidisk, and block—are shown in this figure.

Figure 9 demonstrates the results of transforming a *force-to-force* spatial element into generic physical elements. The generic form is a lever1, the support interface is a revolute pair which provides one degree of freedom (rotation), and the motion interface has various possible input and output areas which are the hinge, groove, or plane.

Figure 10 shows the results of transforming another *force-to-force* spatial element into generic physical elements. Four generic forms—wedge1, wedge2, wedge3, and wedge4 are presented. The generic physical elements with wedge1 generic form and wedge4 generic form are transformed as assemblies of components rather than a single component.

Theoretically, all generic physical elements can be considered in terms of single components without assemblies. The reason for using components as well as assemblies is that there are some assemblies (such as pulley-and-belt, or screw-and-nut) that are often treated as a single building block. Therefore, if we use only components in the database, such building blocks require the use of more than one basic element. To reduce the number of elements used in a solution (which is important to contain combinatorial explosion), components and assemblies are used together.

3.2. Example of Two Consecutive Spatial Elements and Their Physical Realizations. Two examples are given below to illustrate the results of transforming spatial configurations into their generic physical embodiments. Figure 11(a) shows a spatial configuration combining a *torque-to-force* element taking an input torque, to produce and transfer a translational output to a *force-to-torque* element that produces a rotational output at the desired output point. Five generic physical embodiments are shown in Figures 11(b), 11(c), 11(d), 11(e), and 11(f). Figure 11(b) shows a pair of traction wheels or spur gears. Figure 11(c) shows an embodiment similar to that in Figure 11(b) but generates an intermittent output motion. The embodiment shown in Figure 11(d) is similar to Figure 11(c) but provides different output motion which is a repeatedly intermittent output, while that in Figure 11(e) is similar to Figure 11(c) with the same output motion. Figure 11(f) describes a rotating element driving another rotating element, through a contact surface, to transfer the rotational motion. Figure 12(a) shows a spatial configuration combining a *force-to-force* element taking input force, to produce and transfer a translational inverse motion to a *force-to-force* element that produces a perpendicular translational output at the desired output point. Four possible generic physical embodiments are shown in Figures 12(b), 12(c), 12(d), and 12(e). Figure 12(b) shows a lever connected to a wedge. Figure 12(c) shows a lever connected to a wedge assembly. The contact type in-between is a plane. Note that the wedge in the pin diagram can be more general than simply a physical wedge, as illustrated in Figures 12(d) and 12(e). Figure 12(d) shows as lever connected to a rotating rod. The contact type in-between is a groove. Figure 12(e) shows a lever connected to a double-slider crank assembly. These generic physical embodiments describe different elements with their forms, support interfaces, and motion interfaces so as to enlarge or

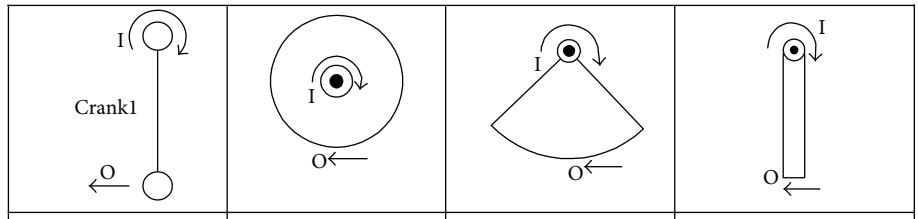

Form	Plate	Semidisk	Block
Support interface	Revolute pair	Revolute pair	Revolute pair
Motion interface (Input area) (Output area)	Plane Tooth, traction	Plane Tooth, traction	Plane Plane, hinge, groove

Figure 7: A torque-to-force spatial element and its generic physical elements.

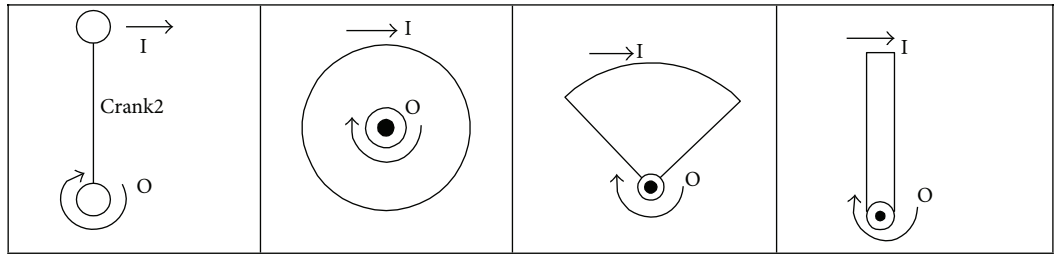

Form	Plate	Semidisk	Block
Support interface	Revolute pair	Revolute pair	Revolute pair
Motion interface (Input area) (Output area)	Tooth, traction Plane	Tooth, traction Plane	Plane, hinge, groove Plane

Figure 8: Crank2 spatial element and its generic physical elements.

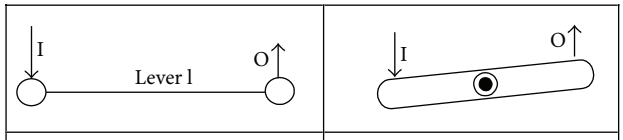

Form	Lever1
Support interface	Revolute pair
Motion interface (Input area) (Output area)	Hinge, groove, plane Hinge, groove, plane

Figure 9: A Lever1 spatial element and the generic physical element.

decrease the magnitude of the input, as well as to change its direction.

4. Discussion

Developing physical embodiments from an abstract spatial configuration is more than one-to-one mapping. This is because an abstract spatial configuration of a solution provides little information as to what physical objects (i.e., components or assemblies of components) and their interfaces should be. The reasons to develop a level of generic physical object are as follows. Firstly, very little supporting theory is available, and hence the designer must rely on his/her intuition and experience for transforming spatial into physical solutions. There is no general theory that relates a spatial element to its possible physical objects, and thus developing a reasoning procedure is necessary to link the two. Secondly, each spatial element can be represented in terms of numerous physical objects, if considering these objects at the physical level with their form, dimensions, and spatial constraints. However, if all possible geometric and dimensional variants of these are considered, the number of physical objects for the spatial element could be infinite. Therefore, it is still necessary to find a way to generalize their geometry and dimensions so as to control the number of the transformed objects. Lastly, a connection between spatial elements in a spatial configuration does not explicitly consider the characteristics of that interface. However, interfaces between connecting objects in mechanical designs can have various geometric forms and dimensions. We, therefore, need to address the question of how to reason about suitable interfaces for connecting two physical objects, each of which represents a spatial element at the physical level. As reported in previous studies [17, 18], physical interface compatibility was addressed before under the framework of Function-Behavior-Structure (FBS) model. Compatibility was checked

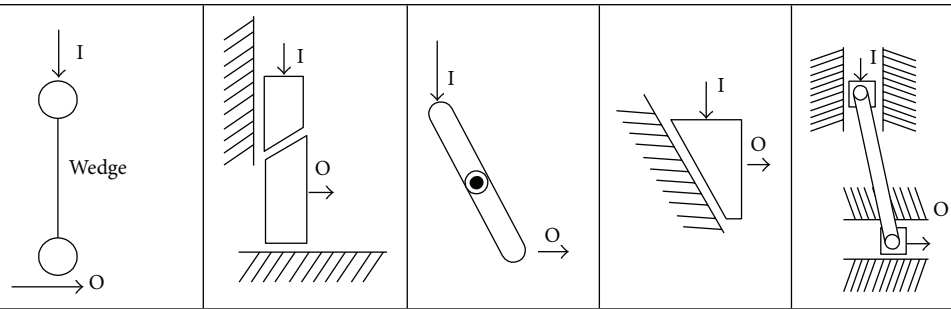

Form	Wedge1	Wedge2	Wedge3	Wedge4
Support interface	Prismatic pair	Revolute pair	Prismatic pair	Prismatic pair
Motion interface (Input area) (Output area)	 Plane Plane	 Hinge, plane Hinge, plane	 Plane Plane	 Plane Plane

Figure 10: A Wedge spatial elements and its possible generic physical elements.

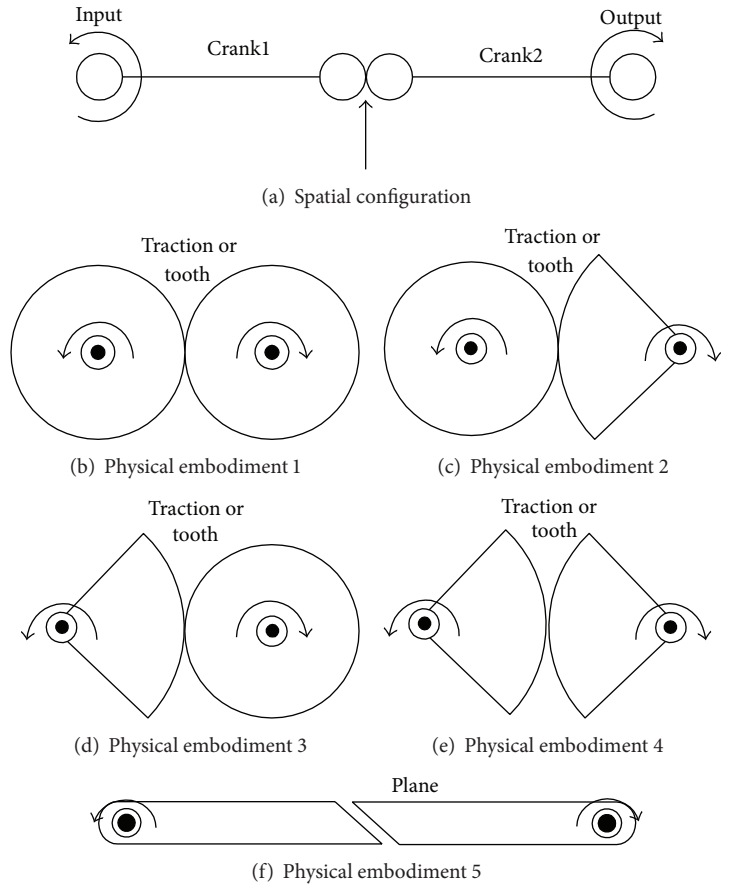

Figure 11: The spatial configuration and its five possible physical embodiments.

to derive types of contact (e.g., point contact or line contact). However, the major difference of this previous approach to the one proposed in this paper is as follows: while earlier work [17, 18] describes how an interface is to be connected (e.g., line contact), our proposed method proposes that, in addition to the type of contact needed, a physical interface should include information on the interface shape (e.g., groove) and the position of the contact point.

The range of physical elements of a specific spatial element would affect the variety of physical objects, while

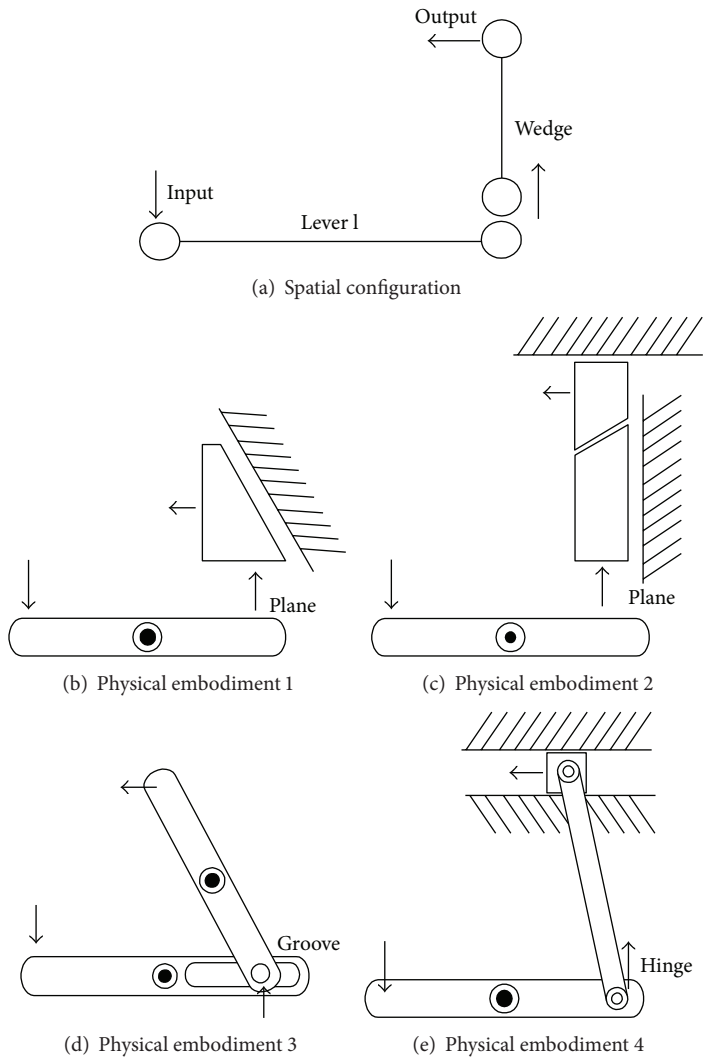

Figure 12: The spatial configuration and its four possible physical embodiments.

the type of spatial elements would decide the variety of the space of abstract solutions. In our method, a database of generic physical elements needs to be developed. Therefore, this raises the question: how to develop and validate generic physical embodiments from existing designs? We propose the following procedure: (a) abstract existing designs to strip irrelevant information from them in order to transform them into their generic physical embodiments, (b) from the designs identified in Step 1, distil subsolutions which are relevant to this research (because e.g., this methodology is developed based on the consideration of mechanical movements and their transformation), (c) compare these subsolutions with the ones independently generated by the proposed method. Take a corkscrew as an example. Two parts relevant to mechanical movements are considered in this case study: (1) Part I (such as the spiral-shaped metal rod) to screw the spiral into the cork so as to combine with the cork so that they can be removed together from the bottle, and (2) Part II (such as the handle) to transfer or transmit motion from hand to Part I. To develop a database, a collection of design catalogues could be used from the literature, for example, catalogues of corkscrews in Wallis [19] and Watney and Babbidge [20]. Also, machines with mechanical movements are shown in Brown [21], Jensen [22], and Sclater [23] as benchmark.

One problem of our method is that since the variety of building blocks at each solution level is wide, the number of generic physical embodiments becomes increasingly large when dealing with solutions which contain many spatial elements and may result in a combinatorial explosion. Two possible ways of resolving this are as follows.

(1) To divide a design problem into subproblems. Each subproblem can then use fewer spatial elements. As a result, the number of solutions can be reduced.

(2) To prune solutions at the earliest possible opportunity. A solution space can be pruned by using relevant heuristics, at the topological solution, spatial configuration, and generic physical embodiment levels (see, e.g., [1, 24]).

The present method is restricted in several ways: only single input single output (aspects of) designs are currently embodied, and the databases of building blocks are all from mechanical domain. Future work involves extending and modifying the set of building blocks, integrating mechanical building blocks with building blocks from other engineering domains, and considering multiple-input multiple-output requirements.

5. Conclusion

This paper investigates a key issue in conceptual design-how to develop spatial solutions into their possible physical embodiments. The method proposed contains knowledge for transforming spatial elements into generic physical elements, as well as rules for ensuring motion interface compatibility between connecting physical elements that together form an assembly to carry out the function. The outcome of the method is generation of generic physical embodiments of spatial configurations which should lead to an improved visualisation of spatial configurations, and an increase in the number of possible concepts explored. There are three important contributions of this method. The first is that both components and assemblies are used as building blocks. The second is that motion interfaces between physical objects are explicitly considered. And finally, there are explicit rules for ensuring interface compatibility that can be used by computers rather than only implicitly handled by designers.

Acknowledgments

This research is partly funded under Grant no. CMRPD2C0021 by the Chang Gung Memorial Hospital and NSC 102-2410-H-182-014 by the National Science Council of the Republic of China.

References

[1] Y.-C. Liu, A. Chakrabarti, and T. Bligh, "Towards an "ideal" approach for concept generation," *Design Studies*, vol. 24, no. 4, pp. 341–355, 2003.

[2] A. Chakrabarti, P. Langdon, Y.-C. Liu, and T. P. Bligh, "Supporting compositional synthesis on computers," in *Engineering Design Synthesis: Understanding, Approaches and Tools*, pp. 179–197, Springer, London, UK, 2002.

[3] A. Chakrabarti, K. Shea, R. Stone et al., "Computer-based design synthesis research: an overview," *Journal of Computing and Information Science in Engineering*, vol. 11, no. 2, Article ID 021003, 10 pages, 2011.

[4] M. S. Hundal and L. D. Langholtz, "Conceptual design by computer-aided creation of function structures and the search for solutions," *Journal of Engeering Design*, vol. 3, no. 2, pp. 127–138, 1992.

[5] N. F. Roozenburg and J. Eekels, *Product Design: Fundamentals and Methods*, John Wiley & Sons, Chichester, UK, 1995.

[6] N. Cross, *Engineering Design Methods: Strategies for Product Design*, John Wiley & Sons, Chichester, UK, 4th edition, 2007.

[7] G. Pahl, W. Beitz, J. Feldhusen, and K. H. Grote, *Engineering Design: A Systematic Approach*, Springer, London, UK, 2007.

[8] S. Kota and S.-J. Chiou, "Conceptual design of mechanisms based on computational synthesis and simulation of kinematic building blocks," *Research in Engineering Design*, vol. 4, no. 2, pp. 75–87, 1992.

[9] C. L. Li, S. T. Tan, and K. W. Chan, "A qualitative and heuristic approach to the conceptual design of mechanisms," *Engineering Applications of Artificial Intelligence*, vol. 9, no. 1, pp. 17–31, 1996.

[10] K. H. Roth, "Design models and design catalogs," in *Proceedings of the International Conference on Engineering Design (ICED '87)*, pp. 60–67, 1987.

[11] K. H. Roth, "Foundation of methodical procedures in design," *Design Studies*, vol. 2, no. 2, pp. 107–115, 1981.

[12] Y.-H. Han and K. Lee, "A case-based framework for reuse of previous design concepts in conceptual synthesis of mechanisms," *Computers in Industry*, vol. 57, no. 4, pp. 305–318, 2006.

[13] T. Murakami and N. Nakajima, "Mechanism concept retrieval using configuration space," *Research in Engineering Design*, vol. 9, no. 2, pp. 99–111, 1997.

[14] C.-C. Gu, J. Hu, Y.-H. Peng, and S. Li, "FCBS model for functional knowledge representation in conceptual design," *Journal of Engineering Design*, vol. 23, no. 8, pp. 577–596, 2012.

[15] A. Chakrabarti and T. P. Bligh, "An approach to functional synthesis of mechanical design concepts: theory, applications, and emerging research issues," *Artificial Intelligence for Engineering Design, Analysis and Manufacturing*, vol. 10, no. 4, pp. 313–331, 1996.

[16] A. Chakrabarti and T. P. Bligh, "An approach to functional synthesis of solutions in mechanical conceptual design—part III: spatial configuration," *Research in Engineering Design*, vol. 8, no. 2, pp. 116–124, 1996.

[17] D. X. Cao and M. W. Fu, "Port-based ontology modeling to support product conceptualization," *Robotics and Computer-Integrated Manufacturing*, vol. 27, no. 3, pp. 646–656, 2011.

[18] D. X. Cao, Q. L. Jia, Y. H. Han, and C. X. Cui, "Port-based description of functional modeling for product conceptual design," *Journal of Advanced Manufacturing Systems*, vol. 7, no. 1, pp. 101–105, 2008.

[19] F. Wallis, *British Corkscrew Patents from 1795*, Vernier Press, London, UK, 1997.

[20] B. M. Watney and H. D. Babbidge, *Corkscrews for Collectors*, Sotheby Parke Bernet, London, UK, 1981.

[21] H. T. Brown, *Five Hundred and Seven Mechanical Movements*, Coombs & Co., New York, NY, USA, 1871.

[22] P. W. Jensen, *Cam Design and Manufacture*, The Industrial Press, New York, NY, USA, 1965.

[23] N. Sclater, *Mechanisms and Mechanical Device Sourcebook*, McGraw-Hill, New York, NY, USA, 5th edition, 2011.

[24] Y. C. Liu, A. Chakrabart, and S. J. Lu, "Design heuristics for pruning the number of mechanism solutions in computer-based conceptual design," in *Proceedings of the 2nd International Conference on Computer and Automation Engineering (ICCAE '10)*, pp. 235–239, February 2010.

Hindawi Publishing Corporation
Advances in Mechanical Engineering
Volume 2013, Article ID 816438, 9 pages
http://dx.doi.org/10.1155/2013/816438

Research Article

Research on SDG-Based Qualitative Reasoning in Conceptual Design

Kai Li, Zhen-Zhen Yi, Wei Xu, Ke Zhao, and Lin Wang

School of Mechanical Engineering, Xidian University, Xi'an 710071, China

Correspondence should be addressed to Kai Li; kli@mail.xidian.edu.cn

Received 10 April 2013; Revised 25 August 2013; Accepted 31 August 2013

Academic Editor: Dongxing Cao

Conceptual design is the initial stage throughout the product life cycle, whose main purposes include function creation, function decomposition, and function and subfunction designs. At this stage, the information about product function and structure has the characteristics of imprecision, incompleteness, being qualitative, and so forth, which will affect the validity of conceptual design. In this paper, the signed directed graph is used to reveal the inherent causal relationship and interactions among the variables and find qualitative interactions between design variables and design purpose with the help of causal sequence analysis and constraint propagation. In the case of incomplete information, qualitative reasoning, which has the function of qualitative behavior prediction, can improve conceptual design level aided by the computer. To some extent, qualitative reasoning plays a supplementary role in evaluating scheme and predicting function. At last, with the problem of planar four-bar mechanism design, a qualitative reasoning flowchart based on the Signed Directed Graph is introduced, and an analysis is made of how to adjust design parameters to make the trajectory of a moving point reach to the predetermined position so as to meet the design requirements and achieve the effect that aided designers expect in conceptual design.

1. Introduction

Rapidly growing complexities of the product in function and structure are enabling engineers to adopt multiple design means and combine them together to shorten the time to market. Exploring advanced conceptual design theories and methodologies and their applications is used to improve the product functions and performances.

According to the requirements of the various stages of the product life cycle [1], conceptual design involves such work as product creation, functional decomposition, and function and subfunction designs, realizing carrier program and idea of systematic design that meet the function and working principle [2]. Conceptual design is the initial stage of the design process, which aims at obtaining the basic form or shape information and related description of the product. In conceptual design, detailed design information is not likely to be obtained; instead, only a rough description of the system is needed [3].

The key technologies of Computer-aided conceptual design are the product information modeling and reasoning techniques, in which design object abstract description and expression are the important part. Currently used in the conceptual design stage reasoning techniques are knowledge-based reasoning, artificial neural networks, case-based reasoning, and qualitative reasoning. Seely Brown and John de Kleer propose the theory based on the concept of "stream" theory, and B. J. Kuipers uses constraint-based qualitative simulation theory described by qualitative differential equations [4]. Cao [5] researches the function, behavior, and structure framework which can be further achieved by product conceptual design process modeling. Von-Wun and Wang [6] designed a compression spring design system with qualitative and quantitative techniques.

The information obtained during the conceptual design is usually incomplete, imprecise, and fuzzy. It is very difficult and sometimes even impossible to set up an accurate quantitative model using conventional numerical analysis tools. We need not establish a precise mathematical model of the problem at many times; instead, we just need rely on the understanding of the principles behind the research questions and qualitative analysis to get the results we want. The foundation

of such a principle understanding of the problem is the application of qualitative knowledge, which is very useful in practical problem solving. In this process, we are often interested in qualitative knowledge about the nature of the system, while numerous, redundant, precise quantitative knowledge is usually not necessary. And the conceptual design is a design-analysis-redesign spiral process; a lot of repetitive designs are inevitable. Take advantage of the knowledge of the initial design phase to build qualitative modeling, qualitatively giving the system's behavior prediction, and approximate direction of the design can effectively reduce repetitive design process, improve efficiency, and reduce design costs [7].

In many cases, such as in the conceptual design of the transmission program, what need to do are to determine the transmission type, to select the drive level, and to make a preliminary analysis of the eventual impact of the transmission scheme on the product [8]. In this analysis process, it is not necessary or possible to get the design details. At the conceptual design stage, a large amount of experience knowledge of designers is to be used, and it is not feasible to adopt numerical analysis tools like the finite element to provide effective help for designers. Qualitative reasoning is one of the reasoning methods in artificial intelligence, which uses qualitative information on the system's structure, behavior and function description. It studies the relationship among them and causality, draw qualitative interpretation, in order to mimic human commonsense qualitative reasoning [9].

The knowledge of qualitative reasoning mainly comes from the objective laws described in terms of mathematical formulas. Through the establishment of qualitative constraint equations, the system behavior change caused by some local changes can be qualitatively predicted. For the parts that do not meet the design requirements, qualitative reasoning can give directional suggestions for improvement.

Conceptual design involves the application of knowledge of various types [10, 11], including empirical knowledge, common sense, and structural knowledge, which generally requires the use of multilayer knowledge representation patterns of metaknowledge, qualitative knowledge, and mathematical models and methods [12]. Therefore, in conceptual design, different corresponding representations need to be adopted according to the characteristics of different types of knowledge, with comprehensive considerations in terms of representation ability, reasoning efficiency, maintainability, and so on.

Combined with the design process, the types of knowledge and structures the conceptual design stage involves are shown in Figure 1. The paper uses the qualitative reasoning method based on the Signed Directed Graph to organize the reasoning process from requirements analysis to scheme solving.

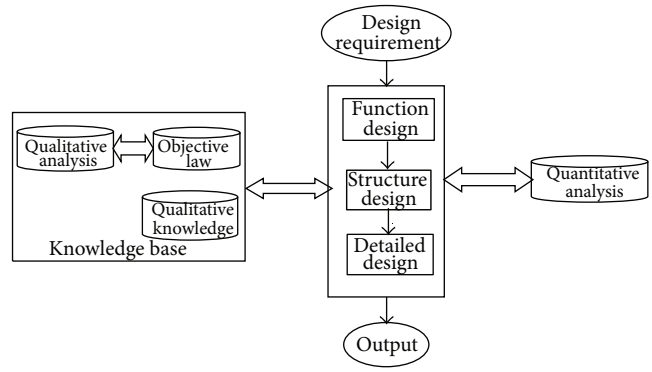

Figure 1: The knowledge model of conceptual design.

2. Signed Directed Graph

Signed Directed Graph is a kind of graph which is constituted by the directed connections among the nodes, referred to as SDG [12, 13], wherein the node can represent a variable, operating member or an event. The SDG model considers the links among the design variables and interactions. The state variables in the object being studied can be represented as nodes, connected with the edge between the nodes associated. The influence among the nodes can be expressed by the qualitative description method, indicating whether each node has incremental or decremental influence on other related nodes, and indicating what impact the state of a node has on the state of other related nodes. SDG can reveal the inherent causal relationship and interactions among the variables of the system, and thus it is suitable for the analysis of problems with root causes and multiple causal relationships. As a deep knowledge model, SDG has the ability to accommodate large-scale potential information.

Definition 1. The SDG model consists of nodes, directed branches, and branch sign among nodes, which is actually a collection of the three things.

The mathematic description of the SDG mode is what follows:

$$\gamma = (G, \psi), \tag{1}$$

where G stands for directed graph and ψ stands for sign set.

The directed graph G consists of the following four items:

$$G = (V, E, \partial^+, \partial^-), \tag{2}$$

where node set $V = \{v_i\}$, branch set $E = \{e_k\}$, adjacent associated character $\partial^+ : E \to V$ stands for the start node of branch, and $\partial^- : E \to V$ stands for the end node of branch.

Sign set ψ can be written as

$$\psi : E \in \{+, -\}. \tag{3}$$

Sign of branch can be written as

$$\psi(e_k) = \psi(v_i, v_j). \tag{4}$$

Definition 2. The signed branch indicates the positive and negative influence among nodes and represents the constraint propagation path. If the initial node of the branch increases or decreases, resulting in the synchronic increase or decrease of the end node, then the branch effect is called incremental influence or positive influence, abbreviated as "+," usually indicated with a solid line with arrows. If the initial node and the

end node change in the opposite way, then the branch effect is called decremental influence or negative influence, abbreviated as "–," indicated with a dotted line with the arrow.

Definition 3. Compatible path: in $\gamma = (G, \psi)$, concerning the instantaneous sample ϕ, if $\phi(\partial^+ e^k)\phi(e^k)\phi(\partial^- e^k) = +$, the branch e^k is called a compatible branch, and the end-to-end compatible branches form a compatible path. It can also be further expanded as a branch combination that meets $\phi(\partial^+ e_i)\phi(e_i)\cdots\phi(e_j)\phi(\partial^- e_j) = +$.

3. Qualitative Reasoning Model of SDG

3.1. SDG Model. The key to the SDG reasoning is to construct the corresponding SDG model, namely, the process of knowledge acquisition and knowledge representation in the normal sense. Through the method based on experiential knowledge or mathematical model to get the constraint relations among variables [14], to determine the qualitative influence among variables is actually to determine the state of SDG branch, and then the influence relationship among variables can be described clearly.

To convert the SDG model directly into the corresponding reasoning model involves the following steps.

(1) According to the SDG model structure, search for all compatible paths from the node with its state known to the parameter node concerned.

(2) Except the node with its state known in compatible paths, add rules to each remaining node n_i according to the following forms.

(a) If $k_1, k_2 \ldots k_n$ are forward nodes of n_i, and relationship among them are "and". Then only all these forward nodes meet the requirement at the same time, can we infer the state of node n_i:

[(node, k_1, status) and (arc, k_1, n_i, influence)] and [(node, k_2, status) and (arc, k_2, n_i, influence)]…and [(node, k_n, status) and (arc, k_n, n_i, influence)].

(b) If $k_1, k_2 \ldots k_n$ are forward nodes of n_i, and relationship among them are "or". As long as one node among these forward nodes meets the requirement at the same time, can we infer the state of node n_i:

[(node, k_1, status) and (arc, k_1, n_i, influence)] or [(node, k_2, status) and (arc, k_2, n_i, influence)]…or [(node, k_n, status) and (arc, k_n, n_i, influence)].

Qualitative reasoning includes two factors: causal sequence analysis and constraint propagation [15]. The most important part of the knowledge in the analysis of the system is causality. In general cases, this causal relationship is expressed as a function relation, but the function does not show the direction of causality [16]. Therefore, we need to use the causal sequence theory to get the causal diagram among variables after obtaining the qualitative equation [17]. This paper studies two main conditions among qualitative reasoning.

(1) When some variables in the system change, we need to find out how the rest variables are influenced, that is, making the analysis from reason to result.

(2) When some variables in the system change, we need to find out what factors cause these changes, that is, making the analysis from result to reason.

In the context of qualitative reasoning, the mechanism of both forward and backward ones is explored, which are two fundamentally different approaches to reasoning [18]. With forward reasoning, propositions are combined with rules to deduce new propositions. Forward reasoning is of special interest in situations where no specific goals are obtainable, and where most rules and the antecedent portion to be considered are well known. As opposed to forward reasoning, backward reasoning works in a consequence-driven way.

In the first case, we use forward reasoning. Based on the established SDG model, we search backward all the pathways which use it as the predecessor, make a qualitative reasoning of these pathways, and find out the status of the affected nodes, a process of constraint propagation.

In the second case, we use backward reasoning, starting from the changed nodes by the depth-first search method to find out all possible cause nodes and identify one or more paths from the target node to cause nodes. When the causality is transmitted along these valid paths, the tendency of the variables and the cause of the corresponding state can be explained.

3.2. Knowledge Representation of SDG. Knowledge-based reasoning systems need to express the information contained in the SDG model, and in this paper knowledge representation is achieved through the frame representation and production rules. The main structure of qualitative analysis is the description of the SDG model. The corresponding knowledge representations are listed as follows:

```
(deftemplate arc
    (slot predecessor (default null))
    (slot successor (default null))
    (slot relation (default null)))

(deftemplate node
    (slot name (default null))
    (slot father (default null))
    (slot status (default null))
    (slot var1 (default null))
    (slot var2 (default null))
    (multislot predecessor (default (create$)))
    (slot mark (default null)))

(deftemplate causality
    (multislot mode (default (create$)))
    (multislot relation (default (create$)))
    (multislot influence (default (create$)))
    (multislot stack (default (create$)))).
```

3.3. Framwwork of SDG Model. The paper uses frame representation and production rule method for knowledge representation and knowledge-based reasoning system to complete the sequence of causal reasoning and explanation. Figure 2 shows the main flowchart of SDG qualitative reasoning model.

In the process of qualitative reasoning, the main algorithms are constraint propagation algorithm and backward reasoning calculus algorithms, which show in Figures 3 and 4, respectively.

4. Qualitative Reasoning Model of Planar Four-Bar Mechanism

4.1. Constraint Relationship among Components. In the conceptual design of the planar four-bar mechanism, generally six design variables are concerned: active rod, connecting rod, followed rod, basement rod, fixed rod, and the angle between the fixed rod and the connecting rod, which are expressed by a, e, g, c, d, f, and Φ, respectively. For the sake of simplicity, it is agreed that the x-coordinate of the system coincides with the basement rod, with the origin A on left of d, as shown in Figure 5.

The paper uses the position method to analyze the four-bar mechanism. As shown in Figure 5, given the rotation angle θ_1 of the active rod a, components e, g, c, d, f, and Φ, and the coordinates X_A, Y_A, X_D, and Y_D of the fixed hinge points A and D, other parameters can be obtained through the displacement constraint analysis, and the assembly relations in the four-bar mechanism are the following

$$\theta_2 = \theta_3 - \theta_4, \tag{1}$$

$$X_C = X_B + (e+g)\cos\theta_2, \tag{2}$$

$$Y_C = Y_B + (e+g)\sin\theta_2, \tag{3}$$

$$\alpha = \arctan\left[\frac{Y_C - Y_D}{X_C - X_D}\right] = \arctan\left[\frac{Y_C}{X_C - d}\right]. \tag{4}$$

The link curve is the trajectory of any point P on the link planar. For any given θ_1, the displacement coordinate of point P is as follows:

$$X = X_B + e\cos\theta_2 + f\cos\theta, \tag{5}$$

$$Y = Y_B + e\sin\theta_2 + f\sin\theta, \tag{6}$$

$$\theta = \phi + \theta_2. \tag{7}$$

4.2. SDG Model of the Four-Bar Mechanism. The relationship among the variables of four bar mechanism is more complicated. The paper considers the qualitative influence relationship among them. Equation (8) represents the more accurate

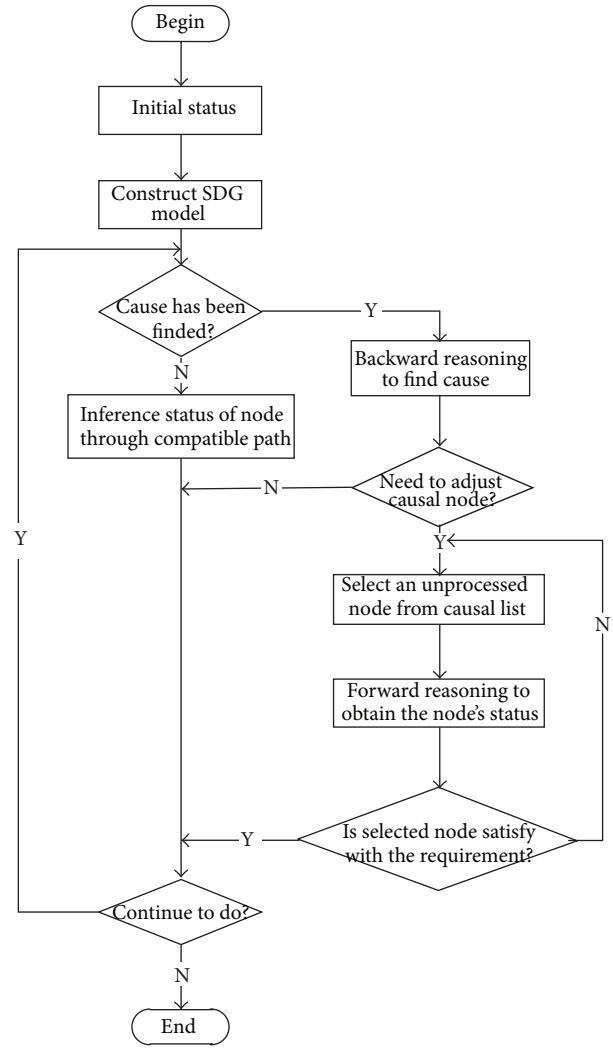

Figure 2: The qualitative reasoning flowchart based on SDG.

constraint among other variables with angle constraint premise:

$$\begin{aligned}
&\text{if } \theta_1 \in \left(0, \frac{\pi}{2}\right) \quad \text{then } X_B - d < 0,\\
&\text{if } \theta_1 \in (0,\pi) \quad \text{then } Y_B > 0,\\
&\text{if } \theta_3 \in (0,\pi) \quad \text{then } \left[(e+g)^2 + b^2 - c^2\right] > 0,\\
&\text{if } \theta_3 \in (0,\pi) \quad \text{then } \left[b^2 + c^2 - (e+g)^2\right] > 0,\\
&\text{if } \theta_2 \in \left(0, \frac{\pi}{2}\right) \quad \text{then } X_C - d > 0,\\
&\text{if } \theta_2 \in \left(0, \frac{\pi}{2}\right) \quad \text{then } Y_C > 0.
\end{aligned} \tag{8}$$

The above formula can reveal the causal dependency among variables in the structure, which is the basis of constraint propagation and qualitative reasoning. Therefore, the qualitative relationship among variables can be obtained from

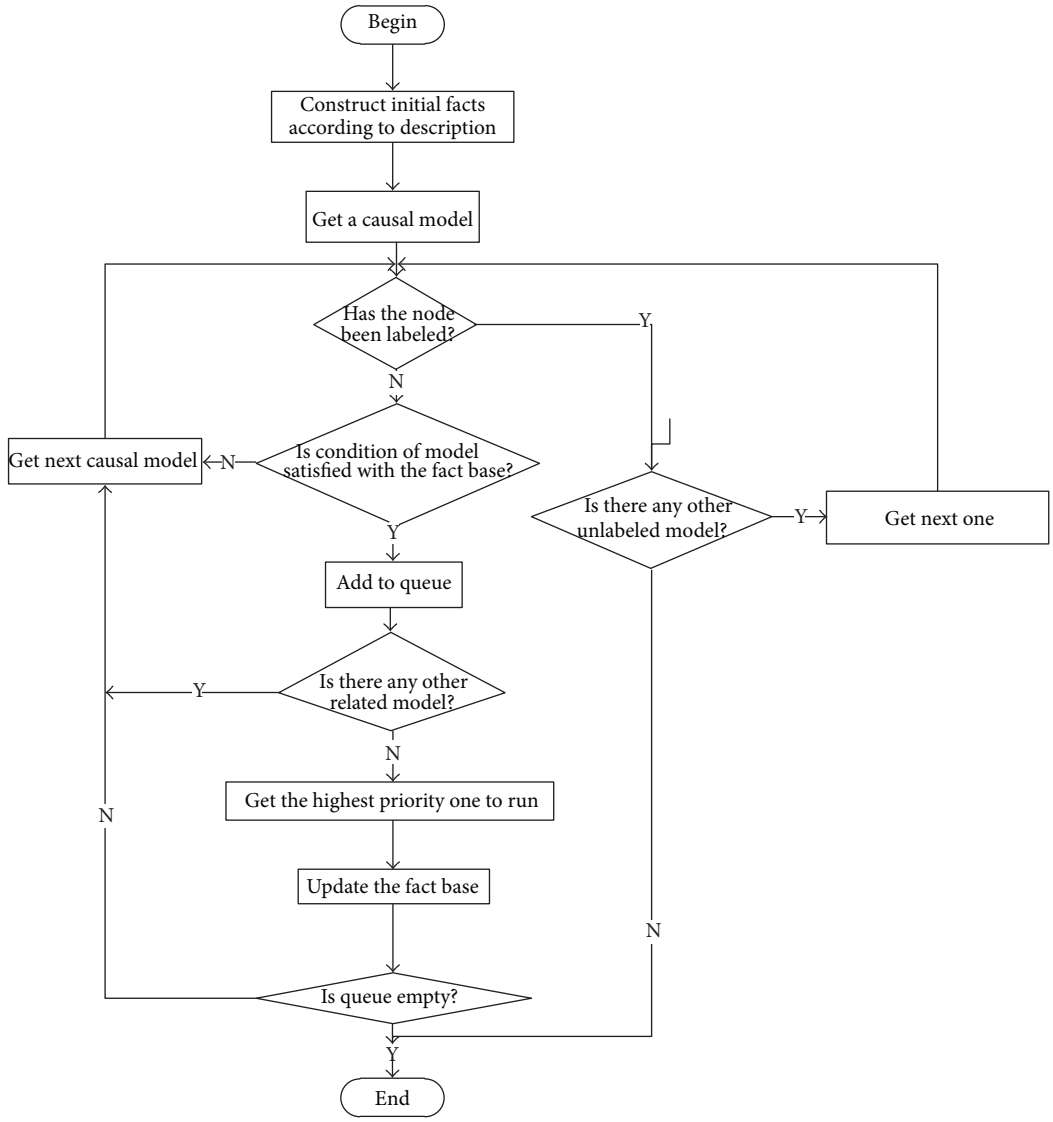

Figure 3: The flowchart of constraint propagation.

the above constraints in the four-bar mechanism. Based on the influence relations among variables, related variables can be connected, and then the SDG mode of four-bar mechanism is obtained, as shown in Figure 6.

4.3. Qualitative Analysis of the Four-Bar Mechanism's Trajectory. In the design of the four-bar mechanism, we often encounter the problem that the point's trajectory in the initial design is not in a predetermined position so that it may not meet our requirements. Then we need to find the reasons that affect it, make adjustments accordingly sometimes, or need to find out what influence will happen to the remaining variables when certain variables change sometimes.

In the design of the four-bar mechanism, the initial design result is obtained by the connecting rod curve trajectory synthesis. The trajectory of point P on fixed rod is shown by the solid line in Figure 7.

As seen from Figure 7, base point P has some gap with actual requirements on the positions of $P1$, $P2$, $P3$, and $P4$. The values of $\theta 1$ on $P1$, $P2$, $P3$, and $P4$ are, respectively, 30°, 130°, 230°, 300°. The analysis starts from $p1$ position, which corresponds to $\theta 1$ of 30°, and other parameters also meet the constraints of the SDG model. The position of P involves two main variables, namely, the abscissa X and ordinate Y. Then abscissa X will be discussed as an example.

It is known from Figure 7 that a, e, and f are directly influencing factors, considering other indirect factors, and then the main factors of $P1$ in a horizontal deviation may be collection $V = \{a, e, d, c, f, g, \theta_1, \theta, \theta_4\}$, and thus they are likely to become factors of disturbance and may be possible cause nodes. The four-bar mechanism, as the adjustment object, must meet the following requirements.

(1) The states of target variables through different paths must be consistent.

(2) The disturbance of the variables in different locations can make the mechanism shift toward a more rational direction, which is reasonable consistency of change.

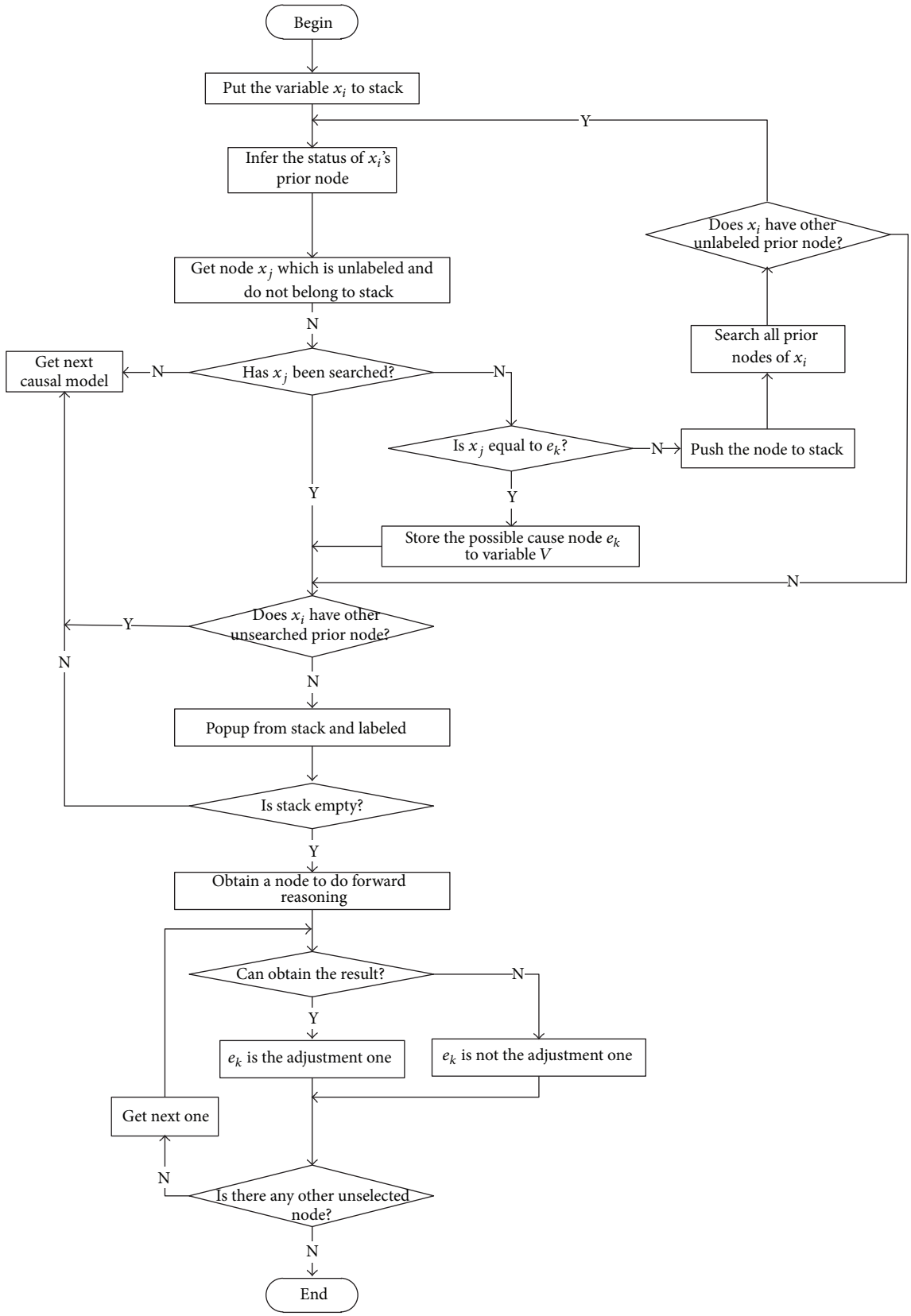

Figure 4: The flowchart of forward verification to backward reasoning.

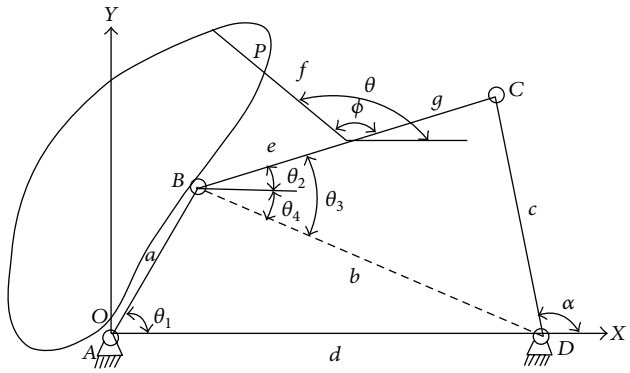

Figure 5: Four-bar mechanism.

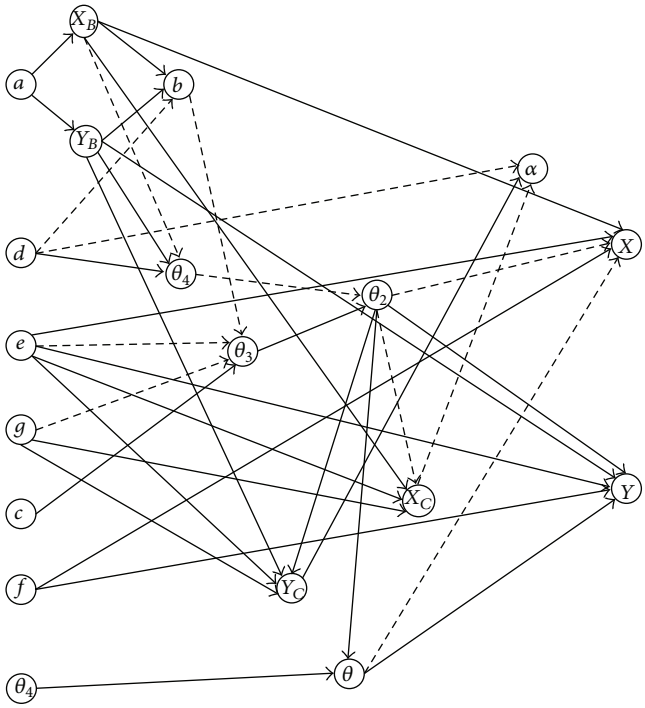

Figure 6: SDG model of four-bar mechanism.

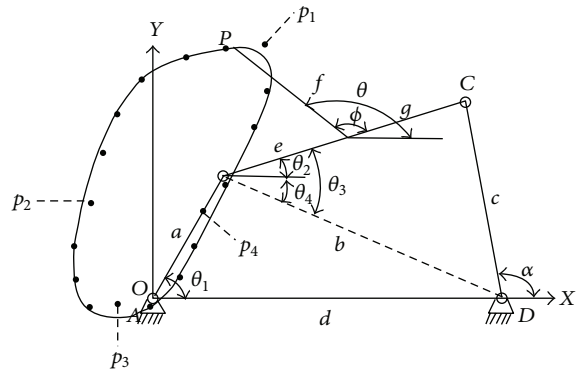

Figure 7: Initial design of four-bar mechanism by curve trajectory synthesis.

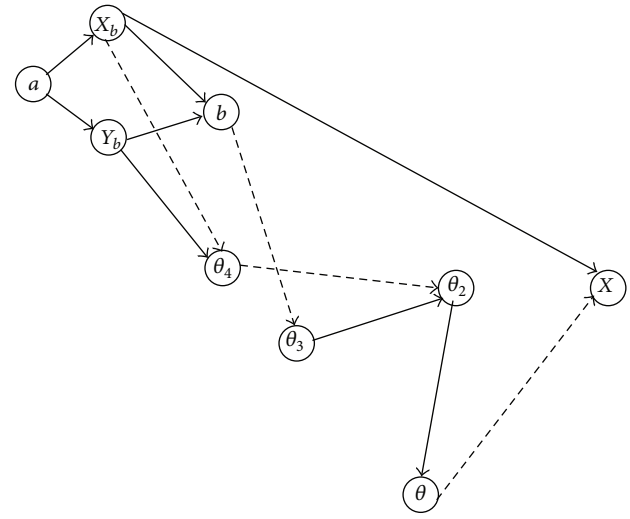

Figure 8: Compatible path between disturbance factor and variable x.

Factor **a** in influencing factor set V is selected for the analysis. Since we want to know how to adjust factor **a** to meet our requirements, we need to start from the constructed four-bar mechanism SDG model and find all compatible paths between this node and abscissa X of the concerned node. The compatible path that can be found is shown in Figure 8.

Then, reasoning needs to be done along the above compatible path. If the state of the target node variable derived from reasoning is consistent, then appropriate adjustment to disturbance variables can be received; otherwise, it is unable to make a judgment based on qualitative information. Some rules summarized from compatible paths are as follows.

Rule 1.

If (node, a, +1) and (arc, a, X_B, positive) then (node, X_B, +1).

Rule 2.

If (node, a, +1) and (arc, a, Y_B, positive) then (node, Y_B, +1).

Rule 3.

If [[(node, X_B, +1) and (node, Y_B, +1)] or [(node, X_B, +1) and (node, Y_B, 0)] or [(node, X_B, 0) and (node, Y_B, 1)]] and (arc, X_B, b, positive) and (arc, Y_B, b, positive) then (node, b, +1).

Rule 4.

If (node, X_B, +1) and (arc, X_B, θ_4, negative) and (node, Y_B, +1) and (arc, Y_B, θ_4, positive) then (node, θ_4, uncertain).

Since uncertain situations appear in the fourth rule reasoning, it is impossible to tell how to do the adjustment of factor **a** to meet our needs according to our qualitative knowledge. Then we need to re-select a disturbance factor from the possible cause set. Factor **g** is be selected as a new disturbance

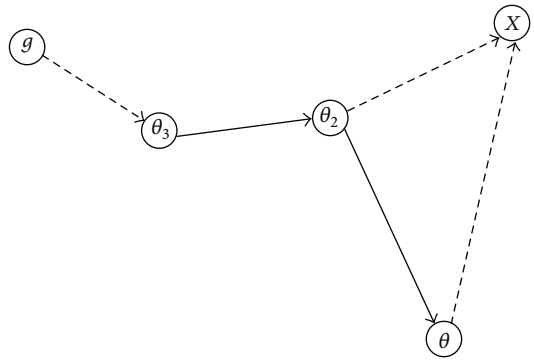

Figure 9: Compatible path between disturbance node g and variable x.

variable, using the same method to find the compatible path from node **g** to abscissa X of node P, as shown in Figure 9. Some rules summarized are as follows.

Rule 5.

If (node, g, +1) and (arc, g, θ_3, negative) then (node, θ_3, –1).

Rule 6.

If (node, θ_3, –1) and (arc, θ_3, θ_2, positive) then (node, θ_2, –1).

Rule 7.

If (node, θ_2, –1) and (arc, θ_2, θ, positive) then (node, θ, –1).

Rule 8.

If [[(node, θ_2, –1) and (node, θ, –1)] or [(node, θ_2, –1) and (node, θ, 0)] or [(node, θ_2, 0) and (node, θ, –1)]] and (arc, θ_2, X, negative) and (arc, θ, X, negative) then (node, X, +1).

The situation of the node's uncertain state does not appear in the above rules, so we can change the state of the abscissa X by adjusting node g. Also, it can be known from the above rules that abscissa X increases with the increase in node g and decreases with the decrease in node g.

Similar to the analysis process of abscissa X, we can use the same method to deal with Y of node p. It is known from the analysis that ordinate Y decreases with the increase in node g and increases with the decreases in node g. In view of the initial design situation, the X value at the location of the point $P1$ is larger than the actual position, and Y is smaller than the actual position. $P1$ is at the bottom right location of the desired position. In accordance with the requirements of the designer, X needs to become smaller, and Y needs to become bigger. Therefore, we can meet the requirement by reducing factor g, namely, the distance between the fixed rod and hinge B.

After the adjustment of factor g, though it may be satisfied that the position of the connecting rod at the point $P1$ is closer to a predetermined position, the requirements of the connecting rod at other predetermined positions may be affected, and there exist the following effects.

(1) The connecting rod at other predetermined positions has not changed.

(2) The connecting rod at other predetermined positions has changed, but it is closer to the desired position.

(3) The connecting rod at other predetermined positions has changed, but on the whole the number of points does not meet the predetermined positions that are greatly reduced.

In order to judge the adjustment effect of the disturbance variables, it is necessary to verify the influence on the rest predetermined positions. For other possible influencing factors, a similar analysis process can be applied to obtain the state of the rest predetermined positions and the number of unsatisfied positions. It is the aim to have a minimal number of positions that do not meet the design accuracy and find the adjustment program that can best meet the user's needs. When there are two or more adjustment programs that can meet this requirement, we need to select the one in which the position that can meet the design accuracy is close to the predetermined position as much as possible. Through a series of procedures, it is known that adjusting factor g makes positions $P2$, $P3$, and $P4$ move toward the expected direction, and there is disturbance to the rest desired predetermined locations, but changes are within the allowable range of accuracy, so adjusting g, namely, the distance between the fixed rod and the hinge C, can meet our requirements.

The same approach can also be adopted to analyze the case of the disturbance of two or more components, which, due to the space limitation, will not be discussed.

5. Conclusion

The product information in the conceptual design stage is qualitative, imprecise, uncertain, incomplete, conceptual design itself belongs to the category of experience design. For those problems that are difficult to access knowledge and not easy to have complete description, the method based on knowledge can also realize the corresponding reasoning, but it is difficult to maintain as knowledge increases knowledge. On the other hand, those problems are relatively easy to deal with in qualitative reasoning. Since the knowledge of qualitative reasoning comes from the objective laws described by mathematical formulas, all the qualitative descriptions of the objective laws can be derived by qualitative reasoning, and thus knowledge is comprehensive and easy to acquire.

Through the directed graph, the SDG qualitative analysis expresses the inner causal relationship and interacting factors among design variables involved in the design system, SDG qualitative analysis system is suitable for the analysis of the root causes and multiple causality problems. Accurate mathematical models are not needed in modeling instead, just experience and knowledge combined with some of the objective laws are needed to lead to corresponding qualitative models,

which can be converted into corresponding rules for qualitative reasoning, and then aid the designer. Based on SDG, a qualitative reasoning system framework has been established, which, after further improvement, can be used conveniently for the establishment of other qualitative reasoning systems of objective laws and can serve as a powerful qualitative analysis tool for designer.

Qualitative reasoning, of course, involves many other aspects [19] that need to be further discussed, conceptual design involves experience knowledge, qualitative knowledge, and quantitative knowledge, which needs multilevel design knowledge from quantitative knowledge to abstract knowledge. SDG qualitative reasoning provides only one of the levels. How to well represent and use such knowledge is the key to constructing the conceptual design support system, and it remains to be solved in the future.

Acknowledgments

The authors are grateful for detailed and insightful comments from the anonymous reviewers which have been invaluable in revising the initial paper. This research was supported by the Fundamental Research Funds for the Central Universities (72124683).

References

[1] Z. X. Cai and G. Y. Xu, *Artificial Intelligence and Application*, Science Press House, 2003.

[2] H. j. Zou, L. Wang, S. G. Wang, and W. Zh. Guo, "Summary of conceptual design and its methods for mechanical products," *Machine Design and Research*, no. 2, 1998 (Chinese).

[3] K. Zhao, X. N. Li, and L. Shi, "Study on application of qualitative reasoning in product conceptual design," *Journal of Mechanical Science and Technology*, vol. 21, no. 6, pp. 1028–1030, 2002 (Chinese).

[4] S. H. I. Chunyi and C. Jian, "Advances in Qualitative Reasoning," in *Proceedings of the 2nd Session of China Joint Conference on Artificial Intelligence*, pp. 128–123, 1992, Chinese.

[5] D. Cao, "Port-based ontology conceptual design theory," *Journal of Mechanical Engineering*, vol. 46, no. 17, pp. 123–132, 2010 (Chinese).

[6] S. Von-Wun and T. -C. Wang, "Integration of qualitative and quantitative reasoning in iterative parametric mechanical design," *Artificial Intelligence for Engineering Design, Analysis and Manufacturing*, vol. 6, no. 2, pp. 95–109, 1992.

[7] S. Q. Sun, E. W. Sun, and H. Chen, "The research status and development trends of computer aided conceptual design," *Journal of Chinese Mechanical Engineering*, vol. 10, no. 6, pp. 697–699, 2004 (Chinese).

[8] Y. H. Yang, Z. P. Zhu, and L. G. Yao, "Survey of reasoning technology of conceptual design for mechanical product," *Journal of Modern Manufacturing Engineering*, no. 2, pp. 4–6, 2010 (Chinese).

[9] S. H. I. Chunyi and Huang, *Changning the Principle of Artificial Intelligence*, Tsinghua University Press, 1996, Chinese.

[10] Y. H. Gu, C. Y. Shi, and Z. H. Zhang, "Current research status of model-based qualitative simulation," *Journal of Computer Science*, vol. 25, no. 6, pp. 40–43, 1998 (Chinese).

[11] C.-L. Li, S. T. Tan, and K. W. Chan, "A qualitative and heuristic approach to the conceptual design of mechanisms," *Engineering Applications of Artificial Intelligence*, vol. 9, no. 1, pp. 17–31, 1996.

[12] K. Li, K. Zhao, and G. W. Hu, "Research on application of data mining techniques based on rough sets in product conceptual design," in *Proceedings of the 1st Asia International Symposium on Mechatronics*, pp. 217–220, xi'an, China, September 2004.

[13] N. Lü, H. Zh. Xiong, and X. A. Wang, "Delaminating modeling and hierarchical reasoning method for SDG based fault diagnosis," *Journal of Control Engineering*, vol. 17, no. 4, pp. 562–564, 2010 (Chinese).

[14] D. Gao, C. Wu, B. Zhang, and X. Ma, "Signed directed graph and qualitative trend analysis based fault diagnosis in chemical industry," *Chinese Journal of Chemical Engineering*, vol. 18, no. 2, pp. 265–276, 2010 (Chinese).

[15] R. H. Sturges, K. O. Shaughnessy, and M. I. Kilani, "Computational model for conceptual design based on extended function logic," *Artificial Intelligence for Engineering Design, Analysis and Manufacturing*, vol. 10, no. 4, pp. 255–274, 1996.

[16] H.-J. Zou and Q. Zhang, "Some key problems for computer aided conceptual design of mechanical products," *Journal of Shanghai Jiaotong University*, vol. 39, no. 7, pp. 1145–1154, 2005 (Chinese).

[17] O. Bernard and J.-L. Gouze, "Global qualitative description of a class of nonlinear dynamical systems," *Artificial Intelligence*, vol. 136, no. 1, pp. 29–59, 2002.

[18] A. J. Bugarin and S. Barro, "Fuzzy reasoning supported by petri nets," *IEEE Transactions on Fuzzy Systems*, vol. 2, no. 2, pp. 135–150, 1994.

[19] C.-X. Shao and F.-Z. Bai, "Technology of qualitative simulation and its application," *Journal of System Simulation*, vol. 16, no. 2, p. 202, 2004 (Chinese).

Hindawi Publishing Corporation
Advances in Mechanical Engineering
Volume 2013, Article ID 702590, 10 pages
http://dx.doi.org/10.1155/2013/702590

Research Article

Integrated Knowledge-Based System for Machine Design

Durmuş Karayel,[1] S. Serdar Ozkan,[1] and Fahri Vatansever[2]

[1] *Sakarya University, Sakarya, Turkey*
[2] *Uludag University, Bursa, Turkey*

Correspondence should be addressed to S. Serdar Ozkan; sozkan@sakarya.edu.tr

Received 22 April 2013; Revised 6 August 2013; Accepted 16 August 2013

Academic Editor: Dongxing Cao

An integrated design system (IDS) approach has been developed to integrate various stages of the mechanical design process, including rapid prototyping. The system consist, of design, analysis, calculation, rapid prototyping, and library modules, and it blends artificial intelligence methods, CAD-CAM, and technical computing packages into a single environment. The system has been applied for the design of one-stage gearbox with helical gear. In this case study, all stages of the design process are carried out by using IDS.

1. Introduction

The design process of the mechanical products is tedious and time consuming because of the various stages and complex activities involved. On the other hand, there are strong pressures to reduce overall costs in a competitive market environment [1]. But, the traditional design approach is inadequate in meeting these needs. Today a lot of CAD/CAM/CAE application software, different databases, and web-based services are used for the mechanical design studies, but these technologies are distributed and there is no coordination between them. Therefore, a number of researchers have focused their studies on establishing a cooperative and integrated environment. Su and Wakelam studied an intelligent hybrid system for integration in design and manufacturing. Their approach blends a rule-based system, artificial neural networks, genetic algorithm, hypermedia, and CAD/CAE/CAM packages into a single environment [2]. Zhao et al. described an agent-based approach to systems interoperability in cooperative design systems [3]. Hao et al. developed an agent-based collaborative e-engineering environment for product design engineering. They studied a prototype software system based on the web and a software agent and demonstrated its viability through an industrial case study [4]. Myung and Han introduced the feature representation, a concept of design unit, parametric modeling, and configuration design methods, and they proposed a framework of a design expert system, which describes parametric modeling with design knowledge-based [5]. Ramamurti et al. put forward an integrated system that could be used by the user for the complete design and analysis of a mechanical system. The system consists of two parts, such as initial design and detailed analysis [6]. Zha and Du presented an integrated method and assembly planning. They applied the system as an integration model, and so, CAD/CAM applications in assembly were supported [7]. Chiang et al. proposed a general integrated framework of design knowledge representation and developed a knowledge-based intelligent system to facilitate dynamic design reasoning. Also, they presented a case study of designing a mechanical system to demonstrate the features of the developed system [8]. Chung et al. studied a framework for integrated mechanical design automation, and they developed extended variational design technology using graph theory and numerical solution techniques [9]. Liang and O'Grady studied the object-oriented approach. Their study contained both of the fundamentals of object-oriented design in the development of design process models [10]. Zha et al. proposed a knowledge-based approach and developed an expert design system to support top-down design for assembled products. The proposed approach focused on the integration of product design, assemblability analysis and evaluation, and design for assembly with economical analysis [11]. Chen et al. developed an intelligent approach for generating assembly drawings automatically from three-dimensional

computer assembly models of mechanical products by simulating the experienced human designer's thinking mode with the aid of computer graphics and a knowledge-based expert system [12]. Daabub and Abdallah presented a computer based intelligent system so that the design for assembly can be realized within a concurrent engineering environment. They developed an expert system that supports new techniques for design and for assembly, and the developed system gave users the possibility to assess and reduce the total production cost at an early stage during the design process [13]. Wang et al. described a new framework for collaborative design. This framework adopts an agent-based approach and relocates designers, managers, systems, and the supporting agents in a unified knowledge representation scheme for product design [14]. Wang and Zhang aimed to develop a distributed and interactive system, on which designers and experts can work together to create, integrate, and run simulations for engineering design. Karayel et al. purposed an internet-based intelligent agent system for mechanical design [15]. The reference model and the architecture of the system were developed [16]. The current study can be accepted as a detailed part of this general research. Karayel et al. studied to determine factors affecting safety stress in the machine design by using artificial intelligence technologies [17]. Cao and Fu proposed and employed a design synthetic approach to guide the design process via behavioral reasoning and to obtain an iterative transforming process. They presented the functional representations and design parameters according to the design requirements of a product and established a behavioral matrix model by using the bond graph fundamental elements and then presented a knowledge modeling language for behavioral reasoning. They developed a prototype system for a computer-aided conceptual design and presented an application from the industry consequently [18]. Cao et al. presented an agent-based approach for guiding the mechanical product conceptual design. Firstly, they analyzed the mechanical product design requirements and then gave functional parameters and design variables and proposed a behavioral matrix model using bond graph fundamental elements. After, they established an agent-based framework and so aimed at solving the behavioral matrix model, producing functional means tree and multisolutions with the aid of agent technologies. An application for the special jig design in the machine center was presented as an example of the design synthesis [19]. Goel et al. analyzed CAD dimensions, such as cognitive design, collaborative design, conceptual design, and creative design. Then, they developed a knowledge-based CAD system illustrating CAD characteristics, and this system was called Design by Analogy to Nature Engine (DANE). They proposed that DANE is an important assistant to assess the practical use of CAD dimensions. One of the major contributions of DANE is to provide human interaction with knowledge-based CAD systems [20]. Chen et al. presented a multilevel model for an entirely assembly design. Their model captured abstract information, skeleton information, and detailed information, so that it can effectively support assembly design. This assembly design process contained design steps with an assembly tree structure. They discussed the use of assembly design model for extending the scope and deepness of its application [21]. Jia et al. proposed a novel multilevel system representation modeling framework for supporting design methods. Their framework had the capability to integrate the product design CAD models. Also, the data exchange and transfer in multidomain analyses were made possible by using the framework. The authors illustrated the framework with a case study. So, the applicability of the modeling framework was highlighted for multibody mechanical systems [22]. Li et al. discussed an integrated design method, which thoroughly considers related parameters of the various subsystems in order to optimize the overall system that mainly consists of optomechanical structure CAD, CAE, and the integrated information platform PDM. Their method was based on the model transformation and data share among different design and analysis steps, and so they carried out concurrent simulation and design optimization. Also, they presented an example of application of a mechanical structure [23]. Zheng et al. developed a novel collaborative design approach to improving efficiency. They designed and implemented a prototype system CoAutoCAD to test the approach and to demonstrate a variety of collaborative design activities [24]. Zhongtu et al. described a declarative modeling approach for task implementation and a methodology for problem-solving of knowledge primitives in design task. In the study, task analysis, knowledge management, and design object management module were developed and integrated with a mechanical computer-aided design (MCAD) system. The two-stage gearbox design was given as an example for this approach [25]. Al-Ashaab et al. developed a knowledge-based environment (KBE) to support product design validation of refresh projects, and they implemented KBE on the product lifecycle management platform. This implementation prevented repeating unnecessary and costly physical product tests, and so it also reduced time and costs for these refresh projects [26]. Chandrasegaran et al. aimed to review the product design process. They focused on a time frame of the last 20 years in general and the last decade more specifically, in order to balance the breadth and depth of the review, relaxing the time frame where it was necessary to look further in the past to establish relevance [27]. Rocca presented a broad technological review of knowledge-based engineering (KBE) in the attempt to fill the current information gap. In this study, the artificial intelligence roots of KBE are briefly discussed, and the main differences and similarities with respect to classical knowledge-based systems and modern general purpose CAD systems are highlighted. Finally he investigated evolution and trends of KBE systems and provided a list of recommendations and expectations for the KBE systems of the future [28]. Chen et al. aimed to develop a knowledge-based framework for the creative conceptual design of multidisciplinary systems through reusing and synthesizing known principle solutions in various disciplines together. The framework contained a formal constraints-based approach for representing the desired functions, a domain-independent approach for modeling functional knowledge of known principle solutions. The success of the system was explained with a design case study [29]. Lee et al. prepared a new and efficient collaborative intelligent

computer aided design (CAD) framework in a theoretical study. Their study made an effort for minimizing redundant design stages and design bottlenecks using the design history, while a lot of collaborative CAD frameworks aimed at decreasing the waiting time for updating design among collaborative designers. Also, it generated an efficient reverse-engineered process, while resolving other existing collaborative design issues [30]. Wang et al. presented a new approach of parametric collaborative design based on the analysis of the many disadvantages in serial design for concurrent engineering and developed an overhead travelling crane's parametric collaborative design system for concurrent engineering. The feasibility, availability, and effectiveness of the system were validated by the results obtained from the case study [31]. Wang et al. presented the solution of collaborative simulation environment (CSE) and analyzed its function framework and system architecture. They researched multihierarchy engineering data management (EDM) and simulation flow control. Then, the flow model platform and web portal of some suspension systems CSE were developed in the paper. Finally, they proposed that the product simulation period was shortened and the design efficiency was increased [32]. Zhang et al. proposed an intelligent design system for complex mechanical product. The intelligent design system adopted product family case tree to construct the model of complex mechanical product and case-based reasoning technology to reuse successful product design knowledge. Product design system was constructed by using the engineering database technology. After that, they realized the intelligent crane design platform by Visual Basic.NET programming, and so, saw that the application example demonstrated the feasibility of the approach [33].

This study is part of a comprehensive project which has many subsystems. Here, the general framework of the project is described, and the integration of the subsystems is focused on. When all the processes about the project are completed, it can operate as an intelligent interactive system. In this study, the subsystems such as design, analysis, computation, and rapid prototyping are prepared, and each of them can fulfill its function now. It is an important prerogative of the study that the user can realize all the processes on a single platform. The users can utilize both subsystems individually and can utilize the whole system with little user intervention for now. On the other hand, the system has a suitable structure for users of all levels because all design and prototyping tools used in the system are chosen from practical applications. This case is a difference of the system too. At the same time, the system uses the current training materials; therefore, this study can be used for the training of machine design with small adaptations. This also is another distinctive feature of this study. This study provides an intermediary to integrated different engineering tools such as CAD/CAM packages, technical computing and analysis packages, and databases and knowledge bases. This study is organized as follows: at first, an introduction and literature review are presented. Section two gives a background about the engineering design process. Section three illustrates integrated design system (IDS). Section four presents an implementation of IDS, and section five describes the conclusions of the study and future works.

2. Background of the Engineering Design Process

Engineering design can be defined as the realization of a product which satisfies a certain need [17]. In other words, the first objective of any engineering design project is the fulfillment of some human need or desire. Engineering may be described as a judicious blend of science and art, in which natural resources, including energy sources, are transformed into useful products, structures, or machines that benefit humankind [34]. It is a good design if its product works efficiently and economically within the imposed constraints. The major constraints are cost, reliability, safety, level of performance, legal requirements, sociological considerations, pollution, and energy consumption. Also, engineering design is not a process consisting of only one phase. On the contrary, it is an iterative process involving a series of decision-making steps where each decision establishes the framework for the next one. It is a continuum effort which embodies stages such as preliminary design, intermediate design, detail design, and development. The engineering design process starts with product specification and goes through an interactive process of requirements analysis, conceptual design, detailed design, and design analysis, and it ends with a functional product that fulfills the product specification [9]. Each stage has submodules that are different from each other, and therefore a designer is not expected to be an expert on all stages. However, a successful designer either should be able to communicate effectively with various specialists in the different stages or should utilize an integrated system consisting of expert systems corresponding to design stages. The present study considers detail design and purposes to develop an integrated design system.

3. Integrated Design System (IDS)

The IDS is the detail design module of the model of integrated design system for mechanical design. The flow chart of the IDS is in Figure 1 and its input screen is in Figure 2. The IDS involves submodules such as calculation, analysis, modeling and drawing, rapid prototyping, and library as seen in Figure 3.

All modules are interactive with each other. The calculation module of the IDS is used for engineering calculation, such as dimensions of machine elements and the calculating of the design safety stress. The 3D modeling and 2D drawing of the products can be prepared by using the design module of the IDS. This module uses CAD/CAM software packages such as SolidWorks and Catia. The analysis module of the IDS can perform the numerical analysis of the mechanical system using finite element methods such as Abaqus and Ansys. The library module of the IDS consists of material database, standard tables and diagrams, systematic technical knowledge and firm catalogues and supports the other modules. The final product of the design process can be transformed into a real physical model by using rapid prototype module of the IDS.

Knowledge Representation and Data Transfer of Integrated Design System (IDS). Automatic data transfer between

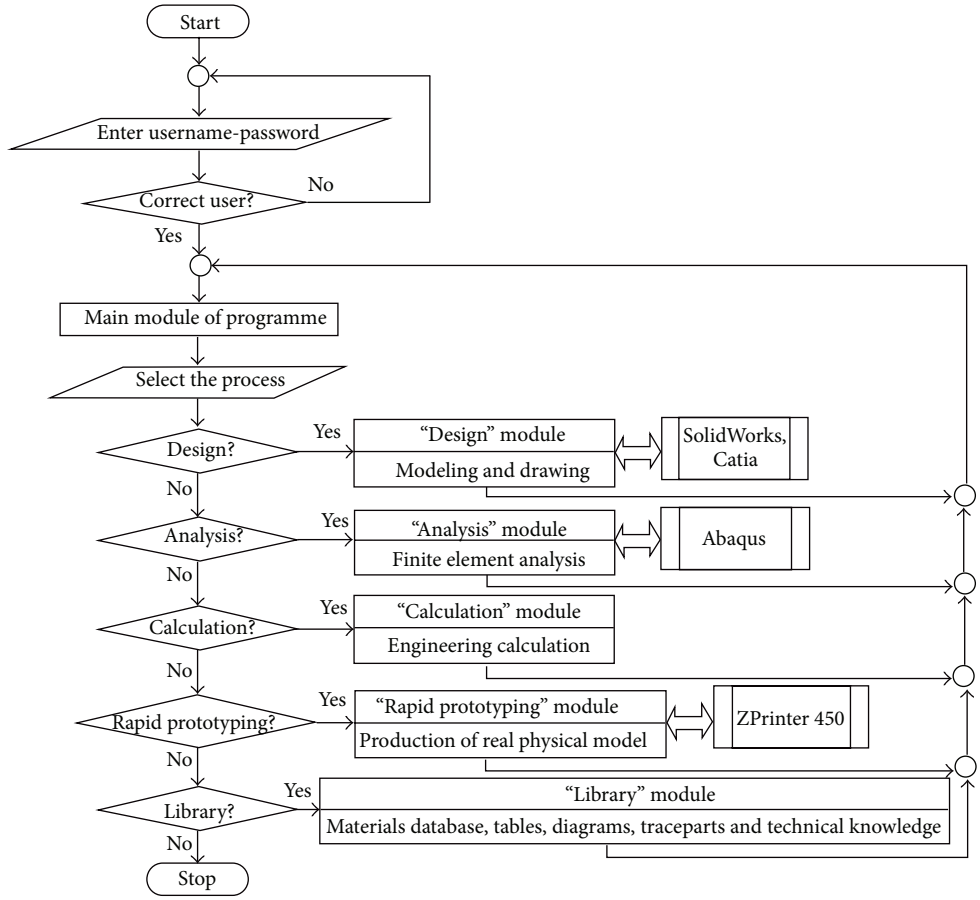

Figure 1: The flow chart of the IDS.

Figure 2: The input screen of the IDS.

Figure 3: The user interface of the IDS.

the units has been carried out using the software agents. In the study, software agents are programs that can perform specific design tasks for a user and possesses a degree of intelligence that permits it to perform parts of its task autonomously and to interact with its environment in a useful manner. There are software agents for each task, and so it can be possible to transfer the knowledge and to use it collectively. The communication and coordination between agents requires a standard knowledge protocol. For this reason, the knowledge exchange schemes and the knowledge forms have been prepared. The design knowledge is determined into specific codes. This knowledge is categorized into main articles and subarticles according to their themes. Also, the activities of knowledge exchange between agents have been categorized and have been prepared into certain formats, such as from who to whom, what is the purpose, and what is the answer. The knowledge protocol layers, which are used by agents of mechanical design, consist of definition, query, and result layers. This knowledge protocol is presented in Figure 14. It is very important that the design knowledge must be prepared into suitable documents so that they can be converted to

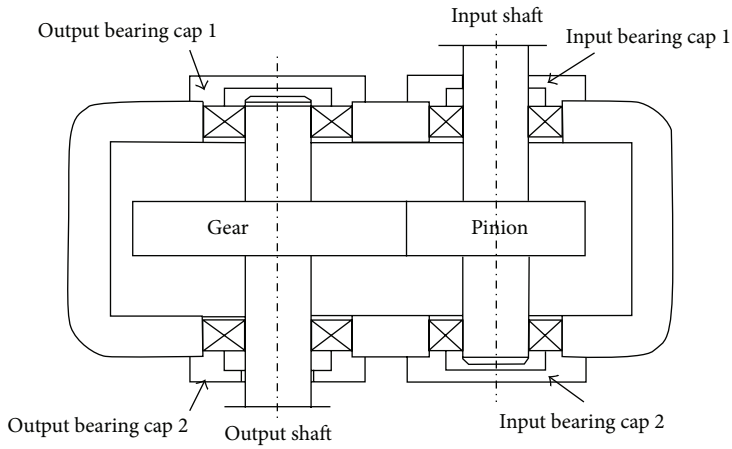

Figure 4: Layout of one-stage gearbox.

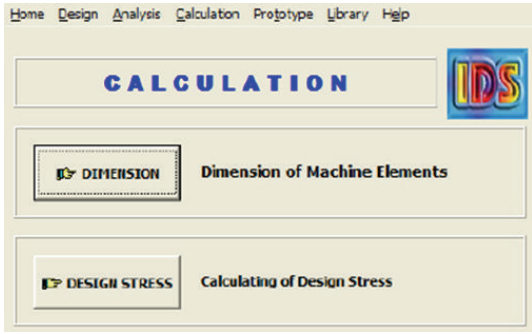

Figure 5: The calculation module of the IDS.

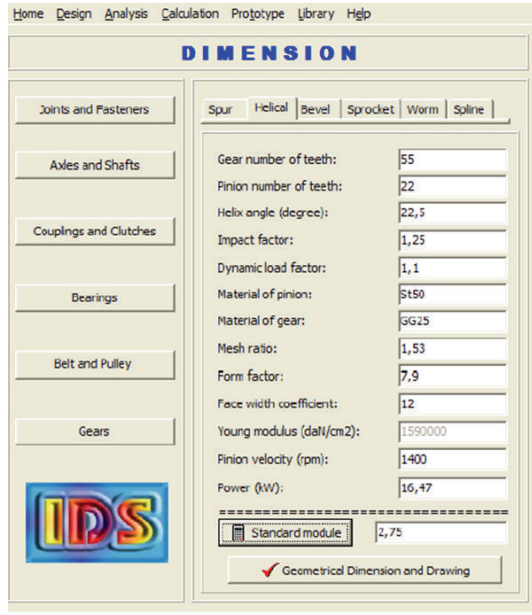

Figure 6: The screen of the gear pair.

digital signals easily because the knowledge stream is in digital form. Therefore, the documents which are the defining address of the knowledge and its position number have been prepared.

4. Implementation of the Integrated Design System

In this study, the design of one-stage gearbox with helical gear has been chosen as a design case study to illustrate and test the developed system. The aim of this section is to use the developed system for the complete design and analysis of the gearbox. The gearboxes are used to transmit power and to change speed, and these have an extensive application area such as materials handling, transportation, metallurgical, and chemical engineering. Also, the gearboxes contain the principal machine elements such as gears, shafts, bearings, bearing caps, bolts, and keys and represent a comprehensive mechanical system. Therefore, the gearbox has been selected for this case as an example. Figure 4 shows the layout of the gearbox.

The graphic user interface (GUI) has been prepared to allow the user to select the design stages (Figure 3). First, the dimensions of each element of the gearbox are calculated. Then, these are drawn according to the calculated dimensions. After, these elements are analyzed and the part dimensions are considered again in case of need. The assembly of the gearbox is realized finally. The last stage of the design process is prototyping the whole gearbox together with all the elements. The use of the IDS has been described in accordance with the elements of the gearbox, which is shown in Figure 4.

4.1. Gear Design. The design of the gear pair begins with the calculation of the gear dimensions, and so the calculation module has been selected from GUI, and then a new window is opened as seen in Figure 5.

The calculation module consists of the dimension and the design stress submodules. When the dimension module is selected from here, second new window containing the machine elements is open, as shown in Figure 6. Again,

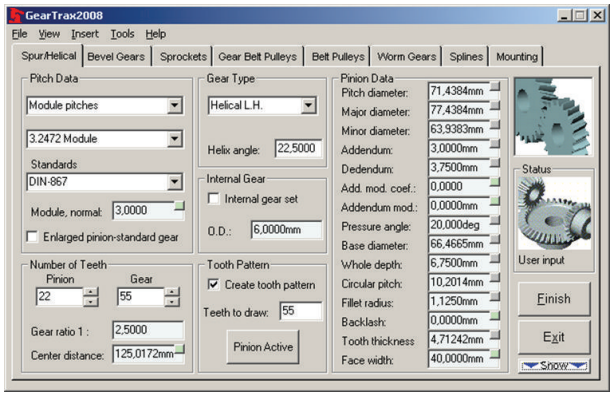

Figure 7: The screen for the geometrical dimension and drawing of the gears.

the gears are selected from this window and the input data of the gear pair are entered.

In the calculation of the gear mechanism, the pinion has been considered because it is forced more than the other gear. The corresponding gear can be selected accordingly [6]. The module of the gears (m) is calculated using the equations according to bending stress and contact stress as shown in the following.

The module according to bending stress:

$$m_{n1} = 6 \cdot \sqrt[3]{\frac{k \cdot \zeta \cdot M_b \cdot \gamma_n \cdot \cos \beta_0}{Z_1 \cdot \sigma_{em} \cdot \psi \cdot \varepsilon_p}}, \quad (1)$$

and the module according to contact stress:

$$m_{n2} = 9 \cdot \sqrt[3]{\frac{k \cdot \zeta \cdot M_b \cdot E\,(i+1) \cdot \cos^4 \beta_0}{Z_1 \cdot P_{em} \cdot i \cdot \psi \cdot \varepsilon_p}}. \quad (2)$$

The design of the gears is done in two steps: step 1 is to determine the module and step 2 is to calculate the geometrical dimensions and drawing. The module of the gears can be easily determined when the input data of the gear pair are entered and the standard module icon is clicked, as shown in Figure 5. The IDS calculates the module (m) by means of (1) and (2). The system accepts the maximum of two values obtained from equations as the module (m) and selects standard module. When the geometrical dimension and drawing icon is clicked, the new window is opened for entering geometrical data, as seen Figure 7.

GearTrax is a submodule of the SolidWorks software package and is used for the geometrical dimension and drawing of the gears. The designed gears are presented in Figure 8. The design of shafts, the bearings, and the keys is achieved in two stages, as the dimensional calculating and geometrical forming. The geometrical forming of these elements depends on each other, and so this process is postponed until the second stage.

4.2. Shaft Design. There are two shafts belonging to the pinion and the gear in the assembly of the gearbox. The design methods of these shafts are the same as each other. Therefore, one of these is described more in detail than the other. The diameter of the shaft can be automatically calculated using the dimension module of IDS. When the axles and shafts icon of this module is clicked, a new window is opened, as shown in Figure 9. In this window, if the input parameters of the shaft are written, the diameter of the shaft can be obtained. The shafts are forced by the combined torsion and bending load because these are required to transmit the torque, as well as withstanding the bending stresses due to the gear teeth loads and bearing reactions. The shafts are modeled as beam elements, and so their diameters are calculated. The diameter of the shaft (d) is given by

$$d = \sqrt[3]{\frac{32 \cdot M_B}{\pi \cdot \sigma_{em}}}, \quad (3)$$

where M_B is combined moment and σ_{em} is safety stress. The combined moment consists of the bending moment M_e and the twisting moment M_b and it is given by

$$M_B = \sqrt{M_e^2 + \frac{1}{2} M_b^2}. \quad (4)$$

4.3. Bearing Design. The use of the radial ball bearing is suitable. The gearbox has two shafts as the input shaft and the output shaft, and four bearings are required for these shafts. Because the load is applied from the middle of the shaft, the bearings belonging to the same shaft are forced with the same loading value. Therefore, the bearings to be selected are two types for the input shaft and the output shaft. The bearings can be selected by using the axles and shaft icon of the dimension module of IDS, as seen in Figure 10.

When the bearing parameters are entered and the select icon is clicked, the calculation of the bearing is realized and the suitable bearing can be selected. For this process, the principal bearing equations used by the software of the IDS are as follows. For the deep grove ball bearing the equivalent dynamic load, F_{es} is given by

$$F_{es} = X \cdot F_r + Y \cdot F_a, \quad (5)$$

where X, Y, F_r, and F_a are radial factor, thrust factor, radial force, and axial force, respectively.

The basic dynamic load rating is

$$C = F_{es} \sqrt[3]{L}, \quad (6)$$

where L is life of bearing. Finally, IDS selects the suitable bearing according to the diameter of the shaft and the dynamic load rating from the catalogue in the library module of the IDS.

4.4. Key Design. When power is supplied from the rotating shaft, it is necessary to attach gears to the shaft. To prevent relative rotation between the shaft and the gear, the connection between the gears' hub and the shaft must be secured [35]. Here, the parallel key is used to prevent relative rotation. Recommendations for key width and height, as a function

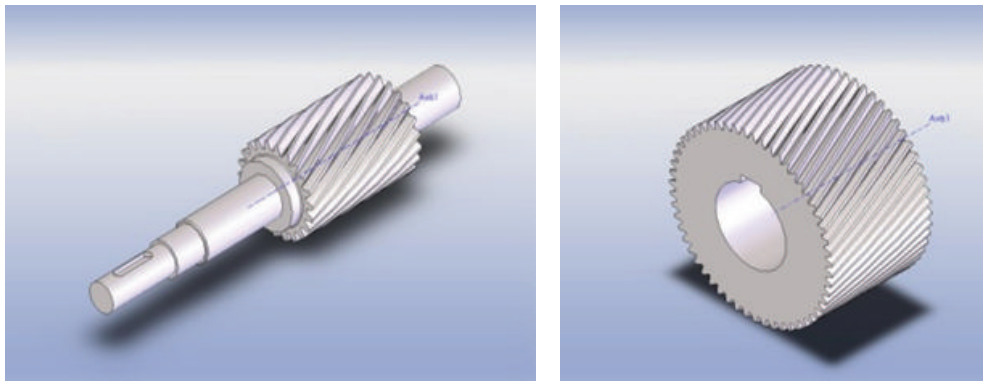

(a) (b)

Figure 8: The designed gears: (a) the pinion and (b) the gear.

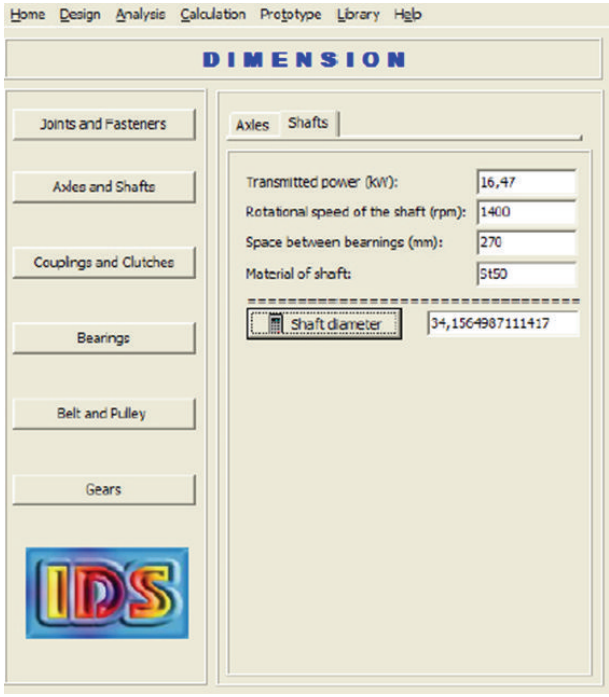

Figure 9: The calculation screen of the shaft diameter.

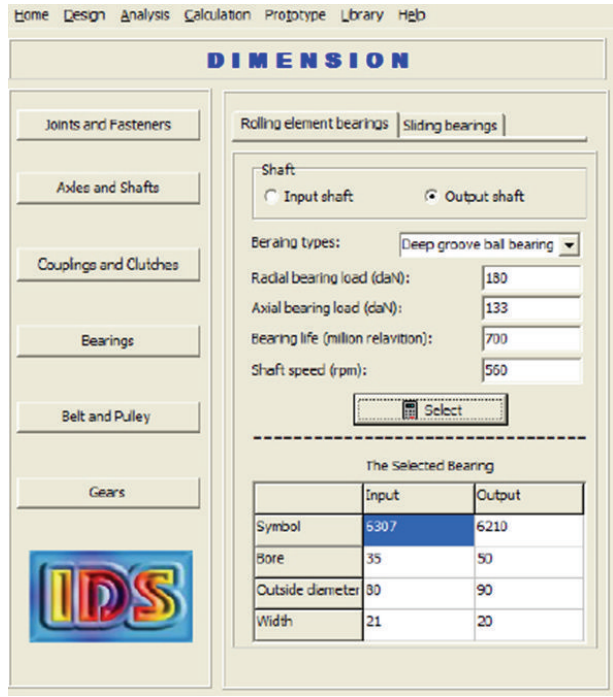

Figure 10: The screen for the selection and the design of the bearings.

of shaft diameter, are provided by standards, as shown in Figure 11. The key length (l) is obtained as a function of the transmitted torque. The key is forced by the shearing stress and the comprehensive bearing stress. Therefore, the calculation of the key length is based on these stresses. These processes about the key are realized by the dimension module of the IDS, as shown Figure 11.

4.5. Geometrical Forming and Assembly. The geometrical forming of the parts of the gearbox and their assembly are achieved by the design module of the IDS. This consists of two submodules such as SolidWorks and Catia for present, as seen in Figure 12.

SolidWorks is used for the current study, and the assembly of the gearbox into 3D is presented, as seen in Figure 13. Due to pages limitation of the paper, the analysis and rapid prototyping module of the IDS could not be discussed. However, the numerical analysis of the designed products can be carried out, and both the elements and the assembly of the gearbox can be produced as a prototyping by using ZPrinter 450 machine connected to the IDS.

5. Conclusion

This study is the first part of a comprehensive project which has many subsystems. Here, the general framework of

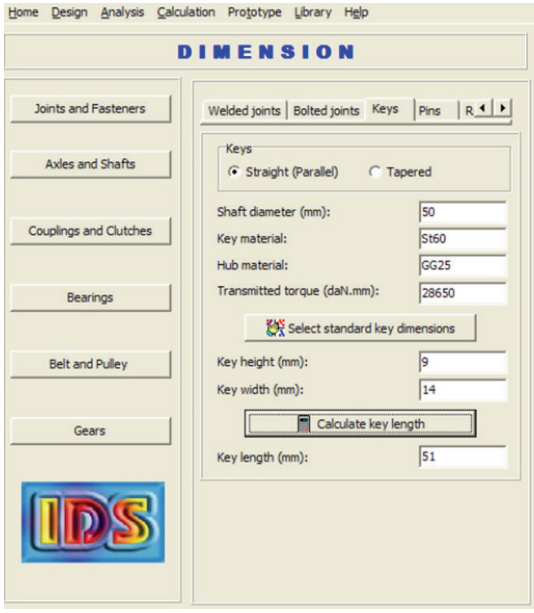

Figure 11: The screen for the key design.

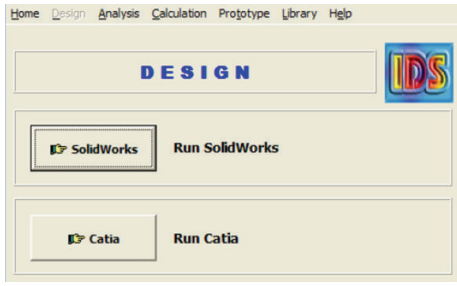

Figure 12: The design module of IDS.

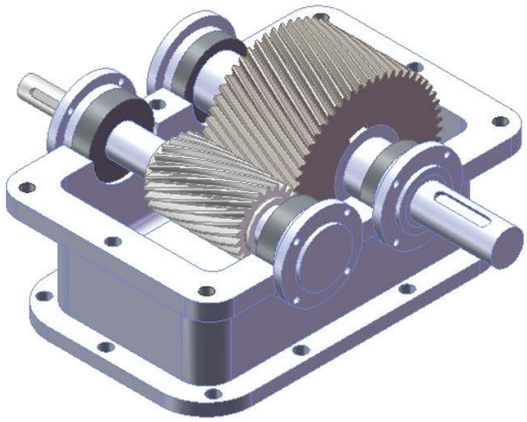

Figure 13: The assembly of the gearbox.

the project is described and the integration of the subsystems is prepared. When all processes related to the project are completed, it can operate as an intelligent interactive system. In this study, the subsystems such as design, analysis, computation, and rapid prototyping are prepared, and each of them

From		To		Definition
0101		0104		
Aim	Question		Task	Query layer
0 (question)	001		001	
	002		002	
	003		003	
1 (answer)				
2 (knowledge)				
Knowledge source	Response status		Response signal	Response layer
D0104020803	01		01 (done)	
D0104020301				
...				
...	02		02	
...				
	00		00 (wait)	

Figure 14: The knowledge protocol.

can fulfill its function now. It is an important prerogative of the study that the user can realize all the processes on a single platform. The users can utilize both subsystems individually and can utilize the whole system with little user intervention for now. On the other hand, the system has a suitable structure for users of all levels because all design and prototyping tools used in the system are chosen from practical applications. This case is a difference of the system too. At the same time, the system uses the current training materials; therefore, this study can used as a course tool for the training of machine design if the small adaptations are realized on the system. This also is another distinctive feature of this study. Also, all stages of the design of the gearbox have been achieved by using the IDS only, and so the IDS has been tested. It is expected that the IDS will be a favorable computer aided tool for industrial users because it reduces the design cost, design errors, and time to market. The next works about this subject will be focused on the intelligent features of the system.

Nomenclature

M_b: Torsional moment, N·m
E: Elasticity module, Pa
β_0: Helix angle, radians.

Subscripts

k: Impact factor
ζ: Dynamic load factor
Z_1: Number of teeth of gear
ψ: Dimension factor
ε_p: Engage ratio
γ_n: Form factor
i: Gear ratio.

References

[1] B. Lees, C. Branki, and I. Aird, "A framework for distributed agent-based engineering design support," *Automation in Construction*, vol. 10, no. 5, pp. 631–637, 2001.

[2] D. Su and M. Wakelam, "Intelligent hybrid system for integration in design and manufacture," *Journal of Materials Processing Technology*, vol. 76, no. 1–3, pp. 23–28, 1998.

[3] G. Zhao, J. Deng, and W. Shen, "CLOVER: an agent-based approach to systems interoperability in cooperative design systems," *Computers in Industry*, vol. 45, no. 3, pp. 261–276, 2001.

[4] Q. Hao, W. Shen, Z. Zhang, S.-W. Park, and J.-K. Lee, "Agent-based collaborative product design engineering: an industrial case study," *Computers in Industry*, vol. 57, no. 1, pp. 26–38, 2006.

[5] S. Myung and S. Han, "Knowledge-based parametric design of mechanical products based on configuration design method," *Expert Systems with Applications*, vol. 21, no. 2, pp. 99–107, 2001.

[6] V. Ramamurti, P. Gautam, and A. Kothari, "Computer-aided design of a two-stage gearbox," *Advances in Engineering Software*, vol. 28, no. 1, pp. 73–82, 1997.

[7] X. F. Zha and H. Du, "A PDES/STEP-based model and system for concurrent integrated design and assembly planning," *Computer-Aided Design*, vol. 34, no. 14, pp. 1087–1110, 2002.

[8] T. A. Chiang, A. J. C. Trappey, and C. C. Ku, "Using a knowledge-based intelligent system to support dynamic design reasoning for a collaborative design community," *International Journal of Advanced Manufacturing Technology*, vol. 31, no. 5-6, pp. 421–433, 2006.

[9] J. C. H. Chung, T.-S. Hwang, C.-T. Wu et al., "Framework for integrated mechanical design automation," *Computer-Aided Design*, vol. 32, no. 5, pp. 355–365, 2000.

[10] W.-Y. Liang and P. O'Grady, "Design with objects: an approach to object-oriented design," *Computer-Aided Design*, vol. 30, no. 12, pp. 943–956, 1998.

[11] X. F. Zha, H. J. Du, and J. H. Qiu, "Knowledge-based approach and system for assembly oriented design—part I: the approach," *Engineering Applications of Artificial Intelligence*, vol. 14, no. 1, pp. 61–75, 2001.

[12] K.-Z. Chen, X.-A. Feng, and L. Ding, "Intelligent approaches for generating assembly drawings from 3-D computer models of mechanical products," *Computer-Aided Design*, vol. 34, no. 5, pp. 347–355, 2002.

[13] A. M. Daabub and H. S. Abdalla, "Computer-based intelligent system for design for assembly," *Computers and Industrial Engineering*, vol. 37, no. 1, pp. 111–115, 1999.

[14] J. X. Wang, M. X. Tang, L. N. Song, and S. Q. Jiang, "Design and implementation of an agent-based collaborative product design system," *Computers in Industry*, vol. 60, no. 7, pp. 520–535, 2009.

[15] H. Wang and H. Zhang, "A distributed and interactive system to integrated design and simulation for collaborative product development," *Robotics and Computer-Integrated Manufacturing*, vol. 26, no. 6, pp. 778–789, 2010.

[16] D. Karayel, R. Keles, and S. S. Ozkan, "A reference model of multi agent system mechanical design," in *Proceedings of the 4th International Symposium on Intelligent and Manufacturing Systems (IMS '04)*, pp. 359–368, 2004.

[17] D. Karayel, S. S. Ozkan, and F. Vatansever, "Determination of factors affecting safety stress in machine design by using artifical intelligence technologies," in *Proceedings of the 3rd International Conference Mechatronic Systems and Materials Conference*, 2007.

[18] D. X. Cao and M. W. Fu, "A knowledge-based prototype system to support product conceptual design," *Computer-Aided Design and Applications*, vol. 8, no. 1, pp. 129–147, 2011.

[19] D. X. Cao, N. H. Zhu, C. X. Cui, and R. H. Tan, "An agent-based framework for guiding conceptual design of mechanical products," *International Journal of Production Research*, vol. 46, no. 9, pp. 2381–2396, 2008.

[20] Goel, A. K, Vattam, S, B. Wiltgen, and M. Helms, "Cognitive, collaborative, conceptual and creative-four characteristics of the next generation of knowledge-based CAD systems: a study in biologically inspired design," *Computer-Aided Design*, vol. 44, pp. 879–900, 2012.

[21] X. Chen, S. Gao, Y. Yang, and S. Zhang, "Multi-level assembly model for top-down design of mechanical products," *Computer-Aided Design*, vol. 44, pp. 1033–1048, 2012.

[22] M. Jia, G. Ding, S. Qin, R. Li, and Y. He, "Research of design and analysis integrated information modeling framework for multibody mechanical system: with its application in the LHD design," *The International Journal of Advanced Manufacturing Technology*, vol. 66, pp. 2107–2122, 2013.

[23] A. Li, Y. Bian, Y. Liang, and Y. Zhu, "Integrated design for large-scale opto-mechanical structure," *Optica Applicata*, vol. 39, no. 2, pp. 383–389, 2009.

[24] Y. Zheng, H. Shen, and C. Sun, "Collaborative design: improving efficiency by concurrent execution of Boolean tasks," *Expert Systems with Applications*, vol. 38, no. 2, pp. 1089–1098, 2011.

[25] L. Zhongtu, W. Qifu, and C. Liping, "A knowledge-based approach for the task implementation in mechanical product design," *International Journal of Advanced Manufacturing Technology*, vol. 29, no. 9-10, pp. 837–845, 2006.

[26] A. Al-Ashaab, M. Molyneaux, A. Doultsinou et al., "Knowledge-based environment to support product design validation," *Knowledge-Based Systems*, vol. 26, pp. 48–60, 2012.

[27] S. K. Chandrasegaran, K. Ramani, R. D. Sriram et al., "The evolution, challenges, and future of knowledge representation in product design systems," *Computer-Aided Design*, vol. 45, pp. 204–228, 2013.

[28] G. L. Rocca, "Knowledge based engineering: Between AI and CAD. Review of a language based technology to support engineering design," *Advanced Engineering Informatics*, vol. 26, no. 2, pp. 159–179, 2012.

[29] Y. Chen, Z.-L. Liu, and Y.-B. Xie, "A knowledge-based framework for creative conceptual design of multi-disciplinary systems," *Computer-Aided Design*, vol. 44, no. 2, pp. 146–153, 2012.

[30] H. Lee, J. Kim, and A. Banerjee, "Collaborative intelligent CAD framework incorporating design history tracking algorithm," *Computer-Aided Design*, vol. 42, no. 12, pp. 1125–1142, 2010.

[31] Z. A. Wang, G. B. Yu, S. A. Wu, and H. A. Qin, "Parametric collaborative design of mechanical products for concurrent engineering," *Journal of Central South University*, vol. 44, no. 2, pp. 552–557, 2013.

[32] H. Wang, G. Liu, X. Yang, and Z. He, "Collaborative simulation environment for mechanical system design," *International Journal of Product Development*, vol. 13, no. 1, pp. 38–46, 2011.

[33] X.-L. Zhang, D.-M. Hu, and B.-G. Wu, "Research on knowledge-based design of complex mechanical product," *Journal of Dalian University of Technology*, vol. 50, no. 6, pp. 917–920, 2010.

[34] A. M. Farag, *Selection of Materials and Manufacturing Processes for Engineering Design*, Prenticel Hall International, Cambridge, UK, 1989.

[35] J. A. Collins, *Mechanical Design of Machine Elements and Machines*, John Wiley & Sons, New York, NY, USA, 2003.

Hindawi Publishing Corporation
Advances in Mechanical Engineering
Volume 2013, Article ID 932684, 13 pages
http://dx.doi.org/10.1155/2013/932684

Research Article

A Simulation Model Design Method for Cloud-Based Simulation Environment

Chunsheng Hu, Chengdong Xu, Guochao Fan, He Li, and Dan Song

School of Aerospace Engineering, Beijing Institute of Technology, Beijing 100081, China

Correspondence should be addressed to Chengdong Xu; xucd@bit.edu.cn

Received 12 April 2013; Revised 24 June 2013; Accepted 12 July 2013

Academic Editor: Yu-Shen Liu

Simulation technologies provide necessary validation tools for the conceptual design of complex products involving multiple disciplines. A variety of simulation models are developed in specific organizations or enterprises to verify the design plan, while they are hard to be shared and to be reused. Based on the analysis of several typical solutions to share and reuse different kinds of resources, a simulation model design method is proposed to provide a simple implementation of simulation model reuse for cloud-based simulation environment. This paper firstly creates the simulation models' metamodel and ontology for their universal description. Secondly, four rules are proposed to design/reprogram a simulation model into service-oriented form for its interoperability, and the ontology of service-oriented simulation model is established. Thirdly, the way to call one simulation model and the way to compose several simulation models into a simulation process are elaborated. Finally, a simple case of using this method to design an aircraft dynamic model is elaborated, and a prototype simulation system is constructed, and then a simple simulation process is composed to verify the practicability of the method. The result shows that the new design/reprogram method has big advantages on the compatibility, expansibility, and reusability despite the decreasing efficiency.

1. Introduction

The design process of modern product is a process in which uncertainties are gradually reduced, and it involves a series of iterative stages mainly including conceptual design, detailed design, simulation analysis, manufacturing, and sale. In this process, as much information as possible is gradually collected, and the engineers need to make design plan firstly and then improve them based on the information. The least amount of information is at the conceptual design stage which usually contains only some vague requirements, so engineers have to add a lot of background information by using variety of tools, their experiences, and their knowledge to get a solution to meet these requirements. As the starting point of the design process, the conceptual design puts significant influences on the subsequent stages, and its design result directly determines the consumptions of time, money, and manpower in the whole design process. For engineers, it is an eternal pursuit to reduce the number of iterations in the design process, and one of the efficient ways is to improve the quality of conceptual design.

Researches are carried out by scholars from different angles to improve the quality of the conceptual design, they typically include the quality function deployment (QFD), house of quality (HoQ), theory of inventive problem solving (TRIZ) and fuzzy set theory [1–7]. When some key parameters of a design plan in the conceptual design stage are determined, computer simulation technology is an efficient way to verify its validity. Different simulations in fact bring additional and hypothetical information which embedded in the simulation models to verify the design plan under some established conditions. Because most of the simulation models are mathematical, and they could be ran on some computer at small consumption of time and money, engineers develop variety of simulation models which plays an important role in specific organizations or enterprises.

With increasing degree of product complexity, more and more disciplines are involved and large-scale interdisciplinary collaboration design becomes mainstream. More and more simulation models are needed to perform different kinds of simulations, and some problems emerge, for example: (1) sometime, it is not possible to find a suitable

simulation model to do a simulation task, because an enterprise cannot have all the simulation models which are available only within some specific organizations or enterprises; (2) sometimes, it is hard to find a suitable simulation model to do a simulation task according to some requirements, because these models are managed out of order; (3) sometimes, it is hard to reuse existed simulation models, because they are programmed to be ran under specific environments; (4) sometimes, it is hard to put some simulation models together to perform a simulation process, because they are interdisciplinary and heterogeneous, and they are programmed by different people in different programming languages at different times. These problems mainly are caused by (1) limited application scope and low sharing degree of simulation models; (2) unordered management of simulation models; (3) high dependency to specific environment (operation system or software) of simulation models; (4) interaction difficulties of interdisciplinary heterogeneous simulation models.

Faced with similar problems, different groups made some specific attempts to achieve the goal of sharing and reusing different kinds of resources. Some typical solutions are listed as follows.

(i) Simulation model portability (SMP) [8] is an attempt to enable reuse and portability of simulation models between simulator applications. It is a standard for simulation models developed by European Space Agency (ESA) together with various stakeholders in the European space industry. SMP is based on the ideas of component-based design and model-driven architecture (MDA) as promoted by the Object Management Group (OMG) and is based on the open standards of UML and *XML*. The development of a simulation model and the run-time environment according to the SMP standard is very complicated, but good interaction between different models can be guaranteed, and a large-scale simulation process can be composed by using these simulation models quickly.

(ii) MyExperiment [9] is designed as a social web site for discovering, sharing, and curating scientific workflows and experiment plans. The MyExperiment builds a collaboratively supported workflow repository over the internet, and all the myExperiment services are accessible through simple representational state transfer (REST) programming interfaces. A developer can develop a workflow in specific development environment and share it on myExperiment. A user can find and download a workflow from myExperiment and then run it in Taverna [10] on his own computer.

(iii) NanoHUB [11] is designed to be a resource to the entire nanotechnology discovery and learning community. The NanoHUB collects simulation tools and flash-based animations/presentations from different groups or individuals and shares them over the internet. A developer can develop a simulation tool by using the Rappture Toolkit [12] and share it on the nanoHUB easily. A user can find a simulation tool and run it directly on the web page, and all the software needed for a user is just the Java for web browser.

(iv) RunMyCode [13] is a cloud-based platform allowing people to run computer codes associated with a scientific publication (articles and working papers) using their own data and parameter values. The RunMyCode is possible to create a companion website from a code written in R, Matlab, C++, Fortran, and Rats. A user can find and run a code directly on the web page, and the result is shown in the form of *.pdf.

While the above solutions have different emphases, their core concepts (sharing and reusing) are the same. A simple comparison of these solutions is shown as follows (Table 1).

Regardless of the involved or not involved specific cloud computing technologies, the MyExperiment, nanoHUB, and RunMyCode are all in line with the core concept of cloud computing which offers different kinds of resources as services for users over the internet [14, 15]. The cloud computing brings bright prospects for the resources sharing and reusing, and more and more scholars propose cloud-based simulation environment. The schema and paradigm of cloud-based environment are stated [16, 17]. The calling method of simulation models by using intelligent agent is proposed [18], and the integration method to plant existing simulation software into the cloud is studied [19]. These jobs are more concerned about the theory and some specific methods of this new concept. All these attempts are trying to build an ideal simulation environment in which all the interdisciplinary heterogeneous simulation models: (1) can be freely called within a large scope (over the internet); (2) can be managed orderly; (3) can be decoupled from specific environment (operation system or software); (4) can interact with each other easily.

The above solutions can be said to be some specific implementations for these goals; however, they only partially meet these goals. The SMP mainly achieves the fourth goal above, and it is powerless to the first three goals. Besides, the high development difficulty and limited application scope of SMP determine that it is not an efficient way to achieve the sharing and reusing simulation models. The MyExperiment achieves the first two goals, but it is highly dependent on some specific software. The nanoHUB and RunMyCode achieve the first three goals. While these resources (workflows/tools/codes) are being shared well over the internet, the MyExperiment, nanoHUB, and RunMyCode are not able to achieve the fourth goal, because these resources are designed without the consideration of interaction capability. It is obviouse that simulation processes cannot be composed freely by using simulation models which has no interaction capability with other simulation models.

In order to build a cloud-based simulation environment which can achieve these four goals, the most basic thing is to make the simulation models well designed for the sharing, reusing, and interaction, and there is almost no relevant work that pays attention on the design method of a simulation model. Aiming to provide a simple design method of simulation model for cloud-based simulation environment, this paper proposed a design/reprogram method. Section 2 creates the simulation models' metamodel and

Table 1: Comparison of typical sharing and reusing solutions.

Solutions	Main goals	Sharing scope	Typical reusing method	Reusing difficulty	Where the shared resources will run	Management mode	Users' dependencies	Development difficulty	Main development tools (language)	Interactive capabilities of different resources
SMP	Reusing simulation models in large-scale collaborative simulation	Within specific organization	Integrate the simulation models in an independent developed run-time environment	High	Uncertain	Dispersedly managed by different small groups	Specific simulation environment and tools	High	C++, Fortran	Strong
MyExperiment	Sharing scientific workflows	Over the internet	Download and run in Taverna	Medium	Users' computers	Centrally managed by MyExperiment	Taverna	High	Ruby, Taverna, Rails, MySQL, ImageMagick, RMagick, Graphviz, and so forth	No
NanoHUB	Sharing simulation tools	Over the internet	Run directly on the web page	Low	NanoHUb's hosts	Centrally managed by NanoHUB	Java for web browser	Medium	Rappture Toolkit	No
RunMyCode	Sharing computer codes	Over the internet	Run directly on the web page	Low	RunMyCode's hosts	Centrally managed by RunMyCode	Pdf plugin for web browser	Low	Matlab, C++	No

ontology for their universal description. In Section 3, four rules are proposed to design/reprogram a simulation model into service-oriented form for its interoperability, and the ontology of service-oriented simulation model is established. In Section 4, the way to call one simulation model and the way to compose several simulation models together into a simulation process are elaborated. In Section 5, a simple case of using this method to design an aircraft dynamic model is elaborated, and a prototype simulation system is constructed, then a simple simulation process is composed to verify the practicability of the method.

2. The Metamodel and Ontology of Simulation Model

In order to eliminate the ambiguity in this paper, the simulation model is defined as computer program or code programmed according to some formula, algorithm, or rules, it has fixed inputs, functions, parameters, and outputs, and it has many kinds of forms typically including *.exe, *.c, *.dll, *.lib, and *.m.

The characteristics of different simulation models are not the same. Some can run automated without human, and some take knowledge and experience of the people involved. Some do not have the ability to interact with the others, and some can directly read/write data from/to some specially formatted files. Some can be directly invoked, and some must be precompiled. Some depend on specific software environment, and some do not. Based on some common features, a metamodel of simulation model is represented as a seven-tuple: $M_i = \langle P_i, \mathrm{ID}_i, \mathrm{OD}_i, \mathrm{CC}_i, \mathrm{SC}_i, \mathrm{DC}_i, C_i \rangle$.

(1) $P_i = \{p_{i1}, p_{i2}, \ldots, p_{in}\}$ is a set of configurable parameters of one model. The parameters are defined in this paper as some data items that directly participate in the operation of the model, and they can be flexibly configured before a simulation, and they do not change during the simulation process. Each p_{ij} $(1 \leq j \leq n)$ can be described by its significant properties including name, index, data type, default value, range of value, and dimension.

(2) $\mathrm{ID}_i = \{\mathrm{id}_{i1}, \mathrm{id}_{i2}, \ldots, \mathrm{id}_{im}\}$ is a set of input data items of one model. The input data items are defined in this paper as some date items that directly participate in the operation of the model, and the values of these data items are changing with the simulation time's changing, and the values of these input data items can be obtained from different places including user's input, other models' output, and some global variables (e.g., global clock tick of time-driven simulation environment, global message of event-driven simulation environment). An input data items set is an ordered data block, and each id_{ij} $(1 \leq j \leq m)$ is marked by its name, index, data type, memory size and offset address, and so forth.

(3) $\mathrm{OD}_i = \{\mathrm{od}_{i1}, \mathrm{od}_{i2}, \ldots, \mathrm{od}_{io}\}$ is a set of output data items of one model. The out data items are defined in this paper as some data items for the recording of the operation results, and the values of these data items are generated by the calculation of the model according to its parameters and input data items. An output data items set is an ordered data block, and each od_{ij} $(1 \leq j \leq o)$ is marked by its name, index, data type, memory size and offset address, and so forth.

(4) $\mathrm{CC}_i = \{\mathrm{cc}_{i1}, \mathrm{cc}_{i2}, \ldots, \mathrm{cc}_{ip}\}$ is a set of control commands of one model. The control commands are defined in this paper as names of some functions that drive the status changing of this model. The typical control commands include initialization, start, step, pause, and end. Generally, the control commands are some functional gateway exposed by the model for the necessary controlling from the outside.

(5) $\mathrm{SC}_i = \{\mathrm{sc}_{i1}, \mathrm{sc}_{i2}, \ldots, \mathrm{sc}_{iq}\}$ is a set of static characteristics of one model. The static characteristics are defined in this paper as some properties that do not change with the changes of simulation process or simulation environment. The static characteristic typically includes model name, model version, model function, model accuracy, single-step-generated data size, and step range.

(6) $\mathrm{DC}_i = \{\mathrm{dc}_{i1}, \mathrm{dc}_{i2}, \ldots, \mathrm{dc}_{ir}\}$ is a set of dynamic characteristics of one model. The dynamic characteristics are defined in this paper as some properties that change with the changes of simulation process or simulation environmental. The dynamic characteristics typically includes calling method, calling path, and computation time in single-step.

(7) $C_i = \{c_{i1}, c_{i2}, \ldots, c_{is}\}$ is a set of applications (including operating system) and components that depend on one model.

The metamodel reflects the most essential features of simulation models without the consideration of specific implementation method. According to this metamodel, the ontology of simulation model can be established as shown in Figure 1.

3. The Service-Oriented Simulation Model

Once the metamodel of simulation model is created, it can be used to create a management system for the simulation models, and users can search appropriate simulation models according to their characteristics for different simulation tasks. If simulation models are chosen for simulations separately without the need of interaction between different models, there is no need to do any change to different kinds of simulation models, but there is need to construct different calling engines for them. But in most cases, different kinds of simulation models are needed to be composed together into a simulation process to do a specific simulation task, and some problems emerge including (1) some models have no ability to interact with others, and (2) while some models have the ability to interact with others, the interaction methods are not the same. So, some design/reprogram works and some design/reprogram rules are needed for the free

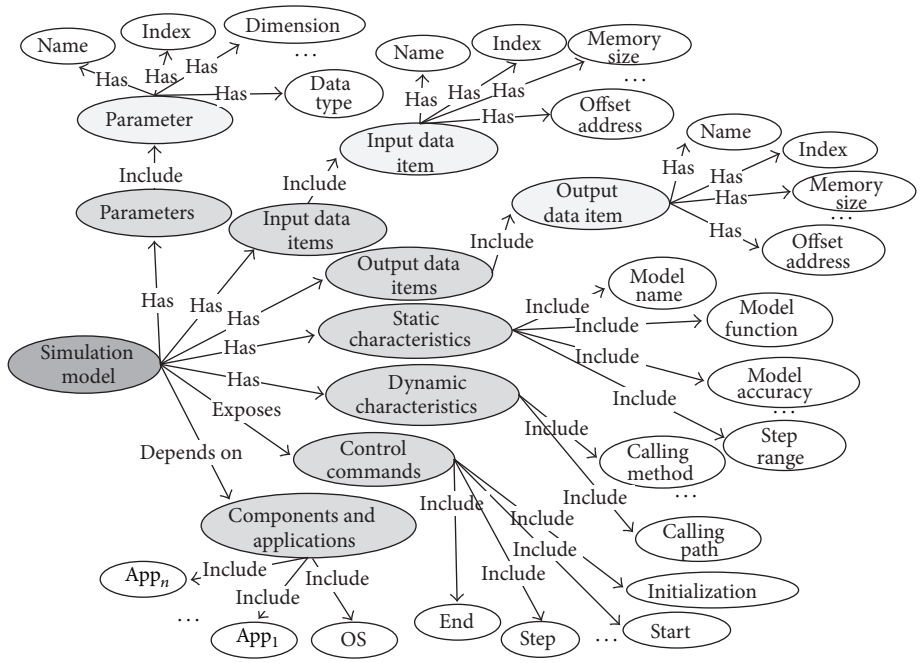

Figure 1: The ontology of simulation model.

interactions among different simulation models. Service-oriented architecture (SOA) can be a powerful technology for the design/reprogram work of simulation models.

SOA is proposed as a kind of architecture for developing distributed system by Gartner Group in 1996. It is a software design methodology based on structured collections of discrete software modules, known as services that collectively provide the complete functionality of a large or complex software application [20]. SOA separates functions into distinct units or services, which developers make accessible over a network in order to allow users to combine and reuse them in the production of applications [21]. SOA can achieve seamless combination and interaction between heterogeneous applications/programs/modules through the well-defined interfaces, contracts and by passing data in a well-defined, shared format [22]. It is a proper way to design/reprogram a simulation model into a SOA-based service.

As a software design methodology, there are many SOA implementation methods. Take the Windows Communication Foundation (WCF), for example, for the above meta-model, where the general strategy is to define the P_i, ID_i, and OD_i as data contract, to define the CC_i as operation contract, to define the message contract, fault contract, and service contract, and then publish these contracts by metadata through a uniform resource identifier (URI). When a user wants to compose several simulation models together into a simulation process, he needs to find these models and get their contacts through their URIs, and then write a program to call these models without rewriting them. Despite the fact that programming workload will be more less than rewriting all the models, there are still some annoying programming works such as defining different classes and data structures for the parameters described in the operation/data contract of different models. The problem is caused by the need of getting the data structure in the model and the need of passing parameters to the model's operations. To eliminate these programming works, a set of rules are proposed to construct a simulation model.

(1) Each model has one named *modelOnto.xml file*, in which all the information shown in Figure 1 is recorded. According to this file, details about a simulation model can be easily parsed and stored into a models database.

(2) Each model has one named *dataInterRela.xml* file and its structure as shown in Algorithm 1.

This file records a set of **.xml* file paths marked by <From></From> or <To></To>. All the parameters corresponds to one **.xml* file, while each input/output data item corresponds to one **.xml* file. These **.xml* files are used as the intermediate files for the data interaction between different models, and these **.xml* files' structures are very simple (see Algorithm 2).

It is noteworthy that multiple input/output data items could point to one same file.

(3) Each model exposes an "*init*" function to read the *dataInterRela.xml* to get all the paths of data interaction files.

(4) Each model exposes a "*step*" function to drive it to get parameters and input data from the corresponding **.xml* files pointed by the file paths mentioned in rule 3, does calculation, and puts output data into the corresponding **.xml* files.

These rules can be described by Figure 2.

```
<DataInteRela>
  <Parameters>
    <From>FileDirectory/FileName.xml</From>
  </Parameters>
  <InputDataItems>
      ......
      <InputDataItem Id="......">
        <From>FileDirectory/FileName.xml/NodeID</From>
      </InputDataItem>
      ......
  </InputDataItems>
  <OutputDataItems>
      ......
       <OutputDataItem Id="......">
         <To>FileDirectory/FileName.xml/NodeID</To>
       </OutputDataItem>
       ......
  </OutputDataItems>
</DataInteRela>
```

Algorithm 1

```
<InteractionRelation>
  <Datas>
      ......
      <Data Id="......">
        <DataType>......</DataType>
        <Value>......</Value>
      </Data>
      ......
  </Datas>
</InteractionRelation>
```

Algorithm 2

When a simulation model is designed or reprogrammed in accordance with these rules, only service contract and operation contract are needed to be defined, and there is no need to pass values for the operation contract, so there is no need to define the data contract. All the work to call a simulation is to operate some fixed format temporary *.*xml* files, and this work can be easily done by some XML parser and XML generator.

The ontology of service-oriented simulation model can be established as shown in Figure 3.

There are three main parts to describe a service-oriented simulation model: the "*Model Ontology*" is employed to describe the most essential information mentioned in Section 2 of a simulation model without the service-oriented implementation, and the model ontology is recorded and presented by the "*modelOnto.xml.*" The "Interactions" is employed to describe the data interaction relationships which are defined as the mapped relationships among multiple *.*xml* files and the parameters/input/output data items, and these mapped relationships are recorded and presented by the "*dataInterRela.xml.*" The "Service Profile" is employed to describe the service information of service-oriented simulation model, and the service information is usually recorded and presented by a "*ServiceConfig.cfg*" based on specific SOA implementation method.

Based on the concept above, the overall architecture of a service-oriented simulation model is shown in Figure 4.

A service-oriented simulation model should include four parts: (1) a hosting process (*.exe or IIS) which hosts the specific implementation of a simulation model; (2) a "*Service-Config.cfg*" file which controls the EndPoint exposed by this service-oriented simulation model; (3) a "*modelOnto.xml*" file which describes the information of the simulation model; and (4) a "*dataInterRela.xml*" which records the mappings between all parameters/input/output data items and some temporary generated *.*xml* files.

In a classic service-oriented architecture, the EndPoint is used to expose the details of a service. The EndPoint includes three parts: (1) the Address identifies a URL where the service can be found, (2) the Binding identifies what communication ways should be used to access this service, and (3) the Contract identifies what operations can this service do through the interfaces defined in this service. There are two interfaces in the specific implementation of a simulation

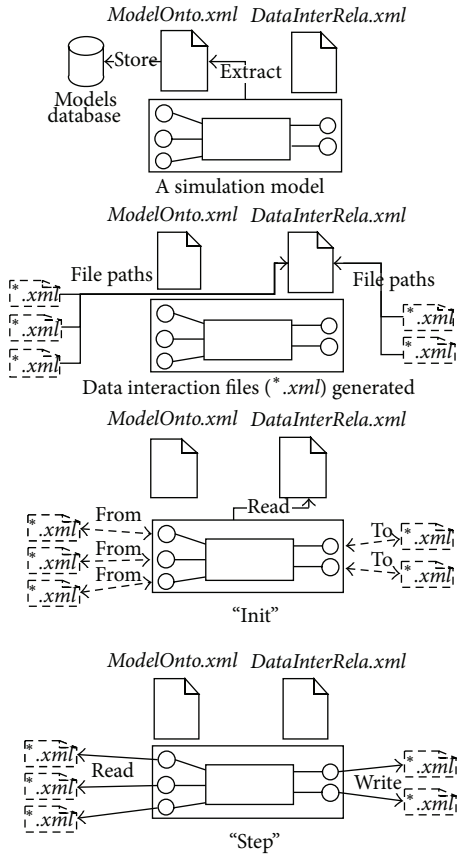

Figure 2: Four rules to design/reprogram a simulation model.

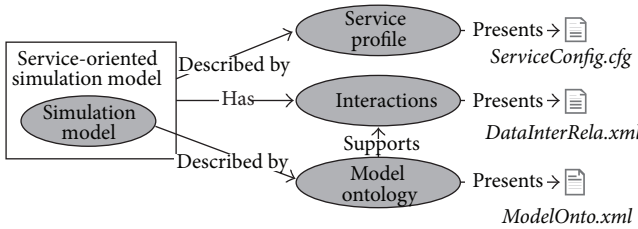

Figure 3: The ontology of service-oriented simulation model.

model: (1) the *IModel* exposes the main operations expressed as OperationContract; (2) the *ImodelCallBack* is used to expose the callback states of the two operations include *init()* and *step()*. The main logic of *init()* and *step()* is shown in Algorithm 3.

When some service-oriented simulation models are built, a service consumer client can be constructed to manipulate these models. A ModelController can be built to read and edit the *modelOnto.xml* file to manipulate the information of a model. A ServiceController can be built to read, edit, and delete the *ServiceConfig.cfg* to manipulate the information of this service, and it can control the service to Start or Stop. A ModelController can be built to drive a model to *init()* or *step()*. Based on these basic function modules, more function modules can be built in the service consumer client, for example, the Service Manager to control all the services, the ModelManagere to control all the models information. This paper will not go into detail contents of the Client because it is not the focus.

4. The Calling of Simulation Models

When a simulation model is programmed into its service-oriented form according to the rules above, it needs to be registered to a simulation models registry as the UDDI (Universal Description, Discovery and Integration) registry. In this Simulation Models Registry, in addition to the description, discovery and integration of simulation models, there is a very important task to establish coarse-grained classification rules in a specific field to support the model searching and model matching for users. Users can search a simulation model or some simulation models according to these coarse-grained rules and then get further information about it/them by reading the database or by parsing the corresponding *modelOnto.xml* files.

If only one simulation model is selected and to be called, a dynamic user input interface which contains the P_i and ID_i, a temporary *input.xml* and a temporary *output.xml* in a structure described in Section 3 are generated, and the paths of the *input.xml* and *output.xml* are wrote into the model's *dataInterRela.xml*; the user input interface will collect the user's inputs and write them into the *input.xml* and then drive the model to get these data and do calculation; the results will be written into the *output.xml*. The data interact process is as shown in Figure 5.

When several simulation models are selected to compose a simulation process, the data interaction relationships among these models need to be configured manually, and each data interaction relationship can be expressed as a mapping from one model's one output data item to another model's one input data item. Finally, a simulation process SP_i $(i \in N)$ can be represented as a five-tuple: $\mathrm{SP}_i = \langle \mathrm{SPC}_i, \mathrm{SPM}_i, \mathrm{SPMR}_i, \mathrm{SPS}_i, \mathrm{SPE}_i \rangle$.

(1) $\mathrm{SPC}_i = \{\mathrm{spc}_{i1}, \mathrm{spc}_{i2}, \ldots, \mathrm{spc}_{in}\}$ is a set of characteristics of the simulation process. They typically include the process name, simulation purpose, step length, start time, and end time.

(2) $\mathrm{SPM}_i = \{M_{i1}, M_{i2}, \ldots, M_{in}\}$ is a set of models employed in the simulation process. Each $M_{ij} = \langle P_{ij}, \mathrm{ID}_{ij}, \mathrm{OD}_{ij}, \mathrm{CC}_{ij}, \mathrm{SC}_{ij}, \mathrm{DC}_{ij}, C_{ij} \rangle$ $(i \in N,\ 1 \leqslant j \leqslant n)$.

(3) $\mathrm{SPMR}_i = \{\mathrm{MR}_{i1}, \mathrm{MR}_{i2}, \ldots, \mathrm{MR}_{im}\}$ is a set of data interaction relationships among these modules. The SPMRi is a set of mappings between the collection of all models' outputs $O_i = \{\mathrm{OD}_{i1}, \mathrm{OD}_{i2}, \ldots, \mathrm{OD}_{in}\}$ and the collection of all models' inputs $I_i = \{\mathrm{ID}_{i1}, \mathrm{ID}_{i2}, \ldots, \mathrm{ID}_{in}\}$, and $\mathrm{SPMR}_i : O_i \rightarrow I_i$. Each MR_{ij} $(i \in N,\ 1 \leqslant j \leqslant m)$ is a rule point from a model's one output to another's one input, $\mathrm{MR}_{ij} : \mathrm{od}_{irk} \rightarrow \mathrm{id}_{isl}$ $(\mathrm{od}_{irk} \in \mathrm{OD}_{ir}, \mathrm{OD}_{ir} \subset O_i, 1 \leqslant r \leqslant n, k \in N, \mathrm{id}_{sl} \in \mathrm{ID}_s, \mathrm{ID}_s \subset I, 1 \leqslant s \leqslant n, l \in N, i \in N, r \neq s)$.

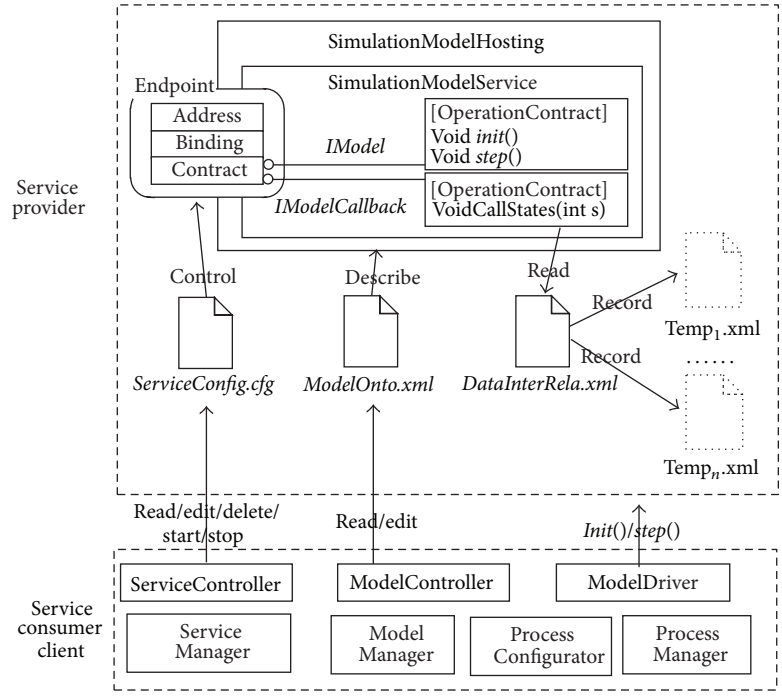

Figure 4: The overall architecture of service-oriented simulation model.

```
init(){
paraFileList<> ReadFile(dataInterRela.xml);
inputFileList<> ReadFile(dataInterRela.xml);
outputFilelist<> ReadFile(dataInterRela.xml);
paraData<> parsePara(paraFileList<>);
initModel(paraData<>);
CallStates(ready);
}
step()
{
inputData<> parseInput(inputFileList<>);
outputData<> doCal(inputList<>);
writeData(outputData<>,outputFileList<>);
CallStates(done);
}
```

Algorithm 3

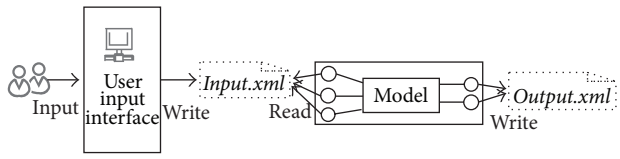

Figure 5: The data interaction process of the calling of one simulation model.

(4) $SPS_i = \{MS_{i1}, MS_{i2}, \ldots, MS_{io}\}$ is a set of modules marked as the starting point of a simulation process, and each $MS_{ij} \in SP_{Mi}$ $(1 \leqslant j \leqslant n)$.

(5) $SPE_i = \{ME_{i1}, ME_{i1}, \ldots, ME_{ip}\}$ is a set of modules marked as the ending point of a simulation process, and each $ME_{ij} \in SPM_i$ $(1 \leqslant j \leqslant n)$.

The ontology of simulation process can be established as shown in Figure 6.

The configuration of a simulation process mainly includes model selection, data interaction relationships configuration, and model parameters/input configuration. Model selection is responsible for selecting appropriate models to meet the simulation demands. When several models are selected, the user input interface of each model's P_i and ID_i is generated for the configuration by users, and then users need to input appropriate values for each model's parameters, create data

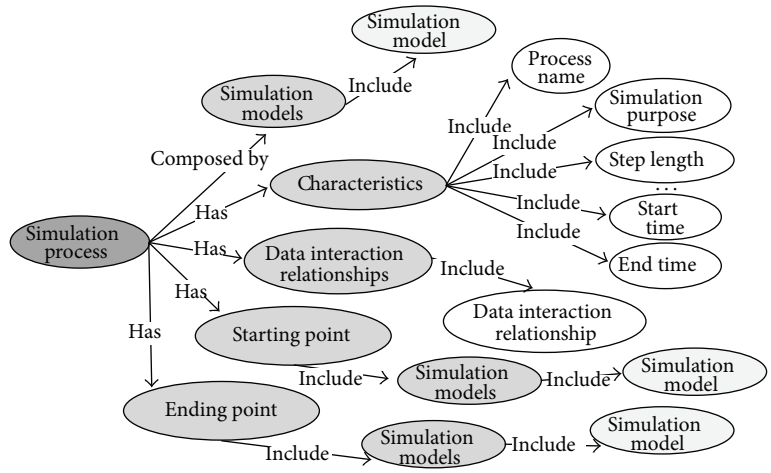

Figure 6: The ontology of simulation process.

```
<SimProcess id="......">
   <SimProcessDescription>
      ......
   </SimProcessDescription>
   <Models>
         ......
      <Model id="213" RunOrder="2" IsStart="false" IsEnd="false">
         ......
            <URI>......</URI>
            <Parameters>
                  <Parameter>
                     <DataType>Int32</DataType>
                     <Value>24</Value>
                       ......
                  </Parameter>
            </Parameter>
      </Model>
          ......
   </Models>
   <InteractionRelations>
      ......
      <InteractionRelation Id="......">
         <From>Model213/Output3</From>
         <To>Model241/Input2</To>
         <FormatConverter>Int64ToInt32</FormatConverter>
         ......
      <InteractionRelation>
      ......
   </InteractionRelations>
</SimProcess>
```

Algorithm 4

interaction relationships between different models' inputs and outputs, and manually input necessary data for some models' input data items which cannot get data from other models' output. All the configuration information is formatted into a process description file in the form of *.xml*. The structure of this *.xml* is described in Algorithm 4.

After this, some temporary*.xml* files are generated for the data interaction according to the data interaction relationships marked by <InteractionRelations></InteractionRelations> in the simulation process description file. The simulation process can be driven by a workflow engine which can parse the simulation process description file to get the

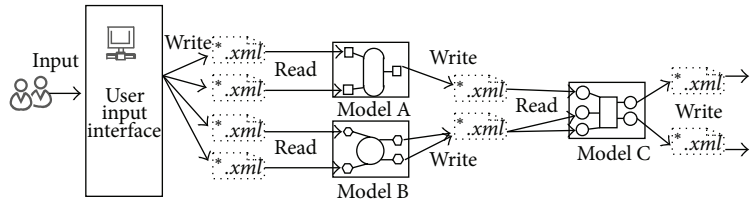

Figure 7: The data interaction process of the calling of several simulation models.

execution order of each model. The data interaction process of a simulation process SP_i is as shown in Figure 7.

5. Case Study

Based on the concepts above, a 6 degree of freedom (DOF) aircraft dynamic model built in Geodetic Coordinates is programmed into two different ways to get flight paths. A flight path is divided into 5 stages including taxi, ascending, level flight, harmonize turn, and landing in this model. The first way is written in Matlab by using fourth-order Runge-Kutta method to calculate the position of the aircraft, and the second one is written in C# by using Newton's method to calculate the position of the aircraft.

Both of the two ways contain the same parameters and input data items. The parameters include the step *st*; the initial rate v_0, the initial azimuth ψ_0 (North by East), and the initial height h_0 in the taxi stage; the ascending start time t_{as} in the ascending stage; the level flight start time t_{lf} in the level flight stage; the harmonize turn start time t_{ht} and the turn angle ψ_t in the harmonize turn stage; the landing start time t_l in the landing stage. The input data item only includes the flight time t expressed in seconds. It is important to note that all parameters related to the aircraft characteristics are built into the dynamic model and do not support external configuration.

The Matlab-way generates an *aircraft-matlab.m* file which cannot be directly a service, so some more programming works are carried out to make it a service by using WCF and Matlab Engines. The main logic of "*init()*" is listed as follows.

(1) Start the Matlab Engine through the calling of corresponding **.dll* and **.lib* provided by Matlab and load the *aircraft-matlab.m* file;

(2) Read the *aircraft-matlab-dataInterRela.xml* to get the file paths *paraFileList*<> of parameters configuration files, the file paths *inputFileList*<> of input data items files, and the file paths *outputFilelist*<> of output data items files.

(3) Parse all the parameters in *paraFileList*<> and send them to the *aircraft-matlab.m* through the Matlab Engine.

The main logic of "*Step()*" is listed as follows.

(1) Parse the input data items from the corresponding **.xml* files according to the *inputFileList*<> and send them to the *aircraft-matlab.m* through the Matlab Engine.

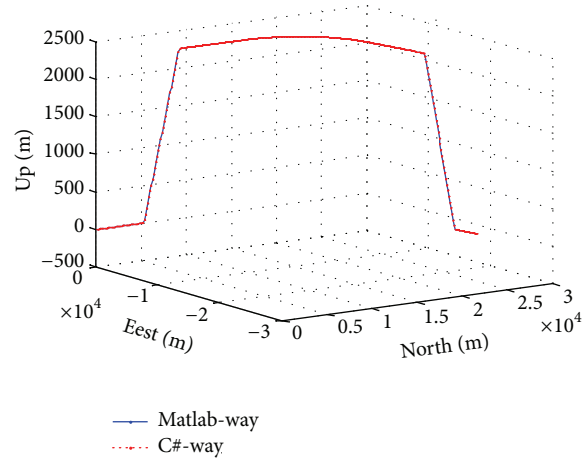

Figure 8

(2) Drive the Matlab Engine to run the *aircraft-matlab.m*.

(3) Get the results and write them into corresponding **.xml* files according to the *outputFilelist*<>.

Unlike the Matlab-way, the C#-way can be directly programmed into a service by using WCF. The main logic of "Init()" and "step()" is similar to the functions in Matlab-way except the Matlab Engine part.

Because the level flight distance of a true flight path is too long to be shown in one scene, a simplified flight path between two different airports in a same city is planned. All the parameters are configured as $st = 1$, $v_0 = 0$, $\psi_0 = 0$, $h_0 = 0$, $t_{as} = 40$, $t_{ht} = 70$, $t_{ht} = 120$, $\psi_t = 15$, and $t_l = 250$, and the whole flight path costs 300 seconds. The two flight paths in North-East-Up (NEU) coordinates are shown in Figure 8, and the projections of altitude changes in North are shown in Figure 9.

The two flight paths have very small differences so that the curves almost coincide with each other. But the two ways' execution time of a single step has huge differences, as shown in Figure 10.

Each time the "*Step()*" is executed, the execution time is recorded, so there are 300 sampling points. These time differences are due to the program logics and algorithms. The fourth-order Runge-Kutta method spend more time than Newton's method, and the calling of Matlab Engine spend extra time.

Then some more simulation models are reprogrammed in WCF, and a prototype simulation system is constructed. A simple global navigation satellite system (GNSS) simulation

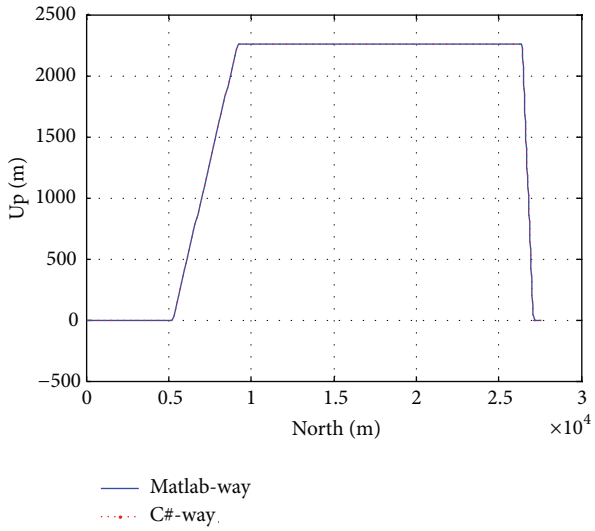

Figure 9: Two flight paths' projections in North.

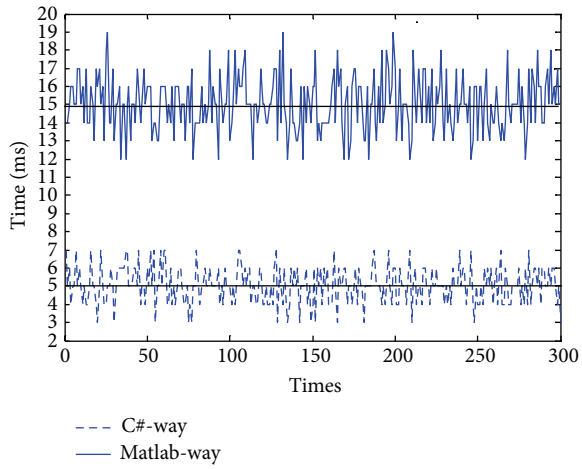

Figure 10: The comparison of two ways' execution time of a single step.

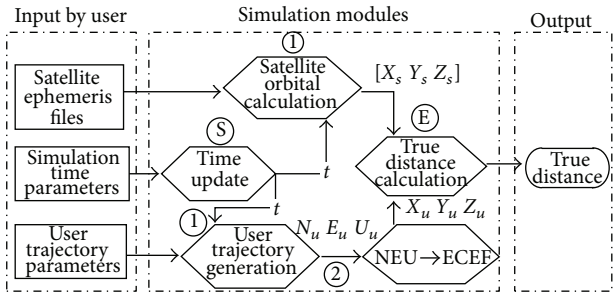

Figure 11: A simple simulation process.

process shown in Figure 11 is composed by using the 6 DOF aircraft model and some other models.

This simple simulation process has five simulation models, and its main function is calculating the true distances between the satellites and a moving vehicle in a period of time. Each model's parameters, input data items, and output

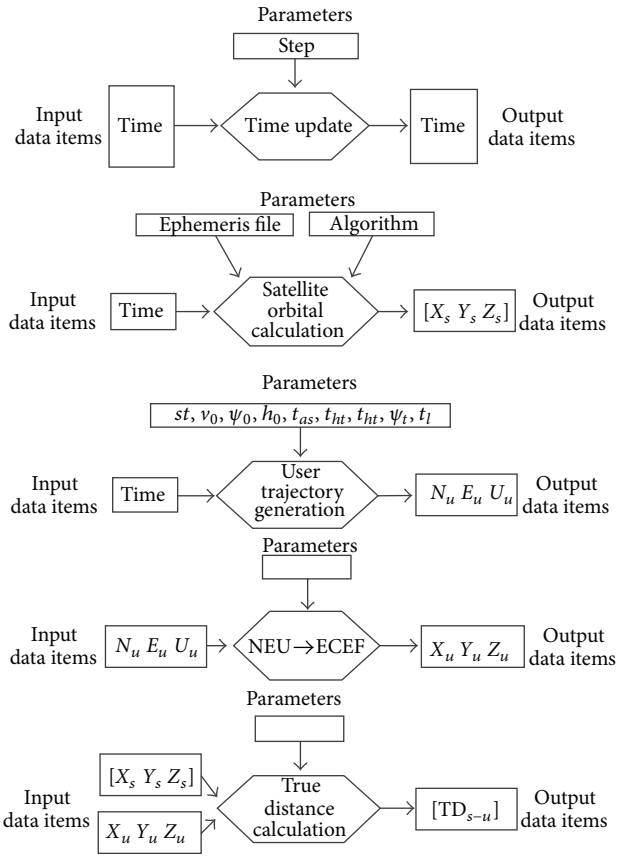

Figure 12: The structure of these five models.

Figure 13: The active service-oriented simulation models.

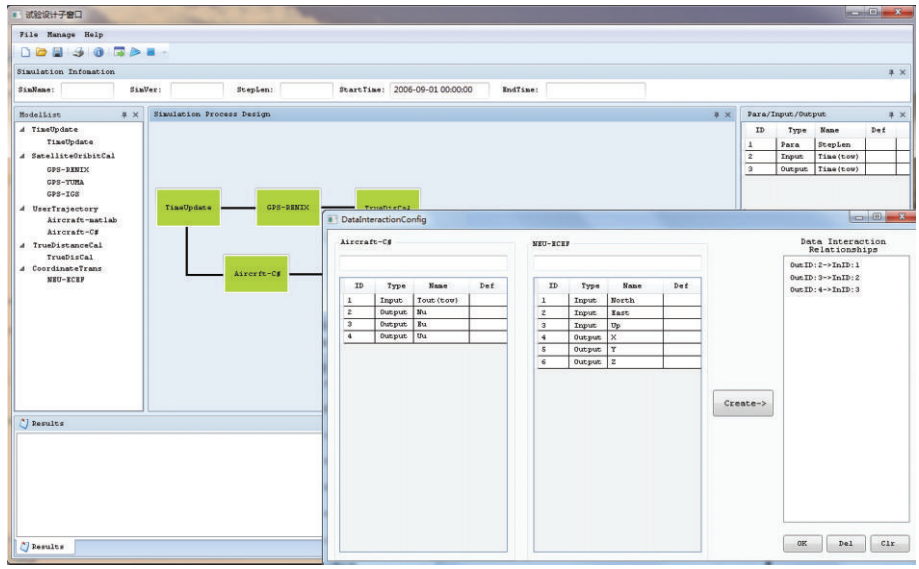

Figure 14: The main interface of simulation model selection, simulation process design, and data interaction relationship.

data items are shown in Figure 12. The $[X_sY_sZ_s]$ stands for the earth centered earth fixed (ECEF) coordinate array of satellites, and the $X_uY_uZ_u$ stands for the ECEF coordinate of a vehicle, and the $[TD_{s-u}]$ stands for the true distance array of these satellites to the vehicle.

Figure 13 shows the active service-oriented simulation models in the Simulation Models Registry. Figure 14 shows the main interface of simulation model selection, simulation process design, and data interaction relationship configuration.

The simulation models used in this process are deployed on a local host to simplify the verification process, but they can be easily deployed on other hosts. The models can be selected from the "ModelList" panel which shows the active service-oriented simulation models. When clicked, a model's parameters/input-data-item/output-data-item are listed in the "Para/Input/Output" panel on the right side, and the parameters can be configured here. A simulation process can be composed by creating interaction relationships between different models just as shown in the subwindow "DataInteractionConfig." The simulation process is driven by a simple event-driven engine, and each service's callback function triggers the engine.

Although this prototype system is performed on a local host, all the models are programmed in WCF according to SOA standards and are formed into some $^*.exe$ files. So when be configured to a Public IP, all the models will be shared over the internet. In addition, the client as a validator is not necessary, because all the functions could be implemented on web pages. And we can know that users can run a $^*.m$ model without the Matlab on his computer from the running of the Matlab-way, that is to say that the decoupling of the users' clients from some specific software is implemented. Finally, users can compose some models to perform a simulation process.

6. Conclusion

Despite that the validation of this structure is relatively simple, conclusions can be drawn from the limited works: (1) service-oriented simulation models can be an available way of encapsulating specific simulation algorithms, programs, methods, and knowledge; (2) a well-designed/well-reprogrammed simulation model only interacts with some fixed format *.xml* files, and it reduces the coupling between the model and specific applications, and it is easy to reuse and easy to integrate; (3) different models interact by reading and writing some fixed format *.xml* files, and it reduces the interaction difficulties of heterogeneous modules; (4) a simulation model resource pool can be easily constructed for cloud-based or distributed environment by collecting these well-reprogrammed simulation models.

The design method proposed in this paper has some disadvantages: (1) this method is not suitable for time-driven simulation mode, because the increased file reading and writing operations will reduce the execution efficiency, and any failed execution of one model could crash the whole simulation process; (2) the parameters/input-data-item/output-data-item need to be format fixed; (3) the work to reprogram an existing simulation is a little hard although simple in form of this method; (4) there is no tools to design a model, and all the work need to be done manually by using a SOA implementation method such as the WCF.

Future works includes (1) improving this design method to fit the situation that the input/output data items' format is not fixed; (2) improving the process interpreter to support more complicated simulation process which contains the looping and branching structure; (3) developing web-based client; (4) doing more tests on distributed environment.

Acknowledgments

This work was supported by the National High-Tech, R and D Program, China (nos. 2011AA120505 and 2011AA040503), and the National Natural Science Foundation, China (no. 61173077).

References

[1] L.-K. Chan and M.-L. Wu, "Quality function deployment: a literature review," *European Journal of Operational Research*, vol. 143, no. 3, pp. 463–497, 2002.

[2] C. Temponi, J. Yen, and W. A. Tiao, "House of quality: a fuzzy logic-based requirements analysis," *European Journal of Operational Research*, vol. 117, no. 2, pp. 340–354, 1999.

[3] L. H. Chen, W. C. Ko, and C. Y. Tseng, "Fuzzy approaches for constructing house of quality in QFD and its applications: a group decision-making method," *IEEE Transactions on Engineering Management*, vol. 60, no. 1, pp. 77–87, 2013.

[4] C. Kahraman, T. Ertay, and G. Büyüközkan, "A fuzzy optimization model for QFD planning process using analytic network approach," *European Journal of Operational Research*, vol. 171, no. 2, pp. 390–411, 2006.

[5] H. Yamashina, T. Ito, and H. Kawada, "Innovative product development process by integrating QFD and TRIZ," *International Journal of Production Research*, vol. 40, no. 5, pp. 1031–1050, 2002.

[6] J. M. Xie, X. W. Tang, and Y. F. Shao, "Research on product conceptual design based on integration of TRIZ and HOQ," *Growth and Development of Computer-Aided Innovation*, vol. 304, pp. 203–209, 2009.

[7] Y.-S. Kim and D. S. Cochran, "Reviewing TRIZ from the perspective of Axiomatic Design," *Journal of Engineering Design*, vol. 11, no. 1, pp. 79–94, 2000.

[8] Simulation model portability, European Space Agency, A. Milstedvega.de/smp/.

[9] G. F. Jeremy, M. Andrew, M. Danius, and D. R. David, "My Experimental Science, extending the "workflow"," *Concurrency and Computatation: Practice and Experience*, vol. 25, pp. 481–496, 2013.

[10] http://www.taverna.org.uk/.

[11] G. Klimeck, M. Mclennan, S. B. Brophy, G. B. Adams III, and M. S. Lundstrom, "NanoHUB.org: advancing education and research in nanotechnology," *Computing in Science and Engineering*, vol. 10, no. 5, Article ID 4604500, pp. 17–23, 2008.

[12] https://nanohub.org/infrastructure/rappture/.

[13] L. Sliman, B. Charroux, and Y. Stroppa, "RunMyCode: an Innovative platform for social production and evaluation of scientific research," in *Proceding of 4th International Conference on Compuatational Aspects of Social Networks*, pp. 109–114, Sao Carlos, Brazil, 2012.

[14] "The NIST Definition of Cloud Computing", National Institute of Science and Technology, 2011, http://csrc.nist.gov/publications/nistpubs/800-145/SP800-145.pdf.

[15] M. Armbrust, A. Fox, R. Griffith et al., "A view of cloud computing," *Communications of the ACM*, vol. 53, no. 4, pp. 50–58, 2010.

[16] G. D'Angelo, "Parallel and distributed simulation from many cores to the public cloud," in *2011 International Conference on High Performance Computing and Simulation (HPCS '11)*, pp. 14–23, July 2011.

[17] R. M. Fujimoto, A. W. Malik, and A. Park, "Parallel and Distributed simulation in the cloud," *SCS M&S Magazine*, vol. 1, no. 3, pp. 1–10, 2010.

[18] A. Jávor and A. Fur, "Simulation on the Web with distributed models and intelligent agents," *Simulation*, vol. 88, no. 9, pp. 1080–1092, 2012.

[19] X. C. Liu, Q. He, X. G. Qiu, B. Chen, and K. D. Huang, "Cloud-based computer simulation: towards planting existing simulation software into the cloud," *Simulation Modelling Practice and Theory*, vol. 26, pp. 135–150, 2012.

[20] V. Toby, T. Anthony, and E. Rober, *Cloud Computing: A Practical Approach*, McGraw Hill, New York, NY, USA, 2010.

[21] B. Michael, *Service-Oriented Modeling (SOA): Service Analysis, Design, and Architecture*, John Wiley & Sons, Hoboken, NJ, USA, 2008.

[22] B. Michael, *SOA Modeling Patterns for Service-Oriented Discovery and Analysis*, John Wiley & Sons, Hoboken, NJ, USA, 2010.

Hindawi Publishing Corporation
Advances in Mechanical Engineering
Volume 2013, Article ID 125291, 8 pages
http://dx.doi.org/10.1155/2013/125291

Research Article

Equilibrium Design Based on Design Thinking Solving: An Integrated Multicriteria Decision-Making Methodology

Yi-Xiong Feng,[1] Yi-Cong Gao,[1] Xuan Song,[2] and Jian-Rong Tan[1]

[1] *State Key Laboratory of Fluid Power Transmission and Control, Zhejiang University, Hangzhou 310027, China*
[2] *Department of Industrial and Systems Engineering, University of Southern California, Los Angeles, CA 90089-0193, USA*

Correspondence should be addressed to Yi-Cong Gao; gaoyicong@zju.edu.cn

Received 31 January 2013; Revised 9 June 2013; Accepted 9 July 2013

Academic Editor: Dongxing Cao

A multicriteria decision-making model was proposed in order to acquire the optimum one among different product design schemes. VIKOR method was introduced to compute the ranking value of each scheme. A multiobjective optimization model for criteria weight was established. In this model, projection pursuit method was employed to identify a criteria weight set which could keep classification information of original schemes to the greatest extent, while PROMETHEE II was adopted to keep sorting information. Dominance based multiobjective simulated annealing algorithm (D-MOSA) was introduced to solve the optimization model. Finally, an example was taken to demonstrate the feasibility and efficiency of this model.

1. Introduction

Generally, designers tend to get more than two schemes in product conceptual design because multiple alternatives can make the design more innovative. After different schemes are obtained, the designers should further decide which one is the best. This is exactly a multicriteria decision making problem. Many researches have been conducted on multicriteria decision making in different application fields. Gu and Wu [1] introduced fuzzy set theory and analytic hierarchy process into the evaluation process to determinate the weights of evaluation factors. Kaya and Kahraman [2] proposed integrated VIKOR-AHP methodology to the selection of the best energy policy and production site. Kong et al. [3] construct the comprehensive evaluation model of enterprise's technological innovation abilities and evaluate technological innovation abilities of four enterprises based on VIKOR method. Macharis et al. [4] discussed the strengths and weaknesses of the Preference Ranking Organization Method for Enrichment Evaluations (PROMETHEE) and analytic hierarchy process (AHP) methods. Opricovic and Tzeng [5, 6] illustrated a comparative analysis of two multiple criteria decision-making methods VIKOR and TOPSIS. Sayadi et al. [7] extended the VIKOR method for decision-making problems with interval number. Lin et al. [8] presented a framework that integrates the analytic hierarchy process (AHP) and the technique for order preference by similarity to ideal solution (TOPSIS) to assist designers in identifying customer requirements and design characteristics and achieving an effective evaluation of the final design solution. Shih et al. [9] proposed a multiattribute decision-making model based on TOPSIS, which is indeed a unified process and it will be readily applicable to many real-world decision-making situations without increasing the computational burden.

In these researches, criteria weight should be given at the beginning in order to calculate the ranking value. It is inevitable to bring subjective factors into criteria weight by these methods. In order to reduce subjective uncertainty in weight calculation to the greatest extent, we put forward a multicriteria decision-making method for product design schemes. In our method, a multiobjective optimization model for criteria weight was established, by which classification and sorting information of original schemes are kept in the final priority sequence.

In Section 2, VIKOR method is explained in detail. VIKOR method is the basis of the proposed model because the optimized criteria weight by the model will eventually

be substituted into this method. In Section 3, a multi-objective optimization model for criteria weight is established, respectively, based on projection pursuit method and PROMETHEE II. In Section 4, a new multi-objective optimization algorithm D-MOSA is introduced to optimize the proposed multi-objective optimization model for criteria weight. In Section 5, a mechanism example is taken to demonstrate the efficiency and feasibility of our model.

2. VIKOR Method

VIKOR was proposed by Opricovic to deal with discrete multicriteria decision-making problem [10]. It uses different aggregation function and normalization method from TOPSIS and calculates ranking value of each scheme with maximum group utility and minimum individual regret. Given a scheme set $A = \{x_{ij} \mid i = 1 \sim m, j = 1 \sim n\}$, in which x_{ij} denotes the rating of scheme a_i with respect to criteria S_j, we perform multicriteria decision making using VIKOR method as follows.

Step 1. Normalize the rating x_{ij} in set A. We assume that all the criteria are benefit-type, and then the following equation can be used to normalize the scheme set A:

$$f_{ij} = \frac{x_{ij}}{x_{\max}(j)}, \tag{1}$$

where f_{ij} is the rating after normalization and $x_{\max}(j)$ is the maximum rating of all the schemes with respect to criteria S_j. Through normalization, the rating value with respect to each criterion could be restricted within the closed interval $[0, 1]$.

Step 2. Determine the positive ideal value f_j^* and negative ideal value f_j^-. f_j^* is the maximum rating value with respect to criteria S_j in all schemes, while f_j^- is the minimum with respect to criteria S_j in all schemes. We evaluate the distance between each scheme and positive ideal value or negative ideal value and select the optimum scheme which is closest to the positive idea value but farthest from the negative ideal value.

Step 3. Calculate group utility S_i and individual regret R_i:

$$\begin{aligned} f_j^* &= \max_i f_{ij}, \qquad f_j^- = \min_i f_{ij}, \\ S_i &= \sum_{j=1}^{n} \frac{w_j\left(f_j^* - f_{ij}\right)}{f_j^* - f_j^-}, \\ R_i &= \frac{\max_j w_j\left(f_j^* - f_{ij}\right)}{f_j^* - f_j^-}, \end{aligned} \tag{2}$$

where w_j is the weight of each criterion.

Step 4. Compute the ranking value Q_i. The schemes are sorted according to their ranking values Q_i, and it can be calculated as follows:

$$Q_i = \frac{v\left(S_i - S^*\right)}{S^- - S^*} + \frac{(1-v)\left(R_i - R^*\right)}{R^- - R^*}, \tag{3}$$

where $S^* = \min_i S_i$, $S^- = \max_i S_i$,

$$R^* = \min_i R_i, \qquad R^- = \max_i R_i \tag{4}$$

v is introduced as strategy weight. It determines whether to consider maximum group utility more or minimum individual regret more in ranking value. When it is set to 0.5, they are considered equally.

According to VIKOR method, the final ranking value Q_i should satisfy two conditions: the acceptable advantage and the acceptable stability in decision making. However, it is very difficult to satisfy them at the same time, because the schemes usually vary slightly from each other, and thus it is difficult to get a complete order using these two conditions. In this paper, the authors sort the schemes directly according to their ranking value Q_i. It can be known that the less the ranking value Q_i is, the better its corresponding scheme is.

3. Multiobjective Optimization Model for Criteria Weight

Multicriteria decision making is required to reflect both classification and sorting information in original schemes [11]. In this paper, projection pursuit [12] is employed to guarantee that the obtained criteria weight could keep the classification feature of schemes. It can make the ranking value scatter on the whole scale but at the same time aggregate on the local scale through maximizing the standard deviation of projecting value and local density. Besides, sorting information can be guaranteed by PROMETHEE method.

3.1. Projection Pursuit Based Scheme Classification Optimization Model. Multi-criteria decision making is actually a projecting process from multidimensional criteria to one-dimensional ranking value. Therefore, the criteria weight set $W = \{w_j \mid j = 1 \sim n\}$ can be regarded as the projection direction. If we choose different weight set W, or in other words, we project criteria from different directions, criteria will be understood at different angles. The projection could be expressed by the following formula:

$$Q_i = P(W, F), \quad F = \left(f_{i1}, f_{i2}, \ldots, f_{in}\right), \tag{5}$$

where $P(\cdot)$ is the projection function.

In formula (5), vector F is known at the beginning of evaluation. There are mainly two methods to determine weight set W, namely, subjective weighting and objective weighting [13]. But these methods are deficient in determining weight accurately due to the limited knowledge and experience of decision maker. In projection pursuit, standard

deviation $S(Q)$ and local density $D(Q)$ of the ranking value are calculated firstly based on the result of formula (3):

$$S(Q) = \left[\sum_{i=1}^{m} \frac{Q(i) - \overline{Q}}{m}\right]^{1/2},$$
$$D(Q) = \sum_{i=1}^{m}\sum_{j=1}^{m} \left(R - r_{ij}\right) \cdot u\left(R - r_{ij}\right), \tag{6}$$

where $\overline{Q}$ is the mean of $Q(i)$, R is window radius of local density, usually $R = 0.1S(Q)$, r_{ij} is the distance between two ranking values, $r_{ij} = |Q_i - Q_j|$, and $u(\cdot)$ is unit step function. In order to acquire the best projection direction, the following optimization objective function is established:

$$\max\ I = S(Q) \cdot D(Q), \tag{7}$$

$$\text{or} \qquad I = S(Q) + D(Q), \tag{8}$$

$$\text{s.t.} \qquad \sum_{j=1}^{n} w_j = 1, \quad 0 \le w_j \le 1. \tag{9}$$

According to the literature [14], the final ranking values, respectively, evaluated by formula, (7) and (8) are similar. In this paper, the authors use formula (8) as the objective function.

3.2. PROMETHEE II Based Sorting Optimization Model. Scheme sorting can be easily affected by criteria weight set. The slight change of criteria weight may even lead to drastic change in sorting. In order to make the sorting stable enough, the most efficient way is to maximize the difference of ranking values between each scheme [15]. PROMETHEE method adopts preference function to establish the priority relation between every two schemes [16, 17]. Preference degree of any scheme versus the whole scheme set is defined, combining with criteria weight, further to determine the priority order of all schemes. For the scheme set $A = \{x_{ij} \mid i = 1 \sim m, j = 1 \sim n\}$ given in last section, its criteria weight set is $W = \{w_j \mid j = 1 \sim n\}$.

Preference function is given as $P_k(a_i, a_j) \in [0, 1]$, which denotes the priority degree of scheme a_i under criteria k relative to scheme a_j. The different values of $P_k(a_i, a_j)$ are as follows:

$$P_k\left(a_i, a_j\right) = 0, \tag{10}$$

a_i has no priority over a_j;

$$P_k\left(a_i, a_j\right) = \rho \in (0, 1), \tag{11}$$

a_i is prior to a_j under criteria k, and the priority degree is ρ;

$$P_k\left(a_i, a_j\right) = 1, \tag{12}$$

a_i is absolutely prior to a_j under criteria k.

The priority degree of a_i versus a_j can be calculated as follows:

$$\prod\left(a_i, a_j\right) = \sum_{k=1}^{n} w_k P_k\left(a_i, a_j\right). \tag{13}$$

The outgoing flow, incoming flow, and net flow of a_i can be obtained using the following equation:

$$\phi^+(a_i) = \sum_{j=1}^{m} \prod\left(a_i, a_j\right),$$
$$\phi^-(a_i) = \sum_{j=1}^{m} \prod\left(a_j, a_i\right), \tag{14}$$
$$\phi(a_i) = \phi^+(a_i) - \phi^-(a_i).$$

The scheme set A is sorted according to net-flow $\Phi(a_i)$. When $\phi^+(a_i) \ge \phi^+(a_j)$, $\phi^-(a_i) \le \phi^-(a_j)$, it can be denoted as

$$a_i P a_j. \tag{15}$$

When $\phi^+(a_i) = \phi^+(a_j)$, $\phi^-(a_i) = \phi^-(a_j)$, it can be denoted as

$$a_i I a_j. \tag{16}$$

Given $x_{ij}, y_{ij} \ge 0$, for any a_i and a_j, we have

$$\phi^+(a_i) - \phi^+\left(a_j\right) - x_{ij} = 0, \tag{17}$$

$$\phi^-(a_i) - \phi^-\left(a_j\right) + y_{ij} = 0, \tag{18}$$

$$\sum_{l=1}^{m}\left(\sum_{k=1}^{n} w_k P_k(a_i, a_l)\right) - \sum_{l=1}^{m}\left(\sum_{k=1}^{n} w_k P_k\left(a_j, a_l\right)\right) - x_{ij} = 0,$$
$$\sum_{l=1}^{m}\left(\sum_{k=1}^{n} w_k P_k(a_l, a_i)\right) - \sum_{l=1}^{m}\left(\sum_{k=1}^{n} w_k P_k\left(a_l, a_j\right)\right) + y_{ij} = 0, \tag{19}$$

specifically, when $a_i P a_j$, $x_{ij} = y_{ij} = 0$.

The difference index Z [9] in formula (20) is calculated through summing x_{ij}, y_{ij} of all priority relations in scheme set and can reflect the difference between ranking values. In order to make the scheme sorting stable, this equation can be taken as the maximizing optimization objective:

$$Z = \alpha + \varepsilon \sum_{a_i P a_j}\left(x_{ij} + y_{ij}\right). \tag{20}$$

In this equation, $\alpha = \min\{x_{ij}, y_{ij} \mid A_i P A_j\}$, it is the minimum x_{ij} or y_{ij} of all scheme relation pair. ε is a small positive number.

3.3. Multiobjective Optimization Model of Criteria Weight. Criteria weight is mainly to measure the policymakers' preference degree for product attributes [18]. Multi-objective

optimization model of criteria weight is established as follows:

$$\begin{aligned}
&\max\ I = S(Q) + D(Q)\\
&Z = \alpha + \varepsilon \sum_{a_i P a_j} \left(x_{ij} + y_{ij}\right)\\
&\text{s.t.}\quad \sum_{j=1}^{n} w_j = 1, \quad 0 \le w_j \le 1;\\
&\sum_{l=1}^{m}\left(\sum_{k=1}^{n} w_k P_k\left(a_i, a_l\right)\right)\\
&\quad - \sum_{l=1}^{m}\left(\sum_{k=1}^{n} w_k P_k\left(a_j, a_l\right)\right) - x_{ij} = 0\\
&\sum_{l=1}^{m}\left(\sum_{k=1}^{n} w_k P_k\left(a_l, a_i\right)\right)\\
&\quad - \sum_{l=1}^{m}\left(\sum_{k=1}^{n} w_k P_k\left(a_l, a_j\right)\right) + y_{ij} = 0\\
&\alpha = \min\left\{x_{ij}, y_{ij} \mid A_i P A_j\right\}\\
&\qquad x_{ij}, y_{ij} \ge 0.
\end{aligned} \tag{21}$$

4. Dominance Based Multiobjective Simulated Annealing Algorithm (D-MOSA)

Simulated annealing (SA) is an ideal algorithm to deal with single-objective optimization problem. When optimization parameter is chosen properly and temperature is reduced slowly enough, the result by SA can be very close to global optimum solution. Smith et al. [14] proposed a new simulated annealing algorithm oriented to multiobjective optimization problem, namely, dominance based multiobjective simulated annealing algorithm (D-MOSA). It overcomes the shortcoming of SA in optimizing single objective. This paper introduced this algorithm to optimize the multi-objective model of criteria weight.

4.1. Dominance Based Energy Function. In simulated annealing algorithm, energy function is used to compare the new solution and current solution as the objective function of optimization and determine whether the new proposal should be accepted. In multi-objective optimization, we can use dominance relation between solutions to determine the priority of proposal versus current solution.

In Figure 1, sample 1 is dominated by more points on Pareto front than sample 2, so we could think that sample 1 has higher energy than sample 2. When the sample point is on the Pareto front, the sample is dominated by no points, and accordingly its energy is 0. Pareto front is denoted by set P, and the part in set P which dominates sample $\mathbf{f}(\mathbf{x})$ can be denoted as P_x, so

$$P_x = \left\{\mathbf{y} \in P \mid \mathbf{y} \prec \mathbf{f}(\mathbf{x})\right\}. \tag{22}$$

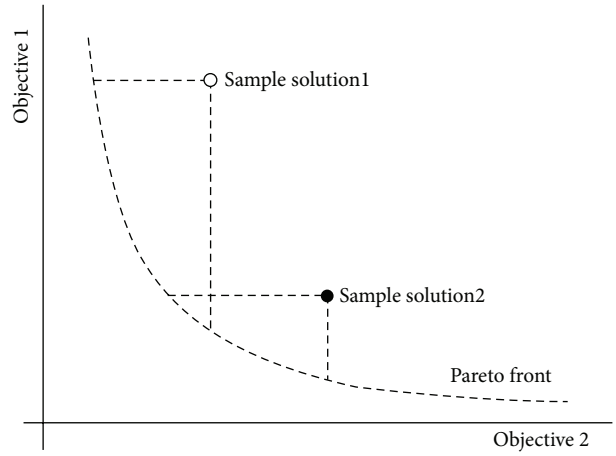

Figure 1: Different samples are dominated by different number of points on Pareto front.

Energy function is defined as $E(\mathbf{x}) = \mu(P_x)$, in which μ is a measure on set P.

In practical application, Pareto front is unknown, so an estimated Pareto front should be used in energy function instead. Set F is constituted by all mutually nondominating solutions so far and can be used to estimate the true Pareto front. Based on set F, set $\widetilde{F}$ can be defined as $\widetilde{F} = F \cup \{x\} \cup \{x'\}$. Then, the set constituted by elements in $\widetilde{F}$ dominating $\mathbf{x}$ can be denoted by $\widetilde{F}_x$:

$$\widetilde{F}_x = \left\{\mathbf{y} \in \widetilde{F} \mid \mathbf{y} \prec \mathbf{x}\right\}. \tag{23}$$

Hence, the energy difference between the new proposal and current solution is

$$\delta E\left(x', x\right) = \frac{1}{\left|\widetilde{F}\right|}\left(\left|\widetilde{F}_{x'}\right| - \left|\widetilde{F}_x\right|\right), \tag{24}$$

where $|\widetilde{F}_x|$ is the number of elements in set $\widetilde{F}_x$ plus 1.

Using the previous energy function, we do not need to be given the weight of every objective function; meanwhile, it encourages the exploration of sparsely populated region of the front because, in this region, the energy of new solution is relatively lower (they are dominated by fewer points), and they can be accepted more easily.

4.2. Attainment Surface Sampling. Though using the estimated Pareto front F provides an estimate of solution energy, the resolution in the energies can be very coarse [14] if F is small. The acceptance probabilities will also become lower and convergence to global optimum will be prevented. In this algorithm, attainment surface sampling (ASS) is used to augment points on estimated Pareto front F.

Firstly, attainment surface S_F of F is determined. As a matter of fact, S_F is the boundary of the region in objective space dominated by elements in F. If

$$\begin{aligned}
F &= \left\{\mathbf{y} \mid \mathbf{u} \prec \mathbf{y},\ \mathbf{u} \in F\right\},\\
U &= \left\{\mathbf{y} \mid \mathbf{u} \lhd \mathbf{y},\ \mathbf{u} \in F\right\},
\end{aligned} \tag{25}$$

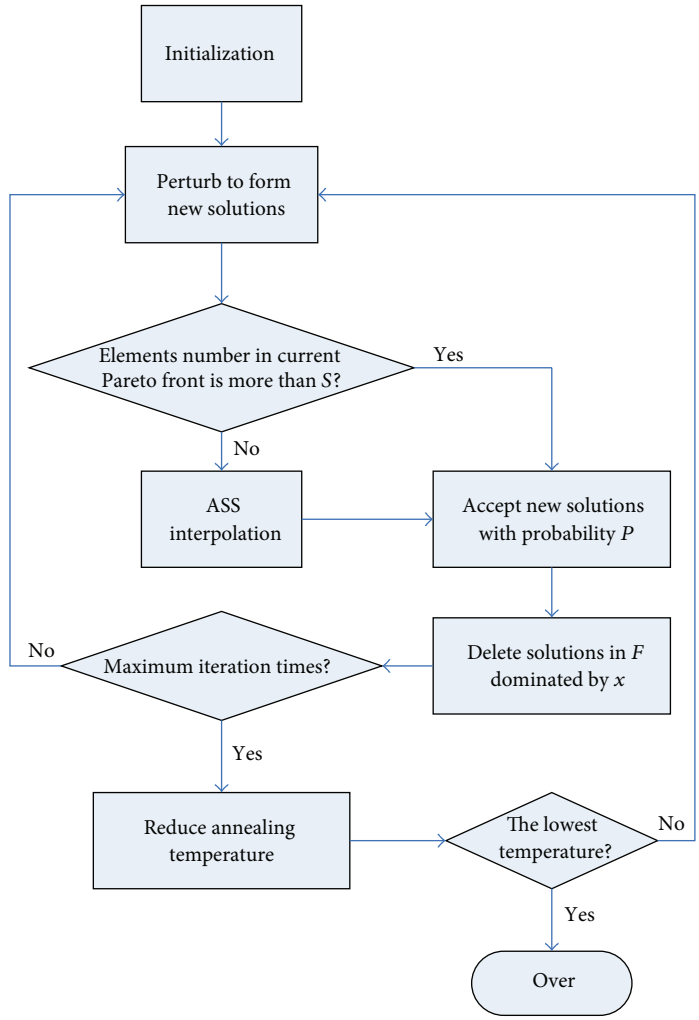

Figure 2: The flow chart of dominance based multiobjective simulated annealing algorithm.

where $\mathbf{u} \lhd \mathbf{y}$ denotes that $\mathbf{u}$ properly dominates $\mathbf{y}$, and for any $i = 1, 2, \ldots, D$ (D is the objective number), $u_i < y_i$. S_F satisfies

$$S_F = F \setminus U. \tag{26}$$

H_F is the minimum hyperrectangle containing F, and

$$H_F = \left[\min_{y \in F}(y_1), \max_{y \in F}(y_1)\right] \times \cdots \times \left[\min_{y \in F}(y_D), \max_{y \in F}(y_D)\right]. \tag{27}$$

After the attainment surface S_F of set F is obtained, uniformly sampling from $S_F \cap H_F$ is performed using Algorithm 1. In the following pseudocode, L_d ($d = 1, 2, \ldots, D$) is the element sequence of F sorted by increasing coordinate d.

4.3. Algorithm Procedure. The flow chart of dominance based multi-objective simulated annealing algorithm is depicted in Figure 2. The detailed process is explained as follows.

```
for i ← 0 to D
    v_i ← rand(min(L_i), max(L_i))
end
d ← randint(1, D)                    choose a dimension, d
for i ← 1 to |F|
    u ← L_{d,i}
    v_d ← u_d
    if F ≺ v
    then return v
end
```

Algorithm 1

Step 1. Initialization. The initial feasible point $\mathbf{x}$ is produced, and the estimated Pareto front is $F = \{\mathbf{x}\}$. Additionally, annealing temperature sequence and epoch duration under each temperature are initialized.

Step 2. Form the proposed solution using perturbation function. Perturb each element of $\mathbf{x}$ singly to form new proposal x'.

Table 1: Evaluation index.

U_1: function	S_1: movement rule, S_2: transmission accuracy
U_2: working performance	S_3: application, S_4: adjustability, S_5: running speed, S_6: bearing capacity
U_3: dynamic performance	S_7: maximum acceleration, S_8: noise, S_9: wear resistance, S_{10}: reliability
U_4: economy	S_{11}: manufacturability, S_{12}: error, S_{13}: processing convenience, S_{14}: energy consumption
U_5: structure	S_{15}: measurement, S_{16}: weight, S_{17}: structural complexity

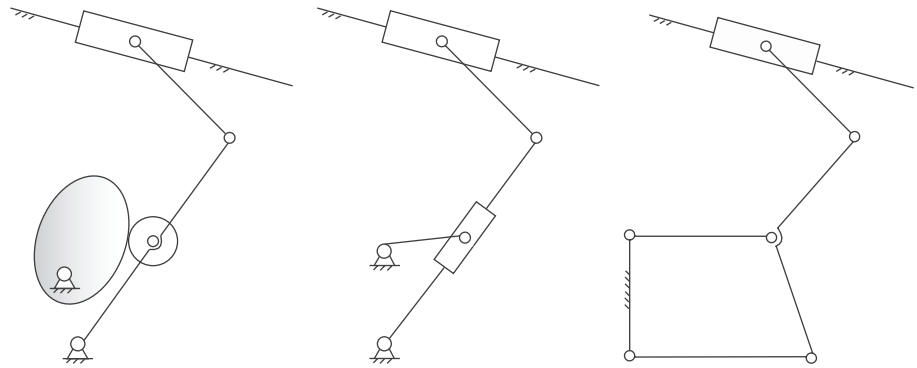

Figure 3: Scheme model. (a) Cam-rocker-slider mechanism. (b) Shaper mechanism. (c) Stephenson mechanism.

Step 3. If there are fewer than S solutions in F, ASS interpolation is performed. One hundred samples are drawn from S_F, and they make up the set S'_F, $\widetilde{F} = S'_F \cup F \cup \{x\} \cup \{x'\}$. Otherwise, skip to Step 4.

Step 4. Consider $\widetilde{F} = F \cup \{x\} \cup \{x'\}$.

Step 5. Determine whether to accept the proposed solution or not. The proposal is accepted with the probability P:

$$P = \begin{cases} 1, & \text{when } x \prec x' \\ \exp\left(-\dfrac{\delta E\left(x', x\right)}{T_k}\right), & T_k \text{ is current temperature.} \end{cases} \tag{28}$$

Step 6. Delete solutions in F dominated by $\mathbf{x}$, and add 1 to iteration times.

Step 7. If the iteration times under current temperature come to the maximum, then go to Step 8 and reduce annealing temperature; otherwise, return to Step 2.

Step 8. If current temperature gets the lowest, then optimization is over; otherwise, return to Step 2.

5. Instance

In this section, we will evaluate three schemes for the paper feeding mechanism in card punching machine [19]: cam-rocker-slider mechanism, shaper mechanism, and Stephenson mechanism, as depicted in Figure 3. We regard product's properties like reliability, maintainability, and green attributes as evaluation parameters, which is shown in Table 1. The rating of each scheme based on 1–9 level is given in Table 2. It can be seen in Table 1 that three schemes are equivalent with respect to criteria S_2 and S_{14}. Therefore, S_2 and S_{14} will not be considered in the following evaluation. The rating values after normalization are shown in Table 3. In PROMETHEE method, preference function was given as

$$P_k\left(f_i, f_j\right) = \left(\frac{\widetilde{d}}{\widetilde{D}}\right)^{1/w_k} \quad \text{when } f_i > f_j; \qquad P_k\left(f_i, f_j\right) = 0 \quad \text{when } f_i \le f_j, \tag{29}$$

where $\widetilde{d} = f_i - f_j$ and $\widetilde{D}$ is maximum $\widetilde{d}$ theoretically.

Through performing D-MOSA, we get the estimated Pareto front. Weight set w = (0.0292, 0.0666, 0.0082, 0.0967, 0.0169, 0.0356, 0.1246, 0.0171, 0.0338, 0.1561, 0.0057, 0.0128, 0.0503, 0.1274, and 0.2190) was chosen from the Pareto front to calculate ranking values of these three schemes, $I = 7.908 \times 10^{-9}$, $Z = 1.1584 \times 10^{-6}$. After substituting weight set W into VIKOR method, we get the ranking values of Schemes 1, 2, and 3 and get the result as is shown in Table 4. From the ranking value sequence, we know that Scheme 1 is the best one and Scheme 3 is the worst one. This conclusion is the same as that in the literature [19].

6. Conclusion

The proposed multi-criteria decision-making model provides designers with an evaluation result objectively. Criteria weight was optimized through the multi-objective optimization model, to maximize the standard deviation and local density of ranking value sequence, as well as the difference index between every two schemes. All of these can guarantee the classification and sorting information of original

Table 2: Rating of each scheme with respect to different criteria.

Criteria		Scheme 1 cam-rocker-slider mechanism	Scheme 2 shaper mechanism	Scheme 3 Stephenson mechanism
U_1	S_1	9	7	7
	S_2	7	7	7
U_2	S_3	7	7	6
	S_4	4	7	7
	S_5	7	6	6
	S_6	5	7	7
U_3	S_7	9	5	5
	S_8	5	7	7
	S_9	7	5	7
	S_{10}	9	7	7
U_4	S_{11}	7	6	5
	S_{12}	5	7	6
	S_{13}	9	7	7
	S_{14}	7	7	7
U_5	S_{15}	7	4	5
	S_{16}	6	7	7
	S_{17}	7	7	5

Table 3: Rating of each scheme with respect to different criteria.

Criteria		Scheme 1 cam-rocker-slider mechanism	Scheme 2 shaper mechanism	Scheme 3 Stephenson mechanism
U_1	S_1	1	0.778	0.778
U_2	S_3	1	1	0.857
	S_4	0.571	1	1
	S_5	1	0.857	0.857
	S_6	0.714	1	1
U_3	S_7	1	0.556	0.556
	S_8	0.714	1	1
	S_9	1	0.714	1
	S_{10}	1	0.778	0.778
U_4	S_{11}	1	0.857	0.714
	S_{12}	0.714	1	0.857
	S_{13}	1	0.778	0.778
U_5	S_{15}	1	0.571	0.714
	S_{16}	0.857	1	1
	S_{17}	1	1	0.714

schemes kept in final ranking value sequence. Meanwhile, the more schemes there are, the closer the result will be to the true Pareto front. During product designing, there is a large quantity of decision makings with fuzzy and uncertain information. This is the field calls for more researches and investigations. Through evaluating and decision of fuzzy information, a knowledge system of artificial intelligence evaluation can be developed to promote the intelligent designing of products.

Table 4: Evaluation result of each scheme.

Scheme	Value	Sorting
Scheme 1 (cam-rocker-slider mechanism)	0.0877	3
Scheme 2 (shaper mechanism)	0.1255	2
Scheme 3 (Stephenson mechanism)	1	1

Acknowledgments

This work was supported by the Science Fund for Creative Research Groups of the National Natural Science Foundation of China (Grant no. 51221004), the National Natural Science Foundation of China (Grant no. 51175456, 51205347).

References

[1] Y. K. Gu and L. H. Wu, "A fuzzy AHP approach to the determination of weights of evaluation factors in mechanism scheme evaluation process," *China Mechanical Engineering*, vol. 18, no. 5, pp. 1052–1067, 2007.

[2] T. Kaya and C. Kahraman, "Multicriteria renewable energy planning using an integrated fuzzy VIKOR & AHP methodology: The case of Istanbul," *Energy*, vol. 35, no. 6, pp. 2517–2527, 2010.

[3] F. Kong, Y. Jia, and J. Jia, "Research on comprehensive evaluation model of enterprise's technological innovation abilities based on VIKOR method," *Technology Economics*, vol. 27, no. 2, pp. 26–30, 2008.

[4] C. Macharis, J. Springael, K. de Brucker, and A. Verbeke, "PROMETHEE and AHP: the design of operational synergies in multicriteria analysis—strengthening PROMETHEE with ideas of AHP," *European Journal of Operational Research*, vol. 153, no. 2, pp. 307–317, 2004.

[5] S. Opricovic and G.-H. Tzeng, "Compromise solution by MCDM methods: a comparative analysis of VIKOR and TOPSIS," *European Journal of Operational Research*, vol. 156, no. 2, pp. 445–455, 2004.

[6] S. Opricovic and G.-H. Tzeng, "Extended VIKOR method in comparison with outranking methods," *European Journal of Operational Research*, vol. 178, no. 2, pp. 514–529, 2007.

[7] M. K. Sayadi, M. Heydari, and K. Shahanaghi, "Extension of VIKOR method for decision making problem with interval numbers," *Applied Mathematical Modelling*, vol. 33, no. 5, pp. 2257–2262, 2009.

[8] M.-C. Lin, C.-C. Wang, M.-S. Chen, and C. A. Chang, "Using AHP and TOPSIS approaches in customer-driven product design process," *Computers in Industry*, vol. 59, no. 1, pp. 17–31, 2008.

[9] H.-S. Shih, H.-J. Shyur, and E. S. Lee, "An extension of TOPSIS for group decision making," *Mathematical and Computer Modelling*, vol. 45, no. 7-8, pp. 801–813, 2007.

[10] S. Opricovic and G.-H. Tzeng, "Multicriteria planning of post-earthquake sustainable reconstruction," *Computer-Aided Civil and Infrastructure Engineering*, vol. 17, no. 3, pp. 211–220, 2002.

[11] J. Ju-liang, W. Yi-ming, and D. Jing, "System evaluation model based on combined weights," *Mathematics in Practice and Theory*, vol. 33, no. 11, pp. 51–59, 2003.

[12] J. H. Friedman and J. W. Turkey, "A projection pursuit algorithm for exploratory data analysis," *IEEE Transactions on Computers*, vol. 23, no. 9, pp. 881–890, 1974.

[13] J. Q. Wang, *Study on multi-criteria decision-making approach with incomplete certain information [Ph.D. thesis]*, Zhongnan Unversity, Changsha, China, 2005.

[14] K. I. Smith, R. M. Everson, J. E. Fieldsend, C. Murphy, and R. Misra, "Dominance-based multiobjective simulated annealing," *IEEE Transactions on Evolutionary Computation*, vol. 12, no. 3, pp. 323–342, 2008.

[15] S. Y. Sun, H. Y. Wang, and Z. M. Qiu, "Robustness analysis method of PROMETHEE weights with incomplete information," *Command Control & Simulation*, vol. 29, no. 1, pp. 47–49, 2007.

[16] J. P. Brans, P. Vincke, and B. Mareschal, "How to select and how to rank projects: the Promethee method," *European Journal of Operational Research*, vol. 24, no. 2, pp. 228–238, 1986.

[17] J. P. Brans and P. Vike, "A preference ranking organization method: the PROMETHEE method," *Management Science*, vol. 31, pp. 647–656, 1985.

[18] J.-L. Jin, M.-W. Wang, and Y.-M. Wei, "Objective combined evaluation model for optimizing water resource engineering schemes," *System Engineering Theory and Practice*, vol. 24, no. 12, pp. 111–116, 2004.

[19] H. J. Zou, *Design Principles of Mechanical Systems*, vol. 3, Science press, Beijing, China, 2003.

Hindawi Publishing Corporation
Advances in Mechanical Engineering
Volume 2013, Article ID 474872, 9 pages
http://dx.doi.org/10.1155/2013/474872

Research Article

Optimum Design of 1st Gear Ratio for 4WD Vehicles Based on Vehicle Dynamic Behaviour

M. H. Shojaeefard,[1] R. Talebitooti,[2] and Sadegh Yarmohammadi Satri[2]

[1] *School of Mechanical Engineering, Iran University of Science and Technology, Tehran, Iran*
[2] *School of Automotive Engineering, Iran University of Science and Technology, Narmak, Tehran 1684613114, Iran*

Correspondence should be addressed to R. Talebitooti; rtalebi@iust.ac.ir

Received 23 January 2013; Revised 26 June 2013; Accepted 24 July 2013

Academic Editor: Yu-Shen Liu

This paper presents an approach that allows optimizing gear ratio and vehicle dimension to achieve optimum gear transmission. Therefore, augmented Lagrangian multiplier method, defined as classical method, is utilized to find the optimum gear ratios and the corresponding number of gear teeth applied to all epicyclical gears. The new method is able to calculate and also to optimize the gear ratio based on dynamics of 4WD vehicles. Therefore, 4WD vehicles dynamic equations are employed assuming that the rear wheels or the front wheels are at the point of slip. In addition, a genetic algorithm is modified to preserve feasibility of the encountered solutions. The basic dimension of a sample commercial vehicle (2009 hummer H3 4dr AWD SUV) and its gearbox are optimized, and then the effects of changing slip angle, wheel base, and engine torque on optimum vehicle dimension are analyzed.

1. Introduction

The gear ratio of a gear train is the ratio of the angular velocity of the input gear to the angular velocity of the output gear, also known as the speed ratio of the gear train [1]. The gear ratio can be computed directly from the number of teeth of the various gears that engage to form the gear train [2]. To achieve a specific set of speed ratios, the designer has to choose a gear train with specific internal-external gear pair combinations, a set of clutches that are to be operated in a chosen sequence, and a set of gear ratios. (In the automotive industry the reciprocal of the reduction ratio is often specified.) The term of gear ratio refers to the ratio of the number of teeth on two mating gears. The classical approach of finding the proper gear ratios has been to choose a gear train and a corresponding clutching sequence and then to vary the gear ratios by trial and error until the best possible reduction ratios have been obtained [3, 4]. Gears are among the most common elements of machine, and therefore, there have been many studies on optimum gear design. Gear optimization can be divided into two categories, namely, single gear pair and gear train optimization [5]. The analysis of these two gears is conventionally done based on classical method which utilizes tooth gears. This method facilitates the design although it does not consider dynamic behaviour of the vehicle.

This paper describes a practical approach to gear train design and optimization. The presented novel algorithm is based on a two-stage optimization process. The first part of the process employs a mathematical optimization method based on dynamic behaviour of vehicle, and the second uses the ratio between gear teeth. This approach concentrates on the following issues related to automotive automatic transmissions:

(i) application of optimization techniques to find the gear ratios in automotive gear trains for a given set of reduction ratios,

(ii) optimizing gear ratio of a commercial car based on genetic algorithm,

(iii) development of a user-friendly method for optimizing basic dimensions of a vehicle based on dynamic equations.

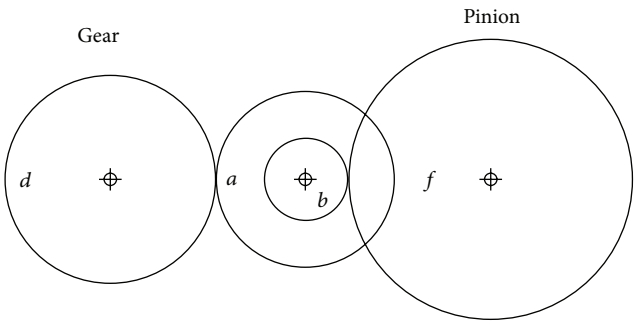

Figure 1: Compound gear train.

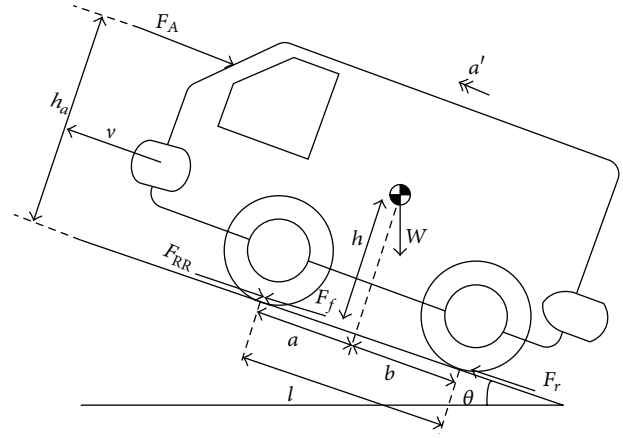

Figure 2: Presentation of a 2D vehicle model.

2. Classical Design of Gear Train

In order to find the required overall gear ratio, the compound gear train contains two pairs of gears, *d*-*a* and *b*-*f* (Figure 1). The desired gear ratio, i_{tot}, between the input and output gears is displayed as

$$i_{\text{tot}} = \frac{w_o}{w_i} = \frac{n_d n_b}{n_a n_f}, \tag{1}$$

where w_o and w_i are the angular velocities of the output and input gears, respectively, and n expresses the number of teeth on each gear wheel.

2.1. Classical Gear Ratio Optimization. In the augmented Lagrangian multiplier method, the objective function is computing the number of teeth for gears *d*, *a*, *b,* and *f* in order to find a gear ratio, i_{tot}. The minimum number of teeth for each gear is assumed between 12 and 60. The target ratio, i_{trg}, is assumed to be 1/6.93, and the function is expressed as follows:

$$\begin{aligned} &X = \left(z_d, z_b, z_a, z_f\right), \quad X \in \{12, 13, \ldots, 60\}, \\ &\text{to } \min f(x) = \left(i_{\text{trg}} - i_{\text{tot}}\right)^2 = \left(\frac{1}{6.93} - \frac{z_d z_b}{z_a z_f}\right)^2 \\ &\text{subjected to} \quad 12 \le x_i \le 60, \quad i = 1, 2, 3, 4. \end{aligned} \tag{2}$$

In other words, the process is going to compute the optimum values of four variables that will minimize the squared difference between the target ratio, i_{trg}, and available gear ratio, i_{tot}. The objective function is expressed as the squared error between the actual and the desired gear ratios.

An alternative solution for the gear train problem is founded by the differential evolution strategy. These solutions have been found to be globally optimal by applying explicit enumeration as mentioned in Tables 1 and 2 [12–14]. In this paper this problem has been resolved with genetic algorithm for 2009 hummer H3 4dr SUV.

Table 1: Alternative solution for gear ratio problem [3].

Solution	z_d	z_b	z_a	z_f
1	19	16	43	**49**
2	16	19	43	**49**
3	19	16	49	**43**
4	16	19	49	**43**

3. 4WD Vehicle Dynamic Gear Ratio

The dynamic gear ratio is obtained with applying dynamic equations as follows [15, 16]:

$$\begin{aligned} F_I &= ma', \\ F_f + F_r - F_{\text{RR}} - W\sin\theta - F_A - F_I &= 0, \\ -W\cos\theta + N_f + N_r &= 0, \\ F_A h_A + F_I h + N_f l - bW\cos\theta + hW\sin\theta &= 0. \end{aligned} \tag{3}$$

F_f and F_r are front and rear traction forces, respectively. m, vehicle mass, a' is the acceleration, F_{RR} is the rolling resistance force, w is the vehicle weight, θ is the road slope, F_A is the aerodynamic force, N_f is the front reaction force, N_r is the rear reaction force, h_A is the height of aerodynamic force, h is the centre of gravity height force, l is the wheel base, and a and b are distances from c.g. to front and rear wheels, respectively. Consider

$$N_f = \frac{b}{l} w\cos\theta - \frac{h}{l}\left(w\sin\theta + F_I\right) - F_A\frac{h_A}{l}. \tag{4}$$

According to Figure 2, the total traction force F_T, which is the combination of rear and front traction forces, is defined as

$$F_T = F_f + F_r. \tag{5}$$

Table 2: Optimal solution for the gear train problem.

Reported by	X_1 (z_d)	X_2 (z_b)	X_3 (z_a)	X_4 (z_f)	Gear ratio	Error%
Sandgren [6]	18	22	45	60	0.1466	1.65
Fu and Wang [7]	14	29	47	59	0.1464	1.17
Loh and Papalambros [8]	19	16	42	50	0.1447	0.33
Wang and Zhang [9]	30	15	52	60	0.1442	0.03
Hsu et al. [10]	19	16	49	43	0.1442	0.01
Kannan and Kramer [11]	13	15	33	41	0.1441	0.11

Also

$$w \sin\theta + F_I = F_T - F_{\mathrm{RR}} - F_A, \tag{6}$$

$$\Delta h = h - h_A, \tag{7}$$

$$F_{\mathrm{RR}} = f_r N, \tag{8}$$

$$N = N_f + N_r. \tag{9}$$

f_r is the rolling resistance coefficient. Solving the previous equations gives (4)–(9) as

$$N_r = \frac{a}{l} W \cos\theta + \frac{h}{l}\left[F_T - F_{\mathrm{RR}}\right] + \frac{\Delta h}{l} F_A, \tag{10}$$

$$N_f = \frac{b}{l} W \cos\theta - \frac{h}{l}\left[F_T - F_{\mathrm{RR}}\right] + \frac{\Delta h}{l} F_A. \tag{11}$$

In a 4WD vehicle, the wheel torques at front and rear axles are distributed such that the ratio of front to rear axle torques is given by r. Assuming that the rear wheels are at the point of slip, an expression is driven for gear ratio of a 4WD vehicle. According to Figure 2, the total traction force is

$$F_T = F_f + F_r. \tag{12}$$

The equal front and rear gear ratios are obtained by dividing the ratio of traction force of the front and rear axes, which is followed as

$$r = \frac{T_f}{T_r} = \frac{F_f}{F_r}. \tag{13}$$

Substitution of (5) into (13) will result in

$$F_T = (1 + r) F_r. \tag{14}$$

When the rear tyres are at the point of slip, (14) can be written as

$$F_{T\max} = (1 + r)\, \mu_p N_r, \tag{15}$$

where μ_p is the road friction coefficient.

In this paper, the vehicle velocity is considered equals to zero which happens in the maximum road slope and tyre slip point. Neglecting the term of $\Delta h F_A$ in (10) and its substitution in (12) leads to

$$N_r = \frac{a}{l} W \cos\theta + \frac{h}{l}\left[(1 + r)\, \mu_p N_r - F_{\mathrm{RR}}\right]. \tag{16}$$

Substituting (8) into (16) and considering $N = W \cos\theta$, (18) is obtained as

$$N_r - \frac{h}{l}\left((1 + r)\, \mu_p N_r\right) = \frac{a}{l} W \cos\theta - \frac{h}{l}\left(f_r W \cos\theta\right), \tag{17}$$

$$N_r = \frac{a - h \times f_r}{l - h\mu_p\,(r + 1)} W \cos\theta. \tag{18}$$

Substituting (16) into (15), the maximum traction force is computed as

$$F_{T\max} = \frac{a - h \times f_r}{l - h\mu_p\,(r + 1)} (r + 1)\, \mu_p W \cos\theta. \tag{19}$$

The equation of gear ratio (n_l) is presented as

$$n_l = \frac{r_w F_{T\max}}{n_d T_e}, \tag{20}$$

Where n_d is the differential ratio, T_e is the motor torque, and r_w is the tyre radius. Also with substituting (12) into (13) the rear gear ratio (nlr) is obtained as follows:

$$n_{lr} = \frac{r_w}{n_d \times T_e} (r + 1)\, \mu_p \frac{a - h \times f_r}{l - h\mu_p\,(r + 1)} W \cos\theta. \tag{21}$$

On the other hand, assuming that the front wheels are at the slip point, an expression for gear ratio of a 4WD vehicle can be obtained. According to (5) and (13) the total traction force can be written as

$$F_T = \left(1 + \frac{1}{r}\right) F_f. \tag{22}$$

When the front tyres are at the slip point, the maximum traction force can be computed as

$$F_{T\max} = \left(1 + \frac{1}{r}\right) \mu_p N_f,$$

$$N_f = \frac{b}{l} W \cos\theta - \frac{h}{l}\left[\left(1 + \frac{1}{r}\right) \mu_p N_r - F_{\mathrm{RR}}\right], \tag{23}$$

$$N_f = \frac{b + h \times f_r}{l + h\mu_p\,(1/r + 1)} W \cos\theta.$$

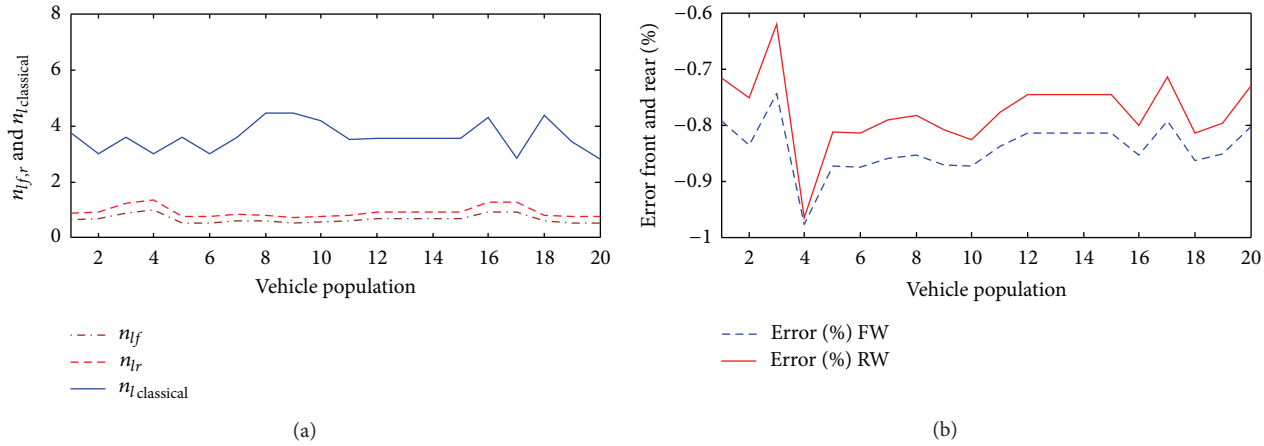

FIGURE 3: Gear ratio and its error when the front or rear tyres are at slips points.

Therefore with substituting the maximum traction force, it can be expressed as

$$F_{T\max} = \frac{b + h \times f_r}{l + h\mu_p\,(1/r + 1)} \left(\frac{1}{r} + 1\right) \mu_p W \cos\theta. \tag{24}$$

Finally, the front gear ratio is expressed as

$$n_{lf} = \frac{r_w}{n_d \times T_e} (r + 1)\, \mu_p \frac{b + h \times f_r}{rl + h\mu_p\,(r + 1)} W \cos\theta. \tag{25}$$

The dynamic gear ratio results are compared in two ways. Firstly, a vehicle population including 20 sample cars is compared in such parameters as gear ratio. Secondly, the method was performed to evaluate dynamic gear ratio. The differences between methods are compared with each other. The idea is to show that even the dynamic form, for let us say 70%, is still performing better than the classical form in the case where both of them are used in commercial car.

The values of 1st dynamic gear ratio are compared with those of the 1st classical gear ratio ($n_{l,\text{real}}$) for 20 sample cars that are used by the car factories. This comparison is illustrated in Figure 3. the conventional method does not consider tire slip and the fact that the front or rear tire slip presents different behaviour and makes the calculation more similar to reality. So the dynamic gear ratio is considerably better than the classical gear ratio. Moreover the difference between classical gear ratio and dynamic gear ratio is illustrated in Figure 3. The first gear ratio should be around 4 to 6 to produce more torque in tires. The gear ratios that are proposed in Table 2 are not vehicle ratios and they are used for presenting the classical gear ratio calculation method. The second vehicle gear ratio and other gear ratios reduce to decrease engine torque. The gear ratios of Figure 3 are different from the ratios presented in Table 2 although the same method is utilized in computing vehicle classical gear ratio.

To optimize the gear ratio in different road slope and for obtaining the optimum basic dimension of 2009 hummer H3 4dr SUV, the effects of gear ratio parameters should be analysed. The effects of basic vehicle dimension variation

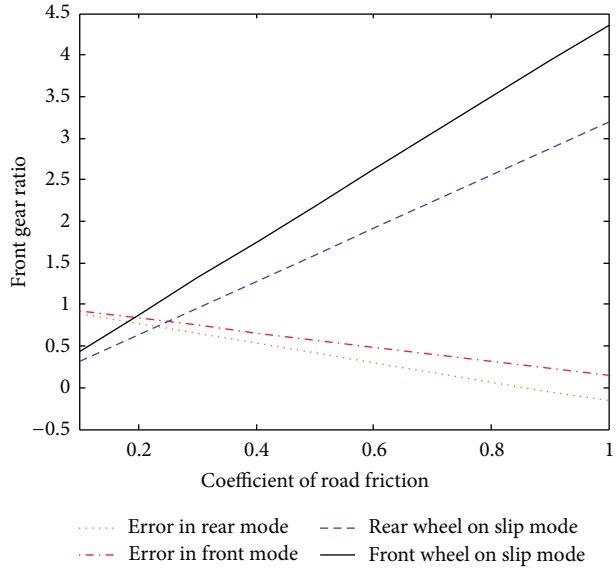

FIGURE 4: Rear/front gear ratio versus displaying coefficient of road friction.

such as friction coefficient, rolling resistance coefficient, and weight distribution evaluation are studied in Figures 4–6. These figures are utilized for determining the bounds of optimization parameters in the case that the gear ratio error is approximately around zero in each parameter. Moreover, Figures 4–6 indicate the effects of changing parameters such c.g. height of vehicle, μ_p, and f_r on gear ratio. In addition it would indicate how changing these parameters will change the gear ratios and presents the optimum gear ratio which refers to the point where the errors of parameters are around zero to increase the efficiency of gearbox.

3.1. Coefficient of Road Friction. Coefficient of road friction variation has an effect on the dynamic gear ratio. Its error with classical gear ratio has been shown in Figure 4. As presented in Figure 4, increasing the coefficient of road

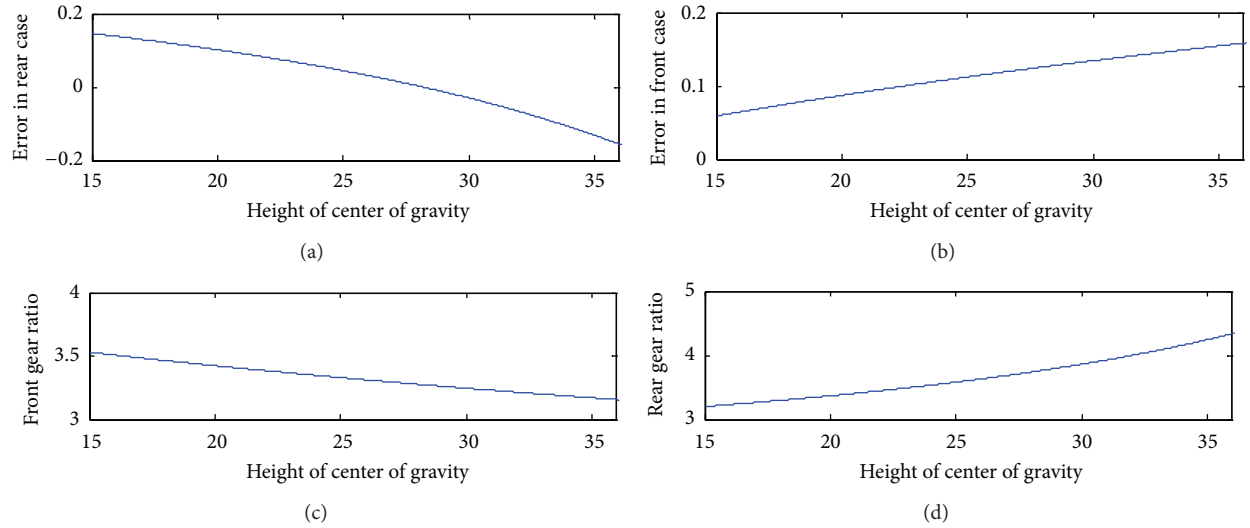

Figure 5: Relationship between error of rear/front gear ratio and height of vehicle c.g..

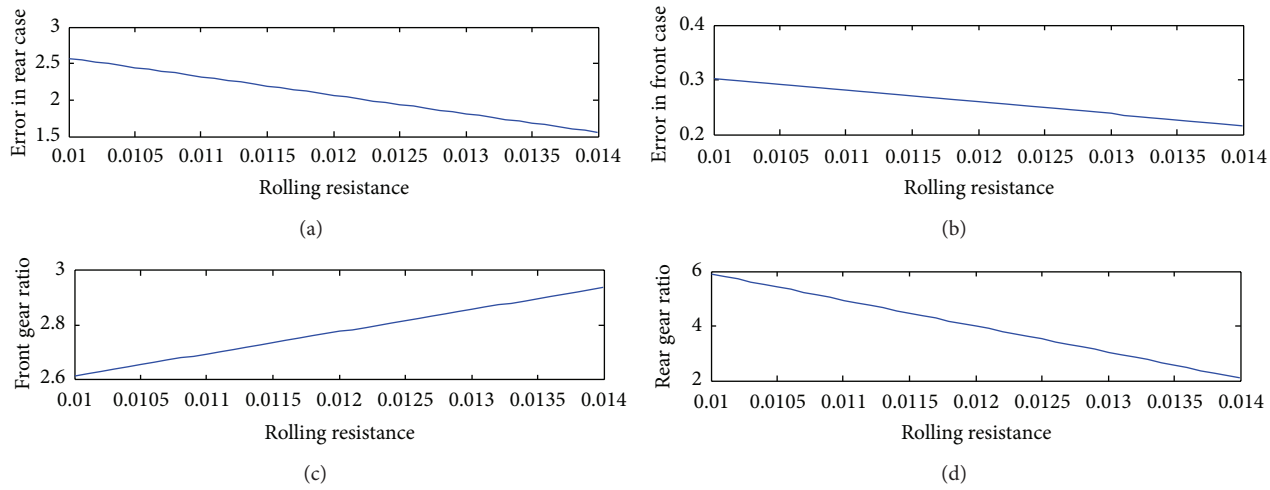

Figure 6: Relationship between error of rear/front gear ratio and rolling resistance.

friction will decrease the difference between classical gear ratio and dynamic gear ratio. In other words, there is a direct relationship between front and rear gear ratios and coefficient of road friction.

3.2. Height of Vehicle c.g. The vehicle c.g. height variation has an effect on the dynamic gear ratio. The error that occurred with classical gear ratio has been shown in Figure 5. As shown, enhancing the c.g. height increases the difference between classic and dynamic gear ratios for frontal mode. On the contrary, this discrepancy will be decreased for rear mode. As a result, front and rear gear ratios have contrariwise effects.

3.3. Rolling Resistance Friction. Rolling resistance, sometimes named rolling friction or rolling drag, is the force resisting the motion when the tire rolls on a surface. It is mainly caused by nonelastic effects; that is, not all of the energy that is needed for deformation of the object is recovered when the pressure is removed. The rolling resistance is presented as a function of velocity, followed as

$$f_r = 0.01 \times \left(1 + \frac{v}{100}\right). \tag{26}$$

Figure 6 shows that enhancing the rolling resistance coefficient decreases the difference between classical gear ratio and dynamic gear ratio. Moreover, increasing the rolling resistance enhances front gear ratio.

4. Genetic Algorithm Optimization

Nowadays using evolution methods to solve optimization problems has a growing trend. Genetic algorithms as the most popular evolution algorithms have an extensive application in esearch studies [17–19]. The 1st dynamic gear ratio in the case that front or rear wheels are at the point of slip

Table 3: 2009 hummer H3 4dr SUV basic dimension.

2009 hummer H3 4dr	Value
Height (m)	1.872
Weight (kg)	2133
First drive ratio	3.75
n_f	3.7
Wheel base (m)	2.864

uses 9 design variables in order to propose an appropriate model of a gear ratio design. The result of the optimization is specifying basic dimensions of vehicle, optimum road slope, 1st gear ratio, and gear train, which minimize the squared difference between the available classical gear ratio, $n_{l,\text{real}}$, and dynamic gear ratio, $n_{l,f,\text{or},r}$. Genetic algorithm begins with a number of solutions called population. These solutions are represented by strings of gene chromosomes [20, 21]. They are taken from a population of solutions and are used to create new populations, with the thought that the new population is better than the original population. Another term in genetic algorithm is mutation rate. Mutation operator changes the integer parts of strings. Mutation of each string is proportional to the initial objective function (the squared difference between the available classical gear ratio, $n_{l,\text{real}}$, and dynamic gear ratio, $n_{l,f,\text{or},r}$), which is chosen to fit the mutation rate (Figure 7). This operator can provide a solution that does not exist in the population to compensate loss of valuable information resulting from inadequate intersection. In this paper, the mutation rate, which determines accuracy and speed of convergence response in the GA program, is investigated. The code developed here includes a large number of explorations for different items such as population number, iteration number, value of cost function, and mutation rate. Thus, the minimum value of iteration and speed of convergence are very important. To explore the effect of mutation rate, classical gear ratio of 3.7 is taken. The mutation rates take the values 0, 1%, 4%, 6%, and 15%. An early convergence occurs without any mutation rate, and GA algorithm cannot satisfy all of the possible values of constraints. For the case of 1% mutation the individual bit changes and the chance of achieving better fitness functions increases. While the mutation equals zero, the best fitness function is obtained at 45 generations. However, while the value of mutation rate takes 1%, proper fitness function is obtained at 100 generations. As mentioned, enhancement of the mutation rate value increases the probability of various individuals in the population. Based on this explanation, the mutation rate should be selected between 4% and 6%, which is obtained with trial and error.

In this paper dynamic gear ratio equation is optimized with genetic algorithm through a diagram that is presented in Figure 8. The objective function is indicated in (27), and it is the squared difference between the available classical gear ratio, $n_{l,\text{real}}$, and dynamic gear ratio, $n_{l,f,\text{or},r}$. This optimization leads to the benefit of vehicle's parameters such as wheel base and inclination angle as listed before, in Table 3. The best cases of gear ratios for a 4WD vehicle are provided.

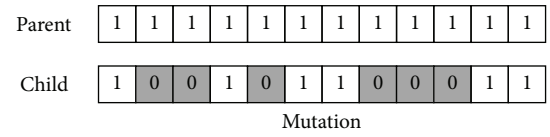

Figure 7: Genetic algorithm operator.

It is also necessary to introduce randomly chosen variables constrained within specific boundaries. These variables and their band are indicated through (28):

$$f(x) = \left(n_{l,\text{real}} - n_{l,f,or,r}\right)^2, \tag{27}$$

$$\begin{gathered} 2 \le l \le 3, \\ 300 \le T_e \le 320, \\ 0.4 \le r_w \le 0.5, \\ 0.4 \le h \le 0.6, \\ 1.5 \le b \le 1.9, \\ 0 \le \theta \le 45, \\ 0.1 \le \mu_p \le 1, \\ 0.3 \le r \le 1, \\ 0.01 \le f_r \le 0.014. \end{gathered} \tag{28}$$

4.1. Applying the Genetic Algorithm (GA). The population size in the gear ratio optimization represents the number of individuals in the population. Usually larger population size increases the amount of variation present in the initial population, and it requires more fitness evaluations. In this case, with a population size of 20, an excellent solution was easily attained. Naturally, a smaller population size will introduce less generations, and the calculation time will be reduced. As presented in Figures 9 and 10, it can be seen that after a sufficient number of generations (around 50 generations), the track for a good (best) solution as well as the track of the average of the population converges to the final solution. Applying genetic algorithm for optimizing basic dimensions of 2009 hummer H3 4dr concludes into optimum data to achieve the most suitable gear ratios. Optimum dimensions of 2009 hummer H3 4dr, noted in Table 4, are suggested in designing the car in order to attain the best dynamic performance.

5. Results and Discussion

The results of gear ratio obtained from genetic algorithm are compared with those of conventional methods reported for hummer H3 4dr. This study confirms the results obtained by Godfrey and Babu. The program is capable of finding excellent results for different constraints that are optional and can consider many parameters. In classical form, in order to

Table 4: Optimum dimensions of 2009 hummer H3 4dr.

2009 hummer H3 4dr	Optimum dimensions (front wheel in slip mode)	Optimum dimensions (rear wheel in slip mode)	Prototype dimensions
Wheel diameter (m)	0.45	0.35	0.4
Torque (N·m)	310	325	326.75
Wheel base (m)	2.5	2.5	2.864
Distance between rear tire and c.g. (m)	1.7	1.7	1.85
c.g. height	0.5	0.5	0.624

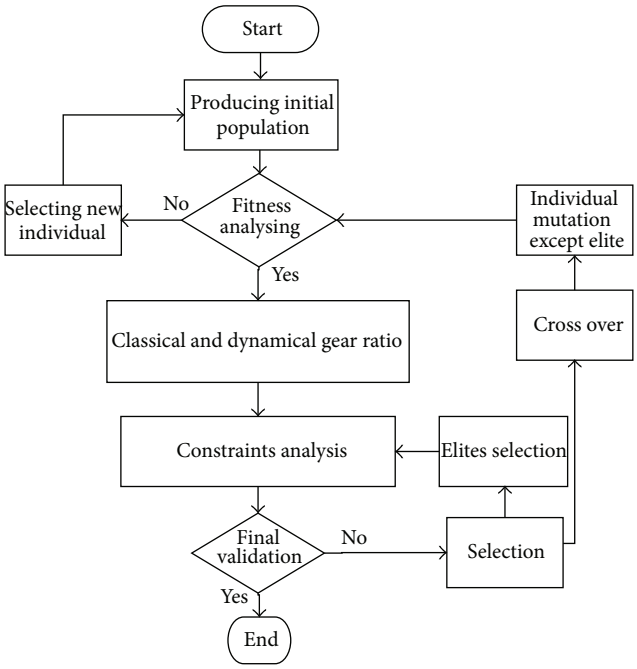

Figure 8: Genetic algorithm diagram.

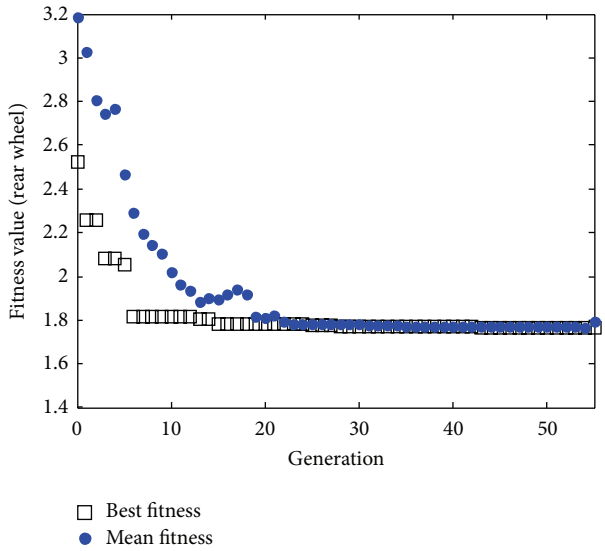

Figure 9: Evolution of the performance for a population = 20 when rear wheel is in slip mode.

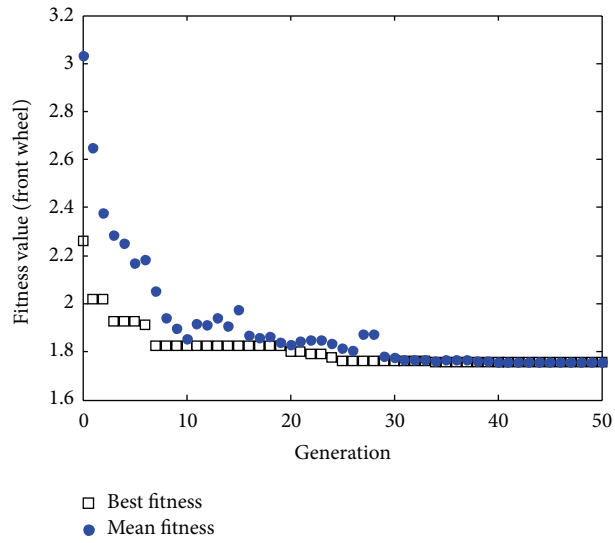

Figure 10: Evolution of the performance for a population = 20 when front wheel is in slip mode.

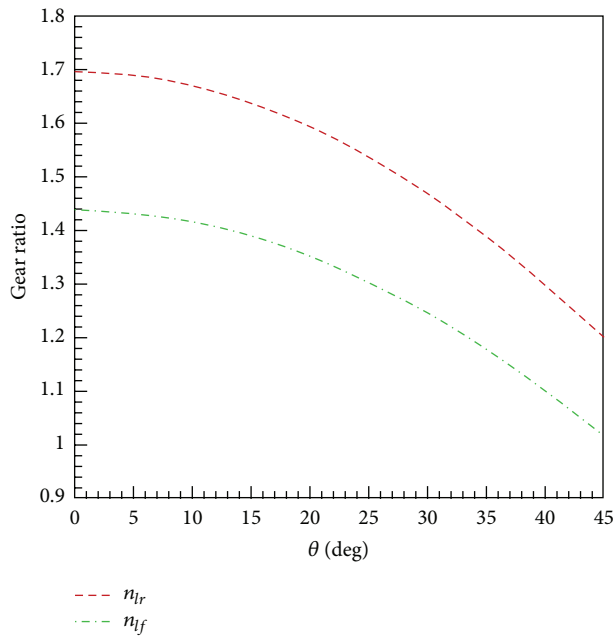

Figure 11: Optimum front and rear gear ratios for different road slope angles.

Table 5: Optimal solution for the gear train of 2009 hummer H3 4dr.

2009 hummer H3 4dr	z_d	z_b	z_a	z_f
Genetic algorithm optimization	19	29	46	45
Hsu et al. [10]	19	16	49	43

find the required overall gear ratio, the compound gear train contains two pairs of gears. The second objective function is expressed as the squared error between actual and desired gear ratios. This optimization introduces a gearbox which is obtained from dynamic gear ratio and presents a proper gear ratio. The Godfrey model is based on conventional gear ratio computation which utilizes the classical gear ratio for determining gear tooth. This model is compared with the dynamic model for precise gear tooth. Table 5 expresses number of teeth which is confirmed with results obtained by Godfrey and Babu [3].

The road slope angle is studied in optimized design to introduce the best ratio compatible with environment particularly to make the vehicle perform in a suitable condition. Figure 11 presents an optimum gear ratio in both front and rear slip modes through different road slopes which means that different cities with average road slope need specific gearbox and gear ratios.

6. Conclusion

In this paper two issues related to automotive gear ratio have been considered. Firstly, the traditional trial and error approach is presented to calculate the gear ratio based on discovering combination of gear teeth numbers which satisfy the geometric constraints.

Secondly, the dynamic gear ratios are computed with the aid of dynamic parameters of a vehicle. Then, comparing the presented results with those of traditional gear ratio design shows the superiority of this research for a commercial car.

Then, a new method is developed to calculate the first gear ratio which has a tendency to minimize the difference between dynamic gear ratio and classical gear ratio. Therefore, dynamic equations for calculating gear ratio have been overstated to study the first gear ratio for optimizing basic dimensions of a sample car (2009 hummer H3 4dr). The presented method was also used to evaluate the optimum dimensions of a vehicle to achieve the minimum differences of classical and dynamic gear ratios. It is also concluded that more road slope yields low first gear ratio due to the effect of c.g. height. The results are also compared with those reported by Godfrey and Babu [3]. Comparing the results shows the reliability of the presented research. The presented algorithm has the high flexibility in comparison with the conventional one. It is more adaptive to get the best gear ratios where dynamic constraints are of high importance. Moreover, this paper indicates the effects of changing parameters such as c.g. height of vehicle, μ_p, and f_r on gear ratio. The presented diagrams are used for determining the bounds of optimization parameters in the case that the gear ratio error is approximately around zero in each parameter. Moreover, the equations of front and rear gear ratios indicate that two parameters of wheel base length and engine torque play an important role to achieve the suitable performance.

References

[1] J. J. Uicker, G. R. Pennock, and J. E. Shigley, *Theory of Machines and Mechanisms*, Oxford University Press, 2003.

[2] B. Paul, *Kinematics and Dynamics of Planar Machinery*, Prentice Hall, New York, NY, USA, 1979.

[3] C. Godfrey and B. V. Babu, *New Optimization Techniques in Engineering*, Springer, New York, NY, USA, 2004.

[4] K. Deb and M. Goyal, "Optimizing engineering designs using a combined genetic search," in *Proceedings of the 7th International Conference on Genetic Algorithms*, pp. 521–528, 1997.

[5] S. Prayoonrat and D. Walton, "Practical approach to optimum gear train design," *Computer-Aided Design*, vol. 20, no. 2, pp. 83–92, 1988.

[6] E. Sandgren, "Nonlinear integer and discrete programming in mechanical design," in *Proceedings of the ASME Design Technology Conference*, pp. 95–105, Kissimme, Fla, USA, September 1988.

[7] J. C. Fu and L. Wang, "A random-discretization based Monte Carlo sampling method and its applications," *Methodology and Computing in Applied Probability*, vol. 4, pp. 5–25, 2002.

[8] H. T. Loh and P. Y. Papalambros, "A sequential linearization approach for solving mixed-discrete nonlinear design optimization problems," *Journal of Mechanisms, Transmissions, and Automation in Design*, vol. 113, no. 3, pp. 325–334, 1991.

[9] Y. Wang and W. J. Zhang, "Stochastic vibration model of gear transmission systems considering speed-dependent random errors," *Nonlinear Dynamics*, vol. 17, no. 2, pp. 187–203, 1998.

[10] C.-H. Hsu, K.-T. Lam, and Y.-L. Lin, "Automatic synthesis of displacement graphs for planetary gear trains," *Mathematical and Computer Modelling*, vol. 19, no. 11, pp. 67–81, 1994.

[11] B. K. Kannan and S. N. Kramer, "An augmented lagrange multiplier based method for mixed integer discrete continuous optimization and its applications to mechanical design," *Journal of Mechanical Design*, vol. 116, no. 2, pp. 405–411, 1994.

[12] K. Deb and M. Goyal, "A flexible optimization procedure for mechanical component design based on genetic adaptive search," *Journal of Mechanical Design*, vol. 120, no. 2, pp. 162–164, 1998.

[13] E. Sandgren, "Nonlinear integer and discrete programming in mechnical design optimization," *Journal of Mechanisms, Transmissions, and Automation in Design*, vol. 112, no. 2, pp. 223–229, 1990.

[14] J. F. Fu, R. G. Fenton, and W. L. Cleghorn, "A mixed integer discrete continuous programming method and its application to engineering design optimization," *Engineering Optimization*, vol. 17, pp. 263–280, 1991.

[15] D. Crolla and B. Mashadi, *Vehicle Powertrain Systems*, John Wiley & Sons, New York, NY, USA, 2011.

[16] R. G. Pennock, J. J. Uicker, and J. E. Shigley, *Theory of Machines and Mechanisms*, Oxford University Press, New York, NY, USA, 2009.

[17] C.-H. Ko and S.-F. Wang, "Precast production scheduling using multi-objective genetic algorithms," *Expert Systems with Applications*, vol. 38, no. 7, pp. 8293–8302, 2011.

[18] A. Kaur and A. K. Bakhshi, "Change in optimum genetic algorithm solution with changing band discontinuities and band widths of electrically conducting copolymers," *Chemical Physics*, vol. 369, no. 2-3, pp. 122–125, 2010.

[19] R. L. Haupt and S. E. Haupt, *Practical Genetic Algorithms*, John Wiley & Sons, New York, NY, USA, 2004.

[20] J. D. Dyer, R. J. Hartfield, G. V. Dozier, and J. E. Burkhalter, "Aerospace design optimization using a steady state real-coded genetic algorithm," *Applied Mathematics and Computation*, vol. 218, no. 9, pp. 4710–4730, 2012.

[21] M. Salehi and R. Tavakkoli-Moghaddam, "Application of genetic algorithm to computer-aided process planning in preliminary and detailed planning," *Engineering Applications of Artificial Intelligence*, vol. 22, no. 8, pp. 1179–1187, 2009.

Hindawi Publishing Corporation
Advances in Mechanical Engineering
Volume 2013, Article ID 401492, 9 pages
http://dx.doi.org/10.1155/2013/401492

Research Article

Conceptual Design of Compliant Mechanism Based on Port Ontology

Zhanwei Li and Dongxing Cao

School of Mechanical Engineering, Hebei University of Technology, Tianjin 300130, China

Correspondence should be addressed to Zhanwei Li; lzw@hebut.edu.cn

Received 20 April 2013; Accepted 18 July 2013

Academic Editor: Shengfeng Qin

It is an effective method for port-based ontology (PBO) to be used to represent and organize product design information and, support product conceptualization. As port is used to map and link components together, it plays an important role in capturing component information. This paper establishes a design method of compliant mechanism based on port ontology. Firstly, the coding rules are constituted based on PBO, and knowledge base of compliant mechanism is constructed, which includes stiffness base and inherent frequency base of flexible cells. Secondly, incidence matrix is established to denote the relationship of components, and based on incidence matrix design, schemes are generated by adopting the genetic algorithm. Thirdly, by selecting suitable parameters, scheme populations are generated towards training neural network (NN), and the trained NN model is employed for choosing preferential schemes to be satisfied with users' demands. At last, an application case is given to demonstrate the conceptual design of compliant mechanism based on port ontology.

1. Introduction

Port-based ontology, as an approach to be involved in product design, has been effectively applied to conceptual description of a product. Ontology has been known as an important means to represent design knowledge in the stage of product development. In general, a consistent and sharable description of design knowledge can be summarized as a fundamental concept for capturing the functional knowledge. Such specification of conceptualization is generally called ontology [1].

PBO modeling has been viewed as an effective approach to supporting conceptual design [2]. Methods to be used for matching multi-information, such as functions and constraints, should be further developed. This has been demonstrated by a great lot of work reported in the literatures [3–5]. Port compatibilities are used to map and link two components, which makes it possible to build incidence matrix and allow designers from different backgrounds with various interests to access the functional ontology of components [6].

Researchers have explored multidesign methods to apply to analyze design activities such as axiomatic design, quality function deployment, and theory of inventive problem solving (TRIZ) [7]. At the early stage of design processes, the components constitute the fundamental building blocks of these activities. Benefitting from the varieties of computer aided design research and various methodologies, a rich library set of components has been developed [8]. However, there is no agreement upon standard component library to share with their design processes. As a result, the libraries of components are independently developed on the basis of the domain knowledge. One goal of this research is to obtain flexible component library that can be available to interrelated designs. It is not to capture all component types that physically exist but to create a function-based hierarchical framework of subcategories in order to represent component design knowledge and obtain design alternatives.

It plays an important role in precise positioning and displacement for compliant microdriving mechanism. The flexible cells transfer energy, force, and motion through the deformation of flexible components. Furthermore, they are easy to fabricate due to their monolithic nature. Being lack of friction and wear, compliant mechanism is ideally suited towards obtaining precise motion [9]. Type synthesis of the flexible

Table 1: Rigid mechanism and compliant mechanism for enlarging displacement.

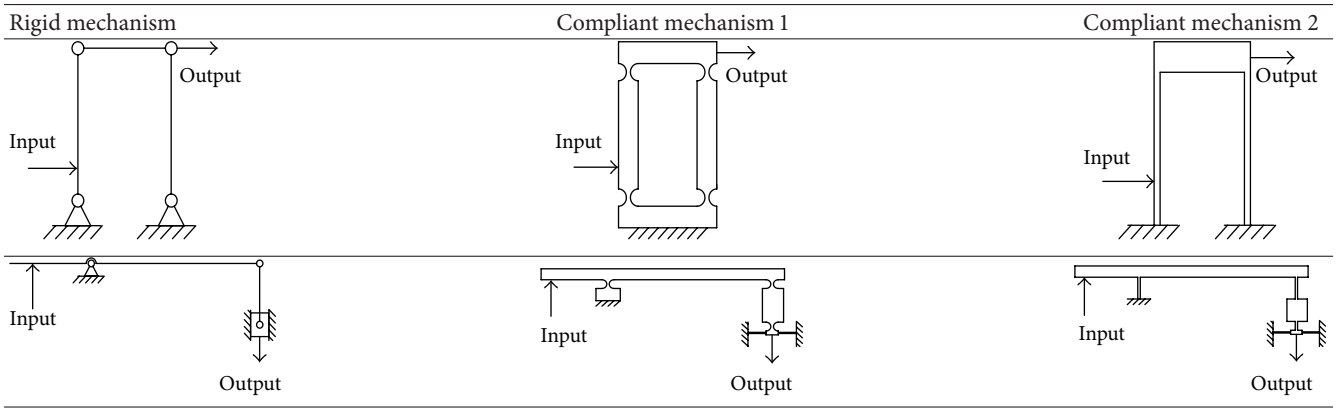

Table 2: Flexible cells of compliant mechanism.

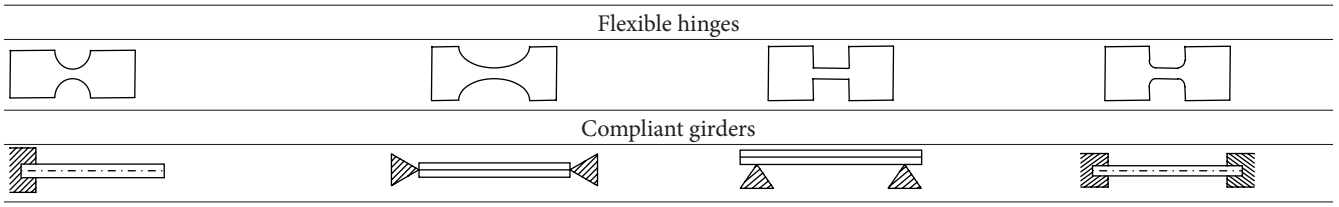

component and the mechanism structure are the decisive factors which determine its performance [10]. Kinematic characteristic is considered at every stage of designing process including preliminary design. For compliant mechanism, the general design method is to estimate all the structure parameters experientially in advance and then analyze its stiffness and inherent frequency. Unfortunately, this process depends mainly on one's experience, and the result usually does not best meet the given requirements. Being devoid of systematic theory foundation, the parameter design method is blindfold and difficult to be put into practice [11].

This paper is to explore the conceptual design theory of compliant mechanism targeting towards content original structure parameters, stiffness, and inherent frequency and also to provide a framework for the latter work and the entire process of design. The rest of the paper is organized as follows. At first, the prototype components of compliant mechanism are introduced; Secondly, PBO component taxonomy and PBO knowledge support for conceptual generation are expounded and analyzed; thirdly, the flow graph of compatibility and solving matching rule is laid out; at last, a case study is given to demonstrate the process of a design scheme generation.

2. Prototype Components of Compliant Mechanism

In general, the prototype components of compliant mechanism are from the rigid mechanism. However, they have a big difference in many respects such as work environment, precise, purpose, manner, linkage, and cost. The similarity between rigid links and flexible behavior makes it easy to scheme out the prototype from rigid mechanism based on kinematic approaches. Table 1 takes a comparison between rigid mechanism and compliant mechanism. Also flexible cells are listed in Table 2, and they include compliant girders and flexible hinges in compliant mechanism.

3. PBO Taxonomy of Compliant Mechanism

3.1. Component Attributes. Three kinds of attributes called taxonomy (TA) are used for capturing each component: descriptive attributes, physical attributes, and functional attributes. They are represented in formula (1) [6]:

$$\mathrm{TA} = \{\mathrm{DA}, \mathrm{PA}, \mathrm{FA}\}, \tag{1}$$

where DA stands for descriptive attributes which particularly include part number, feature quantity, part description, and assembly information. PA means physical attributes which include part weight, type of material, and parametric information such as height, width, length, inside/outside diameters, and thickness. They are physically measured for each component and recorded into the database. FA represents functional attributes which describe each component function, acting interfaces, connectability, and so on.

3.2. Port Attributes. Port, as the location of intended interaction between component and its environment, plays an important role in the product conceptual design. In a system the relationship of component and its port is described in formula (2) [4, 12]:

$$\sum_{i,j=1}^{k} C_{ij} = \mathrm{INT}\left(\sum_{i=1}^{n}\mathrm{IOC}_i, \sum_{j=1}^{n}\mathrm{IOC}_j\right) \quad i \neq j, \tag{2}$$

where IOC represents a component; INT indicates the interaction between i and j component; and C_{ij} stands for

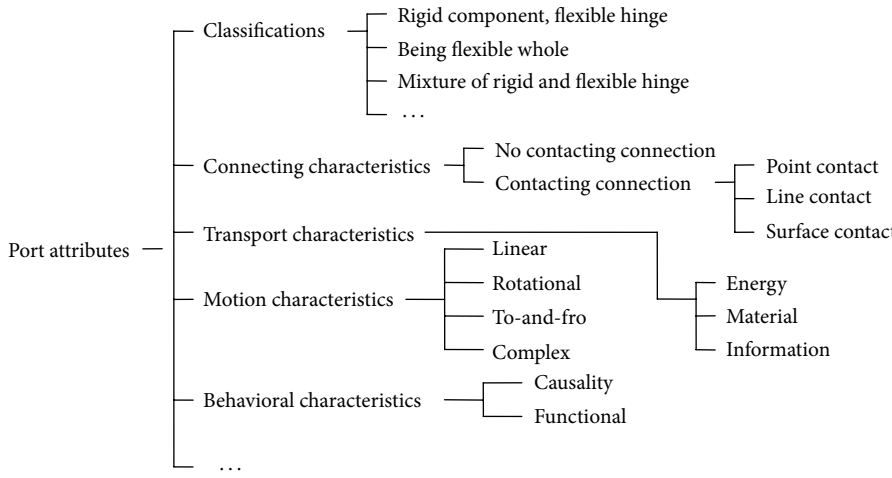

Figure 1: The port attributes of flexible mechanism.

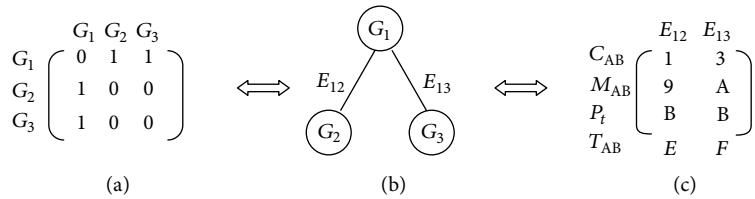

Figure 2: The process of generating incidence matrix.

the connection between i and j. In addition, i, j, k, and n are integers, in which k stands for the number of connection and n for the number of components.

The proposed port taxonomy plays an essential role. The definition of function based on the classes of hierarchical component provides a consistent means of representing component design knowledge that is used for subsequent computational design synthesis. The taxonomy of port attributes is shown in Figure 1.

3.3. PBO Incidence Matrix and Coding Rules. The taxonomy allows us to capture specific relationships between functional needs and components that are used to build incidence matrix.

Port not only constitutes the interface but also defines the boundary of two components. PBO can be expressed with vertex G and edge E as follows [6]:

$$F = (G, E), \tag{3}$$

where G stands for the component number of a product and E means the relationships between two components. Considering a product with three components, vertex G and edge E can be used to build a relation matrix as follows:

$$\begin{matrix} & G_1 & G_2 & G_3 \\ G_1 \\ G_2 \\ G_3 \end{matrix} \begin{bmatrix} E_{11} & E_{12} & E_{13} \\ E_{21} & E_{22} & E_{23} \\ E_{31} & E_{32} & E_{33} \end{bmatrix}. \tag{4}$$

Also, the relationship between component and function can be further described on the basis of attributes of PBO connection. Figure 2 presents the process of incidence matrix generation. Four levels of function-form relations are considered in the proposed incidence matrix. The first one is at the contact relation level, and it corresponds to contact types of two individual components of a product. The second one is at the moving relation level, and it corresponds to the moving relation of two individual components. The third one is at the port type level, and it corresponds to port types of a component in different energy domain. The last one is at the constraint relationship level, and it corresponds to constraint types of two individual components of a product.

Figure 2(a) stands for the matrix of the corresponding components, in which "1" means that they exist in the corresponding relationship. Contrarily, they are marked as "0." Figure 2(b) gives the corresponding structural graph. Figure 2(c) represents incidence matrix with port attribute, in which C_{AB}, M_{AB}, P_t, and T_{AB} are the functional attributes, as shown in Table 3 in detail [6].

4. PBO Knowledge Support for Conceptual Generation

4.1. PBO Prototype Base for Components. The attributes of port include type, contact relationship, moving relationship, constraint relationship and capability, and complexity.

Table 3: The coding rules of compliant mechanism.

Attributes		Contact types	Description
Contact relationship (C_{AB})	0	No contact	There is no contact between two components
	1	Circle	One dof flexible hinge
	2	Ellipse	Two dof flexible hinge
	3	Rounded rectangle	Two dof flexible hinge
	4	Rectangle	One dof flexible hinge
	5	Cantilever	Compliant girder
	6	Two end points	Compliant girder
	7	Two fulcrums	Compliant girder
	8	Two sides	Compliant girder
Moving relation (M_{AB})	9	Straight	The moving relation is linear between two components
	A	Rotational	The moving relation is rotational between two components
Port types (P_t)	B	Mechanical port	Mechanical port (MP) with transfer motion and force
	C	Information port	Transfer various pieces of information from different domains
Constraint relationship (T_{AB})	D	No	No constraint relationship between two components
	E	Size constraint	Size constraint between two components
	F	Movement constraint	Movement constraint between two components

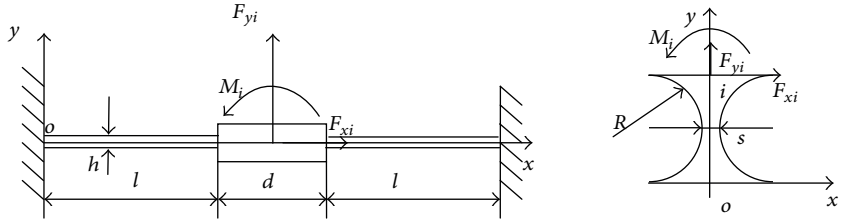

(a) Flexible sliding pairs (b) Flexible circle hinge

Figure 3: Two flexible cells.

Therefore, port attribute performance (PAP) is further expressed in the following:

$$\begin{aligned}\mathrm{PAP} = \big(&\text{number, type, contact relationship,}\\ &\text{moving relationship, constraint relationship,}\\ &\text{purpose, manner, shape, size}\big),\end{aligned} \tag{5}$$

where purpose stands for what the PAP is used for and manner means how the PAP works. For example, according to formula (5), PAP of the port E_{12} is expressed below (see Figure 2):

$$\begin{aligned}\mathrm{PAP} = \big(&E_{12}, \text{Mechanical port, Circle contact,}\\ &\text{Straight, Size constraint,}\\ &\text{Transfer movement, Hinge, Shape, Size}\big),\end{aligned} \tag{6}$$

where PAP.shape and PAP.size are provided from the prototype base and also the parameters of PAP.shape are defined on the basis of PAP.size.

In addition, for E_{12}, parameters include variables (R_1, s_1, and b), which are put into the prototype base. R_1 and s_1 are indicated in Figure 3(b), and b means the thickness.

4.2. Flexible Cells' Stiffness Base and Vibration Frequency Base. Flexible cells are the hinge of compliant mechanism. The influence of its stiffness is essential for the whole compliant mechanism.

Figure 3 presents two flexible cells; one is flexible sliding pairs as shown in Figure 3(a) and the other is circle hinge shown in Figure 3(b), in which u_i represents the displacement of the middle point i and F_i represents the outside force of the point i. They are particularly expressed in the following:

$$\begin{aligned}u_i &= \begin{pmatrix}u_{xi} & u_{yi} & \theta_i\end{pmatrix}^T,\\ F_i &= \begin{pmatrix}F_{xi} & F_{yi} & M_i\end{pmatrix}^T.\end{aligned} \tag{7}$$

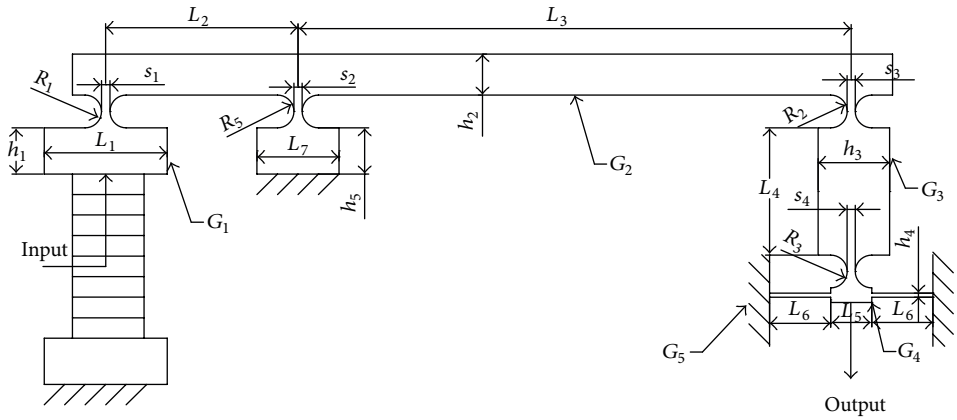

(a) Compliant mechanism

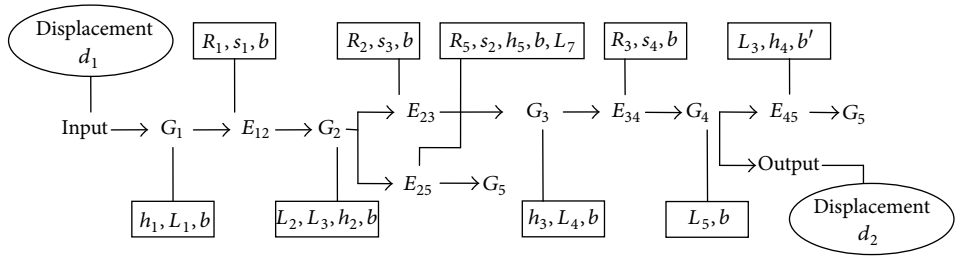

(b) Parameters indexing of compliant mechanism

FIGURE 4: Parameters indexing from the libraries of flexible cells. The amplificatory ratio of displacement is d_2/d_1.

The stiffness model formally describes the relationship between the displacement and the force, as shown in formula (8) [13]:

$$u_i = c_x F_i, \tag{8}$$

where $c_x = \begin{bmatrix} c_{11} & c_{12} & c_{13} \\ c_{21} & c_{22} & c_{23} \\ c_{31} & c_{32} & c_{33} \end{bmatrix}$; in general, c_x stands for the stiffness matrix of flexible cell. For flexible sliding pairs, the stiffness matrix c_x is expressed below:

$$c_x = \begin{bmatrix} \dfrac{l}{2Ebh} & 0 & 0 \\ 0 & \dfrac{l^3}{24EI} & 0 \\ 0 & 0 & \dfrac{l}{8EI} \end{bmatrix}, \tag{9}$$

where $I = bh^3/12$, while b represents thickness of the hinge and E represents elastic modulus of material.

Also a quantitative formula can be given for the other flexible hinges. And the formulae of c_x are not listed for them here.

Every flexible cells' stiffness can be determined according to their geometric relationships and constraint energy distributions. For any given precision requirements, the structure parameters can be modified based on the stiffness-parameters relationship model.

The algorithms libraries of finite element are also established to associate the vibration frequency and the structural parameters of the flexible cells. The detailed arithmetic is described in [14].

4.3. The Base of the Flexible Cells' Parameters. Figure 4(a) is an example of compliant mechanism for enlarging displacement; the amplificatory ratio theoretically is l_3/l_2 and actually is d_2/d_1 because of the stiffness of every flexible cell. The stiffness of the compliant mechanism is influenced by the flexible cells' parameters. For example, in the flexible sliding pairs shown in Figure 3(a), if parameters l are larger, then the stiffness of the hinge will become smaller. It is the same as for other parameters. All value scopes of the parameters and their representations are recorded in the libraries of the flexible cells. For the mechanism in Figure 4(a), the parameters indexing from the libraries of the flexible cell are shown in Figure 4(b). The robustness of amplificatory ratio d_2/d_1 depends on the stiffness of all the flexible cells in the mechanism.

5. Compatibility and Scheme Generation

5.1. Compatibility. The conceptual design solutions can be obtained from the functional decomposition and the associated constraints for a specific design problem. It includes the function and constraint attribute, the relations between these attributes, and the methods that are used to construct the conceptual solutions. It may be constructed in the hierarchy by inheriting the definition from its higher level class. The methods defined for the conceptual solutions include operations such as function queries, adding a new function, modifying and deleting a function, defining a new constraint, and firing an existing constraint [15]. When these operations are

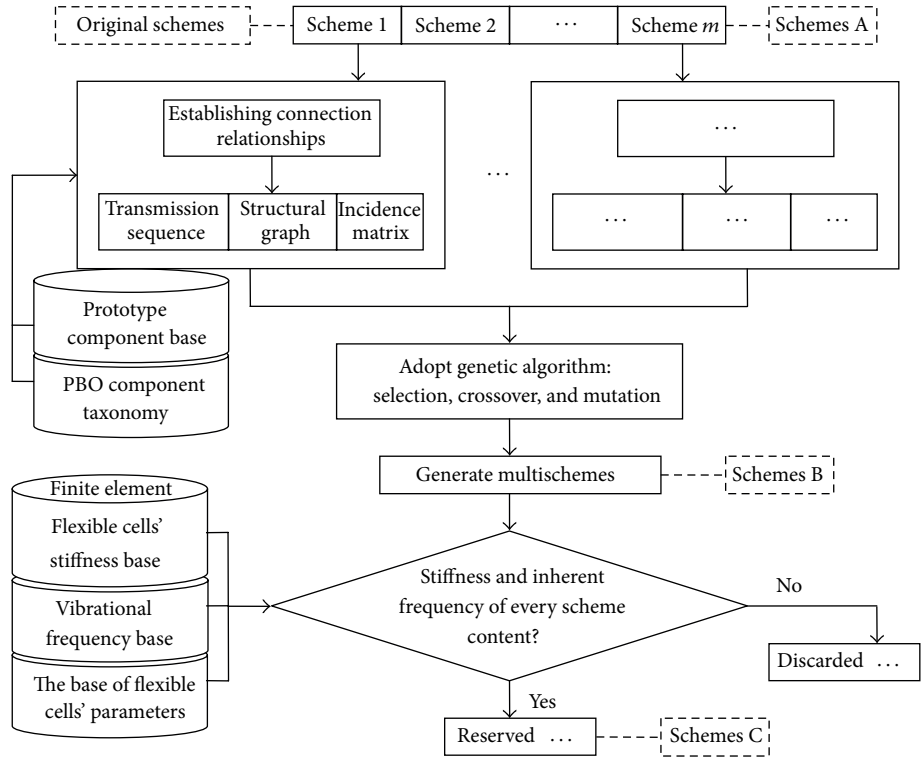

Figure 5: The flow graph of scheme generation based on PBO.

performed, the integrity of the whole object can be described by indexing knowledge libraries corresponding to port ontology. The flow graph as shown in Figure 5 is the process of obtaining the preference scheme of compliant mechanism.

5.2. Multischemes Generation. Hinge types are optional at the same level such as circle hinges, ellipse hinges, rectangle hinges, and rounded rectangle hinges. The process of multischeme generation adopts a roulette method to select from genetic algorithms as shown in Figure 6(a). The algorithms of crossover, and mutation are also employed in Figures 6(b) and 6(c). Scheme populations (schemes B in Figure 5) are to be increased using selection, crossover, and mutation.

Setting a range with eligible or preferable stiffness and vibration frequency, the inconsequent ones are discarded while proper ones (schemes C in Figure 5) are reserved by filtering those schemes (schemes B in Figure 5).

5.3. Neural Network Model from Sample Schemes. It is a challenge to assign an appropriate value to each parameter so as to obtain an optimum scheme. The value of each parameter in the scheme (schemes C in Figure 7) will influence the design objective. Every parameter is designated several different values in the range of its boundary, which are defined in the base of flexible cells' parameters. For example in the cell in Figure 3(b), s, b, and R are three parameters. Generally considering convenience in matching operation for all cells in the mechanism, thickness (parameter b) is appointed the same value, while R and s are alterable parameters. If there are two appointed values respectively for R and s, there are four combinations for R and s, as shown in Table 4. Hence there are four schemes of different parameters values. And they are viewed as to be sample schemes (schemes D in Figure 7).

Table 4: R and s combinations.

R	s	R and s
R_1, R_2	s_1, s_2	R_1 and s_1, R_1 and s_2, R_2 and s_1, R_2 and s_2

Another group schemes (schemes D in Figure 7) are produced by selecting different values for every parameter. All these schemes (schemes D in Figure 7) are as the specimen for training neural networks. Subsequently two trained NNs are obtained, flexible cells' parameters as input and respectively stiffness and vibration frequency of the system as output.

6. Case Study

It is increasingly used in precise mechanism for the microdisplacement amplification mechanisms with flexible hinges [11]. The significant performance parameters, including input displacement, output displacement, and robustness of amplification ratio, are very important for analyzing and designing the mechanism. Two of the original schemes are shown in Table 1. Firstly, to obtain a large amplification ratio, to connect in series two or more original schemes is adopted; hence structural graph and incidence matrix of each scheme (schemes A in Figure 5) are generated. Secondly multischemes (schemes B in Figure 5) are generated by adopting genetic algorithm with PBO modeling, transforming port

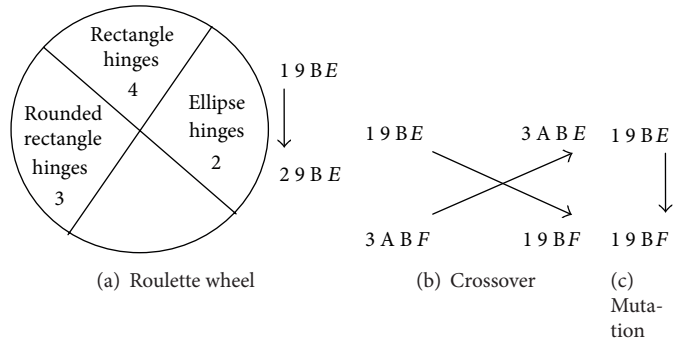

Figure 6: Genetic algorithms.

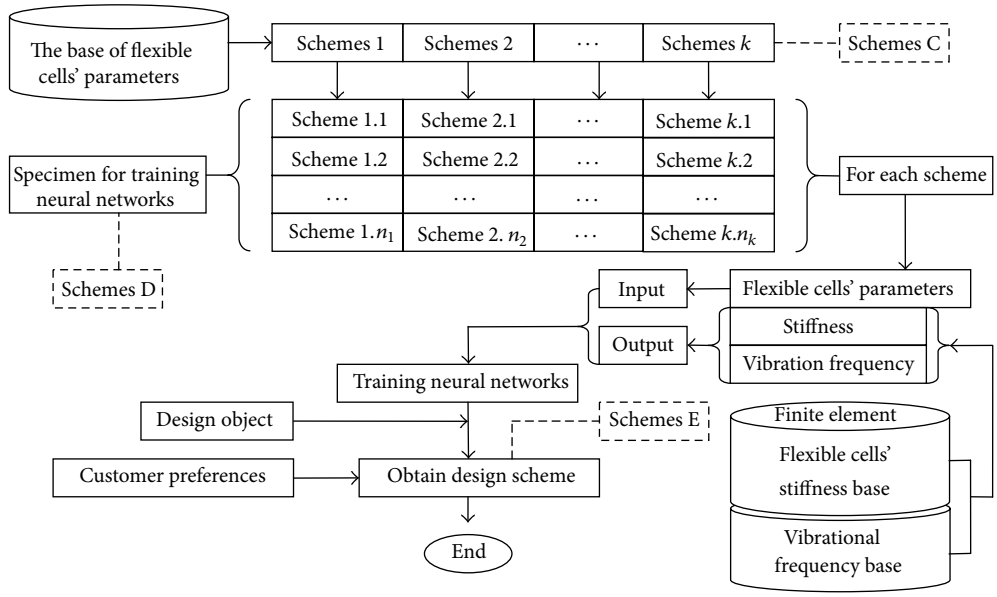

Figure 7: Obtaining preferable schemes.

taxonomical codes to implement iterative design process, and reconstructing system design schemes. Thirdly, by choosing the different values of the parameter, group schemes (schemes D in Figure 7) are generated as the specimen for training neural networks. The nonlinear mapping relation between structural vibration frequency and structural parameters as well as between stiffness and structural parameters is built up by training the artificial neural network with the specimen (schemes D). At last the structural parameters, which met the design requirements aiming at inherent frequency and stiffness, are obtained from the trained neural network. Figure 9(a) gives one result of compliant mechanism for enlarging displacement, which is chosen from customer preferable inherent frequency and stiffness. Figure 9(b) shows the transmission sequence of all the components and the relation between ports and components. The amplificatory ratio desired is 30. 30 is assigned to the two series parts (see Figure 9(a)) and each is $\sqrt{30}$; that is, $L_2/L_1 * L_4/L_3$ theoretically equals to 30. Figure 8(a) shows the structural graph denoting the relationship of vertex G and edge E. $G_1 \sim G_8$ represents components. E_{ij} in Figure 8(b) represents the port linking G_i and G_j.

Thus, eight components and ten hinges are obtained in the mechanism shown in Figure 8. The hinges E_{23}, E_{34}, E_{48}, and E_{28} are at the first grade. The hinges E_{56}, E_{67}, E_{78}, and E_{58} are at the second grade. The hinges E_{12} and E_{35} are the transitional linkages. The relationship between input and output is nonlinear. So it is necessary for error compensation feedback to input in the precise positioning and displacement. The port between G_6 and G_1 is information port. The sensor returns displacement of output component G_6 to the input component G_1 instantaneously to adjust the offset between input and output in real time. The structural graph and incidence matrix are shown in Figure 8.

The attributes of circle hinges, ellipse hinges, rounded rectangle hinges, and components G_1–G_8 are indexed from the prototype base. The boundary of flexible cells' parameters is determined from the parameters base. Contact relationship of E_{23}, E_{34}, E_{48}, E_{28}, E_{56}, E_{67}, E_{78}, E_{58}, E_{12}, and E_{35} is chosen by adopting roulette wheel selection. The result is shown in

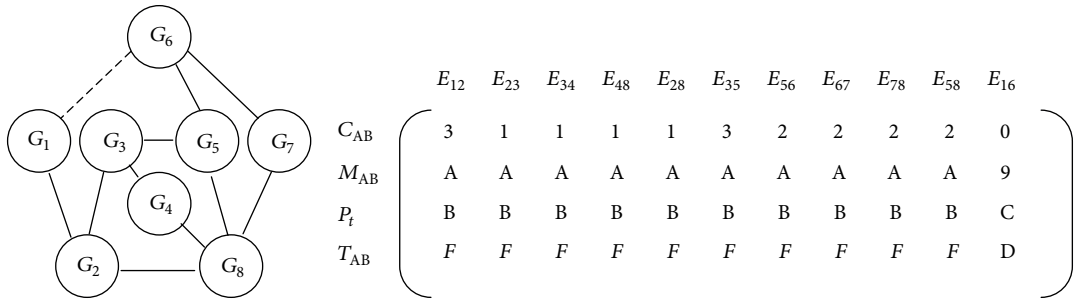

Figure 8: Microdisplacement amplification mechanisms.

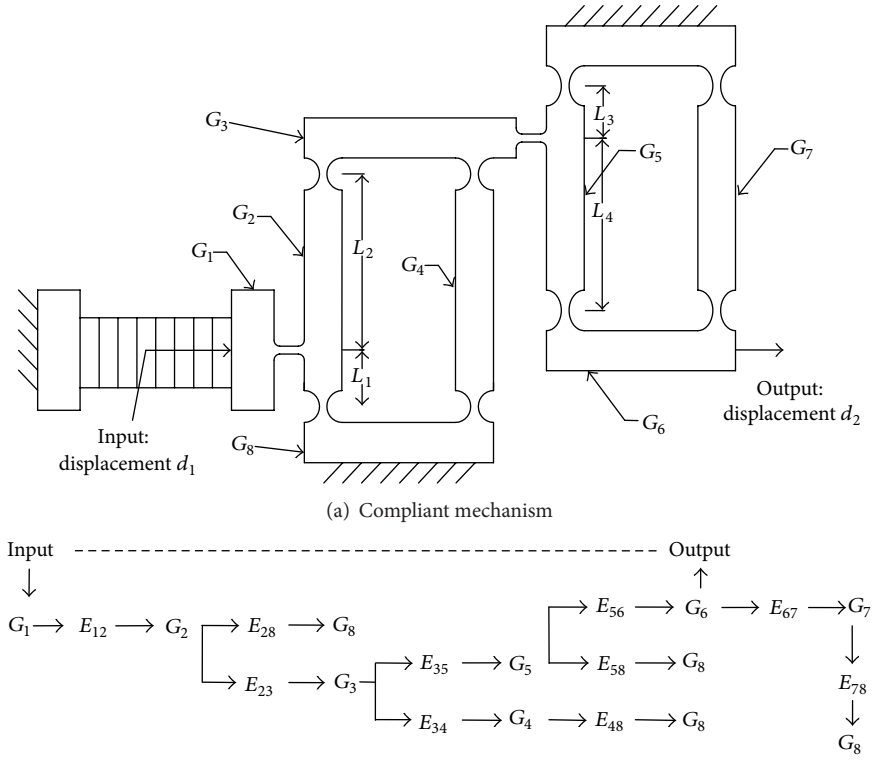

Figure 9: Microdisplacement amplification mechanisms.

Table 5. E_{12} and E_{35} are the transitional linkages, and optimal result is rounded rectangle hinges because of its flexibility. E_{23}, E_{34}, E_{48}, and E_{28} are in the first grade, whose distortion is low. The optimal result is circle hinge because of circle hinge's large rigidity. E_{56}, E_{67}, E_{78}, and E_{58} are in the second grade, whose distortion is large, and the optimal result is ellipse hinges to fit.

Table 5: The optimal result.

E_{12} and E_{35}	E_{23}, E_{34}, E_{48}, E_{28}	E_{56}, E_{67}, E_{78}, E_{58}
Rounded rectangle hinges	Circle hinges	Ellipse hinges

7. Conclusions

The paper presents a PBO method to generate design schemes of compliant mechanism. It is convenient for PBO to link multicomponents into a product system and implement conceptual design. Incidence matrix can capture not only geometrical information but also nongeometrical information such as port functions and constraints. It can be used to represent the preliminary design in two different but interrelated domains, namely, function domain and physical domain. The two domains are linked through function-form mapping relations that allow the designers to identify possible

design solutions through function reasoning. Furthermore, the product is to be modeled on different levels of abstraction corresponding to the port ontology knowledge in different stages of the design process. Incidence matrix is preponderant to increase the number of scheme populations by the multi-objectives of genetic algorithm. The inappropriate schemes are discarded, and they are not suitable to aiming at stiffness and vibration frequency of the system. At last, using trained model of neural networks, the design scheme is selected according to customer preference. However, the paper only refers to the conceptual design of plane compliant mechanism. The coding rules of compliant mechanism are also aimed at plane mechanism. Further study will be needed and extended for the space mechanism design.

Acknowledgments

This research is partially sponsored by the NSFC (Grant nos. 50775065 and 51275152) and Science Foundation of Hebei Province (Grant nos. E2008000102 and E2013202123).

References

[1] Y. Kitamura, M. Kashiwase, M. Fuse, and R. Mizoguchi, "Deployment of an ontological framework of functional design knowledge," *Advanced Engineering Informatics*, vol. 18, no. 2, pp. 115–127, 2004.

[2] D. Cao, Y. Gu, M. W. Fu, and H. Jia, "Port-based ontology modeling for product conceptual design," in *International Design Engineering Technical Conferences and Computers and Information in Engineering Conference (DETC '08)*, pp. 163–172, New York, NY, USA, August 2008.

[3] S. K. Sim and A. H. B. Duffy, "Towards an ontology of generic engineering design activities," *Research in Engineering Design*, vol. 14, no. 4, pp. 200–223, 2003.

[4] V.-C. Liang and C. J. J. Paredis, "A port ontology for conceptual design of systems," *Journal of Computing and Information Science in Engineering*, vol. 4, no. 3, pp. 206–217, 2004.

[5] P. C. Breedveld, "Port-based modeling of mechatronic systems," *Mathematics and Computers in Simulation*, vol. 66, no. 2-3, pp. 99–127, 2004.

[6] D. Cao, Z. Li, H. Li, and K. Qi, "An incidence matrix support for conceptual design based on port ontology," *Key Engineering Materials*, vol. 419-420, pp. 49–52, 2010.

[7] R. A. Shirwaiker and G. E. Okudan, "Triz and axiomatic design: a review of case-studies and a proposed synergistic use," *Journal of Intelligent Manufacturing*, vol. 19, no. 1, pp. 33–47, 2008.

[8] T. Kurtoglu, M. I. Campbell, C. B. Arnold, R. B. Stone, and D. A. Mcadams, "A component taxonomy as a framework for computational design synthesis," *Journal of Computing and Information Science in Engineering*, vol. 9, no. 1, pp. 1–10, 2009.

[9] S. Awtar and A. H. Slocum, "Constraint-based design of parallel kinematic XY flexure mechanisms," *Journal of Mechanical Design*, vol. 129, no. 8, pp. 816–830, 2007.

[10] S. B. Choi, S. S. Han, Y. M. Han, and B. S. Thompson, "A magnification device for precision mechanisms featuring piezoactuators and flexure hinges: design and experimental validation," *Mechanism and Machine Theory*, vol. 42, no. 9, pp. 1184–1198, 2007.

[11] J. Gong, G. Hu, and Y. Zhang, "Closed loop design method of micro-driving displacement amplifier module targeting for stiffness," *Journal of Mechanical Engineering*, vol. 48, no. 15, pp. 58–64, 2012.

[12] D. Cao, "Port-based ontology conceptual design theory," *Chinese Journal of Mechanical Engineering*, vol. 46, no. 17, pp. 123–132, 2010 (Chinese).

[13] J. Wang, K. Chen, and J. Li, "Study of geometrical parameters of typical flexible hinges' influence on its rigidity," *Robot*, vol. 23, no. 1, pp. 51–57, 2001.

[14] Y. Qin and Z. Feng, "Structural dynamic modification of flexure hinge structure based on artificial neural network," *Aviation Precision Manufacturing Technology*, vol. 42, no. 5, pp. 25–27, 2006.

[15] P. Singh and B. Bettig, "Port-compatibility and connectability based assembly design," *Journal of Computing and Information Science in Engineering*, vol. 4, no. 3, pp. 197–205, 2004.

Hindawi Publishing Corporation
Advances in Mechanical Engineering
Volume 2013, Article ID 791071, 12 pages
http://dx.doi.org/10.1155/2013/791071

Research Article

Matrix-Based Conceptual Solution Generation Approach of Multifunction Product

Yuyun Kang[1,2,3] and Dunbing Tang[1,3]

[1] *College of Mechanical and Electrical Engineering, Nanjing University of Aeronautics & Astronautics, Nanjing 210016, China*
[2] *College of Mechanical Engineering, Linyi University, Linyi 276005, China*
[3] *Jiangsu Key Laboratory of Precision and Micro-Manufacturing Technology, Nanjing 210016, China*

Correspondence should be addressed to Dunbing Tang; d.tang@nuaa.edu.cn

Received 11 April 2013; Revised 6 July 2013; Accepted 20 July 2013

Academic Editor: Yu-Shen Liu

In order to integrate two single-function products to a multifunction product, a matrix-based conceptual solution generation approach is proposed in this paper. In the approach, the overall function of a single-function product is decomposed into a number of subfunctions. The sub-functions are described by the functional basis and are used to construct the function model of the single-function product. By analyzing the function models of two single-function products, a functional similarity matrix is constructed based on the quantified similarity indexes of two sub-functions. For indicating the relationship between the sub-functions and the components, a function-component matrix of each single-function product is constructed, and then a component-component matrix of two single-function products can be acquired by multiplying the function-component matrix and the functional similarity matrix. There are three kinds of components' relationships in the component-component matrix, namely, no-correlation, simple-correlation, and complex-correlation. The components of two single-function products can be, respectively, removed, modified, and reserved according to the different correlation relationships, and a design solution of a new multi-function product can be obtained by combining the reserved and modified components. As a case study, a conceptual solution of a new shaver is acquired under the help of the provided approach.

1. Introduction

Some products have one function and others have two or more functions. The former is a single-function product and the latter is a multifunction product. The multifunction product has become more prevalent in recent years, as customers' desire both increased capabilities and reduced complexity to decrease waste in our society. In order to clearly describe the multifunction products, they are divided into four categories in this paper. The first kind of multifunction product is what can multiple functions perform at the same time. For example, the wheat combine cannot only incise straws and convey ears of the wheat but also screen and store grain at the same time. The second is what can multiple functions perform by changing different working status. For example, the microwave oven can heat food, barbecue meat, and make popcorn in different working status. The third is what can multiple functions perform by reconfiguring components. For example, the sofa bed can realize two functions by changing compound mode of the base and the back. The fourth is what can multiple functions realize through changing different executive components on the basis of a common component. For example, the food processer can grind soya-bean milk, mince steak, grind flour, and squeeze juice by changing the self-contained complete blade and cup. The four examples of multifunction products introduced above are shown in Figure 1.

Many methods are well equipped for use with some design problems. But few computational tools are specialized for the multifunction product. Therefore, it is more and more important to specially investigate the design approach of the multifunction product [1, 2]. The multifunction product is defined as complex function product by Feng et al. [3]. They have proposed a conceptual design cycle mapping model and studied the cycle solving process and realization for conceptual design of the multifunction product. Hu et al. have incorporated the fuzzy set theory into the reconfigurable design and proposed a fuzzy reconfigurable design method of

(a) Wheat combine [15] (b) Microwave oven [16] (c) Sofa bed [17] (d) Food processor [18]

Figure 1: Multifunction products.

the multifunction products [4]. While these two approaches are useful in the top-down design of new multifunction products, they do not address the bottom-up combination of the existing products. Li has given a design method of the multifunction product family, and an integrated product family reconfigurable design system is developed and applied in the design process of air separation system [5]. But the presented method is effective only for the multifunction product family. Based on the similarity theory, Zhang et al. have constructed a design platform of multifunction products [6]. Liu et al. have proposed a bottom-up platform design method of the multifunction product [7]. Wei et al. have presented a modular design method of multifunction product based on the product module [8]. However, these three approaches may be effective only for the similar multifunction products.

Recently, a new design principle named as Transformational Design Theory has been proposed in [1]. It provides an avenue for developing transforming systems. In [9], the transformation design is refined to be simpler, easier to learn and follow, and more effective in drawing out untapped potential from the design process. In addition, a research presents a twofold process known as the Transformer Diagram Matching Method and shows the results on a fully functioning prototype of an office supply transformer [2]. The process takes transformation design methodology a large step forward by bridging its two ways of design together, directive and intuitive. According to the categories of the multifunction product, the transforming systems or products shall be the third kind of multifunction product, and the principle is appropriate for this kind of multifunction product. But for other categories of multifunction product, it is not known whether the transformational design theory is effective or not. Furthermore, mathematical design tools for other categories of multifunction product are still needed.

Matrix is a stylized tool and widely used in product conceptual design. By applying different matrix operations, the design activities can be organized and analyzed [10]. One example of a matrix-based method is the House of Quality from Quality Function Deployment (QFD) where customer requirements are mapped to engineering characteristics [11]. Other matrix-based methods include the incidence matrix [12], the design structure matrix [13], and the function impact matrix [14]. These matrixes are best suited for specific domains or applications of the product conceptual design. But there is a lack of matrix-based methods to support the combination of two or more existing single-function products or subsystems into a new multifunction product or system.

Table 1: Example of the expanded flow.

Primary class	Secondary	Tertiary	Correspondents
Energy	Electrical	Electrical	Electromotive force, current
	Mechanical	Rotational energy	Torque, angular velocity
		Translational energy	Force, linear velocity
	Pneumatic	Pneumatic	Pressure, mass flow

Based on the above understanding, a matrix-based stylized bottom-up approach is proposed and attempts to generate a conceptual solution of all categories of multifunction product. In the approach, a few matrixes are used to analyze the reconfiguration of two single-function products. The construction of function models is introduced in Section 2. The concept generation approach of the multifunction product is introduced in Section 3. Finally, a case study of a shaver design is proposed to illustrate the presented approach.

2. Function Model

The concept design is a complicated thinking activity and the function model is the basis of the concept design [21]. The function model also increases the clarity of the design problem by tracking of the input and output flows. It is used to capture the design knowledge from the existing products and represent a form-independent blueprint of a product.

2.1. Functional Basis. In order to describe the product function, Stone and Wood proposed a language named as functional basis [22]. The functional basis, where product function is characterized in a verb-object (function-flow) format, is a consistent language or coding system required to ensure that others can read it. It is intended to comprehensively describe the mechanical design space without repetition. The functional basis contains three primary flows and eight primary functions. The three primary flows are material, signal, and energy flow. The material has five further specified secondary categories with an expanded list of tertiary categories. The signal has two further specified secondary categories with an expanded list of tertiary categories. The energy has thirteen further specified secondary categories with an expanded list of tertiary categories, as shown in Table 1. Eight primary functions are "branch," "channel," "connect," "control magnitude," "convert," "provision," "signal," and "support." Each primary

Table 2: Example of the expanded function.

Primary class	Secondary	Tertiary	Correspondents
Channel	Import	Import	Form entrance, allow, input, and capture
	Export	Export	Dispose, eject, emit, empty, remove, destroy, and eliminate
	Transfer	Transport	Advance, lift, and move
		Transmit	Conduct, convey

function has several further specified secondary categories with an expanded list of tertiary categories, as shown in Table 2. The clear definitions have been developed for all flows and functions in [23]. The functional basis is applied to the areas of product architecture development, functional model generation, and design information transmittal [24].

2.2. Construction of the Function Model. The product function is a description of the design system. In order to construct the function model and analyze the relationships between energy, material, or signal of the product conveniently, the overall function of a product can be decomposed into a number of subfunctions. The function of a product can be described by the subfunction sets. The subfunctions are the roles' abstractions of the existing parts or process. They are described by the functional basis and are used to construct the function model. The function model of any products can be generated by this approach. The steps of the functional model construction are as follows. (1) The overall function and the input/output flow of the product are confirmed. (2) The overall function is decomposed into subfunctions described by the functional basis. (3) The functional chains of each input flow are constructed. (4) The function model of a product is acquired by interlinking all functional chains [7, 25].

3. Conceptual Solution Generation Approach of the Multifunction Product

The first mission of the proposed approach is the function analysis and the function model construction of two single-function products. Second, the subfunction similarities of two products are analyzed and the functional similarity matrix (FSM) is constructed. Third, the component-component matrix (CCM) of two single-function products is acquired by calculating the FSM and the function-component matrix (FCM). Finally, the conceptual solution of the new multifunction product is generated by analysing the components' relationship in the CCM. In brief, the flow chart of the approach is shown in Figure 2.

3.1. Function Analysis. The function analysis is the first mission in the proposed approach. It includes construction

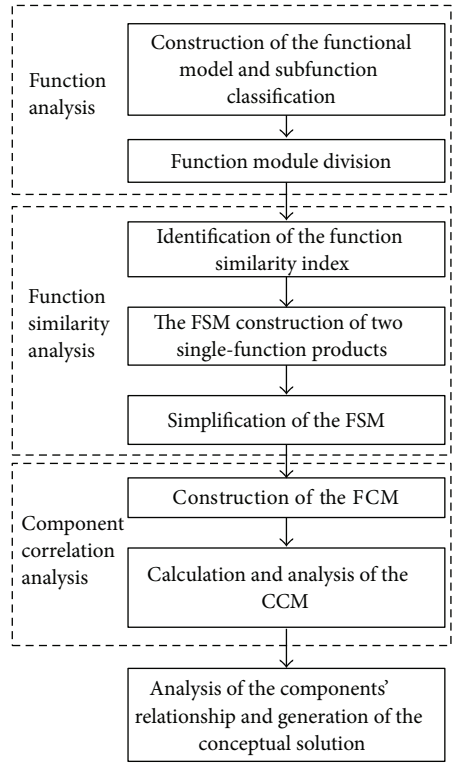

Figure 2: Flow chart of the proposed approach.

of the functional model, identification of the chief subfunctional chain, subfunction classification, and function module division. The construction of the functional model has been introduced in Section 2, and others will be introduced in the following subsections.

3.1.1. Chief Subfunctional Chain Identification and Subfunction Classification. The subfunctional chain is a continuous subfunction set of a product and it may be the energy, material, or signal flow. The subfunctional chains are generated from the functional model by the sequence of the flow. If there are multiple subfunctional chains, a chief functional chain shall be chosen and analyzed primarily. Generally, the chief subfunctional chain is the subfunctional chain that contains most subfunctions. If the chief functional chains of two products are similar, these two products can be integrated into a new product. Otherwise, the integration feasibility of these two products is smaller.

In order to analyze the function similarities of two single-function products, the product subfunctions are divided into three categories: basic function, application function, and accessory function. The basic functions are used to transfer and transform the motive power of the product. The application function indicates the application value of the product and is a function set used to distinguish a product with other products. The accessory function is a discrete function set besides the basic function and the application function.

3.1.2. Functional Module Division. In order to compare and analyze the similarity between the subfunctions of two products, the function model is divided into different modules on the basis of the subfunction categories. The basic functions and the application functions are sequential and divided, respectively, into different modules in the subfunctional chains. The accessory functions are not coterminous like the basic functions or application functions, so they are collected into an alone module. The subfunction similarity is analyzed only in the same type of the functional module.

3.2. Functional Similarity Analysis. In this subsection, the functional similarity index is defined and the FSM is structured and simplified according to the proposed principles.

3.2.1. Functional Similarity Index. The product similarity is introduced in [26]. In their opinion, if there are one or more same important functions in different products, these products are function similar. In [8], the product similarity is analyzed from two aspects: property and characteristic, relation and function. In order to quantify the function similarity, the similarity index is given to represent the similarity and it is classed into seven degrees: 0, 0.3 0.5 0.7 0.9, 1, and −1. The similarity index of a subfunction pair is confirmed by identifying the function/flow descriptors about the primary class, the secondary class, and the correspondents, as shown in Tables 1 and 2. As we move from the primary class to the correspondents, the level of abstraction decreases and the functions become more and more specific in nature. The higher the level of similarity between two subfunctions at all three classes of function and flow sets, the bigger the similarity index of the two subfunctions will be.

3.2.2. Functional Similarity Matrix (FSM). In order to analyze the functional similarity of two existing products, the FSM is constructed, as shown in Figure 3. In the matrix, the subfunctions are ranked by the sequence of the flow in the functional model. The function similarity is analyzed only between same types of the modules. The entry in each square is the similarity index of a subfunction pair.

The entry in the matrix, m_{ij}, indicates the similarity level of a subfunction pair. These entries can assume the following values:

(1) $m_{ij} = 1$ indicates that the corresponding subfunctions i and j are the same.

(2) $m_{ij} = -1$ indicates that the corresponding subfunctions i and j are conflicting.

(3) $m_{ij} = 0$ indicates that there is no similarity between the functions i and j.

(4) $m_{ij} \in [0.3, 0.5, 0.7, 0.9]$ indicates that there is partial similarity between the functions i and j.

3.2.3. Simplification of the FSM. In order to avoid a high degree of internal function coupling in the new product, it is assumed that the similarity relationship only exists between two subfunctions and the corresponding subfunction pair complies with the positive sequence of the flow. The entries that do not conform to the assumption shall be removed by setting to 0. This leads us to the following principle: the values on the diagonal and the higher values below the diagonal shall be preferentially reserved, and this keeps the nonzero values in the FSM to the right and downward trends. Therefore, any similarity relationship between more than two subfunctions must be parsed further, and the feedback and the dual relationship are eliminated by setting the lowest entry to zero. For instance, as shown in Figure 4, F_5^b has the similarity relationships with F_4^a and F_5^a, and the presence of similarity relationships between F_2^a and F_3^b and F_3^a and F_2^b indicate a reversal of flow since it would require a feedback mechanism. Therefore, the value 0.3 corresponding to F_2^a and F_3^b and the value 0.3 corresponding to F_4^a and F_5^b shall be set to zero according to the principle, as shown in Figure 5.

Function similarity matrix			Product B												
			Basic functions					Application functions				Accessory functions			
			F_1^b	F_2^b	F_3^b	F_4^b	·	F_6^b	F_7^b	F_8^b	·	F_{10}^b	F_{11}^b	·	·
Product A	Basic functions	F_1^a	0.9	1	0	0	0								
		F_2^a	0	0	0.7	0	0								
		F_3^a	0	0.3	0	0	1								
		·	·	·	·	·	·								
		·	·	·	·	·	·								
	Application functions	F_6						1	0	0	0				
		F_7						0	0.5	0	0				
		·						·	·	·	·				
		·						·	·	·	·				
	Accessory functions	F_{10}^a										0.7	0	0	0
		F_{11}^a										0	−1	0	0
		F_{12}^a										0	0	1	0
		·										·	·	·	·
		·										·	·	·	·

Figure 3: Function similarity matrix.

For easy calculation in the next section, the matrix in Figure 5 is transformed into

$$M_{\text{FSM}} = \begin{array}{c} \\ F_1^a \\ F_2^a \\ F_3^a \\ F_4^a \\ F_5^a \end{array} \begin{array}{c} \begin{array}{ccccc} F_1^b & F_2^b & F_3^b & F_4^b & F_5^b \end{array} \\ \begin{pmatrix} -1 & 0 & 0 & 0 & 0 \\ 0 & 0 & 0 & 0 & 0 \\ 0 & 0.7 & 0 & 0 & 0 \\ 0 & 0 & 0 & 0 & 0 \\ 0 & 0 & 0 & 0 & 1 \end{pmatrix} \end{array}. \tag{1}$$

3.3. Component Correlation Analysis. In this subsection, the FCM of every single-function product is structured. The CCM can be acquired by multiplying FCM and FSM, and then the component relationships in CCM can be analyzed.

3.3.1. Function Component Matrix (FCM). In order to convert the function similarity relationships in FSM to the components' correlations, the FCM of each product is structured. As shown in Figure 6, two hypothetical FCMs of products A and B are constructed. The columns of the FCM^a must be in

FSM		Product B				
		F_1^b	F_2^b	F_3^b	F_4^b	F_5^b
Product A	F_1^a	−1	0	0	0	0
	F_2^a	0	0	0.3	0	0
	F_3^a	0	0.7	0	0	0
	F_4^a	0	0	0	0	0.3
	F_5^a	0	0	0	0	1

Figure 4: An original function similarity matrix.

FSM		Product B				
		F_1^b	F_2^b	F_3^b	F_4^b	F_5^b
Product A	F_1^a	−1	0	0	0	0
	F_2^a	0	0	0	0	0
	F_3^a	0	0.7	0	0	0
	F_4^a	0	0	0	0	0
	F_5^a	0	0	0	0	1

Figure 5: A simplified function similarity matrix.

Product A					
FCM^a	C_1^a	C_2^a	C_3^a	C_4^a	C_5^a
F_1^a	1	0	0	0	0
F_2^a	0	1	0	0	0
F_3^a	0	0	1	0	0
F_4^a	0	0	0	1	0
F_5^a	0	0	0	1	1

Product B					
FCM^b	C_1^b	C_2^b	C_3^b	C_4^b	C_5^b
F_1^b	1	0	0	0	0
F_2^b	0	1	0	0	0
F_3^b	0	0	1	0	0
F_4^b	0	0	0	1	0
F_5^b	0	0	0	1	1

Figure 6: Function-component matrix.

the same order as the columns of the FSM shown in Figure 5, and the columns of the FCM^b must be in the same order as the rows of the FSM. But the arrangement of components in the FCM does not affect the final results of this phase. This is because the propagation of the function similarity from the FSM to the components of the FCM occurs only through the subfunctions of the products.

3.3.2. Calculation and Analysis of the Component-Component Matrix. In order to use a matrix to describe the components' correlation of two products, the CCM is presented and acquired by

$$\left[\text{FCM}^a\right]_{mi}^T \times [\text{FSM}]_{ij} \times \left[\text{FCM}^b\right]_{jn} = [\text{CCM}]_{mn}, \quad (2)$$

where m and n indicate the total components' number of product A and product B, respectively. This equation is used to map the similarity of the function pair in the FSM into the CCM. The calculation process of the FSM in Figure 5 mapped into a CCM is shown as follows:

$$\begin{array}{c} \\ C_1^a \\ C_2^a \\ C_3^a \\ C_4^a \\ C_5^a \end{array} \begin{array}{c} \begin{array}{ccccc} F_1^a & F_2^a & F_3^a & F_4^a & F_5^a \end{array} \\ \begin{pmatrix} 1 & 0 & 0 & 0 & 0 \\ 0 & 1 & 0 & 0 & 0 \\ 0 & 0 & 1 & 0 & 0 \\ 0 & 0 & 0 & 1 & 1 \\ 0 & 0 & 0 & 0 & 1 \end{pmatrix} \end{array}$$

$$\times \begin{array}{c} \\ F_1^a \\ F_2^a \\ F_3^a \\ F_4^a \\ F_5^a \end{array} \begin{array}{c} \begin{array}{ccccc} F_1^b & F_2^b & F_3^b & F_4^b & F_5^b \end{array} \\ \begin{pmatrix} -1 & 0 & 0 & 0 & 0 \\ 0 & 0 & 0 & 0 & 0 \\ 0 & 0.7 & 0 & 0 & 0 \\ 0 & 0 & 0 & 0 & 0 \\ 0 & 0 & 0 & 0 & 1 \end{pmatrix} \end{array}$$

$$\times \begin{array}{c} \\ F_1^b \\ F_2^b \\ F_3^b \\ F_4^b \\ F_5^b \end{array} \begin{array}{c} \begin{array}{ccccc} C_1^b & C_2^b & C_3^b & C_4^b & C_5^b \end{array} \\ \begin{pmatrix} 1 & 0 & 0 & 0 & 0 \\ 0 & 1 & 0 & 0 & 0 \\ 0 & 0 & 1 & 0 & 0 \\ 0 & 0 & 0 & 1 & 0 \\ 0 & 0 & 0 & 1 & 1 \end{pmatrix} \end{array}$$

$$= \begin{array}{c} \\ C_1^a \\ C_2^a \\ C_3^a \\ C_4^a \\ C_5^a \end{array} \begin{array}{c} \begin{array}{ccccc} F_1^b & F_2^b & F_3^b & F_4^b & F_5^b \end{array} \\ \begin{pmatrix} -1 & 0 & 0 & 0 & 0 \\ 0 & 0 & 0 & 0 & 0 \\ 0 & 0.7 & 0 & 0 & 0 \\ 0 & 0 & 0 & 0 & 0 \\ 0 & 0 & 0 & 0 & 1 \end{pmatrix} \end{array}$$

$$\times \begin{array}{c} \\ F_1^b \\ F_2^b \\ F_3^b \\ F_4^b \\ F_5^b \end{array} \begin{array}{c} \begin{array}{ccccc} C_1^b & C_2^b & C_3^b & C_4^b & C_5^b \end{array} \\ \begin{pmatrix} 1 & 0 & 0 & 0 & 0 \\ 0 & 1 & 0 & 0 & 0 \\ 0 & 0 & 1 & 0 & 0 \\ 0 & 0 & 0 & 1 & 0 \\ 0 & 0 & 0 & 1 & 1 \end{pmatrix} \end{array}$$

$$= \begin{array}{c} \\ C_1^a \\ C_2^a \\ C_3^a \\ C_4^a \\ C_5^a \end{array} \begin{array}{c} \begin{array}{ccccc} C_1^b & C_2^b & C_3^b & C_4^b & C_5^b \end{array} \\ \begin{pmatrix} -1 & 0 & 0 & 0 & 0 \\ 0 & 0 & 0 & 0 & 0 \\ 0 & 0.7 & 0 & 0 & 0 \\ 0 & 0 & 0 & 1 & 1 \\ 0 & 0 & 0 & 1 & 1 \end{pmatrix} \end{array}. \quad (3)$$

The operator × in (2) and (3) has two calculation steps as follows.

Step 1. When the row i of the first matrix (e.g., FCM^a) is multiplied by the column j of the second matrix (e.g., FSM), each element of the row i is multiplied by the corresponding element of the column j, and the results are ranked in a set $\{T_{ij} \mid m_{i1} \times m_{1j}, m_{i2} \times m_{2j}, \ldots, m_{ix} \times m_{yj}\}$, where m_{ix} represents the element of the row i in the first matrix and m_{yj} represents the element of the column j in the second matrix. For instance, the calculation process of the row C_1^a

CCM		Product B				
		C_1^b	C_2^b	C_3^b	C_4^b	C_5^b
Product A	C_1^a	−1	0	0	0	0
	C_2^a	0	0	0	0	0
	C_3^a	0	0.7	0	0	0
	C_4^a	0	0	0	1	1
	C_5^a	0	0	0	1	1

Figure 7: Component-component matrix of two products.

(a) Shaver [19]

(b) Portable cleaner [20]

Figure 8: Single-function products.

in the first matrix multiplied by the column F_1^b in the second matrix in (3) is shown as follows:

$$\begin{aligned} C_1^a \times F_1^b &= [1,0,0,0,0] \times [-1,0,0,0,0] \\ &= \{1 \times -1, 0 \times 0, 0 \times 0, 0 \times 0, 0 \times 0\} \\ &= \{-1,0,0,0,0\}. \end{aligned} \tag{4}$$

Step 2. The element m_{ij} of the new matrix is selected from the results of Step 1 according to the following rules

$$M_{ij} = \begin{cases} 0 & T_{ij} = \{0\}, \\ -1 & \text{if } -1 \in T_{ij}, \\ z & \text{if } -1 \notin T_{ij},\ z \text{ is the minimum in } T_{ij}. \end{cases} \tag{5}$$

The first condition identifies no relationship between two elements. The second condition identifies the conflicting relationship. The third condition ensures that only the minimum in T_{ij} is taken into consideration when there are multiple positive numbers. The lowest number conservatively reflects the minimum similarity.

According to the above principles, the result of C_1^a multiplied by F_1^b is −1, as shown by the following equation:

$$\begin{aligned} C_1^a \times F_1^b &= [1,0,0,0,0] \times [-1,0,0,0,0] \\ &= \{-1,0,0,0,0\} \\ &= -1. \end{aligned} \tag{6}$$

Consequently, the results of (3) are acquired and they are presented visually in CCM as shown in Figure 7.

Table 3: Categories of the modules.

Module category	Product 1: shaver	Product 2: portable cleaner
Basic function	Electrical energy module (1)	Electrical energy module (1)
Basic function	Mechanical energy module (2)	Mechanical energy module (2)
Application function	Material flow module (3)	Material flow module (3)
Accessory function	Accessory function module (4)	Accessory function module (4)

The components' relationships of two products are indicated in CCM. Different types of the values in CCM are as follows. The value −1 indicates that the components C_1^a and C_1^b are conflicting. The value 0 identifies that the components C_2^a and C_3^b are dormant and they are not used in the new product. The values between 0 and 1 indicate that the components have the feasibility to be redesigned into a single component that can perform two functions of the existing products. The value 1 identifies that the components C_4^a, C_4^b, C_5^a, and C_5^b have the same function and can be replaced by each other.

By analyzing the components' relationships in CCM, a few components of two existing products will be reserved in the new product, and a few components will be modified for the new application, and the others will be eliminated. Consequently, the conceptual solution of the new product can be acquired. The detailed application procedure is illustrated in the following case study section.

4. Case Study

4.1. Function Analysis. Two single-function products, a shaver and a portable cleaner, are shown in Figure 8. The overall functions of the two products are, respectively, decomposed into a number of subfunctions that are described by the functional basis, and the function models of the two single-function products are constructed, respectively, as shown in Figures 9 and 10.

In Figures 9 and 10, the function models of the two products are, respectively, divided into four modules according to the types of the energy, material, or signal flow. For instance, in Figure 9, the flow in module 1 is the electrical energy flow. The flow of module 2 is the mechanical energy flow, and the flow in module 3 is the solid material flow. The accessory functions are regarded as an independent module. These modules are divided into three categories according to the subfunction classification introduced in Section 3.1.1. The categories of the modules are listed in Table 3.

As shown in Table 3, module 1 and module 2 of two products belong to the same functional category. Module 3 is a material flow module including a solid material flow and a mixture material flow. This indicates that the application function is the key distinction of two products. Therefore, the

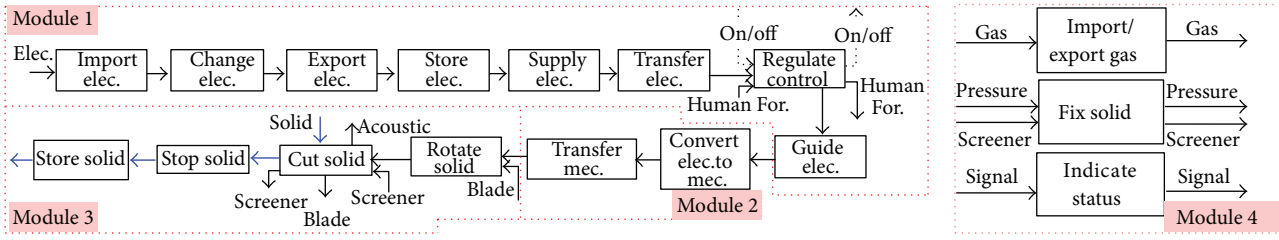

(a) Chief function chain

(b) Accessory functions

Figure 9: Function model of the shaver.

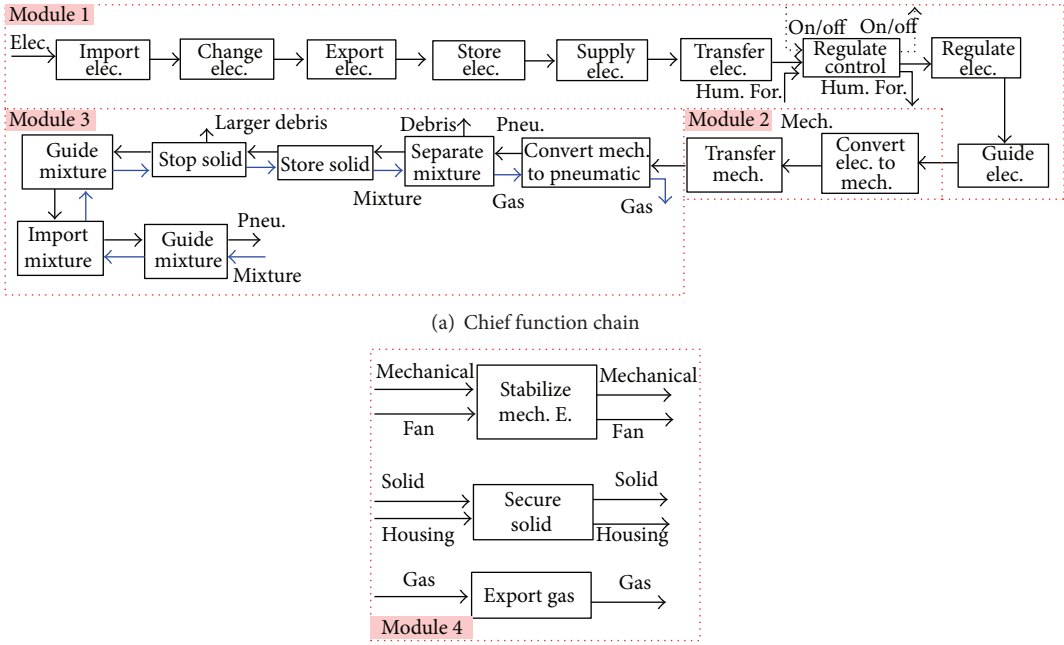

(a) Chief function chain

(b) Accessory functions

Figure 10: Function model of the portable cleaner.

subfunctions in the module 3 are primarily modified for the function of the new product.

4.2. Functional Similarity Analysis. The FSMs between the shaver and the portable cleaner are structured according to their function models, as shown in Figure 11. If two subfunctions are conflicting, the corresponding entry is −1, and it does not exist in Figure 11. Other similarity indexes of the function pairs are represented from 0 to 1 according to the similarity degree. The FSM is simplified according to the principle introduced in Section 3.2.3, and the result is shown in Figure 12. Almost all many-to-many relationships of the subfunction pairs are eliminated, and one-to-one relationships are reserved in the simplified FSM. Only the shaver's subfunction *Guide electrical energy* corresponds to two subfunctions of the portable cleaner: *Regulate electrical energy* and *Guide electrical energy*. In addition, some subfunctions correspond to nothing, such as *Stop solid*, *Indicate status, and Guide mixture.*

4.3. Component Correlation Analysis. The FCMs of the shaver and the portable cleaner are, respectively, constructed according to the relationships between the subfunctions and components, as shown in Figures 13 and 14, respectively. The relationship between the subfunction and component is represented by 0 or 1, and it is not further distinguished. The entry 1 indicates that the subfunction can be performed by the component on the column in the FCM. The entry 0 indicates that the subfunction is irrelevant with the component on the column of FCM. The CCM of the shaver and the portable cleaner is calculated by the FSM multiplied by FCMs of the shaver and the cleaner according to (3), and the result is shown in Figure 15.

5. Results and Discussion

The entry 1 in the CCM shown in Figure 15 indicates the maximal correlation degree of the component pair. The entry 0 indicates that there is no correlation for the components

Function similarity matrix (FSM)				Portable cleaner																				
				Basic functions											Application functions							Accessory functions		
				Import elec.	Change elec.	Export elec.	Store elec.	Supply elec.	Transfer elec.	Regulate con.	Regulate elec.	Guide elec.	Convert elec. to mech.	Transfer mech.	Convert mech. to pneu.	Separate mix.	Store solid	Stop solid	Guide mixture	Import mixture	Guide mixture	Stabilize mech.	Secure solid	Export gas
				1	2	3	4	5	6	7	8	9	10	11	12	13	14	15	16	17	18	19	20	21
Shaver	Basic functions	Import elec.	1	1	0	0	0	0	0	0	0	0	0	0										
		Change elec.	2	0	1	0	0	0	0	0	0.7	0	0	0										
		Export elec.	3	0	0	1	0	0	0.7	0	0	0.7	0	0										
		Store elec.	4	0	0	0	1	0	0	0	0	0	0	0										
		Supply elec.	5	0	0	0	0	1	0.7	0	0	0.7	0	0										
		Transfer elec.	6	0	0	0.7	0	0.7	1	0	0	1	0	0										
		Regulate control	7	0	0	0	0	0	0	1	0	0	0	0										
		Guide elec.	8	0	0	0.7	0	0.7	1	0	0	1	0	0										
		Convert elec. to mech.	9	0	0	0	0	0	0	0	0	0	1	0										
		Transfer mech.	10	0	0	0	0	0	0	0	0	0	0	1										
	Appli. functions	Rotate solid	11												1	0	0	0	0	0	0			
		Cut solid	12												0	0.7	0	0.3	0	0	0			
		Stop solid	13												0	0.7	0.3	1	0.7	0	0.7			
		Store solid	14												0	0	1	0.3	0.7	0	0.7			
	Acce. fun.	Fix solid	15																			0	1	0
		Indicate status	16																			0	0	0
		Import/exp. gas	17																			0	0	1

Figure 11: FSM between the shaver and the portable cleaner.

Filtered total function similarity matrix (FTFSM)				Portable cleaner																				
				Basic functions											Application functions							Accessory functions		
				Import elec.	Change elec.	Export elec.	Store elec.	Supply elec.	Transfer elec.	Regulate con.	Regulate elec.	Guide elec.	Convert elec. to mech.	Transfer mech.	Convert mech. to pneu.	Separate mix.	Store solid	Stop solid	Guide mixture	Import mixture	Guide mixture	Stabilize mech.	Secure solid	Export gas
				1	2	3	4	5	6	7	8	9	10	11	12	13	14	15	16	17	18	19	20	21
Shaver	Basic functions	Import elec.	1	1	0	0	0	0	0	0	0	0	0	0										
		Change elec.	2	0	1	0	0	0	0	0	0	0	0	0										
		Export elec.	3	0	0	1	0	0	0	0	0	0	0	0										
		Store elec.	4	0	0	0	1	0	0	0	0	0	0	0										
		Supply elec.	5	0	0	0	0	1	0	0	0	0	0	0										
		Transfer elec.	6	0	0	0	0	0	1	0	0	0	0	0										
		Regulate control	7	0	0	0	0	0	0	1	0	0	0	0										
		Guide elec.	8	0	0	0	0	0	0	0	0.7	1	0	0										
		Convert elec. to mech.	9	0	0	0	0	0	0	0	0	0	1	0										
		Transfer mech.	10	0	0	0	0	0	0	0	0	0	0	1										
	Appli. functions	Rotate solid	11												0.9	0	0	0	0	0	0			
		Cut solid	12												0	0.7	0	0	0	0	0			
		Stop solid	13												0	0	0	0	0	0	0			
		Store solid	14												0	0	1	0	0	0	0			
	Acce. fun.	Fix solid	15																			0	1	0
		Indicate status	16																			0	0	0
		Import/exp. gas	17																			0	0	1

Figure 12: Simplified FSM between the shaver and the portable cleaner.

FCM of shaver		Charger	Battery	Wire	Switch	Diode	Motor	Motor shaft	Blade bearing	Blade	Screener	Housing	Blade cabin	Luminous diode
		1	2	3	4	5	6	7	8	9	10	11	12	13
Import elec.	1	1	0	0	0	0	0	0	0	0	0	0	0	0
Change elec.	2	1	0	0	0	0	0	0	0	0	0	0	0	0
Export elec.	3	1	0	0	0	0	0	0	0	0	0	0	0	0
Supply elec.	4	0	1	0	0	0	0	0	0	0	0	0	0	0
Store elec.	5	0	1	0	0	0	0	0	0	0	0	0	0	0
Transfer elec.	6	0	0	1	0	0	0	0	0	0	0	0	0	0
Regulate cont.	7	0	0	0	1	0	0	0	0	0	0	0	0	0
Transfer elec.	8	0	0	0	0	1	0	0	0	0	0	0	0	0
Convert elec. to mech.	9	0	0	0	0	0	1	0	0	0	0	0	0	0
Transfer mech.	10	0	0	0	0	0	0	1	0	0	0	0	0	0
Rotate solid	11	0	0	0	0	0	0	0	1	0	0	0	0	0
Cut solid	12	0	0	0	0	0	0	0	0	1	1	0	0	0
Stop solid	13	0	0	0	0	0	0	0	0	0	0	1	0	0
Store solid	14	0	0	0	0	0	0	0	0	0	0	0	1	0
Fix solid	15	0	0	0	0	0	0	0	0	0	1	0	0	0
Indicate status	16	0	0	0	0	0	0	0	0	0	0	0	0	1
Imp./exp. gas	17	0	0	0	0	0	0	0	0	0	1	0	1	0

Figure 13: FCM of the shaver.

FCM of portable cleaner		Adapter	Battery	Contact plate and wire	Switch	Diode	Motor	Motor shaft	Impeller	Filter bag	Rubber flap	Rubber flap holder	Nozzle	Exhaust vents	Housing
		1	2	3	4	5	6	7	8	9	10	11	12	13	14
Import elec.	1	1	0	0	0	0	0	0	0	0	0	0	0	0	0
Change elec.	2	1	0	0	0	0	0	0	0	0	0	0	0	0	0
Export elec.	3	1	0	0	0	0	0	0	0	0	0	0	0	0	0
Supply elec.	4	0	1	0	0	0	0	0	0	0	0	0	0	0	0
Store elec.	5	0	1	0	0	0	0	0	0	0	0	0	0	0	0
Transfer elec.	6	0	0	1	0	0	0	0	0	0	0	0	0	0	0
Regulate cont.	7	0	0	0	1	0	0	0	0	0	0	0	0	0	0
Regulate elec.	8	0	0	0	1	0	0	0	0	0	0	0	0	0	0
Guide elec.	9	0	0	0	0	1	0	0	0	0	0	0	0	0	0
Convert elec. to mech.	10	0	0	0	0	0	1	0	0	0	0	0	0	0	0
Transfer mech.	11	0	0	0	0	0	0	1	0	0	0	0	0	0	0
Convert mech. to pneu.	12	0	0	0	0	0	0	0	1	0	0	0	0	0	0
Separate mixture	13	0	0	0	0	0	0	0	0	1	0	0	0	0	0
Store solid	14	0	0	0	0	0	0	0	0	1	0	0	0	0	0
Stop solid	15	0	0	0	0	0	0	0	0	0	1	0	0	0	0
Guide mixture	16	0	0	0	0	0	0	0	0	0	0	1	0	0	0
Import mixture	17	0	0	0	0	0	0	0	0	0	0	0	1	0	0
Guide mixture	18	0	0	0	0	0	0	0	0	0	0	0	1	0	0
Stabilize mech.	19	0	0	0	0	0	0	0	0	0	0	0	0	0	1
Secure solid	20	0	0	0	0	0	0	0	0	0	0	0	0	0	1
Export gas.	21	0	0	0	0	0	0	0	0	0	0	0	0	1	1

Figure 14: FCM of the portable cleaner.

CCM			Portable cleaner														
			Adapter	Battery	Contact plate and wire	Switch	Diode	Motor	Motor shaft	Impeller	Filter bag	Rubber flap	Rubber flap holder	Nozzle	Exhaust vents	Housing
			1	2	3	4	5	6	7	8	9	10	11	12	13	14
Shaver	Charger	1	1	0	0	0	0	0	0	0	0	0	0	0	0	0
	Battery	2	0	1	0	0	0	0	0	0	0	0	0	0	0	0
	Wire	3	0	0	1	0	0	0	0	0	0	0	0	0	0	0
	Switch	4	0	0	0	1	0	0	0	0	0	0	0	0	0	0
	Diode	5	0	0	0	0.7	1	0	0	0	0	0	0	0	0	0
	Motor	6	0	0	0	0	0	1	0	0	0	0	0	0	0	0
	Motor shaft	7	0	0	0	0	0	0	1	0	0	0	0	0	0	0
	Blade bearing	8	0	0	0	0	0	0	0	0.9	0	0	0	0	0	0
	Blade	9	0	0	0	0	0	0	0	0	0.7	0	0	0	0	0
	Screener	10	0	0	0	0	0	0	0	0	0.7	0	0	0	1	1
	Housing	11	0	0	0	0	0	0	0	0	0	0	0	0	0	1
	Blade cabin	12	0	0	0	0	0	0	0	0	1	0	0	0	1	1
	Luminous diode	13	0	0	0	0	0	0	0	0	0	0	0	0	0	0

Figure 15: CCM of the shaver and the portable cleaner.

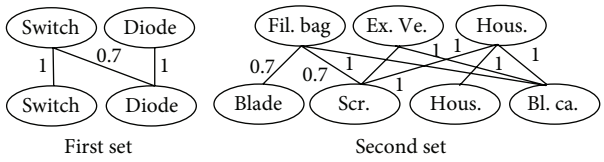

Figure 16: Complex correlations.

in the row and the column. The entries between 0 and 1 indicate the correlation degree of two components. Therefore, the correlation is divided into three kinds: no-correlation, simple-correlation, and complex-correlation. The correlation classifications are shown in Table 4, and the complex correlations are shown in Figure 16.

The no-correlation components are eliminated in the conceptual solution generation of the new product, and these components are 15% of the total components. If the correlation index of a simple-correlation component pair is 1, the component pair is irrelevant with other component pairs, and a component in the pair can be replaced by another one. These components do not need to be modified and are the core components of the new product. These components account for 37% of the total components. If the correlation index of the simple-correlation component pair is not 1, this indicates that the two components in the pair are similar. The two components can be modified and integrated into a component of the new product that performs two similar subfunctions of the existing single-function products. These components account for 7% of the total components. For the complex-correlation components, if one of them is modified, the others will be affected, as shown in Figure 16. Consequently, these components will be considered as a whole and coherently redesigned one with others in the new conceptual solution. These components account for 41% of the total components.

Table 4: Component correlation classifications.

	Shaver	Portable cleaner	Correlation index
No-correlation component	Luminous diode (13)	Rubber flap (10) Rubber flap holder (11) Nozzle (12)	0
Simple-correlation components	Charger (1)	Adapter (1)	1
	Battery (2)	Battery (2)	1
	Wire (3)	Contact plate and wire (3)	1
	Motor (6)	Motor (6)	1
	Motor shaft (7)	Motor shaft (7)	1
	Blade bearing (8)	Impeller (8)	0.9
Complex-correlation components	Switch (4) Diode (5)	Switch (4) Diode (5)	
	Blade (9) Screener (10) Housing (11) Blade cabin (12)	Filter bag (9) Exhaust vents (13) Housing (14)	

The existing single-function product that includes fewer no-correlation components is used for basic architecture of the new product, and this can reduce the ambiguity of the new architecture caused by removing more components. The shaver has a no-correlation component and the portable cleaner has three no-correlation components; therefore, the shaver is used for the basic architecture of the new product. Consequently, the no-correlation components can be removed, such as nozzle. The blade bearing and

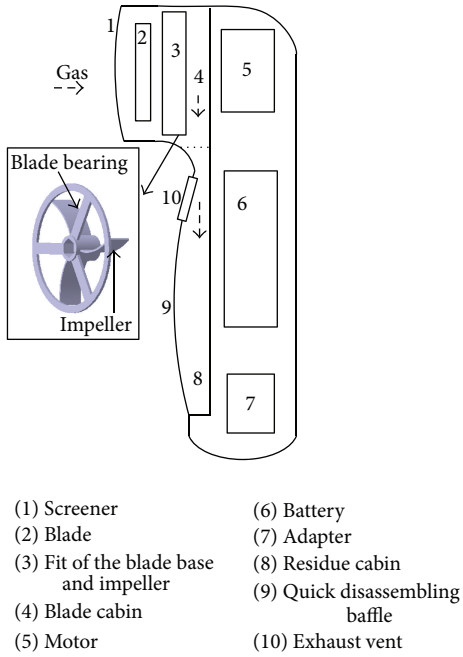

Figure 17: Conceptual solution of the new product.

the impeller are integrated into a component of the new product that performs two subfunctions, *Rotate solid* and *Convert mechanical energy to pneumatic energy,* at the same time. A few components are reserved and used in the new product, and they are motor, battery, adapter, wire, and motor shaft. The blade cabin and the housing are redesigned into a new blade cabin and a dust cabin according to the complex-correlation relationship. On the basis of the above, the conceptual solution of the new product is acquired, as shown in Figure 17. The new product has two functions at the same time: shaving and residue absorption. The beard residue can be collected into an easy dismantling cabin and cleared easily. This cabin is named residue cabin, as shown in Figure 17.

6. Conclusion

In this paper, a conceptual solution generation approach is proposed. It is a concise, stylized, and bottom-up approach and specialized for the multifunction product. In this approach, the overall function of the existing single-function product is decomposed into a number of subfunctions described by the functional basis, and this allows the functions of the different products to be compared and analyzed at the same level. A few matrixes are used to analyze the subfunctions' similarity and the components' correlation of two products, and the stylization, quantification, and automation of the calculation process are easily realized. Using the approach, two single-function products can be combined into a multifunction product. By similar way, a single-function product can be combined with a subfunction chain of a multifunction product, or two subfunction chains of different products can be integrated to generate a multifunction product. A good deal of conceptual solutions of the new multifunction product can be acquired by analyzing, comparing, and integrating two subfunction chains of the existing products under the help of the proposed approach. The proposed approach is effective for the conceptual solution generation of the mechanical and electrical multifunction products. But it is not known whether the approach is effective for other multifunction products, and the verification is needed in the future work. Meanwhile, the redesign process of the complex-correlation components is unordered, and mathematical tools are still needed.

Acknowledgments

This research was supported by National Science Foundation of China (no. 51175262), Jiangsu Province Science Foundation for Excellent Youths (no. BK201210111), Jiangsu Province Industry-Academy-Research Grant (no. BY201220116), NUAA Fundamental Research Funds (no. NS2013053), and Priority Academic Program Development of Jiangsu Higher Education Institutions (PAPD).

References

[1] V. Singh, B. Walther, J. Krager et al., "Design for transformation: theory, method and application," in *Proceedings of the ASME International Design Engineering Technical Conferences and Computers and Information in Engineering Conference (IDETC/CIE '07)*, pp. 447–459, Las Vegas, Nev, USA, September 2007.

[2] R. Kuhr, K. Wood, D. Jensen, and R. Crawford, "Concept opportunity diagrams, a visual modeling method to find multifunctional design concepts," in *Proceedings of the ASME International Design Engineering Technical Conferences and Computers and Information in Engineering Conference (IDETC/CIE '10)*, pp. 193–205, Quebec, Canada, August 2010.

[3] P. E. Feng, S. Zhang, S. X. Pan, Y. Chen, and B. He, "Cyclic solving process and realization for conceptual design of complex function product," *Chinese Journal of Mechanical Engineering*, vol. 41, no. 3, pp. 135–141, 2005.

[4] G. Z. Hu, S. N. Xiao, and Z. B. Liu, "Fuzzy reconfigurable design system of complex mechanical products," *Modern Manufacturing Engineering*, no. 5, pp. 68–73, 2012.

[5] Z. K. Li, *Theories and methodologies for product family reconfigurable design and application in large scale air separation systems [D.E. thesis]*, Zhejiang University, Hangzhou, China, 2009.

[6] H. G. Zhang, W. Y. Zhao, P. Jiang, and R. H. Tan, "Product platform design process model based on similarity and structural sensitivity analysis," *Journal of Mechanical Engineering*, vol. 48, no. 11, pp. 104–118, 2012.

[7] F. Liu, P. Jiang, R.-H. Zhang, and R.-H. Tan, "Platform design of function similar products based on bottom-up method," *Computer Integrated Manufacturing Systems*, vol. 11, no. 7, pp. 947–952, 2005.

[8] Z. Wei, J. R. Tan, Y. X. Feng, and X. Feng, "Construction of product module based on similarity and its applications," *Journal of Computer-Aided Design and Computer Graphics*, vol. 18, no. 12, pp. 1930–1934, 2006.

[9] J. M. Weaver, R. Kuhr, D. Wang et al., "Increasing innovation in multi-function systems: Evaluation and experimentation

of two ideation methods for design," in *Proceedings of the ASME International Design Engineering Technical Conferences and Computers and Information in Engineering Conference (IDETC/CIE '09)*, pp. 965–983, San Diego, Calif, USA, September 2009.

[10] Y. Y. Kang, D. B. Tang, and H. Wang, "Design solutions generation method based on function-component matrix and design structure matrix," *Computer Integrated Manufacturing Systems*, vol. 18, no. 5, pp. 897–904, 2012.

[11] P. Fomin, S. Sarkani, and T. A. Mazzuchi, "Growing the house of quality," *Systems Research Forum*, vol. 4, no. 2, pp. 137–149, 2010.

[12] A. Kusiak, *Engineering Design: Products, Processes and Systems*, Academic Press, Orlando, Fla, USA, 1999.

[13] D. B. Tang, G. J. Zhang, and S. Dai, "Design as integration of axiomatic design and design structure matrix," *Robotics and Computer-Integrated Manufacturing*, vol. 25, no. 3, pp. 610–619, 2009.

[14] D. Ramanujan, W. Bernstein, F. Zhao, and K. Ramani, "Addressing uncertainties within product redesign for sustainability: a function based framework," in *Proceedings of the ASME International Design Engineering Technical Conferences and Computers and Information in Engineering Conference (IDETC/CIE '11)*, Washington, DC, USA, August 2011.

[15] Zhangjiakou agriculture Web, http://www.zjkny.com/news/showarticle.asp?articleid=667.

[16] Galanz Co., http://www.galanz.com.cn/pages/product_list.aspx?catid=78.

[17] Jinhuafang Web, http://member.0579fw.com.

[18] Zhongbaishang Web, http://www.zon100.com/product/1100123016.html.

[19] Alibaba Web, http://detail.1688.com/offer/779711050.html/.

[20] Basha Web, http://www.basha.com.cn/youhuiduo/giftdetail.asp?i=438.

[21] J. M. Zhang, J. X. Wang, and X. P. Wei, "Product modeling for conceptual design based on extended functional basis," *Transactions of the Chinese Society of Agricultural Machinery*, vol. 39, no. 1, pp. 129–133, 2008.

[22] R. B. Stone and K. L. Wood, "Development of a functional basis for design," *Journal of Mechanical Design*, vol. 122, no. 4, pp. 359–370, 2000.

[23] J. Hirtz, R. B. Stone, D. A. McAdams, S. Szykman, and K. L. Wood, "A functional basis for engineering design: reconciling and evolving previous efforts," *Research in Engineering Design*, vol. 13, no. 2, pp. 65–82, 2002.

[24] G. M. Zou, Y. J. Hu, W. S. Xiao, and C. G. Li, "Research on the model of product conceptual design based on the functional basis," *China Mechanical Engineering*, vol. 15, no. 3, pp. 206–210, 2004.

[25] D. McAdams, R. B. Stone, and K. L. Wood, "Understanding product similarity using customer needs," in *Proceedings of the ASME International Design Engineering Technical Conferences (IDETC '98)*, Atlanta, Ga, USA, September 1998.

[26] G.-N. Qi, X.-J. Gu, Q.-H. Yang, and J.-H. Yu, "Principles and key technologies of mass customization," *Computer Integrated Manufacturing Systems*, vol. 9, no. 9, pp. 776–783, 2003.

Hindawi Publishing Corporation
Advances in Mechanical Engineering
Volume 2013, Article ID 985721, 15 pages
http://dx.doi.org/10.1155/2013/985721

Research Article

Fuzzy Dynamic Reliability Model of Dependent Series Mechanical Systems

Peng Gao[1,2] and Shaoze Yan[2]

[1] *Department of Chemical Mechanical Engineering, Liaoning Shihua University, Liaoning 113001, China*
[2] *State Key Laboratory of Tribology, Department of Mechanical Engineering, Tsinghua University, Beijing 100084, China*

Correspondence should be addressed to Shaoze Yan; yansz@tsinghua.edu.cn

Received 8 February 2013; Accepted 7 July 2013

Academic Editor: Shengfeng Qin

Conventional static fuzzy reliability models cannot be directly extended for dynamic reliability analysis of mechanical systems, which consist of correlative components with strength degradation, due to the difficulties in describing the strength degradation process of components under fuzzy load and considering the failure dependence between different components in a system in the possibility context. To deal with these problems, fuzzy dynamic reliability models of mechanical systems in terms of stress and strength are proposed in this paper, which take into account the degradation mechanism of mechanical components in the failure mode of fatigue. The proposed models can be used to represent the dynamic characteristics of fuzzy reliability and analyze the influences of the variation in the parameters of fuzzy stress and strength on the failure dependence of components in a system and the dynamic behavior of fuzzy system reliability. Besides, the explosive bolts for connection between launch vehicle and satellite are chosen as a representative example to illustrate the proposed method. The results show that different parameters of fuzzy stress have different influences on fuzzy system reliability and the failure dependence of components in a system.

1. Introduction

With the high requirements for safe launch and operation of modern technological systems in aerospace engineering, considerable efforts have been involved in the research on developing reliability models and much progress has been made in the methods for reliability estimate associated with their application in practical systems [1–6]. The reliability evaluation of mechanical systems, which are an integral part of most technology systems, plays an important role in the risk assessment of technology systems [7]. Owing to the comprehensive usage of series configuration in mechanical systems [8, 9], we will concentrate our work on dynamic reliability assessment of series mechanical systems in this paper.

For mechanical components and mechanical systems, the stress-strength interference (SSI) model is the most important method for reliability assessment, which is suitable for static reliability calculation. However, as indicated by Martin, it is imperative to extend the static reliability model to dynamic reliability models to take into account the gradual failure of mechanical components due to fatigue, corrosion, wear, and so forth, which exists commonly in practical engineering [10]. In practice, various computational intelligence algorithms have been adopted in the estimation of dynamic reliability. For example, the support vector machines approach is always used in the numerous reliability calculation due to its advantage in computational efficiency, which has applied to particle identification, face identification, data base marketing, and so forth [11, 12]. Xu and Wong extended least squares support vector machines to the domain of hysteresis modeling [13]. Besides, Fu and Xu proposed a method to predict the location of impact on a clamped aluminum plate structure by integrating principal component analysis and support vector machines [14].

In the last two decades, dynamic system reliability models have been well documented with most research focused on electronic systems. Lewis analyzed the time-dependent behavior of a 1-out-of-2 : G redundant system via a Markov model [15]. Brissaud proposed a mathematical framework for dynamic reliability analysis of digital-based transmitters by introducing data variables [16]. Ding presented an approach to dynamic reliability analysis of bilateral contract

electricity providers in restructured power systems by combining the stochastic process theory and the universal generating function technique [17]. Distefano introduced a methodology for evaluating dependent dynamic systems by using dynamic reliability block diagrams [18]. As pointed out by Moss, the methods for reliability analysis of electronic elements and systems are also effective for reliability assessment of mechanical components [7]. However, these methods should be used with some caution [7]. For mechanical systems in the spacecraft, some problems may be encountered in reliability assessment when directly using the existing dynamic reliability models.

(1) It is difficult for mechanical systems in spacecraft to obtain the distribution of stress at any time instant due to insufficient load history samples.

(2) The failure modes and the corresponding degradation behavior of mechanical systems are different from electronic systems. Therefore, dynamic reliability models of mechanical systems should be developed based on the failure modes analysis and the corresponding degradation mechanism of mechanical components.

To address the problems mentioned above, fuzzy dynamic reliability models of mechanical systems consisting of degraded mechanical components in the failure mode of fatigue are established in this paper. As a matter of fact, fuzzy sets theory has been comprehensively used in the performance analysis of various systems under uncertain environment. With the employment of membership function of fuzzy variables, both experimental data and expert information can be used to cope with the uncertainty in the system analysis [19]. For example, neural networks (NNs) and fuzzy logic can be used for robotic control. Li and Liu dealt with dynamic modeling and task-space trajectory following issues for nonholonomic mobile manipulators moving on a slope by using an adaptive neural-fuzzy controller [20] and presented an algorithm for automatic tip-over prevention and path following control of a redundant nonholonomic mobile modular manipulator by using NNs and fuzzy logic [21].

In recent years, some efforts have been made to analyze fuzzy reliability of various engineering systems by employing the fuzzy set theory introduced by Zadeh in 1965 [22]. Ma et al. proposed a method to analyze the dynamic response and reliability of fuzzy-random truss systems under the stationary random load [23]. Roberts presented an approach to analyzing fuzzy system reliability by modeling a single fuzzy probability distribution for a component from some possible distributions [24]. Zhou put forward a fuzzy reliability model of pressure piping system considering both the randomness of assessment parameters and the fuzziness of failure areas [25]. However, these models mainly focused on static fuzzy reliability analysis of systems. Fuzzy dynamic reliability models of mechanical systems are seldom reported. Besides, when considering the gradual failure of mechanical systems, the existing static fuzzy models cannot be directly extended to fuzzy dynamic reliability models of mechanical systems due to the difficulties listed as follows.

(1) Failure dependency takes place commonly in mechanical systems because the mechanical components in the system share the same working environment. Fuzzy dynamic reliability models of mechanical systems in terms of stress and strength, which take account of failure dependence of mechanical components, are seldom reported.

(2) In the case where stress at each load application is a fuzzy variable, methods to determine the statistical characteristics of strength in its degradation process are seldom reported, which is one of the main difficulties of extending static fuzzy reliability models to fuzzy dynamic reliability models.

The fuzzy dynamic reliability models proposed in this paper provide a method for dynamic reliability estimation of mechanical systems in the possibility context, which can also be used to quantitatively analyze the influences of the variation in material parameters and stress parameters on dynamic reliability of mechanical components. The remainder of this paper is organized as follows. In Sections 2 and 3, fuzzy dynamic reliability models of mechanical systems are developed, In Section 4, numerical examples are given to illustrate the proposed models and analyze the impacts of fuzzy characteristics of stress on both the failure dependence of components in a system and the dynamic behavior of reliability and failure rate of a system. Besides, Monte Carlo simulations are carried out to validate the proposed models. Finally, conclusions are summarized in Section 5.

2. Fuzzy Stress

Due to the limitations of technology and cost, it is difficult or impossible to acquire accurate distribution of stress at each time instant with statistical tools. An alternative method is to model the stress at each time instant as a fuzzy variable characterized by its membership function (MF) by employing the fuzzy set theory as shown in Figure 1.

The fuzzy set theory provides a mathematical tool to deal with the uncertainty of parameters involved in reliability models in the possibility context [26]. A fuzzy set $\widetilde{X}$ is characterized by its MF $\mu_{\widetilde{X}}(x)$. The MF defines how each element in the fuzzy set is mapped to the degree of membership ranging from 0 to 1, where 1 represents that the corresponding elements completely belong to the fuzzy set, 0 means that the corresponding elements are completely not in the fuzzy set, and values between 1 and 0 represent that the corresponding elements partially belong to the fuzzy set. As a matter of fact, the triangular membership function is usually taken as the membership function of fuzzy stress for reliability estimation, which is obtained through the fuzzy linear regression method [27–30]. Therefore, in this paper, the triangular membership function is adopted to describe the fuzzy characteristics of stress in the fuzzy reliability calculation. However, it should be noted that the dynamic fuzzy reliability model proposed in this paper is not limited by the format of membership function of stress. The format of the membership function of stress only influences the upper bound and lower bound of the interval of stress at different level of α. The MF of

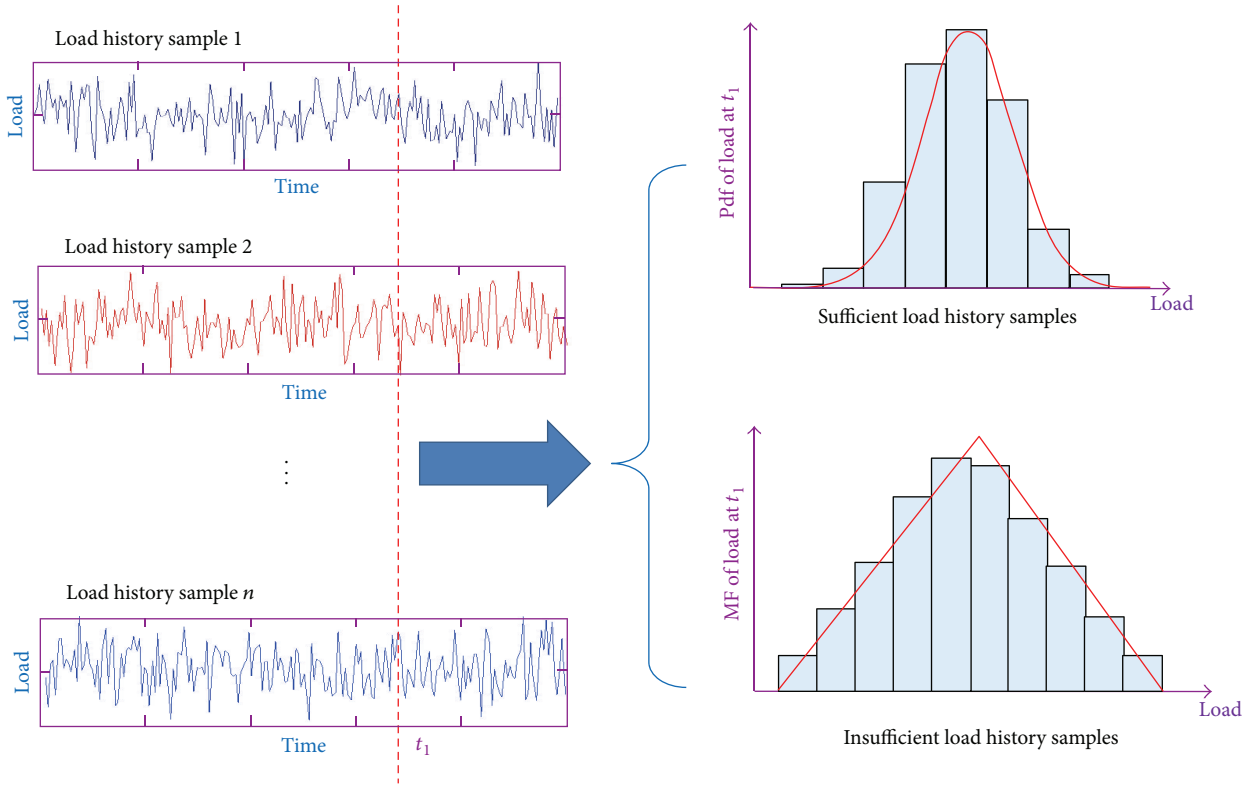

FIGURE 1: Pdf and MF of load.

a triangular fuzzy number, which is denoted by a triplet (a, b, c), can be expressed as follows:

$$\mu_{\widetilde{X}}(x) = \begin{cases} \dfrac{x-a}{b-a}, & a \le x < b \\ 1, & x = b \\ \dfrac{x-c}{b-c}, & b \le x < c \\ 0, & \text{otherwise}, \end{cases} \tag{1}$$

where b is the center point, whose degree of membership is equal to one. a and c are left parameter and right parameter, respectively, which determine the upper bound and lower bound of the fuzzy set, respectively.

For mechanical components, the fuzzy stress can be obtained by integrating the fuzzy linear regression method and the finite element method as follows [31].

(1) Express the fuzzy stress y in the following form:

$$y = A_1 u_1 + A_2 u_2 + \cdots + A_i u_i, \tag{2}$$

where A_j $(j = 1, 2, \ldots, i)$ is the fuzzy regression coefficients and u_j $(j = 1, 2, \ldots, i)$ are the parameters related to stress, such as Youngs modulus of material, weight density, and geometry dimensions.

(2) Obtain the fuzzy regression coefficients in (1), which is denoted by triplets (a_j, b_j, c_j) $(j = 1, 2, \ldots, i)$, by solving the following linear programming problem:

$$\begin{aligned} \min \quad & L = \left|c_1 - a_1\right| + \left|c_2 - a_2\right| + \cdots + \left|c_i - a_i\right| \\ \text{s.t.} \quad & \sum_j b_j u_{ji_1} - (1-\alpha) \sum_j \left|c_j - a_j\right| u_{ji_1} \le y_{i_1} \\ & \sum_j b_j u_{ji_1} + (1-\alpha) \sum_j \left|c_j - a_j\right| u_{ji_1} \ge y_{i_1}, \end{aligned} \tag{3}$$

where α is the threshold of the fuzzy estimate.

(3) Calculate the MF of the fuzzy stress according to the MF of the fuzzy regression coefficients and (2).

3. Fuzzy Dynamic Reliability Model of Dependent Mechanical Systems

Under the failure mode of fatigue, the strength does not degrade in the absence of load application. Therefore, the change of strength is discontinuous and it is more straightforward to establish reliability model with respect to load application times rather than time. Then, the reliability model of mechanical components with respect to time under the failure mode of fatigue can be further developed based on the relationship between load application times and time.

3.1. Fuzzy Dynamic Reliability Models of Dependent Systems with respect to Load Application Times. In a series

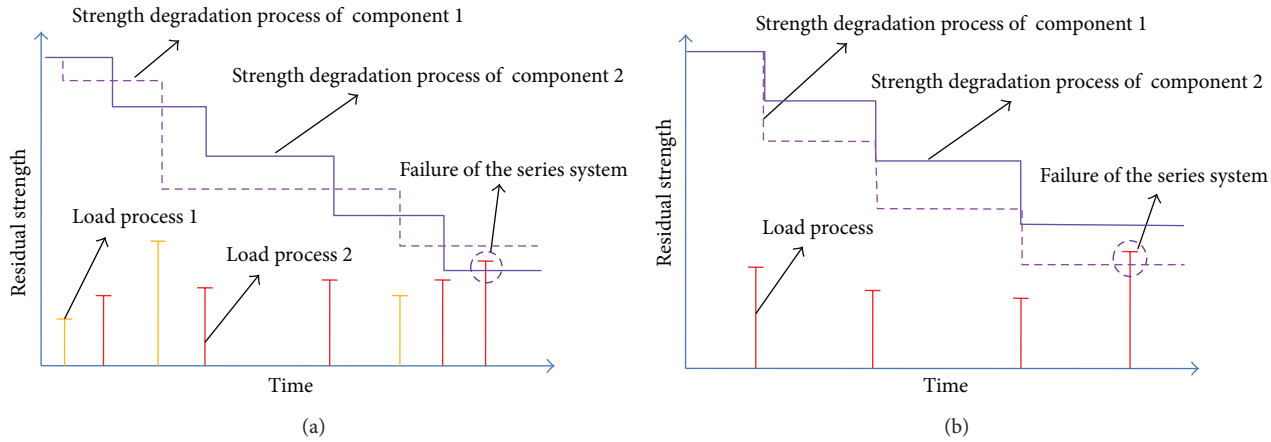

FIGURE 2: (a) Schematic strength degradation process of independent components. (b) Schematic strength degradation process of dependent components.

system with statistically independent components, the strength degradation of each component can be determined independently based on the material properties of the component and the characteristics of load applied on the component as shown in Figure 2(a). However, in practice, the components may be correlative with each other due to sharing the same load, which is a common phenomenon in series mechanical systems, such as the transmission system and kinematic mechanisms. In this case, the strength degradations of the components in the system are mutually correlative. The strength of the components changes simultaneously at the moment when the load appears as shown in Figure 2(b). Besides, the statistical properties of the strength degradation processes of the components are jointly determined by the properties of the load shared by the components.

In addition, even in the probability context, it is difficult to determine the strength degradation process of a component due to the randomness of the magnitude of stress at each load application. Hence, it is more difficult to describe the strength degradation under fuzzy stress, which is seldom reported in the existing literatures. To cope with the problems mentioned above, fuzzy dynamic reliability models of dependent system will be developed in this section.

According to fuzzy probability theory proposed by Zadeh, the fuzzy probability that a random variable x belongs to a fuzzy set $\widetilde{X}$ can be calculated as follows:

$$P(x) = \int_{-\infty}^{\infty} \mu_{\widetilde{X}}(x)\, f(x)\, dx, \tag{4}$$

where $f(x)$ is the probability density function (pdf) of x and $\mu_{\widetilde{X}}(x)$ is the MF of the fuzzy set $\widetilde{X}$. To overcome the difficulty in calculating system reliability directly by using (4) and taking into account both the statistical characteristics of strength and the fuzzy characteristics of stress, the α-cut of fuzzy set is adopted in this paper, which can be used to decompose the fuzzy set and calculate the fuzzy reliability of systems at different levels of α. The α-cut of a fuzzy set provides a basis for fuzzy reliability assessment in the context

$$P(x) = \int_0^1 \int_{\widetilde{X}_\alpha^L}^{\widetilde{X}_\alpha^U} f(x)\, dx\, d\alpha$$

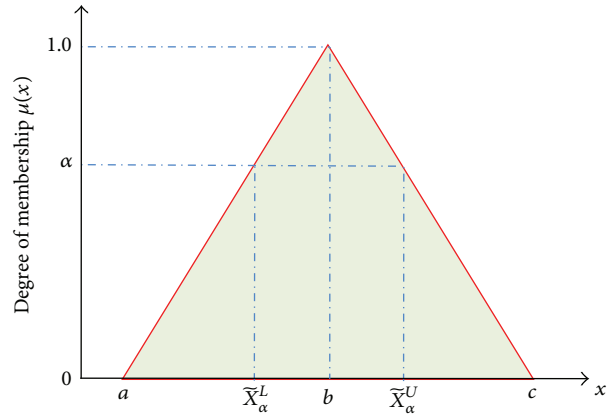

FIGURE 3: MF of the triangular fuzzy number.

of probability. An α-cut, denoted by $\widetilde{X}_\alpha$, is a common set consisting of elements with degree of membership larger than α, whose interval is denoted by $[\widetilde{X}_\alpha^L, \widetilde{X}_\alpha^U]$ as shown in Figure 3. The fuzzy probability $P(x)$ in (4) can be computed by using the α-cut as follows [32]:

$$P(x) = \int_0^1 \int_{\widetilde{X}_\alpha^L}^{\widetilde{X}_\alpha^U} f(x)\, dx\, d\alpha. \tag{5}$$

In practice, the uniform distribution has been widely used as the distribution of a fuzzy variable on the interval of an α-cut in fuzzy reliability calculation according to the maximum entropy approach [33]. In this paper, the uniform distribution is adopted to characterize the uncertainty of stress on the interval of the α-cut. In general, the residual strength of a mechanical component after the application of load for n times can be expressed in the following form [34]:

$$r(n) = r\left[1 - \left(\sum_{i=1}^{n} D_i\right)^{\varepsilon}\right], \tag{6}$$

where $r(n)$ is the residual strength after the application of load for n times and r represents initial strength. D_i stands for the damage of a component caused by the ith load application and ε is a material parameter. According to the Miner linear damage accumulation rule [35], the damage caused by the stress s for once is

$$D = \frac{1}{N}, \tag{7}$$

where N is the lifetime of a component under the stress s. In addition, the S-N curve of mechanical components presents the relationship between the magnitude of the stress s on components and the corresponding lifetime N of components under the stress, which can be mathematically expressed as

$$s^m N = C, \tag{8}$$

where m and C are material parameters, which can be determined by tests. Therefore, the damage caused by the application of load for once can be written as

$$D = \frac{s^m}{C}. \tag{9}$$

Denote the fuzzy stress at the ith load application by (a_i, b_i, c_i). Then, the distribution of the fuzzy stress on the interval of α-cut at the level of α can be given by

$$f_\alpha(s) = \begin{cases} \dfrac{1}{(1-\alpha)(c_i - a_i)}, & (1-\alpha)a_i + \alpha b_i \le x < (1-\alpha)c_i + \alpha b_i \\ 0, & \text{otherwise.} \end{cases} \tag{10}$$

When considering the distribution of the fuzzy stress on the interval of α-cut, the damage caused by the ith application of load at the level of α can be approximately expressed as follows:

$$\begin{aligned} D_{\alpha i} &= \int_{(1-\alpha)a_i + \alpha b_i}^{(1-\alpha)c_i + \alpha b_i} \frac{s^m}{(1-\alpha)(c_i - a_i)C} ds \\ &= \frac{\left[(1-\alpha)c_i + \alpha b_i\right]^{m+1} - \left[(1-\alpha)a_i + \alpha b_i\right]^{m+1}}{(m+1)(1-\alpha)(c_i - a_i)C}. \end{aligned} \tag{11}$$

Therefore, for a deterministic mechanical component with the initial strength of r, the residual strength of a mechanical component after the application of load for n times at the level of α can be written as follows:

$$r_\alpha(n) = r\left\{1 - \left\{\sum_{i=1}^{n}\left\{\frac{\left[(1-\alpha)c_i + \alpha b_i\right]^{m+1} - \left[(1-\alpha)a_i + \alpha b_i\right]^{m+1}}{(m+1)(1-\alpha)(c_i - a_i)C}\right\}\right\}^{\varepsilon}\right\}. \tag{12}$$

From the system reliability theory, it can be learned that the reliable operation of a series system is determined by the weakest component in the system. Therefore, the reliability of a dependent series system at each load application can be obtained by calculating the probability that the minimum residual strength is greater than the stress. For illustrative convenience, in this section, the series system is assumed to be composed of identical components, which are subjected to identical stress in the case of sharing the same environmental load. Denote the fuzzy stress at the ith load application by (a_i, b_i, c_i). When the minimum initial strength of the components in the system is $r_{\min}$, the fuzzy dynamic reliability of the system under the application of load for n times at the level of α can be given by

$$\begin{aligned} R_\alpha(n) = \prod_{i=1}^{n}\Big(&\left(\min\left\{\left[(1-\alpha)c_i + \alpha b_i\right], \right.\right. \\ &\left.\left.\max\left\{\left[(1-\alpha)a_i + \alpha b_i\right], r_{\min\alpha}(n-1)\right\}\right\}\right. \\ &\left. - \left[(1-\alpha)a_i + \alpha b_i\right]\right) \\ &\times \left((1-\alpha)(c_i - a_i)\right)^{-1}\Big), \end{aligned} \tag{13}$$

where

$$r_{\min\alpha}(n) = r_{\min}\left\{1 - \left\{\sum_{i=1}^{n}\left\{\frac{\left[(1-\alpha)c_i + \alpha b_i\right]^{m+1} - \left[(1-\alpha)a_i + \alpha b_i\right]^{m+1}}{(m+1)(1-\alpha)(c_i - a_i)C}\right\}\right\}^{\varepsilon}\right\}. \tag{14}$$

For a dependent series system that consists of k identical components with the initial strength characterized by the pdf of $f_r(r)$, the pdf of the minimum initial strength of components in the system can be given by [36]

$$f_{\min}(r) = k\left[1 - \int_{-\infty}^{r} f_r(r)\, dr\right]^{k-1} f_r(r). \tag{15}$$

Therefore, the fuzzy system reliability under the application of load for n times at the level of α can be given by

$$\begin{aligned} R_\alpha(n) = \int_{-\infty}^{\infty} &k\left[1 - \int_{-\infty}^{r} f_r(r)\, dr\right]^{k-1} f_r(r) \\ &\times \left\{\prod_{i=1}^{n}\Big(\left(\min\left\{\left[(1-\alpha)c_i + \alpha b_i\right], \right.\right.\right. \\ &\left.\left.\left.\max\left\{\left[(1-\alpha)a_i + \alpha b_i\right], r_\alpha(n-1)\right\}\right\}\right. \right. \\ &\left.\left. - \left[(1-\alpha)a_i + \alpha b_i\right]\right) \right. \\ &\left. \times \left((1-\alpha)(c_i - a_i)\right)^{-1}\Big)\right\} dr. \end{aligned} \tag{16}$$

From (5), the fuzzy dynamic reliability of a dependent series system with respect to load applications times can be

calculated by the integral of the fuzzy reliability at different levels of α in the following form:

$$R(n) = \int_0^1 \int_{-\infty}^{\infty} k\left[1 - \int_{-\infty}^{r} f_r(r)\,dr\right]^{k-1} f_r(r) \times \left\{\prod_{i=1}^{n} \left(\left(\min\left\{\left[(1-\alpha)c_i + \alpha b_i\right], \max\left\{\left[(1-\alpha)a_i + \alpha b_i\right], r_\alpha(n-1)\right\}\right\} - \left[(1-\alpha)a_i + \alpha b_i\right]\right) \times \left((1-\alpha)(c_i - a_i)\right)^{-1}\right)\right\} dr\,d\alpha. \quad (17)$$

In addition, when the components in the system are statistically independent, the fuzzy dynamic system reliability can be analogously derived as follows:

$$R(n) = \prod_{w=1}^{k} \left\{\int_0^1 \left\{\int_{-\infty}^{\infty} f_w(r_w) \times \left\{\prod_{i=1}^{n} \left(\left(\min\left\{\left[(1-\alpha)c_{wi} + \alpha b_{wi}\right], \max\left\{\left[(1-\alpha)a_{wi} + \alpha b_{wi}\right], r_{w\alpha}(n-1)\right\}\right\} - \left[(1-\alpha)a_{wi} + \alpha b_{wi}\right]\right) \times \left((1-\alpha)(c_{wi} - a_{wi})\right)^{-1}\right)\right\} dr_w\right\} d\alpha\right\}, \quad (18)$$

where

$$r_{w\alpha}(n-1) = r_w\left\{1 - \left\{\sum_{i=1}^{n-1}\left\{\frac{\left[(1-\alpha)c_i + \alpha b_i\right]^{m+1} - \left[(1-\alpha)a_i + \alpha b_i\right]^{m+1}}{(m+1)(1-\alpha)(c_i - a_i)C}\right\}\right\}^{\varepsilon}\right\}. \quad (19)$$

$f_w(r_w)$ is the pdf of the initial strength of the wth component in the system, and (a_{wi}, b_{wi}, c_{wi}) $(w = 1, 2, \ldots, k)$ is the fuzzy stress on the wth component at the ith application of load.

3.2. Fuzzy Dynamic Reliability Models of Dependent Systems with respect to Time. The fuzzy reliability model developed in Section 3.1 is with respect to load application times. When the frequency function of the occurrence of load is available, which is denoted by $f(t)$, the fuzzy dynamic system reliability with respect to time can be written as

$$R(t) = \int_0^1 \prod_{w=1}^{k} \times \left\{\int_{-\infty}^{\infty} f_w(r_w) \left\{\prod_{i=1}^{f(t)t} \left(\left(\min\left\{\left[(1-\alpha)c_{wi} + \alpha b_{wi}\right], \max\left\{\left[(1-\alpha)a_{wi} + \alpha b_{wi}\right], r_{w\alpha}(n-1)\right\}\right\} - \left[(1-\alpha)a_{wi} + \alpha b_{wi}\right]\right) \times \left((1-\alpha)(c_{wi} - a_{wi})\right)^{-1}\right)\right\} dr_w\right\} d\alpha. \quad (20)$$

However, in the case where the load application times in a given time period is a random variable, it is difficult to provide a straightforward deterministic frequency function of load occurrence times for dynamic reliability analysis, which can only be expressed with the statistical tools. As a matter of fact, the Poisson process has been proved to be an effective stochastic process to describe the randomness of the arrival time of load within a specified time period [15]. Provided that the intensity of the Poisson process is $\lambda(t)$, the probability that the load appears for n times in the time period of t can be given by

$$\Pr[n(t) - n(0) = n] = \frac{\left(\int_0^t \lambda(t)\,dt\right)^n}{n!} \exp\left(-\int_0^t \lambda(t)\,dt\right). \quad (21)$$

In the case where the load process follows the Poisson process, the fuzzy dynamic reliability of the dependent system with respect to time at the level of α can be obtained according to the total probability theorem in the following form:

$$R_\alpha(t) = \exp\left(-\int_0^t \lambda(t)\,dt\right) + \sum_{n=1}^{\infty} \frac{\left(\int_0^t \lambda(t)\,dt\right)^n}{n!} \exp\left(-\int_0^t \lambda(t)\,dt\right) \times \left\{\int_{-\infty}^{\infty} k\left[1 - \int_{-\infty}^{r} f_r(r)\,dr\right]^{k-1} f_r(r) \times \left\{\prod_{i=1}^{n} \left(\left(\min\left\{\left[(1-\alpha)c_i + \alpha b_i\right], \max\left\{\left[(1-\alpha)a_i + \alpha b_i\right], r_{\min}(n-1)\right\}\right\}\right.\right.\right.$$

$$- \left[(1-\alpha)\, a_i + \alpha b_i\right] \Big) \times \left((1-\alpha)\left(c_i - a_i\right)\right)^{-1} \Big) \Big\} dr \Big\}. \tag{22}$$

According to (5), the fuzzy dynamic reliability of dependent system with respect to time can be given by

$$\begin{aligned} R(t) = {} & \exp\left(-\int_0^t \lambda(t)\, dt\right) \\ & + \sum_{n=1}^{\infty} \frac{\left(\int_0^t \lambda(t)\, dt\right)^n}{n!} \exp\left(-\int_0^t \lambda(t)\, dt\right) \\ & \times \left\{\int_0^1 \int_{-\infty}^{\infty} k\left[1 - \int_{-\infty}^{r} f_r(r)\, dr\right]^{k-1} f_r(r) \right. \\ & \quad \times \left\{\prod_{i=1}^{n} \Big(\left(\min\left\{\left[(1-\alpha)\, c_i + \alpha b_i\right], \right.\right.\right. \\ & \qquad \left.\left.\left. \max\left\{\left[(1-\alpha)\, a_i + \alpha b_i\right], \right.\right.\right. \\ & \qquad \left.\left.\left. r_{\min}(n-1)\right\}\right\} \right. \\ & \qquad \left. - \left[(1-\alpha)\, a_i + \alpha b_i\right]\right) \\ & \qquad \left. \times \left(\left(1-\alpha\right)\left(c_i - a_i\right)\right)^{-1}\Big)\right\} dr\, d\alpha \Big\}. \end{aligned} \tag{23}$$

Correspondingly, the fuzzy failure rate of the dependent system at the level of α can be expressed as

$$h_\alpha(t) = -\frac{dR_\alpha(t)}{dtR_\alpha(t)} = \frac{A_1}{B_1}, \tag{24}$$

where

$$\begin{aligned} A_1 = {} & \lambda(t) \\ & \times \left\{1 - \sum_{n=1}^{\infty} \frac{\left(\int_0^t \lambda(t)\, dt\right)^n}{n!} \left[n - \int_0^t \lambda(t)\, dt\right] \right. \\ & \times \int_{-\infty}^{\infty} k\left[1 - \int_{-\infty}^{r} f_r(r)\, dr\right]^{k-1} f_r(r) \\ & \quad \times \left\{\prod_{i=1}^{n} \Big(\left(\min\left\{\left[(1-\alpha)\, c_i + \alpha b_i\right], \right.\right.\right. \\ & \qquad \left.\left.\left. \max\left\{\left[(1-\alpha)\, a_i + \alpha b_i\right], \right.\right.\right. \\ & \qquad \left.\left.\left. r_{\min}(n-1)\right\}\right\} \right. \\ & \qquad \left. - \left[(1-\alpha)\, a_i + \alpha b_i\right]\right) \\ & \qquad \left. \times \left(\left(1-\alpha\right)\left(c_i - a_i\right)\right)^{-1}\Big)\right\} dr \Big\}, \end{aligned}$$

$$\begin{aligned} B_1 = {} & 1 + \sum_{n=1}^{\infty} \frac{\left(\int_0^t \lambda(t)\, dt\right)^n}{n!} \\ & \times \left\{\int_{-\infty}^{\infty} k\left[1 - \int_{-\infty}^{r} f_r(r)\, dr\right]^{k-1} f_r(r) \right. \\ & \quad \times \left\{\prod_{i=1}^{n} \Big(\left(\min\left\{\left[(1-\alpha)\, c_i + \alpha b_i\right], \right.\right.\right. \\ & \qquad \left.\left.\left. \max\left\{\left[(1-\alpha)\, a_i + \alpha b_i\right], \right.\right.\right. \\ & \qquad \left.\left.\left. r_{\min}(n-1)\right\}\right\} \right. \\ & \qquad \left. - \left[(1-\alpha)\, a_i + \alpha b_i\right]\right) \\ & \qquad \left. \times \left(\left(1-\alpha\right)\left(c_i - a_i\right)\right)^{-1}\Big)\right\} dr \Big\}. \end{aligned} \tag{25}$$

The fuzzy failure rate of the system can be written as

$$h(t) = -\frac{dR(t)}{dtR(t)} = \frac{A_2}{B_2}, \tag{26}$$

where

$$\begin{aligned} A_2 = {} & \lambda(t) \\ & \times \left\{1 - \sum_{n=1}^{\infty} \frac{\left(\int_0^t \lambda(t)\, dt\right)^n}{n!} \left[n - \int_0^t \lambda(t)\, dt\right] \right. \\ & \times \int_0^1 \int_{-\infty}^{\infty} k\left[1 - \int_{-\infty}^{r} f_r(r)\, dr\right]^{k-1} f_r(r) \\ & \quad \times \left\{\prod_{i=1}^{n} \Big(\left(\min\left\{\left[(1-\alpha)\, c_i + \alpha b_i\right], \right.\right.\right. \\ & \qquad \left.\left.\left. \max\left\{\left[(1-\alpha)\, a_i + \alpha b_i\right], \right.\right.\right. \\ & \qquad \left.\left.\left. r_{\min}(n-1)\right\}\right\} \right. \\ & \qquad \left. - \left[(1-\alpha)\, a_i + \alpha b_i\right]\right) \\ & \qquad \left. \times \left(\left(1-\alpha\right)\left(c_i - a_i\right)\right)^{-1}\Big)\right\} dr\, d\alpha \Big\}, \end{aligned}$$

$$\begin{aligned} B_2 = {} & 1 + \sum_{n=1}^{\infty} \frac{\left(\int_0^t \lambda(t)\, dt\right)^n}{n!} \\ & \times \left\{\int_0^1 \int_{-\infty}^{\infty} k\left[1 - \int_{-\infty}^{r} f_r(r)\, dr\right]^{k-1} f_r(r) \right. \end{aligned}$$

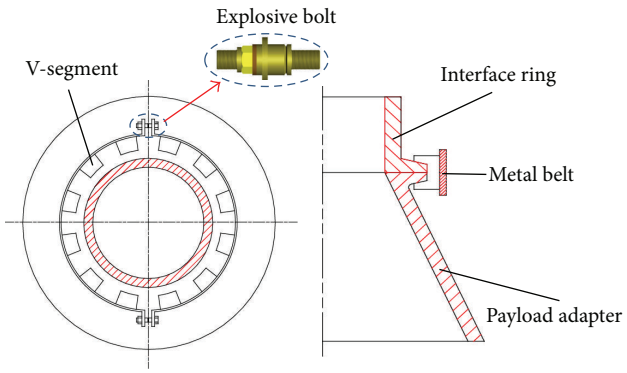

Figure 4: Structure of the joint system.

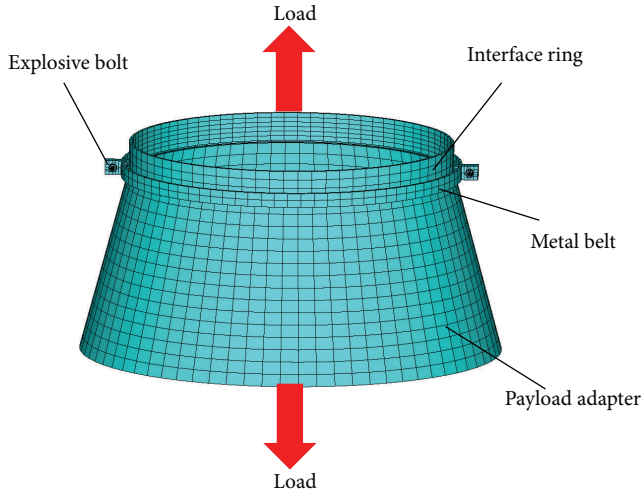

Figure 5: Finite element model of the joint system.

$$\times \left\{ \prod_{i=1}^{n} \left(\left(\min \left\{ \left[(1-\alpha)\, c_i + \alpha b_i \right], \max \left\{ \left[(1-\alpha)\, a_i + \alpha b_i \right], r_{\min} (n-1) \right\} \right\} - \left[(1-\alpha)\, a_i + \alpha b_i \right] \right) \times \left((1-\alpha)\left(c_i - a_i\right) \right)^{-1} \right) \right\} d r\, d\alpha \Bigg\}. \tag{27}$$

4. Numerical Examples

The explosive bolt has been widely used as a connection and pyrotechnical separation device in the aerospace industry, which can provide the joint system with adequate connection strength and produce few pollutants. An important application of the explosive bolt is for the connection and separation of the payload adapter and the interface ring, which are connected to the launch vehicle and the satellite, respectively. The schematic structure and the finite element model of the joint system are shown in Figures 4 and 5, respectively. In the launch process of satellites, the explosive bolts are used to sustain the applied tensile forces and bending moments through the metal belts and the V-segments [37]. In the separation process of the satellite and the launch vehicle, the explosive bolt fractures at the site where a groove is designated with the help of internal power source generated by explosive charge.

To guarantee successful separation of the satellite and the launch vehicle, more than one explosive bolt is always adopted in the joint system. At the separating stage of launch vehicle and the satellite, the explosive bolts constitute a parallel system as shown in Figure 6(a), whose reliability can be analyzed by using the static SSI model. However, in the launch process of satellites, the explosive bolts share the same external load and the failure of a single explosive bolt will result in the failure of the whole joint system. Therefore, the explosive bolts compose a dependent series system in the launch process of satellites as shown in Figure 6(b). Moreover, the fatigue failure of bolts may be caused due to the fluctuating bolt stress in the launch process of satellites, which is a significant and costly failure mode for explosive bolts [38]. Therefore, the reliability of the dependent series system should be estimated considering strength degradation of components. In this section, explosive bolts are chosen as representative examples to illustrate the fuzzy dynamic reliability models proposed in this paper. Moreover, the impacts of various factors on the correlation between different components in a dependent system and further on the fuzzy dynamic reliability will be analyzed through numerical examples.

Consider a joint system with two explosive bolts, which constitute a dependent series system. The fuzzy stress and the material parameters of the explosive bolts are listed in Table 1. The fuzzy dynamic reliability of the dependent system at different levels of α is shown in Figure 7. In addition, to validate the proposed fuzzy dynamic reliability model, the Monte Carlo simulation is carried out in this section with its flow shown in Figure 8. In the Monte Carlo simulation, the actual strength degradation process is simulated based on the fuzzy stress in a strength degradation process, whose occurrence time and magnitude are generated randomly, with the degradation mechanism of the components. The results from the Monte Carlo simulation and the fuzzy dynamic reliability of both the dependent system and the system with independent components are shown in Figure 9.

From Figure 7, it can be learned that the proposed reliability models provide a method to quantitatively analyze the dynamic changing process of fuzzy system reliability that decreases with time. Besides, the level of the cut set has great influences on the assessment of fuzzy system reliability. An increase in the level of the cut set results in a higher reliability. From Figure 9, we can learn that the fuzzy reliability calculated by using the method proposed in this paper shows good agreement with the results obtained from Monte Carlo simulations. In addition, in the case of

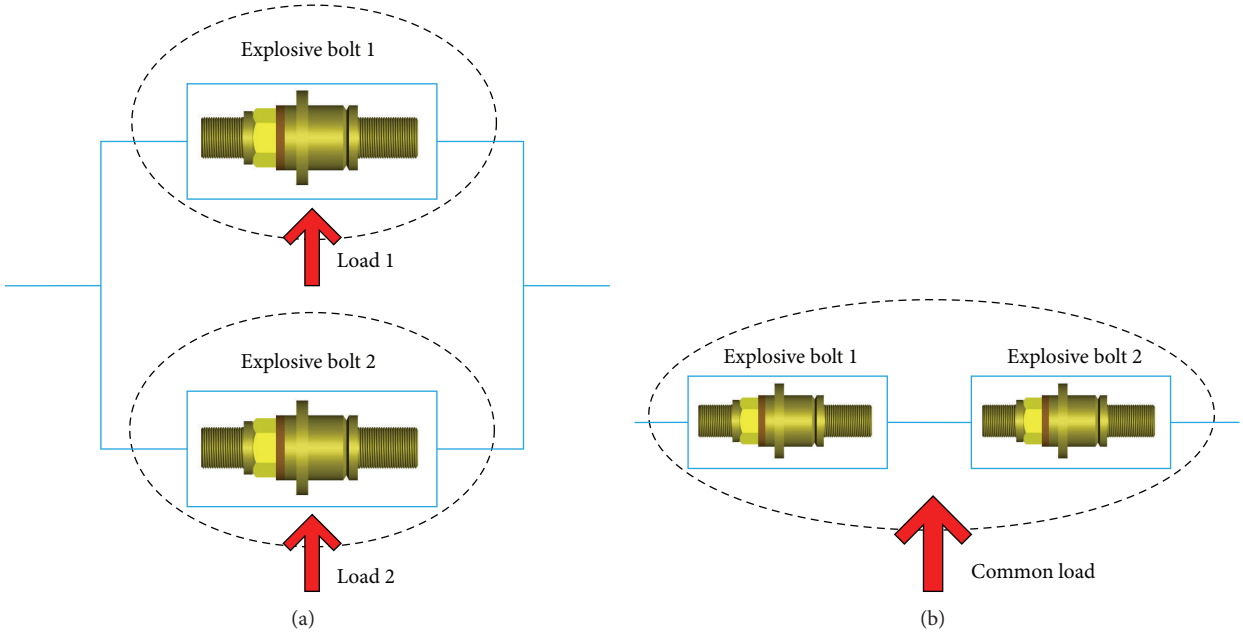

Figure 6: (a) Block program of the independent parallel system, and (b) block program of the dependent series system.

Table 1: Stress parameters and material parameters of explosive bolts.

$\mu(r_0)$ (MPa)	$\sigma(r_0)$ (MPa)	a (MPa)	b (MPa)	c (MPa)	C (MPa^2)	m	ε	λ (s^{-1})
700	10	550	650	720	10^9	2	1	0.3

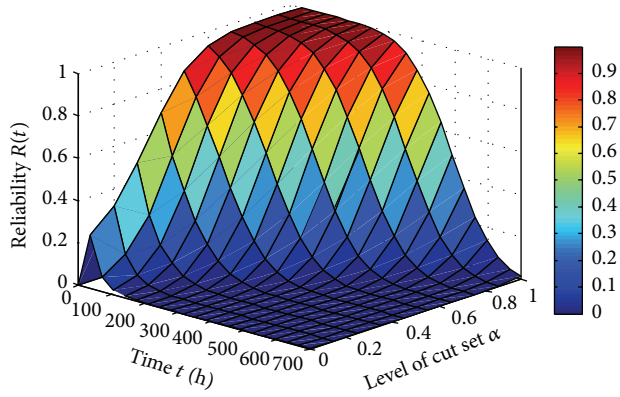

Figure 7: Reliability of explosive bolts at different levels of α.

fuzzy stress, the failure dependence of components in a series system leads to a higher reliability.

In order to analyze the impacts of the fuzzy characteristics of the stress on the failure dependence of the components in a dependent system and the dynamic behavior of fuzzy system reliability, consider the following three cases.

Case 1. To analyze the influences of the left parameter a of the fuzzy stress on the fuzzy dynamic reliability and fuzzy failure rate of the system, the center point b and the right parameter c of the fuzzy stress and the material parameters are kept constant as listed in Table 2. The reliability and failure rate of both the dependent system consisting of correlative components and the system composed of independent components under the fuzzy stress with different left parameters are shown in Figures 10 and 11, respectively.

From Figures 10 and 11, we can learn that the left parameter of the fuzzy stress has few influences on the fuzzy system reliability and the fuzzy failure rate. In general, the fuzzy reliability increases and the fuzzy failure rate decreases with the decrease in the left parameter of the fuzzy stress. Furthermore, the failure dependence of the components in a series system causes the fuzzy system reliability less sensitive to the variation in the left parameter of the fuzzy stress. Besides, when considering strength degradation of components under fuzzy stress, the fuzzy failure rate calculated by using the method proposed in this paper is consistent with the bathtub curve assumption used in the probability context.

Case 2. To analyze the influences of the right parameter c of the fuzzy stress on the fuzzy dynamic reliability and fuzzy failure rate of the system, the left parameter a and the center point b of the fuzzy stress and the material parameters are kept constant as listed in Table 3. The reliability and failure rate of both the dependent system and the system with independent components under the fuzzy stress with different right parameters are shown in Figures 12 and 13, respectively.

From Figures 12 and 13, we can learn that the right parameter of the fuzzy stress has great influences on the

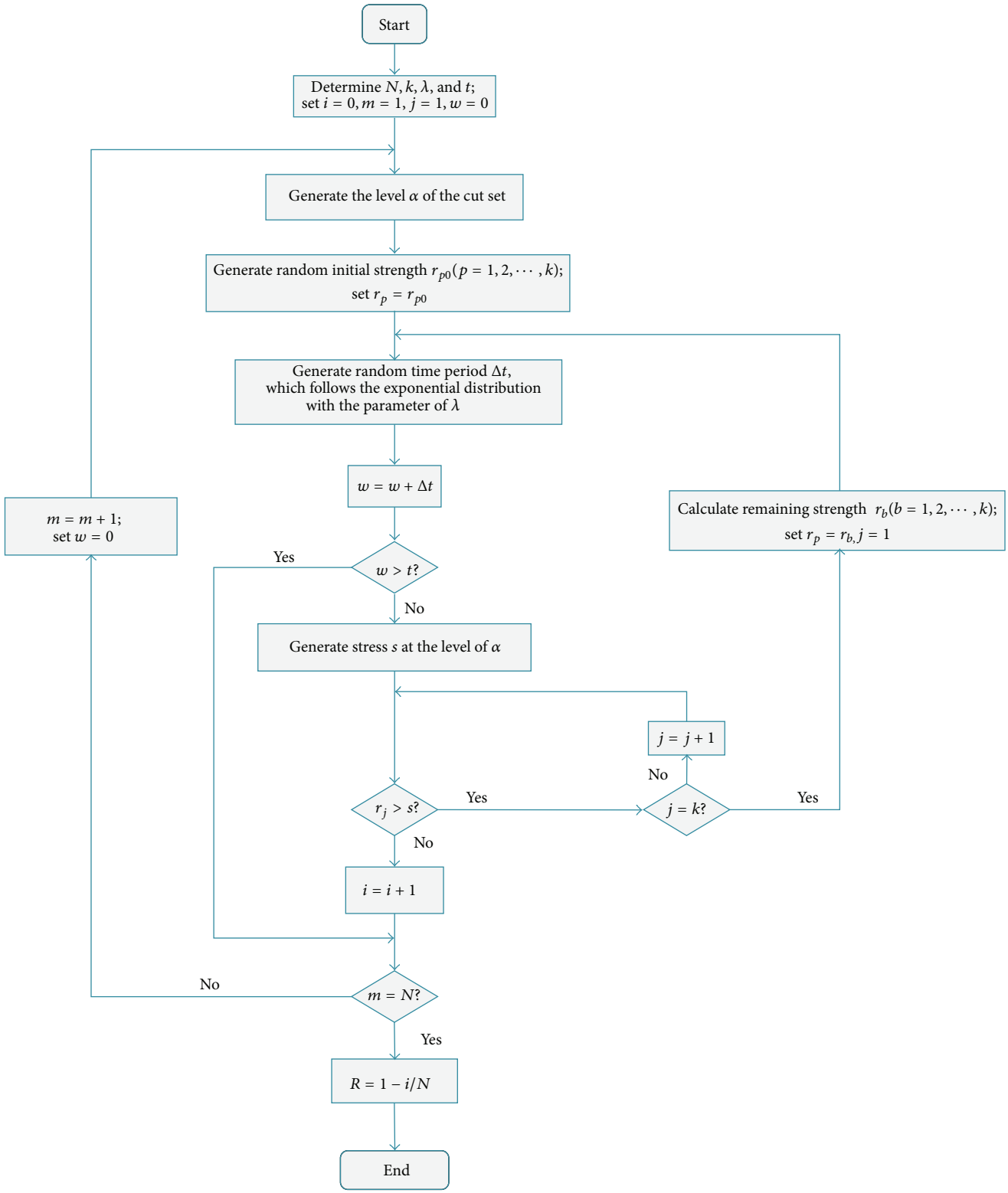

Figure 8: Flowchart of Monte Carlo simulation.

Table 2: Stress parameters and material parameters of explosive bolts.

	$\mu(r_0)$ (MPa)	$\sigma(r_0)$ (MPa)	a (MPa)	b (MPa)	c (MPa)	C (MPa^2)	m	ε	λ (s^{-1})
1	700	10	500	650	720	10^9	2	1	0.3
2	700	10	550	650	720	10^9	2	1	0.3
3	700	10	600	650	720	10^9	2	1	0.3

Table 3: Stress parameters and material parameters of explosive bolts.

	$\mu(r_0)$ (MPa)	$\sigma(r_0)$ (MPa)	a (MPa)	b (MPa)	c (MPa)	C (MPa^2)	m	ε	λ (s^{-1})
1	700	10	550	650	680	10^9	2	1	0.3
2	700	10	550	650	700	10^9	2	1	0.3
3	700	10	550	650	720	10^9	2	1	0.3

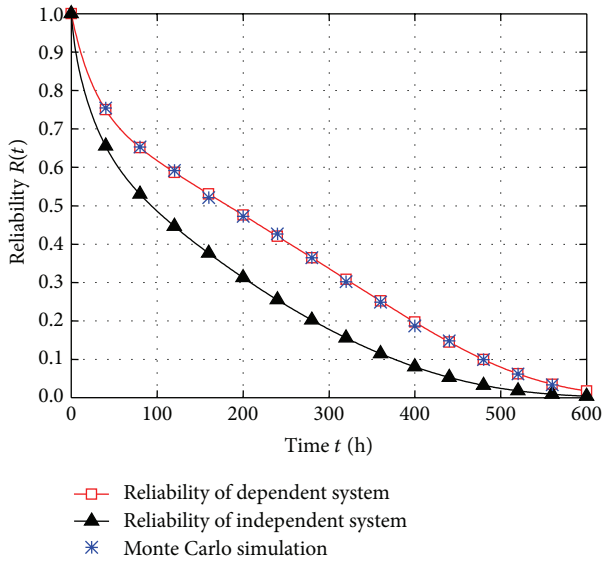

Figure 9: Comparison between the results by using the proposed method and the results from Monte Carlo simulation.

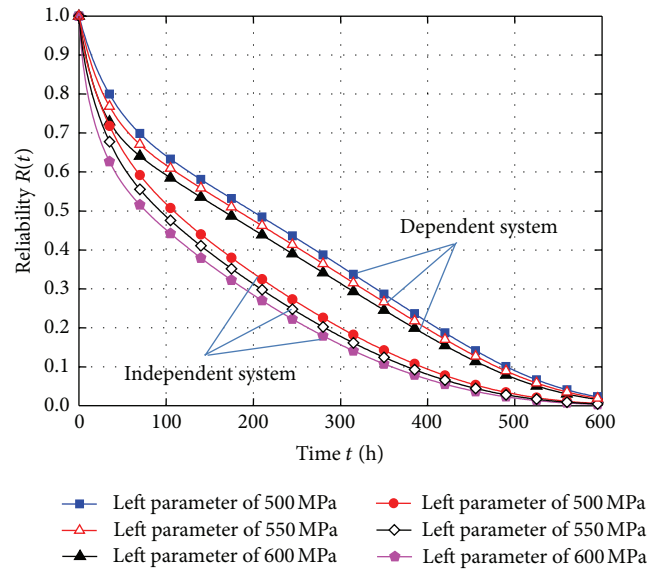

Figure 10: Reliability of independent system and dependent system with different left parameters.

fuzzy system reliability and the fuzzy failure rate. The fuzzy system reliability decreases and the fuzzy failure rate increases with the increase in the right parameter of the fuzzy stress. Moreover, the fuzzy system reliability is more sensitive to the variation of the right parameter of the fuzzy stress when the value of right parameter is lower. In addition, the right parameter of the fuzzy stress has considerable influences on dependence of components in a system. The failure dependence of the components in a series system becomes more obvious when the right parameter of the fuzzy stress is larger. Correspondingly, the difference between the reliability of the dependent system and the reliability of the independent system increases with the increase in the right parameter of the fuzzy stress.

Case 3. To analyze the influences of the center point b of the fuzzy stress on the fuzzy dynamic reliability and fuzzy failure rate of the system, the left parameter a and the right parameter c of the fuzzy stress and the material parameters are kept constant as listed in Table 4. The reliability and failure rate of both the dependent system and the independent system composed of independent components under the fuzzy stress with different center points are shown in Figures 14 and 15, respectively.

From Figures 14 and 15, we can learn that the center point of the fuzzy stress has significant influences on the fuzzy system reliability and the fuzzy failure rate. The fuzzy system reliability decreases and the fuzzy failure rate increases with the increase in the center point of the fuzzy stress. Furthermore, in the case where the value of the center point of the fuzzy stress is higher, the fuzzy system reliability is more sensitive to the variation of the center point of the fuzzy stress. Besides, the center point of the fuzzy stress has great influences on the dependence of components in a system. The failure dependence of the components in a series system is more obvious in the case of smaller center point of the fuzzy stress, which results in a larger difference between the reliability of the dependent system and the reliability of the independent system.

Table 4: Stress parameters and material parameters of explosive bolts.

	$\mu(r_0)$ (MPa)	$\sigma(r_0)$ (MPa)	a (MPa)	b (MPa)	c (MPa)	C (MPa^2)	m	ε	λ (s^{-1})
1	700	10	550	620	720	10^9	2	1	0.3
2	700	10	550	650	720	10^9	2	1	0.3
3	700	10	550	680	720	10^9	2	1	0.3

Table 5: Stress parameters and material parameters of explosive bolts.

	$\mu(r_0)$ (MPa)	$\sigma(r_0)$ (MPa)	a (MPa)	b (MPa)	c (MPa)	C (MPa^2)	k	m	ε	λ (s^{-1})
1	700	10	550	650	720	10^9	1	2	1	0.3
2	700	10	550	650	720	10^9	2	2	1	0.3
3	700	10	550	650	720	10^9	3	2	1	0.3

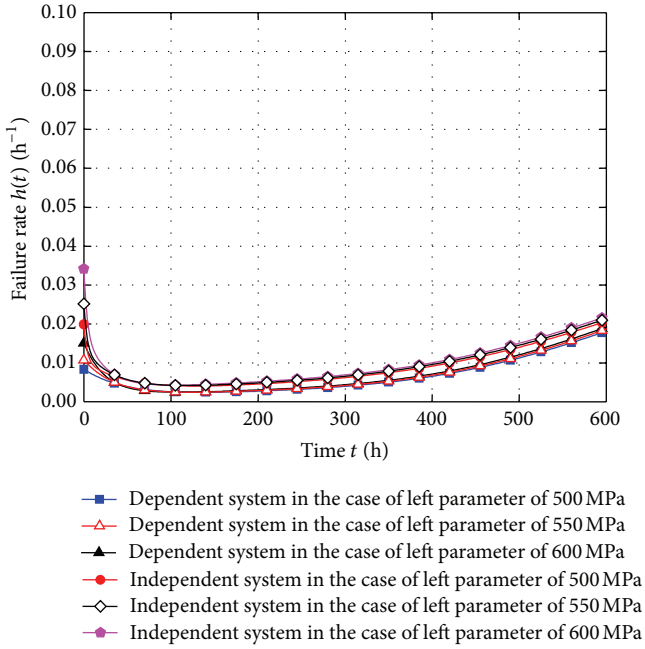

Figure 11: Failure rate of independent system and dependent system with different left parameters.

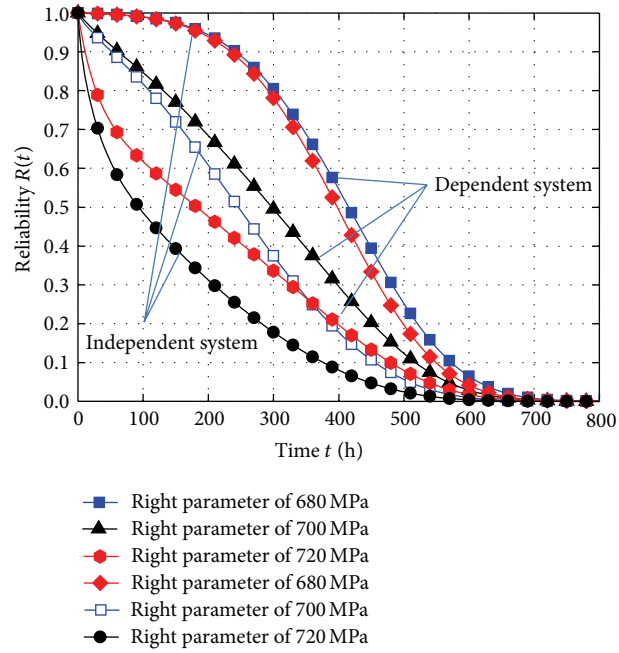

Figure 12: Reliability of independent system and dependent system with different right parameters.

In addition, to analyze the influences of the number of components in the system on the correlation between the components in a dependent system, the material parameters and the parameters of the fuzzy stress are summarized in Table 5. The fuzzy dynamic reliability and fuzzy failure rate of the dependent system and the system consisting of independent components with different number of components are shown in Figures 16 and 17, respectively.

From Figures 16 and 17, it can be learnt that the number of components in a system has great influences on the fuzzy system reliability and the fuzzy failure rate. The fuzzy system reliability decreases and the fuzzy failure rate increases with the increase in the number of components. Furthermore, compared with the reliability of the dependent system, the fuzzy reliability of the independent system is more sensitive to the change of the number of the components in the system. Besides, for both the dependent system and the independent system, the fuzzy system reliability is more sensitive to the variation of the number of components in the system when the number is small. In addition, the number of components has considerable impacts on the failure dependence of components in a system. The failure dependence of the components in a series system becomes more obvious when the number of components is larger, which leads to a larger difference between the reliability of the dependent system and the reliability of the independent system.

5. Conclusion

In this paper, a method for fuzzy dynamic reliability assessment of mechanical systems in terms of stress and strength is presented. The reliability models proposed in this paper take into account the degradation mechanism of mechanical

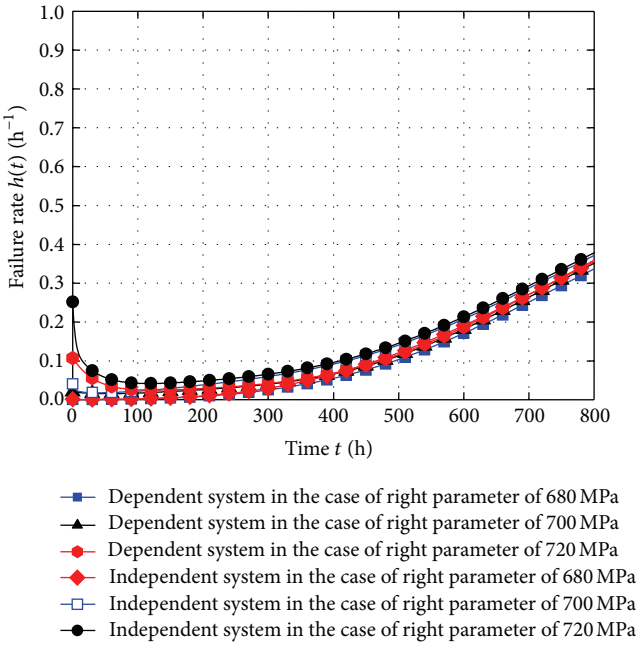

FIGURE 13: Failure rate of independent system and dependent system with different right parameters.

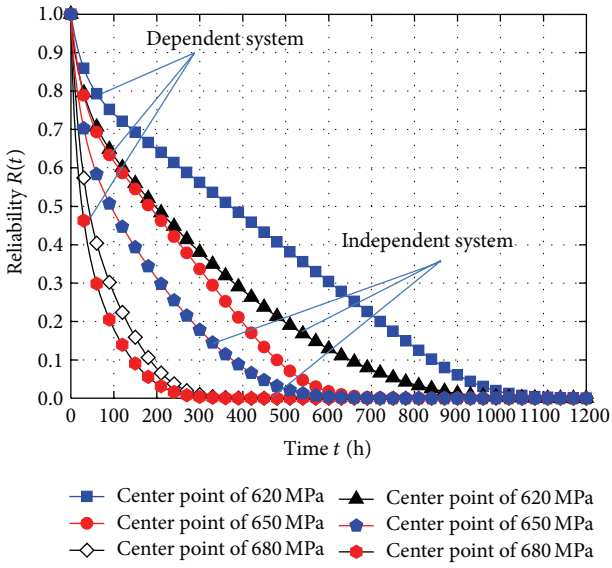

FIGURE 14: Reliability of independent system and dependent system with different center points.

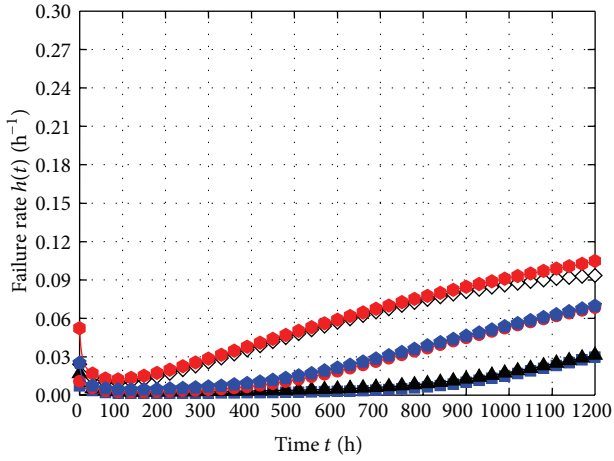

FIGURE 15: Failure rate of independent system and dependent system with different center points.

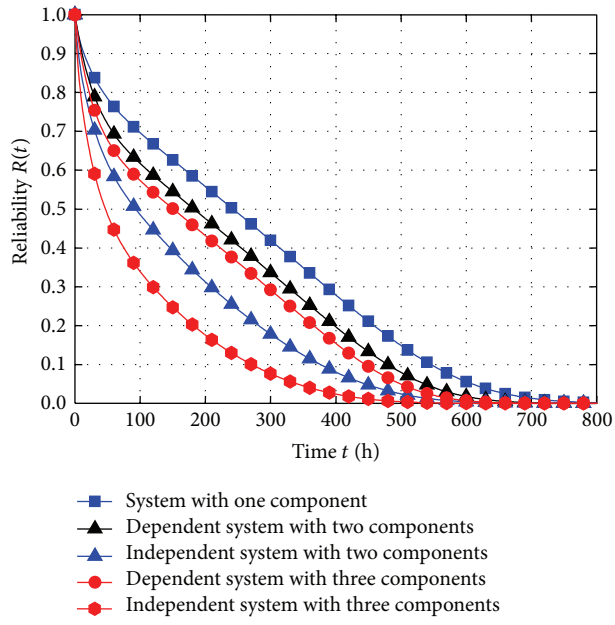

FIGURE 16: Reliability of independent system and dependent system with different number of components.

components and can be used to represent the dynamic characteristics of the fuzzy reliability and failure rate of mechanical systems.

Moreover, the reliability models proposed in this paper provide a method for dynamic reliability analysis of mechanical systems with correlative components in the possibility context. Furthermore, the proposed models can be used to quantitatively analyze the influences of the variation in parameters of fuzzy stress on the failure dependence of components in a system and the dynamic behavior of fuzzy system reliability. The results show that the left parameter of the fuzzy stress has few influences on the fuzzy system reliability. The right parameter and the center point of fuzzy stress and the number of components in a system have significant effects on the fuzzy system reliability and the failure dependence of components in a system.

Further work is in progress to include other variables in the reliability models to achieve more accurate predictive

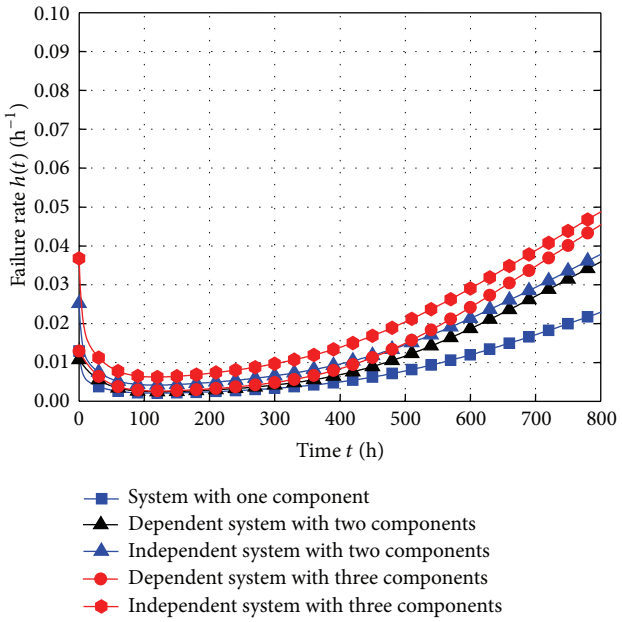

FIGURE 17: Failure rate of independent system and dependent system with different number of components.

results. Besides, extension of the proposed method to problems of reliability-base design optimization is currently being pursued by the present authors.

Acknowledgments

This work was supported by the National Science Foundation of China under Contract no. 11072123, the National High Technology Research and Development Program of China (863 Program) under Contract no. 2009AA04Z401, the Major State Basic Research Development Program of China (973 Program), and the Project-sponsored by SRF for ROCS, SEM.

References

[1] H. W. Brandhorst Jr. and J. A. Rodiek, "Space solar array reliability: a study and recommendations," *Acta Astronautica*, vol. 63, no. 11-12, pp. 1233–1238, 2008.

[2] K. Shen, "An empirical approach to obtaining bounds on the failure probability through stress/strength interference," *Reliability Engineering and System Safety*, vol. 36, no. 1, pp. 79–84, 1992.

[3] J.-F. Castet and J. H. Saleh, "Beyond reliability, multi-state failure analysis of satellite subsystems: a statistical approach," *Reliability Engineering and System Safety*, vol. 95, no. 4, pp. 311–322, 2010.

[4] J. U. Cho, L. Xie, C. Cho, and S.-K. Lee, "Crack propagation of CCT foam specimen under low strain rate fatigue," *International Journal of Fatigue*, vol. 35, no. 1, pp. 23–30, 2012.

[5] Y. Li and Q. Xu, "Stiffness analysis for a 3-PUU parallel kinematic machine," *Mechanism and Machine Theory*, vol. 43, no. 2, pp. 186–200, 2008.

[6] C. Q. Li, "Probability of plastic collapse of a structural system under nonstationary load processes," *Computers and Structures*, vol. 52, no. 1, pp. 69–78, 1994.

[7] T. R. Moss and J. D. Andrews, "Reliability assessment of mechanical systems," *Journal of Process Mechanical Engineering*, vol. 210, no. 3, pp. 205–216, 1996.

[8] S. Yan and P. Guo, "Kinematic accuracy analysis of flexible mechanisms with uncertain link lengths and joint clearances," *Journal of Mechanical Engineering Science*, vol. 225, no. 8, pp. 1973–1983, 2011.

[9] Z. Feng, M. J. Zuo, R. Hao, F. Chu, and M. El Badaoui, "Gear damage assessment based on cyclic spectral analysis," *IEEE Transactions on Reliability*, vol. 60, no. 1, pp. 21–32, 2011.

[10] P. Martin, "A review of mechanical reliability," *Journal of Process Mechanical*, vol. 212, no. 4, pp. 281–287, 1998.

[11] C. M. Rocco and J. A. Moreno, "Fast Monte Carlo reliability evaluation using support vector machine," *Reliability Engineering and System Safety*, vol. 76, no. 3, pp. 237–243, 2002.

[12] P.-K. Wong, Q. Xu, C.-M. Vong, and H.-C. Wong, "Rate-dependent hysteresis modeling and control of a piezostage using online support vector machine and relevance vector machine," *IEEE Transactions on Industrial Electronics*, vol. 59, no. 4, pp. 1988–2001, 2012.

[13] Q. Xu and P.-K. Wong, "Hysteresis modeling and compensation of a piezostage using least squares support vector machines," *Mechatronics*, vol. 21, no. 7, pp. 1239–1251, 2011.

[14] H. Fu and Q. Xu, "Locating impact on structural plate using principal component analysis and support vector machines," *Mathematical Problems in Engineering*, vol. 2013, Article ID 352149, 8 pages, 2013.

[15] E. E. Lewis, "A load-capacity interference model for common-mode failures in 1-out-of-2: G systems," *IEEE Transactions on Reliability*, vol. 50, no. 1, pp. 47–51, 2001.

[16] F. Brissaud, C. Smidts, A. Barros, and C. Bérenguer, "Dynamic reliability of digital-based transmitters," *Reliability Engineering and System Safety*, vol. 96, no. 7, pp. 793–813, 2011.

[17] Y. Ding, A. Lisnianski, P. Wang, L. Goel, and L. P. Chiang, "Dynamic reliability assessment for bilateral contract electricity providers in restructured power systems," *Electric Power Systems Research*, vol. 79, no. 10, pp. 1424–1430, 2009.

[18] S. Distefano and A. Puliafito, "Reliability and availability analysis of dependent-dynamic systems with DRBDs," *Reliability Engineering and System Safety*, vol. 94, no. 9, pp. 1381–1393, 2009.

[19] Y. Liu and Y. Li, "Dynamic modeling and adaptive neural-fuzzy control for nonholonomic mobile manipulators moving on a slope," *International Journal of Control, Automation and Systems*, vol. 4, no. 2, pp. 197–203, 2006.

[20] Y. Li and Y. Liu, "Real-time tip-over prevention and path following control for redundant nonholonomic mobile modular manipulators via fuzzy and neural-fuzzy approaches," *Journal of Dynamic Systems, Measurement and Control*, vol. 128, no. 4, pp. 753–764, 2006.

[21] Y. Li and Y. Liu, "Robust adaptive neural fuzzy control for autonomous redundant non-holonomic mobile modular manipulators," *International Journal of Vehicle Autonomous Systems*, vol. 4, no. 2-4, pp. 268–284, 2006.

[22] L. A. Zadeh, "Fuzzy sets," *Information and Control*, vol. 8, no. 3, pp. 338–353, 1965.

[23] J. Ma, W. Gao, P. Wriggers, T. Wu, and S. Sahraee, "The analyses of dynamic response and reliability of fuzzy-random truss under stationary stochastic excitation," *Computational Mechanics*, vol. 45, no. 5, pp. 443–455, 2010.

[24] I. D. Roberts and A. E. Samue, "The use of imprecise component reliability distributions in reliability calculations," *IEEE Transactions on Reliability*, vol. 45, no. 1, pp. 141–144, 1996.

[25] J. Zhou, "Reliability assessment method for pressure piping containing circumferential defects based on fuzzy probability," *International Journal of Pressure Vessels and Piping*, vol. 82, no. 9, pp. 669–678, 2005.

[26] C. Kai-Yuan, W. Chuan-Yuan, and Z. Ming-Lian, "Fuzzy variables as a basis for a theory of fuzzy reliability in the possibility context," *Fuzzy Sets and Systems*, vol. 42, no. 2, pp. 145–172, 1991.

[27] Y. Liu and H.-Z. Huang, "Reliability assessment for fuzzy multi-state systems," *International Journal of Systems Science*, vol. 41, no. 4, pp. 365–379, 2010.

[28] B. Heshmaty and A. Kandel, "Fuzzy linear regression and its applications to forecasting in uncertain environment," *Fuzzy Sets and Systems*, vol. 15, no. 2, pp. 159–191, 1985.

[29] M. M. Gharpuray and H. Tanaka, "Fuzzy linear regression analysis of cellulose hydrolysis," *Chemical Engineering Communications*, vol. 41, no. 1-6, pp. 299–314, 1986.

[30] M. J. Pardo and D. de la Fuente, "Optimal selection of the service rate for a finite input source fuzzy queuing system," *Fuzzy Sets and Systems*, vol. 159, no. 3, pp. 325–342, 2008.

[31] L. Bing, Z. Meilin, and X. Kai, "Practical engineering method for fuzzy reliability analysis of mechanical structures," *Reliability Engineering and System Safety*, vol. 67, no. 3, pp. 311–315, 2000.

[32] Q. Jiang and C.-H. Chen, "A numerical algorithm of fuzzy reliability," *Reliability Engineering and System Safety*, vol. 80, no. 3, pp. 299–307, 2003.

[33] E. T. Jaynes, *Probability Theory: The Logic of Science*, Cambridge University Press, New York, NY, USA, 2003.

[34] J. R. Schaff and B. D. Davidson, "Life prediction methodology for composite structures. Part I: constant amplitude and two-stress level fatigue," *Journal of Composite Materials*, vol. 31, no. 2, pp. 128–157, 1997.

[35] V. Dattoma, S. Giancane, R. Nobile, and F. W. Panella, "Fatigue life prediction under variable loading based on a new non-linear continuum damage mechanics model," *International Journal of Fatigue*, vol. 28, no. 2, pp. 89–95, 2006.

[36] L. Xie, J. Zhou, and C. Hao, "System-level load-strength interference based reliability modeling of k-out-of-n system," *Reliability Engineering and System Safety*, vol. 84, no. 3, pp. 311–317, 2004.

[37] Z. Y. Qin, S. Z. Yan, and F. L. Chu, "Dynamic analysis of clamp band joint system subjected to axial vibration," *Journal of Sound and Vibration*, vol. 329, no. 21, pp. 4486–4500, 2010.

[38] G. M. Henson and B. A. Hornishy, "An evaluation of common analysis methods for bolted joints in launch vehicles," in *Proceedings of the 51st AIAA/ASME/ASCE/AHS/ASC Structures, Structural Dynamics, and Materials Conference*, pp. 1–27, Orlando, Fla, USA, 2010.

Hindawi Publishing Corporation
Advances in Mechanical Engineering
Volume 2013, Article ID 536820, 10 pages
http://dx.doi.org/10.1155/2013/536820

Research Article

Customer Preference-Based Information Retrieval to Build Module Concepts

Dongxing Cao,[1] Mandun Zhang,[2] and Zhanjun Li[3]

[1] *School of Mechanical Engineering, Hebei University of Technology, Tianjin 300130, China*
[2] *School of Computer Science and Engineering, Hebei University of Technology, Tianjin 300130, China*
[3] *EaglePicher Medical Power, Plano, TX 75025, USA*

Correspondence should be addressed to Dongxing Cao; dongxingcao@gmail.com

Received 11 April 2013; Accepted 3 July 2013

Academic Editor: Yu-Shen Liu

Preference is viewed as an outer feeling of a product, also as a reflection of human's inner thought. It dominates the designers' decisions and affects our purchase intention. In the paper, a model of preference elicitation from customers is proposed to build module concepts. Firstly, the attributes of customer preference are classified in a hierarchy and make the surveys to build customer preference concepts. Secondly, the documents or catalogs of design requirements, perhaps containing some textual description and geometric data, are normalized by using semantic expressions. Some semantic rules are developed to describe low-level features of customer preference to construct a knowledge base of customer preference. Thirdly, designers' needs are used to map customer preference for generating module concepts. Finally, an empirical study of the stapler is surveyed to illustrate the validity of module concept generation.

1. Introduction

Why do the customers prefer to buy a kind of products and not others? Is that their brands, shapes, or reliabilities? How to reduce the risk of product development from evaluating the choices customers make? Of course, if customers could exactly indicate their preference, product development would be fairly risk-free [1, 2]. However, the fact is the opposite, and the uncertainty still appears at the earlier design stage of product development. The difference maybe appears in between designers and customers as the developed product is not what the customer wants [3, 4]. Therefore, in order to reduce risks and fasten the lead time to market, product development should take into consideration rapid responses in customers' voices [5]. In general, design can be viewed as an iterative process, in which customer preference dominates the final result of the conceptual design of a product [6].

At the early stage of product concept generation, customer preference has a direct impact on the number of iterative design, scheme evaluation, and cost. It also will affect the final design decision. Even when reliable customer information is elicited, it is still a great challenge to efficiently implement conceptual design [7]. Customer satisfaction degree can be also described by a conventional fuzzy set, in which fuzzy rules are employed to model the knowledge to evaluate design candidates [8]. Fuzzy reasoning is carried out to obtain the importance of customer needs and design metrics. In the preliminary design stage, the specification of design is usually incomplete. The compromise between designers and customers can be obtained by their negotiations to make a concession with each other.

In this paper, we propose a customer preference model for new product development by automatically mining the text information of customer preference online product reviews [9]. For fast developing products, customer's perceptions and product module concepts are constantly changing depending on customer preference. An automatic analysis approach is fast and simple, and it can remain abreast of changes in the market. In this research, firstly, we review the related literatures at the customer preference. Secondly, we present

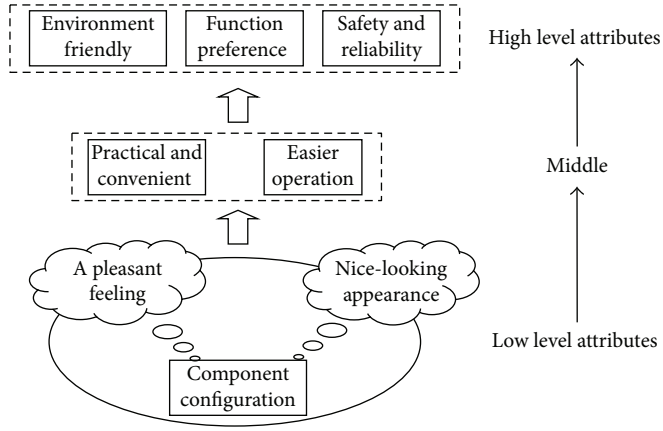

Figure 1: The preference attributes from low to high level.

the proposed approach, and the attributes of customer preference are classified in a hierarchy. Next, the process of ontology preference modeling is described to realize preference semantic extraction. Then, an empirical study is applied to generate module concepts.

2. Related Work

There are several methods for surveying customers' preference. They mainly include conjoint analysis, contingent valuation, direct value surveying, house of quality, and utility analysis [5, 10], in which conjoint analysis requires the survey subject to jointly consider several product attributes. These hypothetical product attributes are defined as a designed experiment, intended to obtain the most accurate information from the least amount of input. Contingent valuation involves directly asking survey respondents about their willingness to pay for a particular product feature. Direct value survey is utilized in value engineering and is a method that integrates features of conjoint analysis, contingent valuation, utility analysis, and prospect theory. House of Quality (HOQ) is a well-known method for eliciting, organizing, and communicating the "voice of the customer" to the design process [5]. A matrix structure is employed. On the vertical axis, the voice of the customer is expressed in a list of customer's desires. These might be entries such as "low cost," "light weight," or "environmentally friendly." The horizontal axis contains design variables that the engineer can directly control to satisfy the stated customer desires. Entries within the matrix and in the "roof" indicate interrelationships between each entry. Utility analysis is an axiomatically based approach to decision making, and it is particularly useful for dealing with decision making under uncertainty. Hauge and Stauffer [11] developed the taxonomy of customer requirements as an initial concept graph structure for questionnaires used for an expert system. The approach was aimed at further elicitation of knowledge from customers.

Since our objective mainly focuses on obtaining module concepts and performing the function of a product, it is also imperative to capture the customer voices. In this work, we discuss how to generate preference knowledge base by processing online product reviews and adaptive text extraction. The objective makes efforts to bridge the gap between low level attributes and high level attributes as shown in Figure 1 [3].

In this research, we carry out the survey by articulating two distinct problems: needs and attribute specifications. First, we differentiate between product attributes and user needs by proposing a method that explicitly addresses needs identification. Second, concept generation requires more than attribute classifications. A single product attribute is specified by using multiple properties and levels. However, our approach is used to cluster and manage categorical data. In the context of words and phrases in reviews, we might treat every word as a node in the graph. Edges would represent the relationship between words. Edges are weighted based upon the number of reviews in which the two words appear together [12].

3. The Proposed Approach

Most of the existing information is disorderly arranged and unsystematic. It needs product designers' analysis and extraction in order to provide useful information [13]. At the beginning of design, the original content of preference from customers, such as from survey reports, transaction data, and customer dialogs, should be filtered. A normal design information text or document is used to extract preference information after transformation [14]. Automatically extracting semantics from the normalized document requires recognizing the syntactic structure as well as the semantic meaning of the text. Linguistic knowledge and domain knowledge are needed to fulfill preference semantic extraction.

Figure 2 gives the infrastructure of a prototype for design preference information extraction. First of all, the original material documents from customers, such as user requirements, survey reports, and transaction data, and are acquired and then transformed into design information texts or documents in which some unstructured information should adopt an effective approach. Second, some terms and concepts can be extracted from preference semantic structures, such as

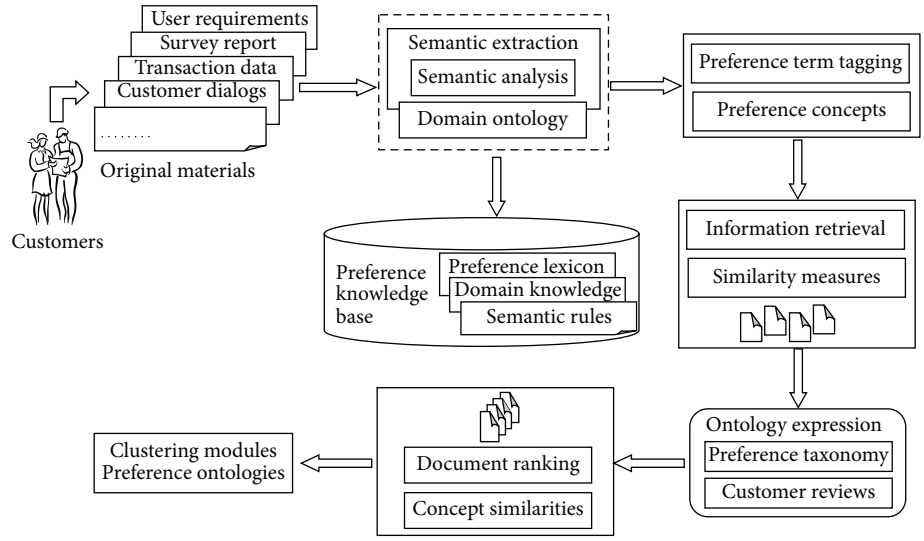

Figure 2: Infrastructure of customer preference ontology.

noun phrases, verb phrases, adverb phrases, and adjective phrases. These can be represented by using an ontology-based design semantic analysis and information extraction. The taxonomy of preference is classified to acquire the relationships between two concepts further. The specific thesauri or lexicons are built to capture preference concepts from the knowledge base of preference. The ontology expression and preference semantics of extraction process are described, and they are based on a shallow NLP algorithm and the domain ontology. Next, the preference ontology concepts are acquired after the extraction process. The extraction algorithm and the preference metrics are described and are used for preference ontology modeling. Finally, an empirical study for design preference extraction is introduced to build module concepts.

4. Customer Preference Analysis

4.1. Attribute of the Preference. The enterprises aim to set up a great reputation for their product on customers' minds. They often inquire about customers in order to find out the needs that are not met by existing products and assess demand degrees for a new product where no product currently exists. Then, they define the product in terms of attributes of preference and develop the product to settle for the market demands. After finishing the analysis of the need preference, product designers can work towards concept generation in order to customize product configurations. However, the preference cannot be viewed as equivalent to demand. Their categories are different. Preference has subjectivity and is related to the behavior of customer's feelings, whereas demand is more objective and mainly depends on other factors, such as availability, familiarity, word of mouth, advertising, and store or shelf location.

Thus, customer preference (CP) includes instinct factors (IF), aesthetic sensibilities (AS), emotional factors (EF), faiths (Fa), appreciation abilities (AA), and time span (TS). There, the instinct factors stand for product characteristics which include functions, performances, reliabilities, cost, and lifecycle. Aesthetic sensibilities include shape, color, operation, decoration, and feel. Faiths include religion, ethnologic culture, and race prejudice. Emotional factors affect the intention of purchase, decide the customers' mood, and include good temper, bad temper, indifferent, inpatient mood, and irritable mood. Appreciation abilities mean the customers' cognition and their contents include knowledge background, educational degree, and habitat. Time span means how many years it lasts, and it is short time or long time. Attribute of the preference is shown in Figure 3.

Customer preference is of certain relativity and is not absolute [14]. It is changeable relative to time span, scene, and attribute. The time span, which depends on the category of the product, is uncertain. Sometimes it is long, sometimes short. The scene, which depends on customer behavior, is associated with different cultures and geographies [7]. In addition, customer preference may change, when the value of some attributes is changed, such as function, shape, and cost.

Therefore, customer preference can be formally represented as follows:

$$\mathrm{CP} = (\mathrm{IF}, \mathrm{AS}, \mathrm{EF}, \mathrm{Fa}, \mathrm{AA}, \mathrm{TS}), \quad (1)$$

where IF = (function, performance, reliabilities, cost, and lifecycle), AS = (shape, color, operation, decoration, and feel), EF = (good temper, bad temper, indifference, inpatient mood, and irritable mood), Fa = (religion, ethnologic culture, and race prejudice), AA = (knowledge background, educational degree, and habitat), and TS = (year, short time, and long time).

4.2. Survey of the Preference. A best-selling product is definitely based on a favorable customer preference. First, the main factors from customer perspectives should be identified and the domain knowledge of the product should be collected in a professional survey before the product is launched. Second, a survey activity is conducted to determine the

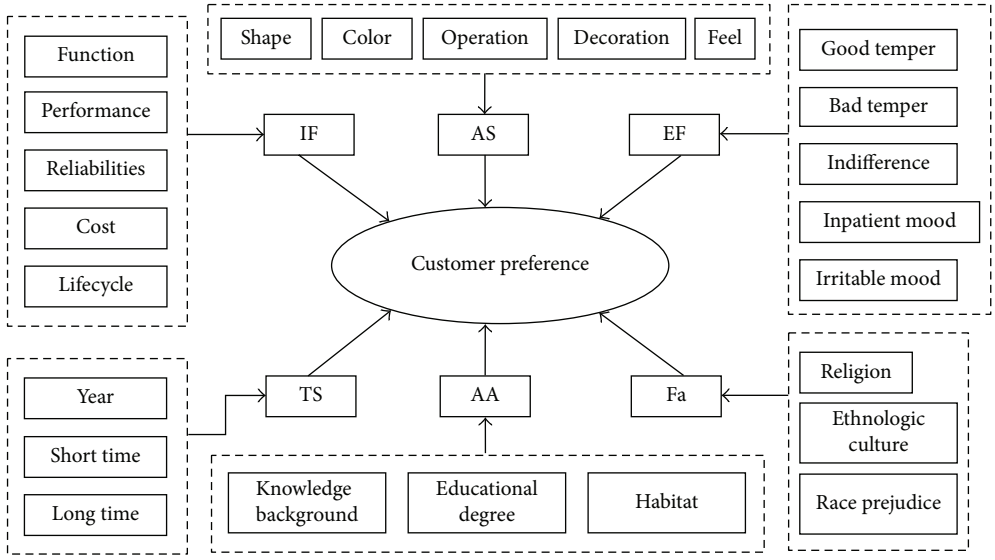

Figure 3: Attribute of the preference.

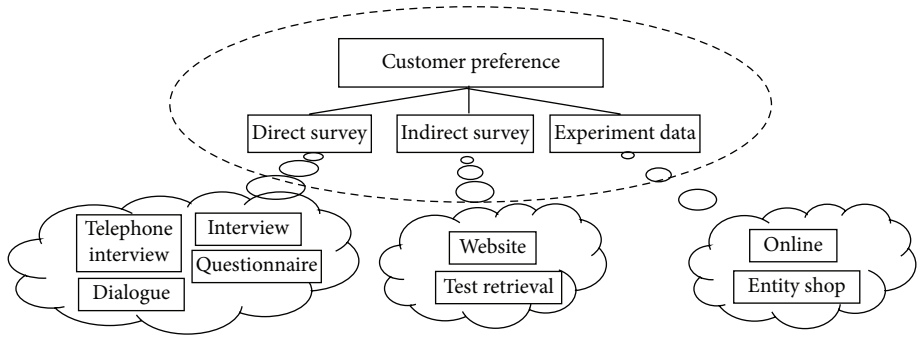

Figure 4: Survey of the preference.

customers' needs and desires before putting the new product on the market. This survey can be analyzed by using a software tool to determine the specific customer preference. Based on this consideration, a measure about the acceptance of potential customers can be taken and market simulations can become feasible. Therefore, customer preference can support demand analysis, conceptual design, and embodiment design, and at the same time, they are related to direct and indirect surveys and experiment results, as shown in Figure 4.

Enterprises routinely ask their customer preference questions, that is, direct survey, and in this way, they can provide better service to their customers or improve customers' satisfaction degree of products [8]. Surveys are sometimes described as informal conversations between product designers and customers. A number of measures can be taken to conduct the survey [15]. A very common method is to ask customers questions about their preference for particular product function, feature, shape, cost, or even service quality. A scale is commonly used in survey questions to elicit preference or evaluations. The value of the labels perhaps has a prejudice against the selected results which depend on customers' personal desires.

Indirect survey is another traditional approach to generate different concepts of a design and to conduct experiments with customers to capture preference [5]. By using a software tool as the customer service platform, it is much easier to run experiments on website. And most of them always ran such experiments and showed a raise in the browsing rate through clicking and determining whether a new design increased sales in a few days. If a product is advertised online, we will discover in a few hours whether experiment results or ad click rates increase, and the transaction data reveals copurchasing patterns for customer services. Some popular websites certainly have a high ad click rate. When customers go shopping, the transaction data can reveal their preference for a particular product and enable results targeted to specific buyer groups or buyer categories. How easy it is to identify customer preference depends on the context online and on the customer's willingness to buy a product. However, these text descriptions are disorganized but do have a great deal of information. It is necessary to extract customer preference by employing some effective methods, such as AHP [16], statistic method [17], and decision algorithm [18]. Therefore, customer preference has the multidimensional

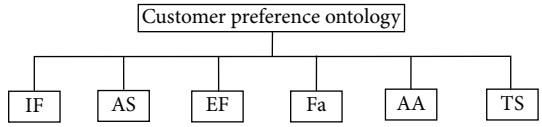

Figure 5: Taxonomy of preference ontologies.

Table 1: Classification of the relationships.

Relationship	Concept	Definitions of the relationship	Examples
is_a	IF-STAPLER/IF-BINDING SHEET	Relationships between parent and son or special and general	Is_a (IF-STAPLER, IF-BINDING SHEET)
is_part	Fa-HEALTH-RISK/Fa-CYCLE	Relationships between part and whole	Has_part (Fa-HEALTH-RISK, Fa-CYCLE)
has_function	IF-MAGAZINE/IF-HOLD STAPLES	Refer to the connection between two concepts	Has_function (IF-MAGAZINE, IF-HOLD STAPLES)
use_material	IF-LOW-END-STAPLER/IF-METAL	The type of materials	Use_material (IF-LOW-END-STAPLER, IF-METAL)
has_property	AS-SQUARE MAGAZINE/IF-METAL	Geometric attribute/physical attribute	Has_property (AS-SQUARE MAGAZINE, IF-METAL)
has_feature	AS-SIVER/AS-BOX LIKE-STAPLER	Geometric shape	Has_feature (AS-SIVER, AS-BOX LIKE-STAPLER)

properties, such as price, features, quality, performance, brand, distribution channel, safety, and usability.

5. Ontology Preference Modeling

5.1. Expression of Preference Ontology. Ontology is a formal, explicit specification of a shared conceptualization [19], where conceptualization refers to an intended model of the world's phenomena identified by its concepts and relation. Explicit means that the concepts and relations are explicitly defined, while formal means that it can be communicated across people and computer. Therefore, ontology defines a set of representational terms we call concepts. They should represent the hierarchical correlations among concepts [20]. On the other hand, the taxonomy is only reviewed as concept classification in the hierarchy. It simply links concepts by domain-independent relationships.

Ontology concepts have multiple parents and form the complex relations of inheritances. They share the genetic attributes. At present, considering ontology modeling for customer preference, there are two main problems: one is the extraction of the semantic concepts from the preference words, and the other is the document indexing from customers' requirements. As for the first problem, the key issue is to identify appropriate preference concepts and build preference lexicon based on design documents, at the same time, indexing the preference terms from customer documents, in which the precision problem of extraction is about the semantic expression employed in customer requests. A hierarchical analysis process has been used to aggregate preference in a group using a pair-wise approach [16]. However, a significant assumption is assumed to be equally important. That is, the information is handled equally without any preference given to one group member over another.

Ontology modeling provides an effective approach to indexing terms/concepts which can be used to match with customer requests. However, the taxonomy acquisition of customer preference of different products is of a certain subjective behavior. Their generation is either by brainstorming or by interviewing or dialoging with customers. Under similar circumstances, we can acquire preference ontologies [21]. Figure 5 presents the taxonomy of customer preference ontology, which comes from stapler handbooks or knowledge resources. For example, stapler handbooks often classify engineering components which can be clustered into an ontology model as concepts and taxonomy in the hierarchy. Each component is described in detail, including its attributes such as instinct, aesthetic, emotional, and religious, which can easily be identified and mapped to preference ontologies as well as corresponding relationships.

Customer preference ontology includes concepts, taxonomies, and relationships. Each taxonomical concept is acquired from various engineering knowledge resources. We can adopt terms or phrases to describe the concepts of the taxonomy as well as their relationships with other concepts. For example, magazine belongs to IF taxonomy of the stapler. We can represent this as IF-MAGAZINE, where the prefix of each concept represents the taxonomy which this concept belongs to. Therefore, the relationships are structured between concepts across taxonomies. For example, relationship "has_feature" has a concept "AS-SIVER/AS-BOX LIKE-STAPLER" as shown in Table 1, in which AS-SIVER stands for a color concept in the instinct taxonomy, AS-BOX LIKE-STAPLER represents a shape concept in the

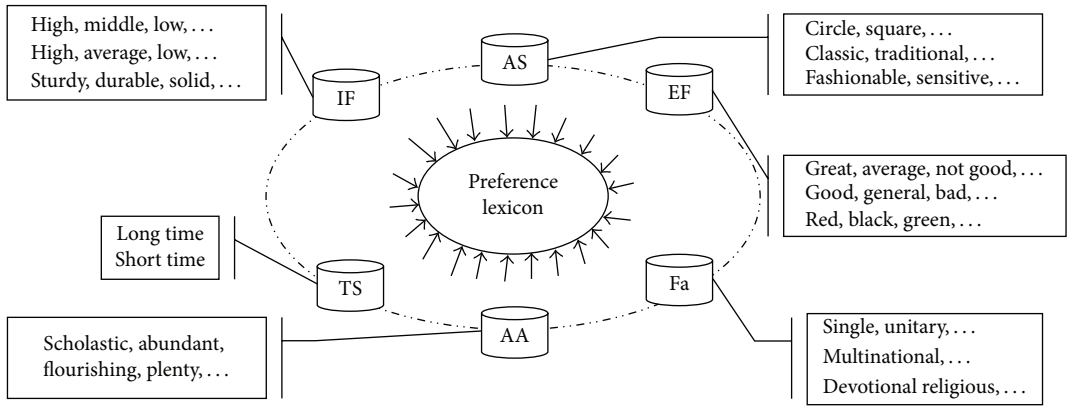

Figure 6: Lexicon of customer preference.

aesthetic taxonomy [14, 21]. Table 1 lists customer preference ontological concepts and their relational classification.

5.2. Knowledge Base of Preference Ontology. Generally speaking, lexical terms are words or phrases corresponding preference concepts in the documents. They are used to map the concepts of different texts. Therefore, word morphs, abbreviations, acronyms, and synonyms of the word/phrase are lexical terms and share the same concepts with the original lexical terms [12]. Also, some noun phrases, verb phrases, adverb phrases, and prepositional phrases can be extracted as preference terms. The morphs of original lexical terms can easily and automatically be obtained by WordNet (http://wordnet.princeton.edu/) [22], whereas other terms can be acquired manually because WordNet is a general lexical resource but not a professional preference lexicon. We aim to extract implicit customer preference based on the domain knowledge. As the existing case studies are almost special products, the extracted texts have a certain limitation. If a preference lexicon is built, it can be used for improving the preference evaluation possibilities. However, it is not easy to model and extract the semantic information of implicit customer preference from design texts which are embedded into natural language. In order to identify linguistic forms of customer preference, we build a preference lexicon to support automatic indexing. Logically speaking, such preference information is implicit within engineering design texts, but it could be difficult to extract from unstructured documents. In order to overcome this difficulty, we build the preference semantic model and its mapping into the ontology concepts. We identify linguistic forms of preference, produce a specific preference lexicon, develop customer preference ontology concepts, and generate design alternatives. A preference lexicon can show what the customers want. Figure 6 presents a common preference lexicon for the stapler, which looks like six planets round the preference lexicon. Each planet has its preference terms and can be decomposed further in the hierarchy. Here, the arrowheads describe the different preference terms which indicate stapler functions, performance, shape, cost, color, and so on.

6. Preference Semantic Extraction

6.1. Expression of Preference Ontology. Semantic ambiguity often occurs in design making when customers do not know the exact expressions or the related concepts they want to pursue though they may have some contextual clues, such as the functional preference of the design and other interacting parts of the product. A preference lexicon is a better way to evaluate customer preference [13].

Semantic rules are used to link preference terms and concepts together to build the customer preference concepts to aid in searching for design information. In general, there are two types of semantic rules. One is from the combination of preference terms and concepts, in which each term includes a noun, verb, adj, adv, and pron, and each concept is composed of several words. For example, the combination of "RED" and "AS-PUPPY DOG-STAPLER" forms a new preference concept "AS-RED-PUPPY DOG-STAPLER." The other is the combination of two concepts. For example, "IF-ANVIL" and "IF-BASE" constitute a new concept "IF-ANVIL-BASE." The concept from semantic synthesis is called Instance Concept (IC) which has a certain entity meaning. Generally speaking, some instance concepts exist in specific relationships, such as is_a, has_function, has_part, and has_material. These relationships are on the basis of forming concept ontology relationships [21, 23].

We use instance concept to construct design semantics through a set of slots and relations [21]. For example, each concept instance has several slots which describe its functions, properties, materials, and relationships. In the process of system work, the documents are scanned to search for instance concept and its specific value. Each concept corresponds to a relative slot value. For example, design object of the stapler has a specific slot "has_part" which corresponds to the instance concept, "HAMMER." It will be scanned and tagged in the process of indexing sentences. Meanwhile, the concept "HAMMER" has a function slot "STRIKING MOTION" and its upper cover exists in a material slot "has_material"; that is, "UPPER COVER" is made of material "PLASTIC." In the same way, we can find the stapler function slot "has_function," and it has

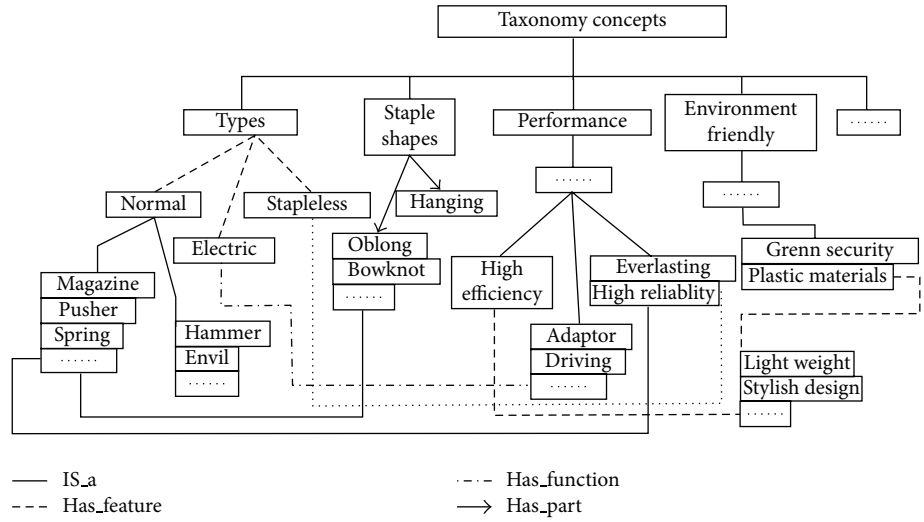

Figure 7: Concept forest derived from multiterm relationships of the stapler.

a function "MAGAZINE" and three properties: "STORING STAPLES, ORIENTATION, and REORIENTATION." Customer preference ontologies exist in the concept forest which is interlinked by means of conceptual and lexical relations as shown in Figure 7. For example, given words "HAMMER," "STAPLES," and "ENVIL," we can construct a concept tree for terms "HAMMER," "STAPLES," and "ENVIL" using "is_a" or "has_part" relationship links based on the hypernymy relationships.

6.2. Preference Concept Extraction and Module Generation. As customers often present their requirements by using natural language; some words, terms, and concepts can be used to represent customer preference. Sometimes different word or term usage can show a big difference in the preference degree [24]. At first, we need to extract some words from documents and dictionaries. These words can be classified as different taxonomies based on semantic description. An analyzer is built to separate these words into different taxonomies. Some independent words will be scaled based on linguist viewpoints. On the other hand, semantic rules are built to compose the concepts, in which rule base is crucial to build concepts. Also according to the viewpoints of linguist, some concepts should be advisably scaled. The scaled words and concepts will be put into preference knowledge base. In addition, we need to classify concept into taxonomies, such as function preference, performance preference, and cost preference.

We can extract different preference concepts from a document based on different semantic structures. It is an effective method to use concept forests to represent the semantic content of a text document; the semantic similarity of two text documents can be determined by comparing their concept forests. Formally, a concept forest (CF) is defined as a graph as follows [25]:

$$\mathrm{CF} = (S, E, R), \tag{2}$$

where S indicates a set of stemmed words, that is, $s_1, s_2, \ldots, s_n$, and E stands for a set of edges, that is, $e_1, e_2, \ldots, e_n$, which connect stemmed words with relationships defined in R, that is, $r_1, r_2, \ldots, r_n$.

Specifically, an edge e is defined as a triplet in the following:

$$e = \left(s_{i1}, s_{i2}, r_j\right), \quad \text{where } s_{i1}, s_{i2} \in S,\ r_j \in R. \tag{3}$$

Assuming the two documents d_1 and d_2, and their concept forests CF1 $= (S_1, E_1, R_1)$ and CF2 $= (S_2, E_2, R_2)$, respectively, calculating the semantic similarity of two documents needs to consider the similarities of the term, edge, and relationship sets in their concept forests; therefore, we calculate the semantic similarity of two text documents by simply comparing the similarity of the terms (S_1 and S_2) in their concept forests, as follows:

$$\mathrm{Sim}\left(d_1, d_2\right) = \frac{\left|S_1 \cap S_2\right|}{\left|S_1 \cup S_2\right|}. \tag{4}$$

Therefore, we can realize document ranking on the basis of the previous semantic similarity. Assuming that module sets $M\{t_i(i = 1, 2, \ldots, n) \mid t_i \subseteq S\}$, in which t_i stands for term concepts, and according to the degree of similarity measures, n term concepts T are clustered into a cluster (C_i) while we will divide module sets into k clusters in the following:

$$C_i = \sum_{i=1}^{k} \omega_i T_i \quad (i = 1, 2, \ldots, k), \tag{5}$$

where ω_i means weight factor of different term concepts. And C_i satisfies the following relationships:

$$C_i \subseteq M \quad C_i \cap C_j = \varnothing \quad (i, j = 1, 2, \ldots, k). \tag{6}$$

Therefore, we obtain the number of modules (m) as follows:

$$M = \sum_{i=1}^{m} \sum_{j=1}^{k} C_{ij}. \tag{7}$$

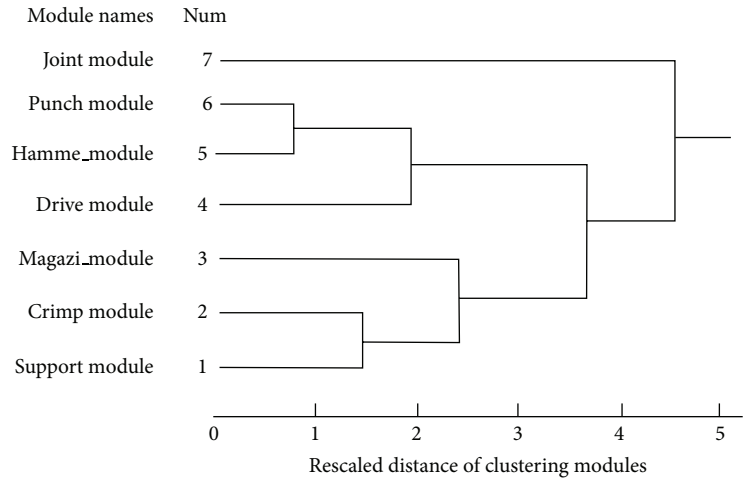

Figure 8: Clustering chart of module concepts.

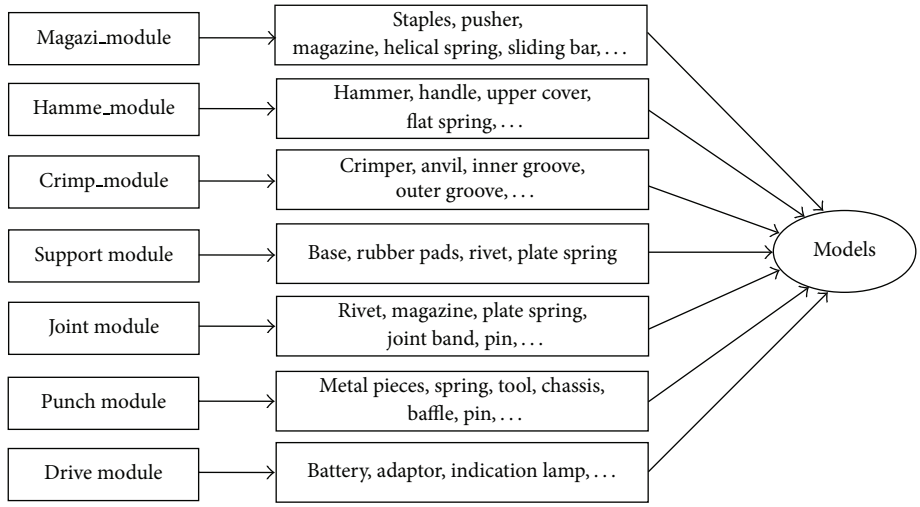

Figure 9: Different modules corresponding to component concepts.

7. Empirical Study

A case study on stapler is used to illustrate the proposed method. We collect 200 documents, totally about 1M memories, in which 100 documents come from stapler specification descriptions, and the other 100 documents for customers' reviews from several familiar websites (http://www.amazon.co.uk/, http://www.ebay.com/, etc.). They delegate most users' requirements for staplers. We only select text documents excluding pictures, charts, and graphs from websites as they are out of the range. Nine brands are selected from several companies, such as Office Depot, Leitz, Rapid, Stanley, and Swingline.

The objective of module concept generation involves identifying customer requirements and then mapping them into a set of stapler attributes or specifications. Considering this case review, the designer would like to generate concept modules of a new stapler by means of clustering algorithms. A formal or normal document is needed to use for text information extraction. We first extract all keywords and their occurrence frequencies from the document, excluding stop words such as pronouns, common verbs, common nouns, adjectives, and frilly words. These words are of little or no value in determining the document's semantic content. Some classifications are annotated as part-of-speech (POS) tagging by indexing preference lexicon [26]. On the basis of domain ontology base, the terms/phrases are recognized to build concept forests. By indexing semantic rule base, jointing relationships are established to classify out different preferences (see Section 5.1). Then, module concepts are clustered by an effective algorithm based on (4) and (5). Figure 8 presents clustering chart of stapler module concepts. Different kinds of components will be clustered into the specific functions of stapler. Figure 9 presents module concepts and their components which form different types of models. They are obtained by extracting 100 documents from stapler specification descriptions.

Any preference concepts can be viewed as a part of stapler or one of components within module. Preference terms are indexed and tagged. Similarity measures are used

Table 2: Types, brands, models, and descriptions.

Types	Model pictures	Brands	Concept descriptions
Normal stapler		Office Depot	Antijam mechanism provides worry-free stapling, and O/D version worked well.
		Leitz	Stapler is with ergonomic touch, easy to press down, well designed, strong, and beautiful piece of office equipment.
		OXO	Locks close for storage and transport; it is perfect for everything and does not fall apart like the tiny tot stapler.
Staple-less stapler		Amazing	The way it fastens paper is novel and it attaches several pieces of paper together, but not strong enough.
		Ecozone	Environmentally friendly, it is small and fits into your pocket, bag, or just looks nice on a desk with its stylish design.
		Kokuyo	Ergonomically designed for fastening paper without using staples; it has a cooler-looking design.
Electric stapler		Rapid	Runs on batteries or adaptors; good product which copes very well with the demands of a busy office.
		Stanley	It has a high volume of stapling work and drive technology that delivers up to 3x faster stapling speeds.
		Swingline	Insert paper for automatic stapling or press the comfortable grip and let the stapler do the work.

to select preference ontology concepts. After text document extraction, we select nine models which have commercial value staplers as shown in Table 2. They are obtained by indexing 100 documents from customers' reviews. These results will provide model references to office enterprises for new product development further. Furthermore, enterprises will increase customer preference degree by improving the performance of their existing staplers. At the same time, different sex and age people can still select more suitable staplers for themselves.

8. Conclusion

In the paper, the customer preference ontology is described and preference design information is extracted to build a preference knowledge base which includes a preference lexicon, domain ontology, and semantic rules. An ontology-based model is given for information retrieval. The concept generation and selection of information are based on customer preference ontology. We have used the preference domain knowledge of the stapler for describing the proposed approach, while the results can be applied to other similar products. However, further research is needed as follows.

(i) The large amount of informal design information is steadily increasing on website. These texts are less likely to comply with the formal documental format. It is difficult to extract the ontology concept semantics from these documents. It is worth investigating further in the future.

(ii) Information extraction of customer preference is currently based on indexing the sentence semantic rules, in which the preference lexicon and domain knowledge are crucial to achieve information retrieval. However, how to avoid semantic blur and improve the indexing precision? Further work is needed.

(iii) At a particular time, customers show a strong liking for certain staplers. But later, they show a change for another stapler. Therefore, how to update dynamically the changes with a fast and simple response to customer preference in the market is needed.

Acknowledgments

This research is partially sponsored by the National Natural Science Foundation of China (NSFC) under Grant nos. 50775065 and 51275152 and Nature Science Foundation of Hebei Province under Grant nos. E2008000102 and E2013202123.

References

[1] E. F. MacDonald, R. Gonzalez, and P. Y. Papalambros, "Preference inconsistency in multidisciplinary design decision making," *Journal of Mechanical Design*, vol. 131, no. 3, pp. 0310091–03100913, 2009.

[2] K. N. Otto and E. K. Antonsson, "Trade-off strategies in engineering design," *Research in Engineering Design*, vol. 3, no. 2, pp. 87–103, 1991.

[3] R. Zhao and W. I. Grosky, "Narrowing the semantic gap: improved text-based web document retrieval using visual features," *IEEE Transactions on Multimedia*, vol. 4, no. 2, pp. 189–200, 2002.

[4] M. Kulok and K. Lewis, "Preference consistency in multiattribute decision making," in *Proceedings of the ASME International Design Engineering Technical Conferences and Computers and Information in Engineering Conference (DETC '05)*, pp. 291–300, Long Beach, Calif, USA, September 2005.

[5] A. Griffin and J. R. Hauser, "The voice of the customer," *Marketing Science*, vol. 12, no. 1, pp. 1–27, 1993.

[6] D. X. Cao, Y. H. Han, J. Yang, G. Yang, and C. X. Cui, "Integrated modeling towards collaborative product development," *Advanced Materials Research*, vol. 44-46, pp. 669–676, 2008.

[7] C.-H. Chen, L. P. Khoo, and W. Yan, "Evaluation of multicultural factors from elicited customer requirements for new product development," *Research in Engineering Design*, vol. 14, no. 3, pp. 119–130, 2003.

[8] R. N. Bolton, "A dynamic model of the duration of the customer's relationship with a continuous service provider: the role of satisfaction," *Marketing Science*, vol. 17, no. 1, pp. 45–65, 1998.

[9] R. Decker and M. Trusov, "Estimating aggregate consumer preferences from online product reviews," *International Journal of Research in Marketing*, vol. 27, no. 4, pp. 293–307, 2010.

[10] P. E. Green and V. Srinivasan, "Conjoint analysis in marketing: new developments with implications for research and practice," *Journal of Marketing*, vol. 4, pp. 3–19, 1990.

[11] P. L. Hauge and L. A. Stauffer, "ELK: a method for eliciting knowledge from customers," in *Proceedings of the ASME Design and Methodology*, pp. 73–81, September 1993.

[12] S. Deerwester, S. T. Dumais, G. W. Furnas, T. K. Landauer, and R. Harshman, "Indexing by latent semantic analysis," *Journal of the American Society for Information Science*, vol. 41, no. 6, pp. 391–407, 1990.

[13] M. C. Yang and H. Ji, "A text-based analysis approach to representing the design selection process," in *Proceedings of the International Conference on Engineering Design (ICED '07)*, pp. 28–31, Cite Des, Paris, France, August.

[14] D. Cao, Z. Li, and K. Ramani, "Ontology-based customer preference modeling for concept generation," *Advanced Engineering Informatics*, vol. 25, no. 2, pp. 162–176, 2011.

[15] R. Mugge, P. C. M. Govers, and J. P. L. Schoormans, "The development and testing of a product personality scale," *Design Studies*, vol. 30, no. 3, pp. 287–302, 2009.

[16] A. Chwolka and M. G. Raith, "Group preference aggregation with the AHP: implications for multiple-issue agendas," *European Journal of Operational Research*, vol. 132, no. 1, pp. 176–186, 2001.

[17] P. M. West, P. L. Brockett, and L. L. Golden, "A comparative analysis of neural networks and statistical methods for predicting consumer choice," *Marketing Science*, vol. 16, no. 4, pp. 370–391, 1997.

[18] T.-K. See and K. Lewis, "A decision support formulation for design teams: a study in preference aggregation and handling unequal group members," in *Proceedings of the ASME International Design Engineering Technical Conferences and Computers and Information in Engineering Conference (DETC '05)*, pp. 177–187, Long Beach, Calif, USA, September 2005.

[19] R. Studer, V. R. Benjamins, and D. Fensel, "Knowledge engineering: principles and methods," *Data and Knowledge Engineering*, vol. 25, no. 1-2, pp. 161–197, 1998.

[20] Y. Kitamura and R. Mizoguchi, "Ontology-based systematization of functional knowledge," *Journal of Engineering Design*, vol. 15, no. 4, pp. 327–351, 2004.

[21] Z. Li, M. C. Yang, and K. Ramani, "A methodology for engineering ontology acquisition and validation," *Artificial Intelligence for Engineering Design, Analysis and Manufacturing*, vol. 23, no. 1, pp. 37–51, 2009.

[22] M. Marcus, B. Santorini, and M. A. Marcinkiewicz, "Building a large annotated corpus of English: the penn treebank," *Computational Linguistics*, vol. 19, no. 2, pp. 313–330, 1994.

[23] G. A. Miller, "A lexical database for English," *Communications of the ACM*, vol. 38, no. 11, pp. 39–41, 1995.

[24] G. Salton, *Automatic Text Process*, Addison-Wesley, Wokingham, Mass, USA, 1998.

[25] J. Z. Wang and W. Taylor, "Concept forest: a new ontology-assisted text document similarity measurement method," in *Proceedings of the IEEE/WIC/ACM International Conference on Web Intelligence (WI '07)*, pp. 395–401, November 2007.

[26] C. McMahon, A. Lowe, S. Culley et al., "An integrated search and retrieval system for engineering documents," *Journal of Computing and Information Science in Engineering*, vol. 4, no. 4, pp. 329–338, 2004.

Hindawi Publishing Corporation
Advances in Mechanical Engineering
Volume 2013, Article ID 590957, 7 pages
http://dx.doi.org/10.1155/2013/590957

Research Article

Conceptual Design of Deployment Structure of Morphing Nose Cone

Junlan Li,[1,2] Jianing Wu,[1] and Shaoze Yan[1]

[1] *State Key Laboratory of Tribology, Department of Mechanical Engineering, Tsinghua University, Beijing 100084, China*
[2] *School of Mechanical Engineering, Tianjin University, Tianjin 300072, China*

Correspondence should be addressed to Shaoze Yan; yansz@tsinghua.edu.cn

Received 20 October 2012; Revised 2 February 2013; Accepted 15 March 2013

Academic Editor: Dongxing Cao

For a reusable space vehicle or a missile, the shape of the nose cone has a significant effect on the drag of the vehicle. In this paper, the concept of morphing nose cone is proposed to reduce the drag when the reentry vehicle flies back into the atmosphere. The conceptual design of the structure of morphing nose cone is conducted. Mechanical design and optimization approach are developed by employing genetic algorithm to find the optimal geometric parameters of the morphing structure. An example is analyzed by using the proposed method. The results show that optimal solution supplies the minimum position error. The concept of morphing nose cone will provide a novel way for the drag reduction of reentry vehicle. The proposed method could be practically used for the design and optimization of the deployable structure of morphing nose cone.

1. Introduction

For a reusable space vehicle or a missile, the nose cone is ejected in the upper parts of the atmosphere. The shape of the nose cone has a significant effect on the drag of the vehicle [1]. Moreover, the temperature of the nose cone caused by aerodynamic heating is about 2000 to 3000 centigrade for reentry vehicles [2] and tactical missiles [3, 4]. Therefore, among a number of design requirements, the reduction of both drag and aerodynamic heating is the major challenge in the design of these supersonic and hypersonic vehicles [5]. So the shape optimization plays an important role in the design of nose cone.

Numerous studies on the design and optimization of the shape of nose cone have been carried out. Ledu and Pollak [6] gave an extensive series of flight tests of a blunt-nosed flare-stabilized re-entry nose cone and deduced drag and stability coefficients. Ericsson et al. [7, 8] discussed combined effects of nose bluntness and cone angle on dynamic stability of the nose cone and provided some useful suggestions on missile design. Deepak et al. [1] described a unique process of shape optimization for drag reduction for the nose cone of hypersonic flight experiments. Lin et al. [9] provided an investigation to determine the optimum nose shape and frustum configuration in an effort to improve reentry vehicle performance. The literature mentioned perviously provided valuable reference for the studies to reduce the drag and aerodynamic heating.

After that, there have been a variety of papers devoted to reducing both the drag and the aeroheating by modifying the flow field ahead of the vehicle's nose [5]. Of these techniques, using spikes is the simplest and the most reliable technique. Gauer and Paull [10] numerically investigated the drag and the heat-transfer reduction of a forward-facing spike with varying length and shape in comparison to the unspiked nose cone. Ahmed and Qin [11] compared the spike and aerodisk with the unspiked nose cone and researched a mechanism to explain the drag reduction and the cause of flow instability based on the shape of an effective body. Marley and Riggins [12] investigated methods for increasing the stability of forward mass injection and presented drag reduction technologies including annular (ring) and swirled injection both with and without upstream energy deposition.

Besides, much research on new techniques for drag reduction has been developed. The breathing blunt nose [13] is proposed to reduce the pressure drag of blunt-nosed body

by passive control at a supersonic Mach number. The side force of a slender body flight vehicle with chine nose at high angles of attack has been studied by Lim et al. [14], and the chine nose shape with chine edge on its both sides is considered for the method to reduce side force.

Although lots of efforts have been made in reducing the drag and the aerodynamic heating of the nose cone, there are still some limitations for re-entry vehicles, of which the drag and aerodynamic heating is varied with the flight phase.

Morphing technology on aircraft and spacecraft has found increased interest over the past 30 years because it is likely to enhance performance and efficiency over a wider range of flight conditions [15, 16]. NASA had started the Aircraft Morphing Program to develop and mature smart component technologies for advanced airframe systems that can be embedded in aircraft structures and provide cost effective system benefits [17]. During these years, a hot issue of morphing technology is morphing wing for which numerous studies have been carried out. Lampani et al. [15, 16] proposed a concept of smart thermal protection system for morphing leading edge. Inoyama et al. [18, 19] present a topology optimization methodology for determining multiple configuration for morphing wing structure. Courchesne et al. [20] studied the configurations of morphing wing by use of shape memory alloys actuators. However, the literature survey indicates that morphing nose cone has not been noticed and reported until now.

The term conceptual design is a type of work which gives precedence to hypothetical function. Many approaches are researched for realizing conceptual design. For example, Cao et al. [21, 22] presented a port-based ontology modeling method to support product conceptualization. Taking the conceptual design of aircraft as an example, the goal is to generate one or more aircraft concepts which will meet the design specifications. And the aircraft concept includes the aircraft configuration and its primary dimensions. Raymer [23] expatiated the entire process of aircraft conceptual design and Rentema [24] presented the issues that should be distinguished, such as the configuration layout, the lift curves, and drag polars, accompanied with some necessary demonstration quantitively ensuring the feasibility of accessories.

In this paper, the conceptual design of morphing nose cone is proposed. The morphing nose cone has deformable shape in different flight phases. It is blunt when the re-entry flies out of the atmosphere, whereas it deforms into a sharper cone to reduce the drag when it flies back into the atmosphere. Furthermore, the conceptual design and optimization method will be developed according to the morphing process and the design procedure of the morphing nose cone will be expatiated.

This paper is organized as follows. In Section 2, the shape representation of the nose cone is given. In Section 3, the conceptual design of morphing nose cone is presented. The optimization method based on genetic algorithm and the optimal result are proposed in Section 4. A numerical example is presented to explain how the optimization method works. Finally, the method for design and optimization of the morphing nose cone is summarized in the last section.

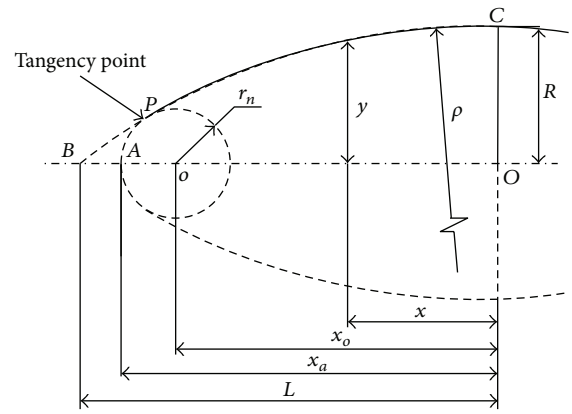

Figure 1: Shape of spherically blunted nose cone.

2. Shape Representation of the Nose Cone

The shape of nose cones can be described as conical, biconic, power series, ogival, elliptical, and Parabolic [9, 25]. The equations describing the various nose cone shapes are expatiated in [3]. In this paper, the ogival nose cone with spherically blunted forebody is considered because it is most commonly used on space vehicle.

The 2D shape of spherically blunted ogival nose cone is shown in Figure 1, where L is the overall length of the nose cone, R is the radius of the base of the nose cone, and y is the radius at any point x, as x varies from the principle tip of the nose cone (O) to the base (B). The principle tip is blunted by capping it with a segment of a sphere, whose radius is r_n. Thus, the real tip becomes A. The arc BC is a segment of a circle, of which the radius is ρ, such that the curve of the nose cone is tangent to the rocket body at its base at C and the spherical cap at P.

For the ogival nose cone, the coordinates of tangency point P are

$$\begin{aligned} x_p &= x_0 + \sqrt{r_n^2 - y_t^2} \\ y_p &= r_n \frac{(\rho - R)}{(\rho - r_n)}, \end{aligned} \tag{1}$$

where the radius ρ can be calculated by

$$\rho = \frac{R^2 + L^2}{2R}. \tag{2}$$

The center of the spherical cap is located at

$$x_0 = \sqrt{(\rho - r_n)^2 - (\rho - R)^2}. \tag{3}$$

Thus, the profile of the nose cone can be expressed as

$$y = \begin{cases} \sqrt{\rho^2 - x^2} + R - \rho & \left(0 < x < x_p\right), \\ \sqrt{r_n^2 - (x - x_0)^2} & \left(x_p < x < x_a\right). \end{cases} \tag{4}$$

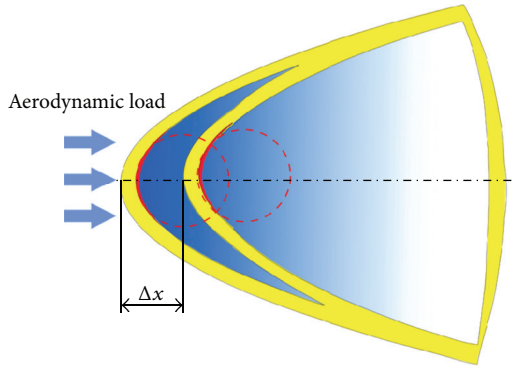

Figure 2: Morphing principle of nose cone.

3. Conceptual Design of Morphing Nose Cone

For the morphing nose cone, the spherical cap is nondeformable, whereas the curvature of the deformable ogive is varied with the changes of aerodynamic load. For a re-entry vehicle, the morphing principle of the nose cone is shown in Figure 2. To reduce the drag, the total length of the nose cone is increased by 20% or more ($\Delta x \geq 0.2L$) so that the cone angle gets smaller, whereas the curvature radius of the ogive is enlarged after morphing.

As far as it is concerned, the design of morphing nose cone is made via three main processes in general, the conceptual design, integrated design, and detailed design, as shown in Figure 3. In conceptual design, the most adaptive mechanism to complete the task of morphing is proposed to make sure it could be used without motion interference and satisfy the requirement of kinematic accuracy.

Considering the morphing principle of nose cone, the mechanism composed of several slider-crank units each of which has 2 links and a slider is selected as the inner deployable structure. Figure 4 represents the deformable mechanism of the morphing nose cone graphically, where the notations A_i, B_i, and C_i ($i = 1, 2 \ldots n$) represent the points on the mechanism which holds the blunt nose cone and A_i', B_i', and C_i' ($i = 1, 2 \ldots n$) belong to the sharp nose cone mechanism; C_i and C_i' ($i = 1, 2 \ldots n$) are directly connected to the key points on the original and final surface of the morphing nose cone, respectively; O is the origin of coordinates xoy; A_i and A_i' ($i = 1, 2 \ldots n$) are located in the x-axis. As the slider translates from A_{i+1} to A_{i+1}', the key points C_i move to C_i' so that the profile of the nose cone changes from the blunt one to the sharp one.

4. Optimal Design of the Structure Using Genetic Algorithm

4.1. Overall Process of Optimal Design. With respect to the morphing principle of morphing nose cone, the general structure can be preliminary designed. Considering the coordination of deformation mechanism, the movement of key points on the skin should be appropriate, which means that the units of the deployable mechanism should be distributed uniformly.

On the one hand, the solution of the first slider-crank elements can be calculated according to the theory of mechanism. But, if the same method is applied to calculate the other elements, the configuration of the whole mechanism may lead to an infeasible solution with unreasonable links and pressure angles. Therefore, optimization of the mechanism is needed. On the other hand, the optimal design of morphing nose cone is an optimization problem with a single objective and multiparameters which has complex relations between the input and output. The optimal solution can be rapidly obtained with good initial parameters. Consequently, the solution of the first slider-crank elements is used as initial parameters and the other elements are calculated through optimization.

Genetic algorithm (GA) is selected in this paper as the tool to get the optimal solution for the reasons listed as follows. Firstly, it should be noted that this is probably an optimization problem with a single objective and multiparameters which has complex relations between the input and output, so GA can be employed to get the optimal solution. Secondly, GA can rapidly locate good solutions, even for large search spaces. The same is of course also true for evolution strategies and evolutionary programming. The amount of calculation is related to the initial parameters. The optimal solution can be easily obtained by GA if adaptive initial parameters are precalculated. With respect to our problem, the range of some initial parameters, which will produce a global optimization solution very rapidly, can be determined by the engineering requirements and empirical information. Thirdly, solving the equations is the main topic of optimization which consumes large computing resources. Fortunately, GA will not join in the equation solving, so it saves a lot of time. Moreover, GA has more concise mathematical descriptions which can be easily applied in our research. Therefore, GA is applied in this paper to get the optimal solution.

To sum up, the overall process of optimization is conducted in two procedures: (1) calculation of the first slider-crank unit and (2) optimization of other units of the mechanism using GA.

4.2. Calculation of the First Slider-Crank Unit. As shown in Figure 4, considering the first unit $A_1B_1C_1A_2$, A_1 is the origin of the coordinate xoy, A_2 is on the slider which moves along the x axis, and C_1 and C_1' are key points on the original and final profiles.

For the original mechanism, the equations of the first slider-crank unit are

$$\begin{aligned} |A_1B_1| \cos\varphi_1 + |A_2B_1| \cos\varphi_2 &= x_{A2}, \\ |A_1B_1| \sin\varphi_1 + |A_2B_1| \sin\varphi_2 &= 0, \end{aligned} \tag{5}$$

where $\cos\varphi_1 = x_{C1}/\sqrt{x_{C1}^2 + y_{C1}^2}$, and $\sin\varphi_1 = y_{C1}/\sqrt{x_{C1}^2 + y_{C1}^2}$.

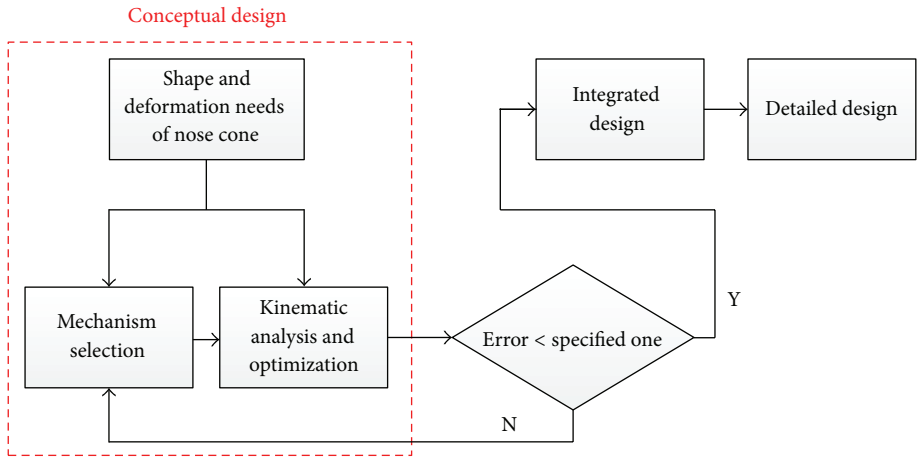

Figure 3: The whole process of morphing nose cone design.

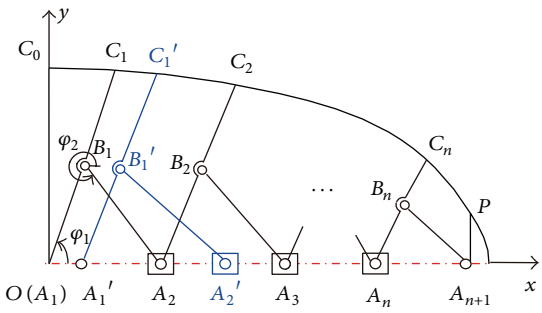

Figure 4: Mechanism of the morphing nose cone.

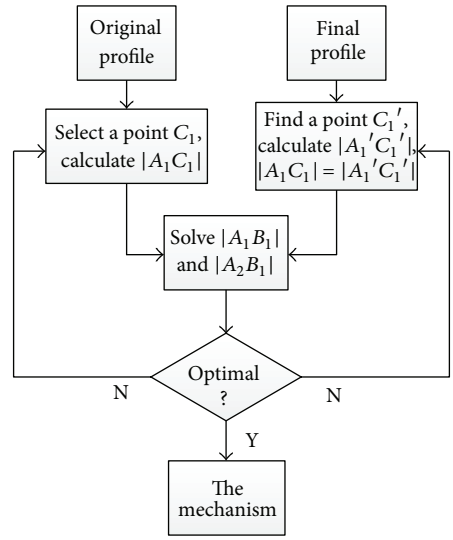

Figure 5: Flowchart of the calculation method.

For the morphed mechanism, the origin of the first slider-crank unit moves from A_1 to A_1'; thus the equations are

$$\begin{aligned} \left|A_1'B_1'\right| \cos\varphi_1' + \left|A_2'B_1'\right| \cos\varphi_2' &= x_{A2}' - x_{A1}', \\ \left|A_1'B_1'\right| \sin\varphi_1' + \left|A_2'B_1'\right| \sin\varphi_2' &= 0, \end{aligned} \tag{6}$$

where $\cos\varphi_1' = x_{C1}'/\sqrt{(x_{C1}')^2 + (y_{C1}')^2}$, and $\sin\varphi_1' = y_{C1}'/\sqrt{(x_{C1}')^2 + (y_{C1}')^2}$.

Because the points C_1 and C_1' belong to the profiles, the coordinates (x_{C1}, y_{C1}) and (x_{C1}', y_{C1}') can be selected according to the profiles. Combining the equations of original and final units, $|A_1B_1| = |A_1'B_1'|$, $|A_2B_1| = |A_2'B_1'|$, giving the position of A_1' and A_2, $|A_1B_1|$ and $|A_2B_1|$ can be solved (see Figure 5).

The calculation method for the first slider-crank unit of the morphing nose cone mechanism can be recapitulated in three steps as follows.

(1) Select a point $C_1(x_{C1}, y_{C1})$ on the original profile and compute $|A_1C_1|$. Find a point $C_1'(x_{C1}', y_{C1}')$ on the final profile which satisfies $|A_1C_1| = |A_1'C_1'|$.

(2) Given the position of A_1' and A_2, $|A_1B_1|$ and $|A_2B_1|$ are solved by (5) and (6). Calculate (x_{B1}, y_{B1}) and (x_{B1}', y_{B1}').

(3) Changing C_1 on the profile, several solutions can be obtained. The optimal solution is selected based on the constraint condition; namely, B_1 is near the middle of the link A_1C_1 to improve its stability.

4.3. Optimization of Other Units. After the first slider-crank unit is solved, the optimization of other units of the mechanism can be conducted using GA [26]. The flowchart of the optimization process by GA is illustrated in Figure 6. The input is the original and final curve functions of morphing nose cone, and the output is the best sample of morphing mechanism with minimum position error, corresponding to the optimal length of the links. The objective function minimizes the position error of the key points between the kinematic and final profile of configuration. The GA program firstly sets the total generation i_g and the population scale determines the iteration times and the scale of samples respectively. Then the samples are generated by the random

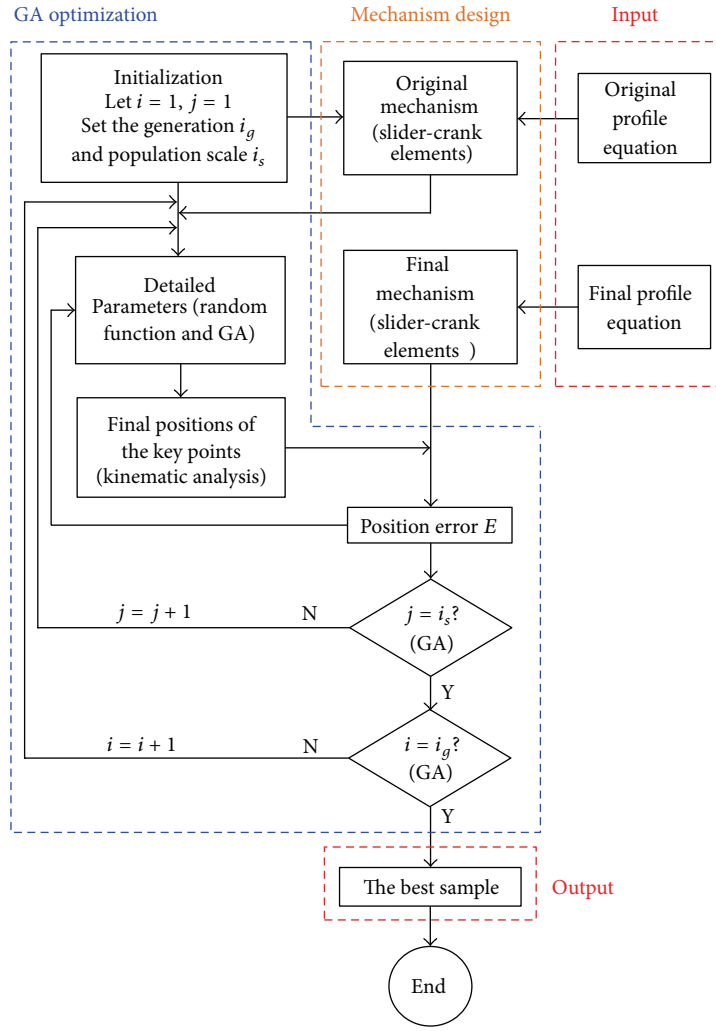

Figure 6: Flowchart of optimization design of the nose cone.

function via uniform distribution. The output position error can be calculated by solving the kinematic equations. After genetic selection, cross, and metamorphosis, one can get the best sample in one generation. Repeating the genetic selection, cross, and metamorphosis for i_g generations, the minimum position error can be obtained as the best sample shown at the bottom of Figure 6.

The output of GA program is the scales n_i $(i = 2, 3, \ldots n)$ of the mechanism units, where n is the number of the units. The proportional indexes S_i are defined as

$$S_i = \frac{n_i}{\sum_{j=2}^{n} n_j} \quad (i = 2, 3, \ldots n). \tag{7}$$

Suppose the elongation contributed by the mechanism is proportional to the indexes S_i. As a result, the length of all the links can be derived from the first slider-crank unit and S_i proportionally. Then the geometric analysis provides key points ($\widehat{C}_i$ and C_i') on the linkage A_nC_n and the final profile.

Therefore, the objective function of optimization can be expressed as

$$E(\mathbf{x}) = \min \sum_{i=1}^{n} \left(\left(\hat{x}_{ci} - x_{ci}' \right)^2 + \left(\hat{y}_{ci} - y_{ci}' \right)^2 \right)^{1/2}, \tag{8}$$

where $(\hat{x}_{ci}, \hat{y}_{ci})$ and (x_{ci}', y_{ci}') are the coordinates of key points $\widehat{C}_i$ and C_i'.

5. Numerical Example

A numerical example is studied to discuss the effect and feasibility of the optimization method. Refer to Figure 1; suppose that $L = 1$ m and $R = 0.25$ m before morphing, whereas the real length of the nose cone increases from x_a to $1.2x_a$. The curvature radius of the egive and the other key parameters are calculated by (1)–(3). The parameters of initial and morphing profiles are listed in Table 1.

Table 1: Parameters of initial and final profiles.

Parameters	Initial profile (m)	Final profile (m)
ρ	2.125	3.053
r_n	0.055	0.055
x_0	0.877	1.063
x_a	0.932	1.118
x_p	0.900	1.086
y_p	0.15	0.15

Table 2: Optimal solution by GA.

i	2	3	4	5	6	7	8
S_i	0.29	0.24	0.11	0.14	0.10	0.10	0.30

The functions of the original and final profiles are

$$y = \begin{cases} \sqrt{2.125^2 - x^2} - 1.875 & \text{Initial} \\ \sqrt{3.053^2 - x^2} - 2.803 & \text{Final.} \end{cases} \quad (9)$$

Figure 7 sketches the position errors of different generations in optimization process by GA and the best sample of S_i is shown in Table 2. It can be concluded from Figure 7 that the error decreases and converges to an optimal solution which supplies the minimum value after 500 generations. The position error may get to 28.4369 mm in the first generation and after 500 generations the error is confined to a lower stage about 28.1150 mm.

The optimal solution of the links is listed in Table 2. According to the optimization results, The 3D model of the morphing nose cone before and after morphing is present in Figures 8(a) and 8(b), respectively. The mechanism morphs from Figure 8(a) to Figure 8(b) under the drive, whereas the shape of the nose cone changes from blunt body to a sharper one.

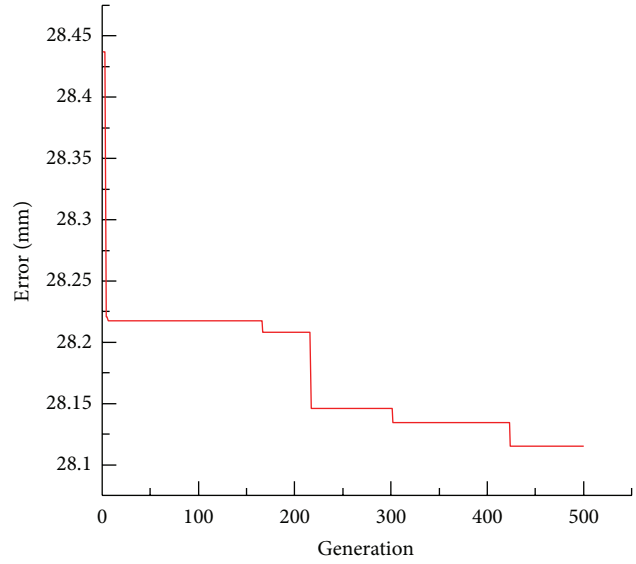

Figure 7: Errors in the generations.

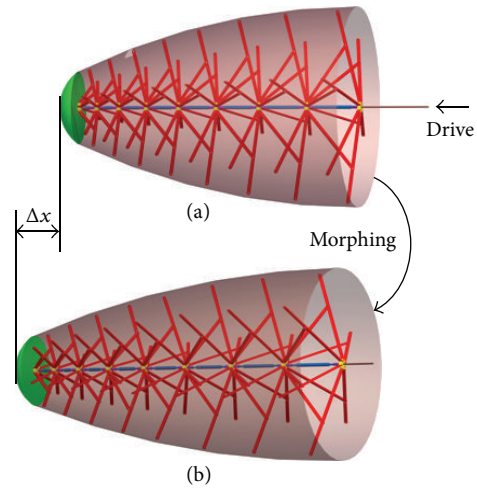

Figure 8: 3D models of the morphing nose cone: (a) before morphing and (b) after morphing.

6. Conclusions

This paper proposed the concept of morphing nose cone to reduce the drag when the re-entry vehicle flies back into the atmosphere. The range of conceptual design is defined and the optimization method of morphing nose cone is conducted. Mechanical design is conducted to obtain the initial mechanism that can be used in the further optimization. The optimization approach for the mechanism of morphing nose cone is developed to find the optimal geometric parameters of the morphing structure by employing genetic algorithm into the calculation. An example is provided by using the proposed method to verify the effect of the design and optimization method. The results show that optimal solution supplies the minimum error. The concept of morphing nose cone will provide a novel way for the drag reduction of re-entry vehicle. The proposed method could be practically used for the design and optimization of the morphing nose cone of the re-entry vehicles in the future.

Future work will be focused on the aerodynamic analysis and the wind tunnel test of the morphing nose cone to study its aerodynamic performance.

Acknowledgments

This work was supported by the National Science Foundation of China under Contract no. 11072123, the Major State Basic Research Development Program of China (973 Program), and the Project sponsored by SRF for ROCS, SEM.

References

[1] N. R. Deepak, T. Ray, and R. R. Boyce, "Evolutionary algorithm shape optimization of a hypersonic flight experiment nose cone," *Journal of Spacecraft and Rockets*, vol. 45, no. 3, pp. 428–437, 2008.

[2] A. K. Noor, S. L. Venneri, D. B. Paul, and M. A. Hopkins, "Structures technology for future aerospace systems," *Computers and Structures*, vol. 74, no. 5, pp. 507–519, 2000.

[3] W. L. Huang, *Ballistic Missiles*, China Astronautics Press, Beijing, China, 2006.

[4] E. L. Fleeman, *Tactical Missile Design*, chapter 4, American Institute of Aeronautics and Astronautics, Inc., 2nd edition, 2006.

[5] M. Y. M. Ahmed and N. Qin, "Recent advances in the aerothrmodynamics of spiked hypersonic vehicles," *Progress in Aerospace Sciences*, vol. 47, no. 6, pp. 425–449, 2011.

[6] J. Ledu and C. Pollak, "Flight testing results on a hypersonic reentry nose cone," *Journal of Spacecraft and Rockets*, vol. 6, no. 9, pp. 1044–1047, 1969.

[7] L. E. Ericsson, R. A. Guenther, W. R. Stake, and G. S. Olmsted, "Combined effects of nose bluntness and cone angle on unsteady aerodynamics," *AIAA Journal*, vol. 12, no. 5, pp. 729–732, 1974.

[8] L. E. Ericsson, "Parametric investigations of slender cone nose bluntness effects," *Journal of Spacecraft and Rockets*, vol. 23, no. 1, pp. 126–128, 1986.

[9] T. C. Lin, W. R. Grabowsky, and K. E. Yelmgren, "The search for optimum configurations for re-entry vehicles," *Journal of Spacecraft and Rockets*, vol. 21, no. 2, pp. 142–149, 1984.

[10] M. Gauer and A. Paull, "Numerical investigation of a spiked blunt nose cone at hypersonic speeds," *Journal of Spacecraft and Rockets*, vol. 45, no. 3, pp. 459–471, 2008.

[11] M. Y. M. Ahmed and N. Qin, "Drag Reduction using aerodisks for hypersonic hemispherical bodies," *Journal of Spacecraft and Rockets*, vol. 47, no. 1, pp. 62–80, 2010.

[12] C. D. Marley and D. W. Riggins, "Numerical study of novel drag reduction techniques for hypersonic blunt bodies," *AIAA Journal*, vol. 49, no. 9, pp. 1871–1882, 2011.

[13] A. Vashishtha and E. Rathakrishnan, "Breathing blunt-nose concept for drag reduction in supersonic flow," *Journal of Aerospace Engineering*, vol. 223, no. 1, pp. 31–38, 2009.

[14] S. Lim, S. D. Kim, and D. J. Song, "The influence of Chine nose shapes on a slender body flight vehicle at high angles of attack," *Journal of Aerospace Engineering*, vol. 226, no. 2, pp. 182–196, 2012.

[15] L. Lampani, K. Keller, E. Pfeiffer, H. Ritter, and P. Gaudenzi, "Variable curvature concepts for smart thermal protection systems (smart TPS)," in *Proceedings of the 56th International Astronautical Congress*, pp. 1–10, Fukuoka, Japan, October 2005.

[16] K. Keller, L. Lampani, H. Ritter, E. Pfeiffer, and P. Gaudenzi, "Smart thermal protection leading edges," in *Proceedings of the 5th European Workshop Thermal Protection Systems and Hot Structures*, pp. 36.1–36.6, Noordwijk, The Netherlands, May 2006.

[17] C. Thill, J. Etches, I. Bond, K. Potter, and P. Weaver, "Morphing skins," *Aeronautical Journal*, vol. 112, no. 1129, pp. 117–139, 2008.

[18] D. Inoyama, B. P. Sanders, and J. J. Joo, "Topology optimization approach for the determination of the multiple-configuration morphing wing structure," *Journal of Aircraft*, vol. 45, no. 6, pp. 1853–1862, 2008.

[19] D. Inoyama, B. P. Sanders, and J. J. Joo, "Topology synthesis of distributed actuation systems for morphing wing structures," *Journal of Aircraft*, vol. 44, no. 4, pp. 1205–1213, 2007.

[20] S. Courchesne, A. V. Popov, and R. M. Botez, "New aeroelastic studies for a morphing wing," in *Proceedings of the 48th AIAA Aerospace Sciences Meeting Including the New Horizons Forum and Aerospace Exposition*, Orlando, Fla, USA, January 2010, AIAA 2010-56.

[21] D. Cao and M. W. Fu, "Port-based ontology modeling to support product conceptualization," *Robotics and Computer-Integrated Manufacturing*, vol. 27, no. 3, pp. 646–656, 2011.

[22] D. Cao, Z. Li, and K. Ramani, "Ontology-based customer preference modeling for concept generation," *Advanced Engineering Informatics*, vol. 25, no. 2, pp. 162–176, 2011.

[23] D. P. Raymer, *Aircraft Design: A Conceptual Approach*, AIAA Education Series, 4th edition, 2006.

[24] W. E. Rentema, *AIDA: artificial intelligence supported conceptual design of aircraft [Ph.D. thesis]*, Delft University of Technology, Delft, The Netherlands, 2004.

[25] G. A. Crowell Sr., http://www.if.sc.usp.br/~projetosulfos/artigos/NoseCone_EQN2.PDf.

[26] O. E. Canyurt, H. R. Kim, and K. Y. Lee, "Estimation of laser hybrid welded joint strength by using genetic algorithm approach," *Mechanics of Materials*, vol. 40, no. 10, pp. 825–831, 2008.